



ISSN INTERNATIONAL STANDARD SERIAL NUMBER eISSN: 2789-858X

SCIENTIFIC JOURNAL FOR THE FACULTY OF SCIENCE - SIRTE UNIVERSITY

DOI: 10.37375/issn.2789-858X - Indexed by Crossref, USA



VOLUME 3 ISSUE 1 APRIL 2023

Bi-Annual, Peer-Reviewed, Indexed, and Open Accessed e-Journal

SJFSSU



معامل التأثير
العربي = 1.02

Legal Deposit Number@National Library (Benghazi): 990/2021



Sjsfsu@su.edu.ly



journal.su.edu.ly/index.php/JSFSU





**Bi-annual, Peer-Reviewed, Indexed, and Open Accessed
e-Journal**

DOI: 10.37375/issn.2789-858X (Indexed by Crossref, USA)

Volume 3, Issue 1, April 2023

Editor in chief

Prof. Dr. Abdussalam S. Mohamed

Editorial Board

Assoc. Prof. Dr. Haniyah A. Ben Hamdin **Co-editor.**

Assis. Prof. Dr. Gazala M. Alhdad. **Co-editor.**

Assis. Prof. Dr. Fathia A. Mosa. **Co-editor.**

Assis. Prof. Dr. Fatima .M. Mohamed. **Co-editor.**

Assis. Prof. Aziza E. Eshtiwi. **Co-editor.**

Assis. Prof. Dr. Mohammed O. Ramadan. **Proof-Reader in English.**

Eng. Mohamed T. Alsriti. **Production Editor.**

Advisory Scientific Committee of the SJFSSU

No	Name	Specialisation	Organisation	Country
1	Prof. Dr. Ahmad F. Mahgoub	Zoology	Science Faculty, Sirte University	Libya
2	Prof. Dr. Salem A. Abuhassia	Statistics	Science Faculty, Omar Al-Mukhtar University	Libya
3	Prof. Dr. Marei M. El-Ajaily	Chemistry	Science Faculty, Benghazi University	Libya
4	Prof. Dr. Huda Shaaban Elgubbi	Botany	Science Faculty, Misurata University	Libya
5	Prof. Dr. Nasser H. Sweilam	Applied Maths	Science Faculty, Cairo University	Egypt
6	Prof. Dr. Osama Ahmed Hlal	Geology	Science Faculty, Tripoli University	Libya
7	Prof. Dr. Mohamed A. Elssaidi	Environment Sciences	Environment & Natural Resources Faculty, Wadi Al-Shatti University	Libya
8	Prof. Dr. Ebrahim M. Dagman	Microbiology	Science Faculty, Misurata University	Libya
9	Prof. Dr. Ali Mohamed Awin	Mathematics	Science Faculty, Tripoli University	Libya
10	Prof. Dr. Ebrahim A. Elmerhaq	Information Technology	Information Technology Faculty, Tripoli University	Libya
11	Prof. Dr. Rafa A. Azzarroug	Physics	Science Faculty, Benghazi University	Libya
12	Prof. Dr. Osams M. Shalabiea	Astronomy	Science Faculty, Cairo University	Egypt
13	Prof. Dr. Abdualhamid S. Alhaddad	Environment Sciences & Natural Resources	Science Faculty, Misurata University	Libya

Editor in-Chief's Word

It is a matter of pleasure, modesty, and expectation that I become the Editor-in-Chief of the **Scientific Journal for the Faculty of Science-Sirte University (SJFSSU)**. On behalf of the SJFSSU editorial team, I would like to extend a warm welcome to our beloved readers. I would also like to take this opportunity to thank the authors, editors and referees, all of whom volunteered to contribute to the success of the journal.

The **Scientific Journal for the Faculty of Science-Sirte University (SJFSSU)** focuses primarily on recent scientific research that follows the rhythm of the era. This research spans a range of fields, including mathematics, physics, chemistry, biology, environment and computer science. The journal covers topics such as biochemistry, pure and synthetic mathematics, statistics, plant taxonomy and microbiology; technological development, astronomy, optics and environmental pollution.

We welcome contributions that can bring practical benefits to science, especially contributions that can contribute to the betterment of our society and our planet.

SJFSSU offers an ideal place to exchange information on all of the above topics and more, in various formats: research papers, and journal articles, written by scientific experts. SJFSSU is published biannually. In order to ensure the rapid dissemination of information, the Journal's editorial board aims to carry out the review process for each article as soon as possible after its initial submission.

SJFSSU is committed to publishing all manuscripts that receive a high or high-priority recommendation during the review process, while those that receive medium priority will be considered for publication on a case-by-case basis. In addition, we will issue semi-annual invitations to receive public papers for publication, so please follow our website to update and enhance the areas of research and development presented in the field of science. They will be published in the best possible manner.



I will end this message by inviting everyone to present their fascinating research to the SJFSSU. All papers that receive a high degree of accuracy in the reviewer's review process will find a place in SJFSSU. Therefore, we are committed to publishing all manuscripts in the field of science and its various applications.

Once again I welcome you to this journal. With your support as authors, examiners, and editors, I see very promising opportunities to better serve science and the scientific community in the future. Ultimately, we will build a better society. For additional questions or suggestions, please contact sjsfsu@su.edu.ly

.
Thank you. We hope you find our journal is spectacular.

Prof. Dr. Abdussalam S. Mohamed

Editor in chief

About the Scientific Journal for the Faculty of Science-Sirte University (SJFSSU)

DOI: <http://www.doi.org/10.37375/issn.2789-858X>

The Scientific Journal for the Faculty of Science-Sirte University (SJFSSU, henceforth) is a bi-annual peer-reviewed and openaccessed journal issued electronically by the faculty of science at Sirte University. The SJFSSU aims to encourage research in the scientific community and publish papers reporting original work that are of high standards and contribute to the development of knowledge in all fields of applied and pure (theoretical) science, namely mathematics, statistics, physics, chemistry, zoology, botany, microbiology, astronomy, computer science, information technology, geology, environment science and oceanography.

The SJFSSU accepts all types of articles such as research articles, review articles, topical review, case study/case reports, monograph, short communication, letters, conference/symposium special issues, editorials research articles and methodology articles.

Any opinions or views expressed in this journal do not reflect the opinions or views of the SJFSSU or its members. Moreover, the designation and the presentation of materials do not reflect any opinion whatsoever of the SJFSSU in terms of legal status of any country, territory...etc.

Policy and Publication Ethics of the Scientific Journal for the Faculty of Science-Sirte University (SJFSSU)

Publishing Cycle

The Scientific Journal of the faculty of science at Sirte University is published electronically on a semi-annual basis during the months of April and October.

Open Access Policy

The Scientific Journal of the faculty of science at Sirte University is an open-access journal that allows readers, authors and their institutions to obtain the full text of the articles published in it for free.

Copyright License Terms

All articles published in the Scientific Journal of the faculty of science at Sirte University are subject to the International Creative Commons License (CC BY 4.0 Creative Common Licence) and the author(s) retain copyright for the articles published by the journal with the guarantee of the following:

- 1- Making the article available on the magazine's website.
- 2- Granting any third party the right to use the article without any restrictions provided that its contents and original authors are preserved and the original source of publication is cited.

Intellectual Property Rights Copyrights

The Scientific Journal of the faculty of science at Sirte University allows authors to keep the copyright of their research without restrictions. The author retains all rights upon publication without prejudice to the open access policy of the journal, meaning:

- 1- Making the article available on the magazine's website.
- 2- Granting any third party the right to use the article without any restrictions provided that its contents and original authors are preserved and the original source of publication is cited.

Plagiarism Policy

2. To fulfil the academic integrity requirements, manuscripts submitted to the SJFSSU must adhere to ethical standards and refrain from plagiarism in any way. Thus all manuscripts submitted to the SJFSSU must be initially screened by plagiarism checker software.
3. If any plagiarism or scientific theft is detected before publication then the SJFSSU will contact the author/s in regard to this matter. If the editorial board of the SJFSSU is not satisfied with the justifications presented by the author, then the following strict actions will be taken against the author:
 - i. Such manuscript(s) will be immediately rejected.
 - ii. The editorial board forever will not consider any request for publication submitted by such author/s in the future.
 - iii. An announcement will be placed in this regard in the journal website and in the author's institution.
4. If any plagiarism or scientific theft is detected after publication then:
 - a. Immediately this article will be withdrawn from publication and republished on the journal's website and in the next issue of the journal with a watermark (RETRACTED).
 - b. An appropriate announcement will be placed in this regard through the journal website and in the author's institution.
 - c. d. An official letter to the author's institution regarding taking legal measures in this regard.
 - d. We can also consider more strict actions against authors based on seriousness of the incident.

Complaints and appeals

Anyone can submit his/her complaints/appeal to the Editor-in-Chief of the journal by email.

Publication fees

Publication in the journal is completely free and there are no fees either for submission, or for article processing APC, or for publication, or fees for the number of papers, or fees for coloured figures.

General Rules:

1. Any manuscript submitted to the SJFSSU must contain an original work which has been neither previously published, nor it is under consideration by another journal, conference, workshop or symposium.
2. The submitted manuscript must fulfil the common requirements of the scientific research, including presenting the problem, reviewing the relevant literature, analysing data, discussing results and draw the conclusion and the recommendations.
3. The SJFSSU accepts all types of articles such as research articles, review articles, topical review, case study/case reports, monograph, short communication, letters, conference/symposium special issues, editorials, research articles and methodology articles.
4. An author is required to write his or her manuscript carefully according to the basic and technical rules of the SJFSSU.
5. The SJFSSU only accepts manuscripts written in English language.
6. The subject of the submitted manuscript must be in the specified categories of the SJFSSU.
7. All individuals involved in the publishing process: from authors, editorial board, reviewers, must comply with standards of ethical behaviour.
8. All submitted manuscripts are subject to double-blind and peer-review process that is the author will be unaware of the reviewer's identity, and also the reviewer is unaware of the author's identity.
9. The SJFSSU follows the Code of Conduct of the Committee on Publication Ethics (COPE) and follows COPE Flowcharts for resolving cases of suspected misconduct. The Journal is particularly committed to the COPE Code of Conduct for Journal Publishers. Journal editors follow COPE's Code of Conduct and best practice guidelines for journal editors.

Author/s Responsibility:

1. The author is alone responsible for the proofreading and spellingcheck of his or her submitted manuscript.
2. The SJFSSU editorial committee has the right to make any editorial changes on the manuscript which is accepted for publication.
3. The author/ authors are prohibited from publishing in the journal for a period of three consecutive years if it appears that they have sent the manuscript to another journal at the same time that it was sent to the journal.
4. The author is not entitled to withdraw the manuscript during the evaluation process, unless the peer-review process exceeds six months. Thus the author could withdraw the manuscript provided that he informs the journal of his desire.
5. An author is kindly requested to disclose any affiliations, including financial, consultant or institutional associations that might lead to bias or a conflict of interest.
6. Any author is required to understand, complete and sign the ‘Authorship, Copyright Transfer, Conflicts of Interest and Acknowledgments statement’ which can be downloaded from the link:
https://drive.google.com/file/d/1jvan4NOS_CFeqJzOw8LR6RwH0vXoiA29/view?usp=sharing

The signed form should be scanned and attached electronically along with the submitted manuscript.

7. An author has to submit his or her manuscript electronically as a MS-Word file through the journal website via the link:
<https://journal.su.edu.ly/index.php/SJFSSU/information/authors>
8. Without the need to contact the editorial committee with regard to submitted manuscript, an author can easily track his or her submitted manuscript electronically through the journal website via the link:
<https://journal.su.edu.ly/index.php/SJFSSU/information/authors>

Author’s Rights:

1. The Author retains the following rights:
 - i. All proprietary rights, such as patent rights.

- ii. Using all or part of the material published in his or her article in further research of his or her own filling, provided that permission is granted from the SJFSSU and an adequate acknowledgment should be appropriately credited and referenced for the SJFSSU.

Disclaimer

The author(s) of each article appearing in this Journal is/are solely responsible for the views, ideas expressed and the accuracy of the data in his or her manuscript. Thus the published papers do not reflect the opinions or views of the SJFSSU or its members. Furthermore, the designation and the presentation of materials do not reflect any opinion whatsoever of the SJFSSU in terms of legal status of any country, territory...etc.

Editors Responsibilities:

1. The editorial committee must ensure a fair double-blind peer- review of the submitted manuscript.
2. The editorial committee will strive to make sure there are no potential conflicts of interests between the author and the editorial and review personnel.
3. The editorial committee will ensure that all the information related to submitted manuscripts is sustained as confidential.

Reviewers Responsibilities:

1. The reviewers must ensure that all the information related to submitted manuscripts is kept as confidential.
2. Reviewer who is unable to review the submitted manuscript for any reason should notify the editorial director to excuse himself or herself from the review process.
3. Reviewers must review the submitted manuscripts objectively according to the journal's evaluation forms and adhere to the specified evaluation period of three months at max.

Review Process

1. If the submitted manuscript initially meets the specified requirements of the SJFSSU and successfully passes the plagiarism check, then directly it should go through the double blind and peer- review process.
2. The submitted manuscript is subject to double blind review by specialized referees suggested by the editorial committee in an undisclosed manner to evaluate the submitted manuscript.
4. The editorial board of the journal informs the author of the opinions of the referees and forwards its assessment report if the manuscript needs any corrections.
5. Any PhD-degree holder with a scientific degree (assistant professor or higher) who would like to be a referee in the SJFSSU should register and send his or her CV through the SJFSSU website.
6. An author is required to make any minor or major corrections that are suggested by the referees within a stipulated date.

Publishing Process

1. Once the decision is made of accepting the manuscript for publication at the SJFSSU, the author will be notified and facilitated with an acceptance letter to confirm that his or her manuscript is accepted for publication in the upcoming issue of the SJFSSU.
2. Once the issue of the journal has been realised, a soft-copy of each published paper will be sent to the author via his or her email address.

Author guidelines for preparing the manuscript

All submissions should strictly be prepared according to the following typing guideline:

1. The submitted manuscript should be approximately up to a maximum of 20 pages and a minimum of 5 pages (including tables, figures, references list, appendixes and supplements).

2. The submitted manuscript of types (review articles, topical review) should be approximately up to 45 pages maximum (including tables, figures, references list, appendixes and supplements).

Rules for the Paper Structure

3. The first page should contain the full title of the manuscript (the title should be concise and informative), then the name(s) of the author(s).
4. Affiliation with contact information including the (The affiliation(s) of the author(s), i.e. institution, (department), city, (state), country). A clear indication and an active, official university email address of the corresponding author.
5. This is followed by the abstract except for review article types which start with the introduction.
6. The abstract length should be of (250) words at the maximum and (150) words at the minimum.
7. In the abstract of the submitted manuscript, the following main points must be available: -
 - i. An introductory sentence related to the research topic to attract readers.
 - ii. Presentation of the research main point (purpose).
 - iii. Description of the method used in the research.
 - iv. Presentation of the achieved results.
 - v. A concluding sentence that includes a recommendation.
8. The keywords should be 4 to 6, which can be used for indexing purposes.
9. In the introduction of the submitted manuscript, the following main points must be available: -
 - i. Introductory sentences related to the research topic to attract readers.
 - ii. An adequate background, then the relevant literature review.
 - iii. Clearly state the object of the research.
 - iv. The limitation of the research.
 - v. The structure of the manuscript.
10. In the Material and methods section of the submitted manuscript, the author should provide sufficient details to allow the work to be

reproduced by an independent researcher. Methods that are already published should be summarized and indicated by a reference. If quoting directly from a previously published method, use quotation marks and also cite the source. Any modifications to existing methods should also be described.

11. Results should be clear and concise and presented separately from the discussion.
12. The discussion should explore the significance of the results of the work, not repeat them.
13. The main conclusions of the study may be presented in a short Conclusions section, which may stand alone or form a subsection of the Discussion section.
14. Collate acknowledgements in a separate section at the end of the article before the reference list and do not, therefore, include them on the title page, as a footnote to the title or otherwise. List contributions that need acknowledging (e.g., acknowledgments of technical help; acknowledgments of financial and material support, writing assistance or proof reading the article, financial arrangement, specifying the nature of the support).
15. Within the acknowledgments section, a conflict of interest statement must be included for all manuscripts even if there are no conflicts of interest.
16. If there is more than one appendix, they should be identified as A, B, etc. Formulae and equations in appendices should be given separate numbering: Eq. (A.1), Eq. (A.2), etc.; in a subsequent appendix, Eq. (B.1) and so on. Similarly for tables and figures: Table A.1; Fig. A.1, etc.
17. The author is asked to switch off the 'Track Changes' option in Microsoft Office files as these will appear in the published version.

Text Formatting Rules:

18. Use a normal, plain font (e.g., 10-point Times New Roman) for text.
19. Use italics for emphasis.
20. Use the equation editor or Math Type for equations.
21. Save your file in docx format (Word 2007 or higher).

Headings: Please use no more than three levels of displayed headings.

22. The manuscript (in two columns) should be single line space and the font type (Times New Roman) and the size should be as specified in this table:

Paper title	14 Bold
Authors names	10
Abstract	9
Address	10 Italic
Main headings	12 Bold
subheadings	10 Bold
Text	10
Figure and table captions	9

23. The metric system should be used, and the Arabic numbers should be used for page numbers and throughout the running text.

24. Abbreviations, if used should be defined at their first mention in the text and used consistently thereafter, and the non-standard ones should be avoided.

25. Mathematical equations should appear in a sequential order and should be numbered between the brackets ().

Tables

26. All tables are to be numbered using Arabic numerals.

27. Tables should always be cited in text in consecutive numerical order. For each table, please supply a table caption (title) explaining the components of the table and an explanatory legend.

28. Identify any previously published material by giving the original source in the form of a reference at the end of the table caption.

29. Footnotes to tables should be indicated by superscript lower-case letters (or asterisks for significance values and other statistical data) and included beneath the table body.

Figures

30. High resolution is required in preparing the figures in the manuscript, the file formats JPEG, PNG are preferred for the figures, images, etc.

31. If the figure, photo... etc. has been published elsewhere, then the original source must be acknowledged and a written permission from

the copyright holder must be obtained and submitted with the manuscript.

32. If photographs of people are used, then the photos must be obscured by clouds or a written permission by the concerned person must be obtained.
33. All figures are to be numbered using Arabic numerals.
34. Figure parts should be denoted by lowercase letters (a, b, c, etc)
35. References to figures and tables should be made in a sequential order as they appear in the running text, and should be numbered between the parentheses (), e.g. (Fig. 1) and (Tab. 1).
36. Ensure all figure and table citations in the text match the files provided.
37. When preparing your figures, pay attention to the size figures to fit in the column width.
38. Figures should have a short label.

References Style:

39. Enclose the references list at the end of the manuscript accordingly to the APA (American Psychological Association) style (5th to 7th) edition. A guide containing examples of common citation formats in APA can be found at the below link:

<https://guides.libraries.psu.edu/apaquickguide/>

40. How to create an APA cited paper in Microsoft Word:

<https://support.microsoft.com/en-us/office/apa-mla-chicago-%E2%80%93-automatically-format-bibliographies-405c207c-7070-42fa-91e7-eaf064b14dbb>

Page margins: The Page margins should be adjusted as,

Top	Bottom	left	Right
2	2	2.5	2

41. To prepare the manuscript, it is highly recommended to use the ready –template that is prepared by the editorial committee which is available electronically on the journal website at the ink:

<https://docs.google.com/document/d/1Q7JFml7kjZAwR0qXLzv6L9nOoOdeRLtK/mobilebasic>

Scientific Journal for Faculty of Science-Sirte University (SJFSSU)

DOI: 10.37375/issn.2789-858X (Indexed by Crossref, USA)

Volume 3, Issue 1, April 2023

DOI: <https://doi.org/10.37375/sjfssu.v3i1>

Contents	page
A new Variety (<i>A. foliolosus</i> var. <i>viscosus</i> (Webb & Berthel.) Essokne & Jury, <i>comb. nov</i>) from Canary Islands. <i>Stephen L. Jury and Rafaa A. Essokne</i> DOI: https://doi.org/10.37375/sjfssu.v3i1.1042	01-08
Metal Chelates of Copper and Nickel with Murexide in Mixed Isopropanol: Water Solvent: Spectrophotometric Study. <i>Zainab Y. Alzalouk, Khaled M. M. Elsherif, Ahmed Zubi, Rafallah M. Atiya and Salima Al-Ddarwish</i> DOI: https://doi.org/10.37375/sjfssu.v3i1.71	09-17
Assessment of Radioactivity in the Soil Samples from Al Bayda city, Libya, and its Radiological Implications. <i>Salha D. Y. Alsaadi, Areej Hazawi and Ahmed S. A. Elmzainy</i> DOI: https://doi.org/10.37375/sjfssu.v3i1.1058	18-23
Investigation of Medicinal Activity of Four Imported Trees to Libya Against Some Pathogens. <i>Amani A. Abdulrazziq, Sami M. Salih and Ahmed A. Abdulrazziq</i> DOI: https://doi.org/10.37375/sjfssu.v3i1.972	24-28
Ground Water Quality Evaluation for Drinking Purposes in Sabratha City, Libya <i>Wafa A. Aldeeb and Bashir M. Aldabusi</i> DOI: https://doi.org/10.37375/sjfssu.v3i1.102	29-34
Formulate the Matrix Continued Fractions and Some Applications. <i>Naglaa F. A. Elfasy</i> DOI: https://doi.org/10.37375/sjfssu.v3i1.1100	35-46

<p>Evaluation of the Healthy of Workers in the Three Cement Factories of Expansion Badoush, New Badoush and Al-Rafidain in Nineveh Governorate.</p> <p><i>Aya A.H. Rasheed, Luay A. Al-Helaly, Ayad F. Qasim</i></p> <p>DOI: https://doi.org/10.37375/sjfssu.v3i1.1169</p>	47-53
<p>Synthesis and Spectral Characterization of New Compounds Containing Benzotriazole Ring from 2 - chloro – N – (Substitutedphenyl) Acetamide.</p> <p><i>Ghazala Hashim, Nsreen Abdalfarg and Hanan Bashir</i></p> <p>DOI: https://doi.org/10.37375/sjfssu.v3i1.837</p>	54-60
<p>Air Pollution: Selected Fuel Stations in Benghazi City, Libya.</p> <p><i>Adel M. Najar, Mohmed A. I Amajbary, Abduslam H. A. Awarfaly, Tahani Aeyad, Mona H. A. Bnhmad, Naima Aeyad, Aliaa M. M. Khalifa</i></p> <p>DOI: https://doi.org/10.37375/sjfssu.v3i1.299</p>	61-67
<p>Improvement the Germination Characteristics in Aged Seeds of <i>Hordeum vulgare</i> Plants by Some Invigoration Solutions.</p> <p><i>Rabha B. Hamad</i></p> <p>DOI: https://doi.org/10.37375/sjfssu.v3i1.1015</p>	68-76
<p>Assessment of the Cytological and Chemical Changes of Some Varieties of Potato Tissues (<i>Solnum tubersum</i> L.) under Salt Stress.</p> <p><i>Ghada Elrgaihy, Adel Elmaghrabi, Said Abojreeda, Huda Abugnia, Elmundr Abugnia</i></p> <p>DOI: https://doi.org/10.37375/sjfssu.v3i1.937</p>	77-87
<p>Growth and Yield of Triticale (\times <i>Triticosecale</i> Wittmack) as Influenced by Different Sowing Dates.</p> <p><i>Amal Ehtaiwesh and Munira Emsahel</i></p> <p>DOI: https://doi.org/10.37375/sjfssu.v3i1.324</p>	88-94
<p>Aqueous Extract of Winter Jasmine Leaves Mediated Biosynthesis of Silver Nanoparticles.</p> <p><i>Kawther E. Adaila, Samia S. E. Elraies, Abdounasser A. Omar, Eman J. Ben Younis, Hiba A. Alhaj, Salsabel A. Shlebek and Sara N. Ali</i></p> <p>DOI: https://doi.org/10.37375/sjfssu.v3i1.1139</p>	95-101
<p>Preptin Hormone in Patients with Type 2 Diabetes Induced Post Coronavirus Infection (Covid-19).</p> <p><i>Zahraa M. Mahmood and Luay A. Al-Helaly</i></p> <p>DOI: https://doi.org/10.37375/sjfssu.v3i1.46</p>	102-108

<p>A study on Using Plant Extracts as Indicators for the Endpoint in the Acid-Base Titrations.</p> <p><i>Aisha AL-Abbasi, Dania Abu Alassad, Ihssin Abdalsamed and Khadija Ahmida</i></p> <p>DOI: https://doi.org/10.37375/sjfssu.v3i1.149</p>	109-114
<p>Assessment of the Antimicrobial Activity of Three <i>Silene</i> Species (Caryophyllaceae) Against Some Microorganisms.</p> <p><i>Miloud M. Miloud and Najma A. Senussi</i></p> <p>DOI: https://doi.org/10.37375/sjfssu.v3i1.1089</p>	115-121
<p>Mobile Phones as a Source of Bacterial Infection.</p> <p><i>Najla A. Najam and Fauzia Garabulli</i></p> <p>DOI: https://doi.org/10.37375/sjfssu.v3i1.155</p>	122-129
<p>Detection of Bacterial Species Causing Urinary Tract Infections in Brega City Region, Isolation, Identification, and Antibiotic Sensitivity Testing.</p> <p><i>Mifthah S. Najem, Suliman F. Alsdig and Youssef F. Lawgali</i></p> <p>DOI: https://doi.org/10.37375/sjfssu.v3i1.1140</p>	130-138
<p>The Effects of Indole Butyric Acid and Seaweed (<i>Posidonia oceanica</i>) and their Mixture in Improving Photosynthetic Pigments of Salt-Stressed Wheat Cultivar (Marjawi).</p> <p><i>Sami M. Salih and Ahmed A. Abdulrazziq</i></p> <p>DOI: https://doi.org/10.37375/sjfssu.v3i1.100</p>	139-144
<p>Phytoremediation of Crude Oil-Polluted Soil by Maize (<i>Zea mays</i>) and Sunflower (<i>Helianthus Annus</i>).</p> <p><i>Farag Abu Drehiba, Abubaker Edkymish, Abdurrazzaq Braydan, Otman Ermithi, Mohamed Mukhtar and Elmundr Abughnia</i></p> <p>DOI: https://doi.org/10.37375/sjfssu.v3i1.940</p>	145-149
<p>Effect of Silver Nitrate (AgNO₃) and Copper Sulphate (CuSO₄) on Callus Formation and Plant Regeneration from Tow Pepper Varieties (Chile Ancho and Misraty) <i>in Vitro</i>.</p> <p><i>Noaman Enfeshi, Elshaybani Abdulali, Mustafa Salama, Zaineb geath, Ahmed Shaaban, Elmundr Abughnia and Zuhear Ben saad</i></p> <p>DOI: https://doi.org/10.37375/sjfssu.v3i1.943</p>	150-157
<p>Hydrogen Sulphide Strategy in Oil and Gas Field. Review</p> <p><i>Ihssin A. Abdalsamed, Ibrahim A. Amar, Aisha A. Al-abbasi, Elfitouri K. Ahmied, Abdusatar A. farouj, Jamal A. Kawan and Mohammed A. Awaj</i></p> <p>DOI: https://doi.org/10.37375/sjfssu.v3i1.74</p>	158-165



A new Variety (*A. foliolosus* var. *viscosus* (Webb & Berthel.) Essokne & Jury, *comb. nov*) from Canary Islands

Stephen L. Jury¹ and Rafaa A. Essokne^{2*}

¹Biological Sciences School (Harborne Building), Reading University, Whiteknights, Reading RG6 6AS, United Kingdom.

²Biology Department, Education Faculty, Benghazi University.

DOI: <https://doi.org/10.37375/sjfssu.v3i1.1042>

A B S T R A C T

ARTICLE INFO:

Received: 16 February 2023

Accepted: 26 March 2023

Published: 17 April 2023

Keywords:

Adenocarpus, Leguminosae, Canary Islands, New variety, Taxonomy.

Twenty four species have been recognised in this genus. Subspecies rank has been applied to geographical variants of a species which are morphologically distinguishable. In addition, one new variety has been recognised which lacks glandular papillae on the calyx, and grows at a different altitude than the type. The range of descriptions, distributions and the key to the species were drawn up from field collections and herbarium material. All the specimens available to me have been examined, except where specimens were missing some parts (e.g. some sheets lacked flowers). The descriptions and the distributions of most of the taxa were taken directly from the type and herbarium specimens. Therefore, the species *Adenocarpus viscosus* (Leguminosae) is proposed as a new Variety to the Canary Islands. Its morphological, and ecological features are discussed, together with its relationship to, and differences from, the other species of *Adenocarpus foliolosus* (Ait.) DC. Furthermore, earlier Reading University fieldwork in Morocco suggested that the genus presently consists of ca. 25 species (Rafaa Essokne, *et al.*, 2012). However, in this paper *A. foliolosus* var. *viscosus* is recognized as a variety and accordingly described.

1 Introduction

The genus *Adenocarpus* contains approximately 23 species and is centered in the western Mediterranean with a few outlying species in tropical Africa and south-central SE Europe. Many different treatments have been published since the last complete revision over 40 years ago by Gibbs (1967). The most radical new treatment was for Flora iberica (Castroviejo, 1999 a&b), where new species are described and subspecies raised in rank. Although rich in *Adenocarpus* taxa, Ouyahya's account in Flora Pratique du Maroc (Ouyahia *et al.*, 2007), has followed that of Med Checklist (Greuter, *et al.*, 1998). The new Index Synonymique de la Flore d'Afrique du

Nord volume 4 account of *Adenocarpus* enumerates eight species, one with two subspecies, plus a hybrid and maintains a traditional view (Dobignard & Chatelain, 2012).

In order to produce a comprehensive modern revision, morphological and phytochemical studies together with a molecular investigation to create a phylogeny using the independent data sets from: morphology, phytochemistry and the nucleotide sequences of non-coding DNA (ITS) and the chloroplast (trnL-F). The basic variation in the genus has been examined, and the distribution of the variants noted (Essokne, R.S., 2011).

2 Materials and Methods

Herbarium specimen data of *Adenocarpus* were obtained from the Herbaria of the University of Reading (RNG), Natural History Museum (BM), the Royal Botanic Gardens Kew (K), the Royal Botanic Garden Edinburgh (E), The Linnean Society of London (LINN), the University of Rabat (RAB) and Institute Agronomique et Vétérinaire Hassan II Rabat (IAV). More than 200 herbarium specimen labels were photographed using a digital camera (Sony Ericsson K800i), and the data of the species entered into the Botanical Research And Herbarium Management System (BRAHMS). This system allows searching and export of data and can link to GIS systems.

A small amount of leaves were reserved in Silica gel ready for morphological, phytochemical analysis and DNA extraction. Morphology was studied mainly on herbarium specimen material examined using light microscope. Flowers and leaflets from herbarium specimens were rehydrated in boiling water for about 5 mins with two drops of detergent for the vegetative morphology of leaves, stipules, flowers and the glandular papillae on both the calyx and fruits, samples were obtained from herbarium specimens in RNG, NHM, and E.

Vegetative morphology

The calyx is described by a bilabiate shape in all the tribe Genisteae consisting of two upper lobes and three lower lobes. The upper lobes separate or joined, from an upper lip (Polhill, 1967). However, in *Adenocarpus* the calyx is normally tubular, with two lips, the lower lip longer than the upper lip. The exception is *A. mannii* which has a long lower lip.

Morphological characters of *Adenocarpus* show relationships between all the species even though the geographical distributions of the species are different. All the species are shrubs with many branches, 3-foliolate leaves, glandular papillae on the calyx, *A. foliolosus* var. *viscosus*, and *A. hispanicus* have a calyx with glandular papillae, whereas absent in *A. foliolosus*, and *A. decorticans* (Gibbs, 1967).

The exception is *A. mannii* which has a long lower lip. Some of the species of the genus have glandular papillae on the calyx: *A. bivonii*, *A. samniticus*, *A. foliolosus* var. *viscosus*, *A. hispanicus*, *A. lainzii*, *A. desertorum*, *A. gibbsianus*, *A. anisochilus*, whereas *A. complicatus*

subsp. commutatus, *A. brutius*, *A. mannii*, *A. foliolosus* var. *foliolosus*, *A. anagyriifolius* var. *foliolosus*, *A. decorticans*, *A. artemisiifolius*, *A. bacquei*, *A. cincinnatus* and *A. boudyi*. *A. faurei*, *A. complicatus* *subsp. Complicatus*. The calyx structure reflects the relationships of significant value to distinguish similar or closely related species.

Similarity between the species

Morphological characters of *Adenocarpus* show relationships between all the species even though the geographical distributions of the species are different. All the species are shrubs with many branches, 3-foliolate leaves, glandular papillae on the calyx, *A. foliolosus* var. *viscosus*, and *A. hispanicus* have a calyx with glandular papillae, whereas absent in *A. foliolosus*, and *A. decorticans* (Gibbs, 1967).

A. foliolosus (Ait.) DC. in Lam & DC., *Fl. Fr.*, ed. 3, 5 (Suppl.) : 549 (1815).

≡ *Cytisus foliolosus* Aiton, *Hort. Kew* 3: 49 (1789).

Type: Canary Islands 7 & 8. 1779, F. Masson (K !, BM !).

Shrub to 200 cm, erect, densely hairy, branches with villous hairs; leaves trifoliolate; leaflets 3.5—5.5 × 1.0—2.5 mm, oblanceolate; upper surfaces dense with villous hairs, lower surfaces glabrous. Inflorescence lax; bracts 3—4 mm, sublinear; bracteoles 3—4.5 mm, narrowly elliptic; calyx 6.5—8 mm, with dense villous hairs, with or without glandular papillae; lips longer than the tube, upper lip 4.0—5(6.5) mm, lower lip 5.5—6.5(8.5) mm; standard 10—12 mm, broadly ovate, with dense sericeous hairs; wings 8—11 mm; keel 8.5—11.5 mm; legume 24—40 × 4—5 mm, narrowly oblong, with glandular papillae; seeds 3—5.

Distribution: Endemic to the Canary Islands: Tenerife, Gran Canaria, Gomera, La Palma, El Heirro, at 250—2200 m.

Key to varieties

1-Calyx without glandular papillae ...**a. var. foliolosus**

1-Calyx with glandular papillae...**b. var. viscosus**

a. var. foliolosus

= *A. ombriosus* Ceballos & Ortuno, *Ins. Forest. Invest. Exper.*, 18, no.33: 12 (1947)

Illustration: Bramwell & Bramwell, *Flores Silvestres de las Islas Canarias*. Ed.4: 197 (2001).

Leaflets 3.5—5.5 × 1.0—2.5 mm, oblanceolate; upper surfaces densely hairy, lower surfaces glabrous; calyx densely hairy, without glandular papillae. (Figure 2).

Distribution: Endemic to the Canary Islands: Tenerife, Gran Canaria, Gomera, La Palma, El Heirro.

Notes:

It differs from *A. foliolosus* var. *viscosus* by the absence of glandular papillae on the calyx, although on the legumes they are present (Figure 1). It lives at lower altitudes, usually beneath 1400 m, while *A. foliolosus* var. *viscosus* lives at higher altitudes up to 2200 m.

Specimens examined:

Tenerife, Near Jcod de los Vinas, 1921, Dr. F. Borgeesen 139 (K); Pinus canariensis, Erica arborea, wald Bei Aguamansa, 1400 m, 1977, Gill 11.I (K); Las Mercedes, 1921, Borgeesen 570 (K); Las Mercedes on dry hill and below wood, 18.6.1913, Sprague & Hutchinson 611 (K); Las Mercedes, ad marginem sylvae in saxosis, 19.5-15-7.1855, Boureau 1304 (E); Guimer, Pico de Badajor, 1857, Ball (E); Las Mercedes, 1.5.1891, Hamilton (E); 5 km after turning to Anaga from Las Cantaras, 28°31' N 16°18' W, 700 m, 30.6.1997, Percy 29 (E); road from La Laguna to parquet del Teide, c. 5km above Las Raicas restaurant, on left at beginning on track to Huelgues, between Eucalyptus plantations, 28°26' N 16°22'30'' W, 1190 m, 22.6.1997, Percy 4 (E); Near Agua Manza, forestry track, 3 km north of Village, 28°21' N 12°48' W, 1400 m, 14.5.1977, Jarvis 693 (RNG); C.821 road, 3 km north of El Portillo, 28°28' N 12°52' W, 1900 m, 30.4.1977, Jarvis 503 (RNG); On hill above San Juan da Rambla, 20.2.1929, Maude (RNG); Agua Lgarica, 750 m, 30.5.1969, Bramwell 1716 (RNG); Monte de las mercedes, Mirador, 4 km west of Pico del Ingles, roadside, 28°31' N 12°35' W, 800 m, 29.4.1977, Jarvis 462 (RNG); Near Agua Manza, Barranco above Village, Pine foresr, roadside weed, 28°21' N 12°48' W, 1100 m, 30.4.1977, Jarvis 478 (RNG); Pine forest above Agua

Manza, 1300 m, 14.4.1969, Bramwell 1289 (RNG); Cistus marguis near La Guancha, 400 m, 9.11.1968 Bramwell 363 (RNG); Gran Canaria: Santa-Brigida, in sylvis regionis mediae, 22.4.1855, Bourgeau (K); 13.5.1892, Murray (K); San Jose near Agaiti, 800 m, 8.8.1966, Gosland D40 (K); Near S. Matteo, 30.5.1902, Murray (K); Cruz de Tejeda to Las Legunetas, 1400-1600 m, 19.4.1981, Davis 67370 (E); Above las Mateo, 853 m, 30.5.1972, Kumkel 15014 (E); By road from Cruz de Tejeda to Tejeda Village 27°59' N 15°36' W, 1480 m, 5.7.1997, Percy 36 (E) Cruz de Tejeda along the rim of the central crater, up to Los Moriscos, 1500 m, 8.8.1954, Lems, 2136 (RNG); Moya, enter Los Tilos de Moya et El Palmital, 400 m, 27.4.1982, Retz, 82913 (RNG); Gomera: Dry hillside above Valle Hermoso, 17.5.1899, Murray (K); Above Arafo, on new road to Mirador Ortuno and EL Diabolo, rocky slopes in scrub, 600-700 m, 26.4.1981, Davis 67533 (E); Between La Orotava and Aquamansa, 800 m, 24.4.1981, Davis 67471 (E); Orotava, 900 m, 21.6.?, Bourchard 51 (E); Alto de Garajonay, in exposed places on tops of Mountain, 5000 ft., 28.8.1957, Gillie 2643 (E); Road from Arure to Las Hayas and Parque Nacional, 28°7'30'' N 17°18'30'' W, 900 m, 13.7.1997, Percy 67 (E); N. coastal road, near Tamagarda and Las Rosas, 28°11'30'' N 17°13'30'' W, 600 m, 26.6.1998, Percy 223 (E); Near Vallehermoso, road to Valle Gran Rey, 4km south of Vallehermoso, roadside, 600 m, 7.3.1973, Aldridge 1065 (RNG); Track to Garajonay, from main track of Vallehermoso to Valle Gran Rey, 1100 m, 8.3.1973, Aldridge 1098 (RNG); Degollada de San Sebasten, between Rio de Villa Agula, 300 m, 6.4.1971, Bramwell, Humphries 3349 (RNG); Roque de Aganda, 1200 m, 27.6.1969, Bramwell 2000 (RNG); Roque de Aganda, in Erica heath, 900 m, 27.6.1969, Bramwell 2000A (RNG); Bco, de Vallehermoso, 4 km south of vallehermoso, 28°9' N 13°35' W, 450 m, 7.5.1977, Jarvis 584 (RNG); 1.25 miles south of El cedro, Roque de Aganda, 1100 m, 4.8.1983, Thompson, Baum & Richards 91 (RNG); La Palma: Los Sauces, at Barranco de los Tilos, 700 m, 14.4.1971, Bramwell 3398 (RNG); Road from Breana Alta to Tigalete in the south, 27.3.1973, Angela & Aldridge 1414 (RNG); Pinan de Fue ncalinte, 800 m, 8.6.1969, Bramwell 1857 (RNG).

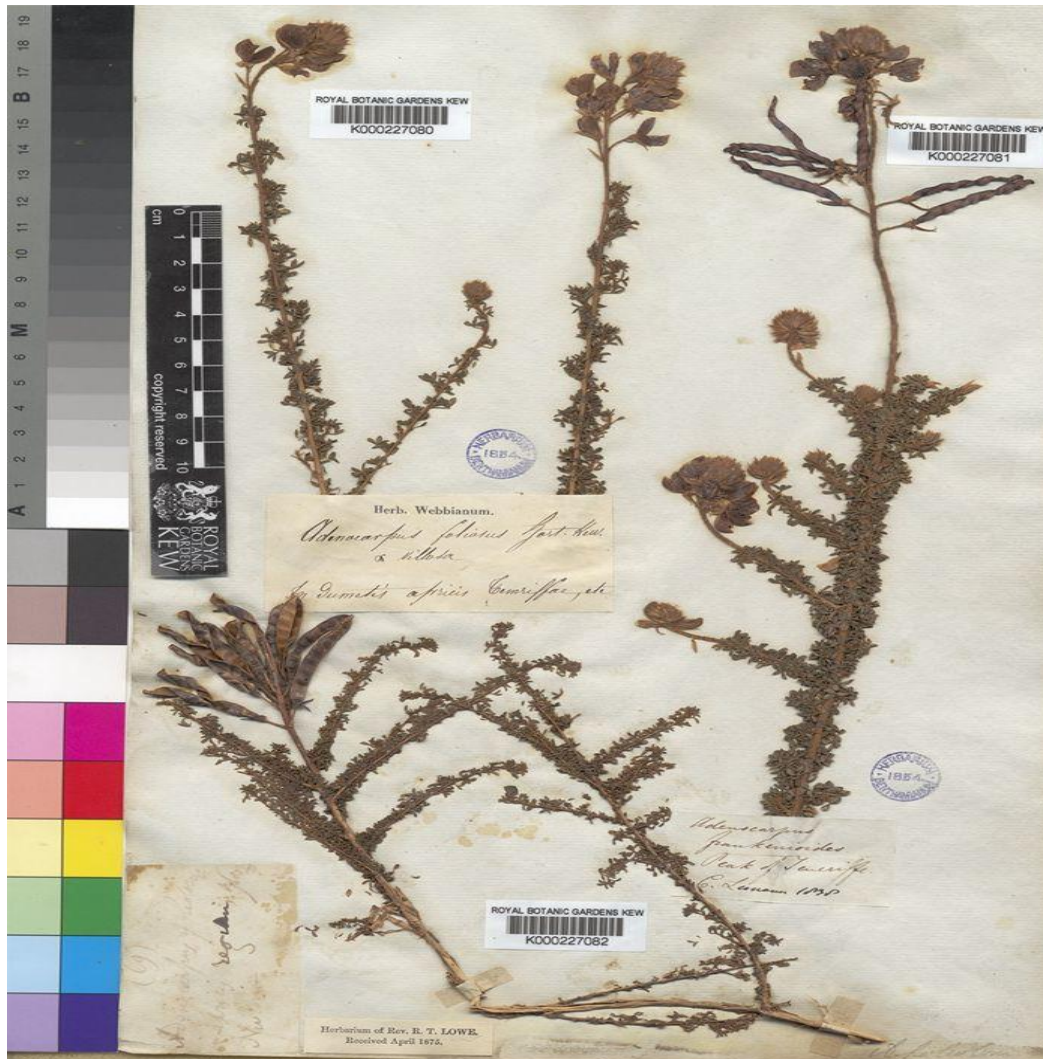


Figure 1. *Adenocarpus foliolosus* DC (<https://plants.jstor.org/stable/10.5555/al.ap.specimen.k000227082>)

B. var. viscosus (Webb & Berthel.) Essokne & Jury, comb. nov.

≡ *A. viscosus* Webb & Berthel., Hist. Nat. Iles. Canaries (Phytogr.) 2: 32 (1842).

= *A. anagyrus* Spreng, Syst. Veg. ed. 16, 3: 226 (1826).

= *A. frankenioides* Choisy, in DC., Prodr 2: 158 (1825).

Illustration: Bramwell & Bramwell, Flores Silvestres de las Islas Canarias, ed.4: 197 (2001).

Leaflets 2.5—6.5 × 1.2—1.8 mm, narrowly elliptic; both surfaces densely hairy; calyx 6.5—8.0 mm, with dense villous hairs, with glandular papillae. (Figure 2).

Distribution: Endemic to the Canary Islands: Tenerife, La Palma.

Specimens examined: Tenerife: Caldera, cliffs above Tenerife, 13.6.1913, Sprague & Hutchinson 467 (K); Cañades, 2000 m, 11.5.1933, Asplund 1233 (K); Cañades, 2000 m, 25.2.1935, Chaytor 5-7 (K); Pico del Teyde, ad radices conii superioris, 7.6.1855, Bourgeau 1313 (K); Codizo del Pies, 1400 ft., 9.6.1890, Muray (K); Above Vilaflor, abundant shrub in pine forest and higher up in superasylvatic zone, 6000 ft., 13.7.1957, Gillie 2754 (E); Tenerife, 9.5.1891, Hamilton (E); Tenerife, 2000 m, 22.5.?, Burchard 124 (E); LaPalma: Pico del Cedro, 4.6.1913, Sprague & Hutchinson 286 (K); In regione alpine, Bourgeau 117 (E); Palma, 1800 m, 21.VI.? Burchard 13 (E); Road from Santa Cruz to Las Calderas, 28°43' N 17°47' W, 1500 m, 15.7.1997, Percy 74 (E); La Caldera rim, 28°45' N 17°51' W, 2200 m, 20.5.1998, Percy 209 (E); El paso, Pine woodlands around Ermita del Pino, and crest of El Paso towards Los

Roques, 800-1500 m, 22.5.1966, Lems 7735 (RNG); Cambres de Los Tilos, 1500 m, 7.6.1969, Bramwell 1841 (RNG); North Coast road from Ti jarafe to Garafe, pine woodlands on slopes with loamy soil, 1000-1200 m, 23.5.1966, Lems 7724 (RNG); Near Fuencaliente, 5 km from Fuencaliente on El Charco road, 28°29' N 14°11' W, 500 m, 22.4.1977, Jarvis, Gibby, Humphries 440 (RNG)



Figure 2. *Adenocarpus viscosus* Webb & Berthel (<https://plants.jstor.org/stable/10.5555/al.ap.specimen.k000227094>)

3 Results and Discussion

According to Gibbs (1967), the genus originated either in North Africa with the ancestors of *A. mannii* moving to Tropical Africa and *A. complicatus* to Southern Europe, or the genus originated in Tropical Africa and extended to Northern Africa and Southern Europe. According to the molecular and chemical data the first explanation is much more likely. However, the combined results from the morphology, phytochemistry and phylogeny shows that there are 24 species, *A. complicatus* with three

subspecies and two species each with two varieties. I have described a new species from the Middle Atlas of Morocco, *A. ronaldii*, based on *Jury & Shkwa 20890* as this does not belong to the *complicatus* complex which I believe is restricted to Europe. However, I believe that *A. bracteatus* is a part of the *A. complicatus* complex, as outlined above, and so I have reduced this to a third subspecies of *A. complicatus* (Rafaa Essokne, *et al.*, 2018).

The Parsimony tree shows slightly different clades than the Bayesian clades. In the Parsimony tree (Figure 3. A), the first clade A consist of two sub-clades: sub-clade A1 contains the High Atlas endemic taxa *A. anagyriifolius* var. *anagyriifolius*, and *A. anagyriifolius* var. *leiocarpa*, *A. cincinnatus* and *A. bacquei* from the (Middle Atlas Morocco) with low value of 54% BS and 100 PP, as a sister group to *A. decorticans* (from both Spain and Morocco), *A. desertorum*, *A. hispanicus* and *A. argyrophyllus* (Spain). The most interesting aspect being their relationships as endemic species to the same geographic area, also this support has a similar topology to the ITS tree. The only difference between the topologies of the ITS and *trnL-trnF* trees concerns the position of *A. faurei* is sister to clade B (the *complicatus* and the endemics taxa from Canary Islands group) with a bootstrap support of 76% (MP analysis) and 1.0 (BI analysis), and the position of the Moroccan endemic *A. artemisiifolius* is unresolved as shown in the parsimony tree cluster with *A. telonensis* (also Moroccan), whereas in the Bayesian Inference tree it is adjacent to the endemics from the High Atlas with a value of 1.00 PP.

Clade B, (Figure 3. B) shows that *A. decorticans* from Spain is nested with the Moroccan *A. decorticans* and the Spanish *A. desertorum* subclade with value of 66% BS. *Adenocarpus decorticans* is adjacent to *A. desertorum* (Spanish) with the low value of 66% BS. This subclade is sister to the *A. hispanicus*, *A. argyrophyllus*, (all Spanish taxa) subclade with value of 69% BS.

Clade B of the parsimony tree (Figure 3. A) consists of two sub-clades, the first sub-clade contains the Middle Atlas taxa *A. ronaldii* (Moroccan), *A. telonensis* adjacent to *A. boulyi* (Moroccan) *A. complicatus* subsp. *bracteatus* and *A. aureus* (Spanish) with a support value of 66% (MP analysis) and 1.0 (BI analysis), this sub-clade is sister to *A. faurei* (Algerian) which cluster with the endemic *A. foliolosus* var. *foliolosus* from Canary Islands, and adjacent to *A. decorticans* (Algerian) and *A. complicatus* subsp. *commutatus*. The second sub-clade

shows slightly different topology between the two trees analysis, and consists of *A. complicatus* subsp. *bracteatus*, *A. anisochilus* (Portugal), *A. lainzii* and *A. gibbsianus* (both from Spain), *A. complicatus* subsp. *commutatus*, *A. bivonii* and *A. brutius* (both from Italy) with low value of 59 % BS. There is a slightly different topology of the species position in the two trees Figure 3. A and 3. B. (Essokne, R.S., 2011).

The endemic taxa from the Canary Islands, *A. foliolosus* var. *foliolosus*, and *A. foliolosus* var. *viscosus* have identical sequences and very strong support value of 100 % BS and 1.0 PP in the *trnL-trnF* tree, and are very closely related taxa to the European *complicatus* complex by the ITS analysis. Those two Canary Islands' taxa are

morphologically distinct, the leaf shape is obovate, and the calyx without glandular papillae in *A. foliolosus* var. *foliolosus*, whereas in *A. foliolosus* var. *viscosus* the leaves are narrowly elliptic and the calyx has glandular papillae. Lems (1954) in his *Botanical notes on the Canary Islands* distinguished a number of varieties and hybrids between these two species which happened as they live within short distance of one another. They grow abundantly in the famed Retama-Codeo and the Canary Pine (*Pinus canariensis*) forest in Tenerife. Our data show that these two taxa have identical sequences, results also suggested by Käss & Wink (1997), Percy & Cronk (2002) and Cubas (2002, 2010). I propose, therefore, to reduce *A. viscosus* to a variety of *A. foliolosus*

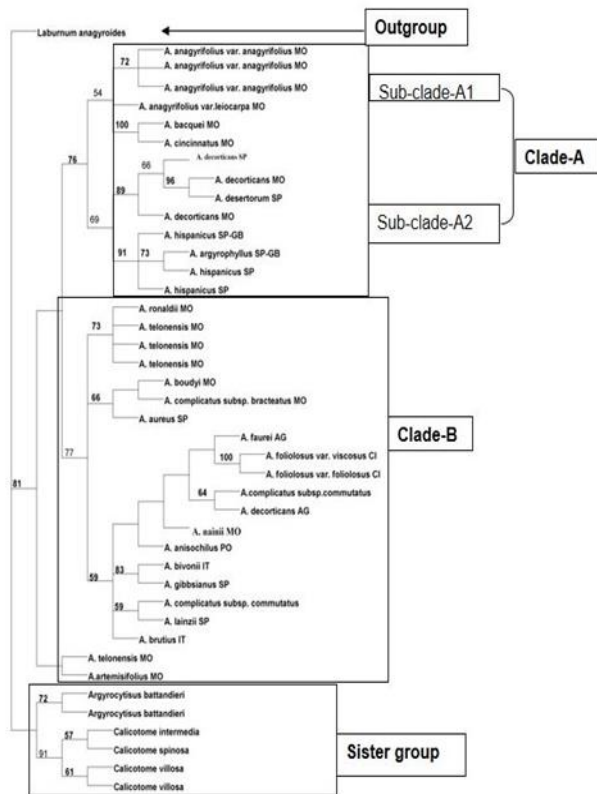


Figure 3.A. One of the 3748 most parsimonious trees based on the *trnL trnF* data sets obtained from maximum parsimony (MP) analysis of 42 *Adenocarpus* accessions. Numbers above branches are bootstrap support percentage values for clades receiving more than 50% bootstrap support (Essokne, R.S., 2011).

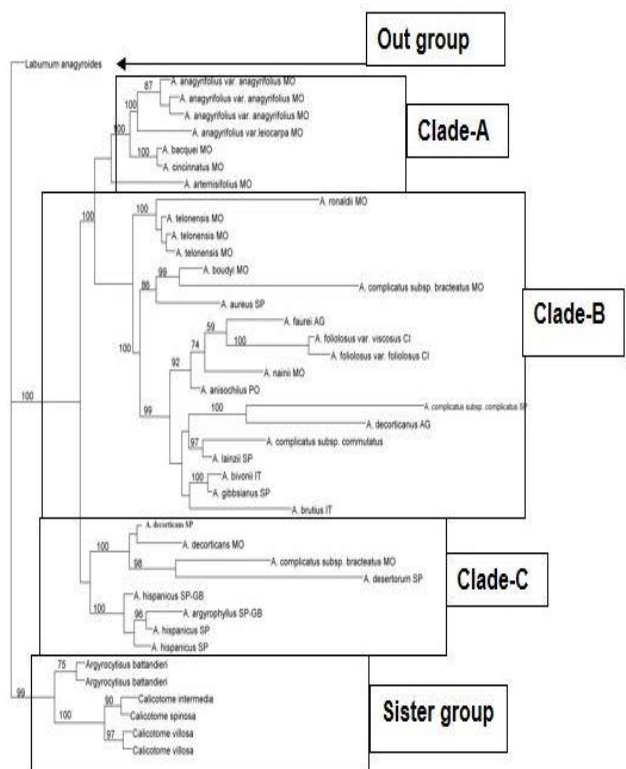


Figure 3.B. Majority-rule consensus tree of the Bayesian inference based on the *trnL trnF* data set of 42 *Adenocarpus*. Posterior probability values of the nodes are indicated above the branches. (Essokne, R.S., 2011).



Figure 4: Calyx with glandular papillae as in *A. viscosus*



Calyx without glandular papillae as in *A. foliolosus*

4 Conclusion

On the basis of the herbarium specimens, phytochemical analysis and the phylogeny of this taxon, Therefore, this taxon must be considered as a variety of *A. foliolosus*. According to our observations (Rafaa Essokne, *et al.*, 2012), and in accordance with the previous revisions (Gibbs, 1967), *A. viscosus* (Figure 4) can be distinguished from *A. foliolosus* by the presence of glandular papillae on the calyx. Therefore, I have sunk *A. viscosus* as a variety of *A. foliolosus* as although I can recognize them by the rather small distinction of the presence of glandular papillae on the calyx in the former species, they are not distinguishable by the molecular studies. Moreover, Google Earth map has been used to present the distribution of the *Adenocarpus* species in the Canary Islands (Figure 5)

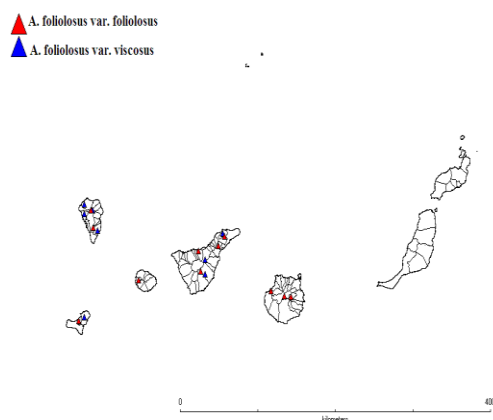


Figure 5. Map showing distribution of the *A. foliolosus* var. *foliolosus* and *A. foliolosus* var. *viscosus* varieties in the Canary Islands

Conflict of Interest: The authors declare that there are no conflicts of interest.

References

- Castroviejo, S.**, (1999a). Apuntes sobre algunos *Adenocarpus* (Leguminosae) Ibericos. *Anales Jardín Botánico de Madrid* 57, 37–46.
- Castroviejo, S.**, (1999b). *Adenocarpus* DC. In S. Castroviejo *et al.* (eds) *Flora iberica*, 7(1): 189–205. Madrid: CSIC.
- Cubas, P., Pardo, C. & Tahiri, H.** (2002). Molecular approach to the phylogeny and systematics of *Cytisus* (Leguminosae) and related genera based on nucleotide sequences of nrDNA (ITS region) and cpDNA (*trnL-trnF* intergenic spacer). *Plant Systematics and Evolution* 233: 223–242.
- Cubas, P., Pardo, C., Tahiri, H. & Castroviejo, S.** (2010). Phylogeny and evolutionary diversification of *Adenocarpus* DC. (Leguminosae). *Taxon* 59: 720–732.
- Dobignard, A., Chatelain, C.**, (2012). Index synonymique de la flore de l’Afrique de Nord, 4. Genève: Ville de Genève, Editions des Conservatoire et Jardins botaniques.
- Essokne, R.S.**, 2011. A Taxonomic Treatment of the Genus *Adenocarpus* (Leguminosae). PhD Thesis, University of Reading.
- Gibbs, P.E.**, (1967). A Revision of the Genus *Adenocarpus*. In: *Boletim Sociedade. Broteriana Série*, vol. 2, pp. 67–121.
- Greuter, W., Burdet, H. & Long, G.** (1989). *Med-Checklist*, 4. Dicotyledones (Lauraceae – Rhamnaceae) : Genève: Conservatoire et Jardin Botanique de la Ville de Genève.

- Käss, E. & Wink, M.** (1997). Phylogenetic relationships in the Papilionoideae (family Leguminosae) based on nucleotide sequences of cpDNA (*rbcL*) and ncDNA (ITS 1 and ITS2). *Molecular Phylogenetics and Evolution* 8: 65—88.
- Lems, K.**, (1954). Botanical Notes on the Canary Islands II. The Evolution of Plant Forms in the Islands: *Aeonium*. Ecology, Vol 41.1: 1— 17
- Ouyahia A., Fennane, M., Ibn Tattou, M., & El oualidi, J.,** (2007). Flore pratique du Maroc, manuel de détermination des plantes vasculaires – volume 2 : Angiospermae (Leguminosae - Lentibulariaceae). Travaux de l'Institut Scientifique, Série Botanique, n°38, Rabat (MA) : 636 p.
- Percy, D. M. & Cronk, C. B.** (2002). Different fates of island brooms: contrasting evolution in *Adenocarpus*, *Genista*, and *Teline* (Genisteae, Fabaceae) in the Canary Islands and Madeira. *American Journal of Botany* 89: 854—864.
- Polhill, R. M.** (1976). Genisteae (Adans.) Benth. and related tribes. *Botanical Systematics* 1: 143—380.
- Rafaa S. Essokne, Mohamed H. Makhoul, Stephen L. Jury.** (2018). *Adenocarpus ronaldii* Essokne & Jury. sp. nov. (Leguminosae). A New Species From Morocco. *American Journal of Life Science Researches* 6(1): 1—5
- Rafaa S. Essokne, Renée J. Grayer, Elaine Porter, Geoffrey C. Kite, Monique S.J. Simmonds, Stephen L. Jury** (2012). Flavonoids as chemosystematic markers for the genus *Adenocarpus*. *Biochemical Systematics and Ecology*, 42: 49–58



Metal Chelates of Copper and Nickel with Murexide in Mixed Isopropanol: Water Solvent: Spectrophotometric Study

Zainab Y. Alzalouk¹, Khaled M. M. Elsherif², Ahmed Zubi¹, Rafallah M. Atiya¹ and Salima Al-Ddarwish¹

¹Chemistry Department, Science Faculty, Misurata University, Misurata, Libya.

²The Libyan Authority for Scientific Research, Tripoli, Libya.

DOI: <https://doi.org/10.37375/sjfsu.v3i1.71>

A B S T R A C T

ARTICLE INFO:

Received: 26 November 2022.

Accepted: 09 February 2023.

Published: 17 April 2023.

Keywords:

Nickel, Copper, Murexide, Stability Constant, Spectrophotometry

A sensitive, accurate, and quick spectrophotometric technique for determining Ni(II) and Cu(II) in analytical samples employing murexide reagent was investigated in a water-isopropanol mixed solvent. UV/Vis spectroscopy was used to characterize the produced complexes. In three mixtures of water-isopropanol mixed solvent, various experimental parameters affecting complex formation were examined. For Ni(II) and Cu(II), the resulting complex in a 3:7 water-isopropanol mixed solvent showed maximum absorbance at $\lambda_{\max} = 458$ nm at pH 3.1 and 470 nm at pH 3.8, respectively. Beer's law was maintained in the concentration ranges of (0.2 to 3.5 ppm) for Ni(II) and (0.2 to 4.0 ppm) for Cu(II). The molar absorptivity (ϵ) and sensitivity values of the Ni(II) and Cu(II) complexes were determined to be (7800 $\text{l.mol}^{-1}.\text{cm}^{-1}$ and 0.32 ppm^{-1}) and (18700 $\text{l.mol}^{-1}.\text{cm}^{-1}$ and 0.20 ppm^{-1}), respectively. The continuous variation method was used to explore the structure of the prepared compound. The acquired results revealed that the complexes have a (1:2) (M:L) molar ratio, indicating that this method was more sensitive, precise, and accurate when the effect of Cl^- , NO_3^- , CH_3COO^- , and SO_4^{2-} was studied.

1 Introduction

Metal chelates are important compounds in numerous fields; i.e., they are used in the paint and dyes industry; such as nickel and copper complexes with some Schiff bases (Wahba et al., 2017; Elsherif et al., 2020a; Elsherif et al., 2020b), they are also used as catalysts in polymerization processes such as Ziegler-Nata catalysts (Cossee and Ziegler, 1964), and are also widely used in the nuclear industry to purify uranium and also in the treatment of nuclear waste (Flett et al., 1983). Furthermore, they play an important role in many biochemical reactions in the body, participate in the composition of many important natural biological compounds; i.e. hemoglobin, enzymes, vitamin B12 and chlorophyll in plants (Spessard and Miessler, 1996), also play a great role in diagnosis and physical therapy like: contrast agents in nuclear magnetic imaging, as active compounds in the treatment of cancer (Erkey, 2011; Elsherif et al., 2021; Elsherif et al., 2018). Large numbers

of complexes are prepared and tested from silver, copper, ruthenium, platinum, and gold, and used as antioxidants and antibacterial (Ndagi et al., 2017; Esmaeili et al., 2019; Lum et al., 2013; Warra, 2011). They are also used in the development of solar energy storage technologies (Erkey, 2011).

Complex formation reactions are also the basis of various analytical methods, such as: solvent extraction, chromatography, gravimetric analysis, UV-VIS molecular absorption and emission spectroscopy (Jeffery, 1981; Elsherif et al, 2020c; Muneer et al., 2020). They are also used in different techniques for determination of metal ions or their compounds in environmental and pharmaceutical samples. There are many analytical techniques that include the determination or extraction of metal ions in the form of chelates such as: molecular absorption methods in the visible and ultraviolet region, molecular fluorometric methods, complex formation titrations, solvent extraction methods, solid phase extraction methods, cloud point

extraction methods (Nasir Uddin et al., 2013; Birghila et al., 2008). However, there are other methods that may or may not use complexes such as voltammetry, polarography, ion exchange methods, and chromatography (Alabidi et al., 2021).

Murexide (Figure 1) is a colorimetric indicator used in the detection of metal ions and is widely used in conventional EDTA titrations (Elsherif et al., 2020c). It is widely used in the determination of calcium ions, and other metal ions like copper, nickel, cobalt, thallium, and alkaline earth elements (Masoud et al., 2006). Murexide dissolves in water and forms complexes with most metal ions with different oxidation states, in aqueous and non-aqueous solutions. The stability constants of these complexes are usually estimated by spectroscopic methods, and are often not high in aqueous solutions causing some limitations when using murexide as a colorimetric agent. The stability of the murexide complexes can be increased by using solvents with a lower dielectric constant than water (Huang et al., 2018; Shamsipur et al., 1989; Shamsipur and Alizadeh, 1992).

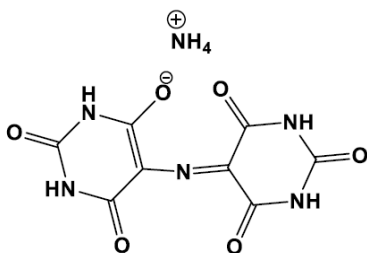


Figure (1). Chemical structure of murexide

In the present paper, a spectrophotometric investigation of the murexide complexes with copper and zinc ions in binary isopropanol-water mixtures at 25°C has been reported.

2 Materials and Methods

2.1 Chemicals and reagents

Murexide was purchased from Merck chemicals and was of ACS reagent grade. Isopropanol ($\geq 99.5\%$) was also from Merck and of ACS reagent grade. Copper (II) sulphate pentahydrate (ACS reagent, $\geq 98.0\%$), Zinc chloride (reagent grade, $\geq 98\%$), Hydrochloric acid (ACS reagent, 37%), and Sodium hydroxide (reagent grade, $\geq 98\%$, pellets (anhydrous)) were all purchased from Sigma-Aldrich. All the reagents and solvents were of analytical grade and chemically pure and were used as received without any further purification.

2.2 Instrumentation

UV-visible spectra of free and complexed murexide were recorded using Cary-60 model UV-visible spectrophotometer from Agilent. Optimum pH monitoring of complex formation was done using 3505 pH meter from Jenway.

2.3 Standard solutions

The stock solutions (5×10^{-3} M) of murexide, copper sulphate pentahydrate, and zinc chloride were prepared by dissolving the compounds in deionized water. Sample dilutions were carried out by taking the appropriate aliquots from the stock solutions followed by dilution with proper quantity of mixed solvent (isopropanol: water). To investigate the effect of various anions on absorption spectra of prepared complexes, stock solutions (1.0 M) of potassium chloride, sodium nitrate, sodium sulphate, and sodium acetate were prepared by dissolving these salts in deionized water.

2.4 The absorption spectra of murexide in different mixtures of isopropanol and water

A series of standard solutions of equal concentration of murexide; contains different proportions of water and isopropanol start from 10% to 100% water, was prepared and then the absorption spectra of these solutions were measured in the UV-VIS region (200-800 nm). The absorption maxima (λ_{\max}) of each complex in different proportions of water and isopropanol were determined. Various parameters that affect complex formation were investigated which include: time and pH.

The pH value of the complex solutions was adjusted using 0.1 M solutions of hydrochloric acid and sodium hydroxide. The absorption of the formed complexes was measured till 3 hours to determine the stability of these complexes with time

2.5 Determination of complex stoichiometry by method of continues variation

Nine solutions were prepared by mixing various proportions of 5.0×10^{-3} M solutions of both metal ion and murexide. The solutions contain various mole (or volume) ratios of both reactants, and these ratios are as follows:

$$1:9, 2:8, 3:7, 4:6, 5:5, 6:4, 7:3, 8:2, 9:1$$

The absorbance of the solutions is measured and plotted against the mole (or volume) fraction of the murexide.

2.6 Determination of complex stoichiometry by method of continues variation

In the linear range of Beer-Lambert Law, solutions with various metal ion concentrations were prepared, the absorbance of these solutions was measured, the linear relationship between the metal ion concentration and the absorbance was plotted, and the sensitivity was calculated as the slope of the straight line. The standard deviation of ten measurements of Blank's solution was used to evaluate the detection limits. The detection and quantification limits were calculated using the following equations:

$$DL = \frac{3xSD}{S} \quad (1)$$

$$QL = \frac{10xSD}{S} \quad (2)$$

Where: DL and QL detection and quantification limits, respectively, S_D standard deviation, S slope.

Different concentrations of interfering ions such as chloride, nitrate, sulfate, and acetate were also investigated.

3 Results

3.1 Absorption spectra of murexide at different proportions of water: isopropanol

Figure 2 depicts the UV-visible absorption spectra of murexide in the 300-700 nm range. As seen in the graph, the presence of two absorption groups is indicated by the presence of two peaks, one at 515-520 nm and the other at 320-330 nm. The higher intensity absorption peak is generated by the $\pi \rightarrow \pi^*$ transition, and the lower peak is caused by the $n \rightarrow \pi^*$ transition, according to the murexide structure (Figure 1). The formation of hydrogen bonds between the solvent and murexide ions causes the absorption peak at 520 nm to shift blue as the solvent polarity decreases (Elsherif et al., 2018). The absorption maxima at each water: isopropanol proportion are shown in Table 1.

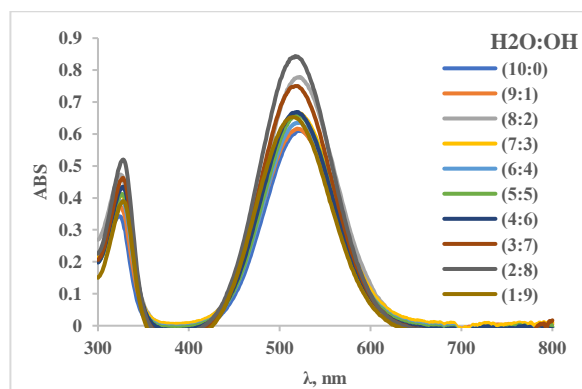


Figure (2). Absorption spectra of murexide at various water: isopropanol proportions

Table (1). λ_{max} values of murexide at various water: isopropanol proportions

Isopro.:H ₂ O	λ_{max} (nm)
0:10	521
1:9	521
2:8	521
3:7	520
4:6	520
5:5	519
6:4	519
7:3	518
8:2	517
9:1	515

3.2 Absorption spectra of metal-murexide complex at different proportions of water: isopropanol

Figure 3 depicts the relations between the absorbance and wavelength of Ni(II) and Cu(II) complexes with murexide in three different mixed solvent ratios (8:2, 6:4, and 3:7 - H₂O: Isopropanol). Blue shifts of complexes absorption peaks are seen, resulting in new, distinct absorption peaks specified to complexes absorption. The reason for these displacements is that when the complex is formed, the contribution of the $n \rightarrow \pi^*$ transitions in the murexide decreases due to the participation of n electrons in the formation of coordination bonds with metal ions (Elsherif et al, 2020c). The blue shifts in the complexes were as follows: 7 nm and 6 nm for the nickel and copper complexes, respectively.

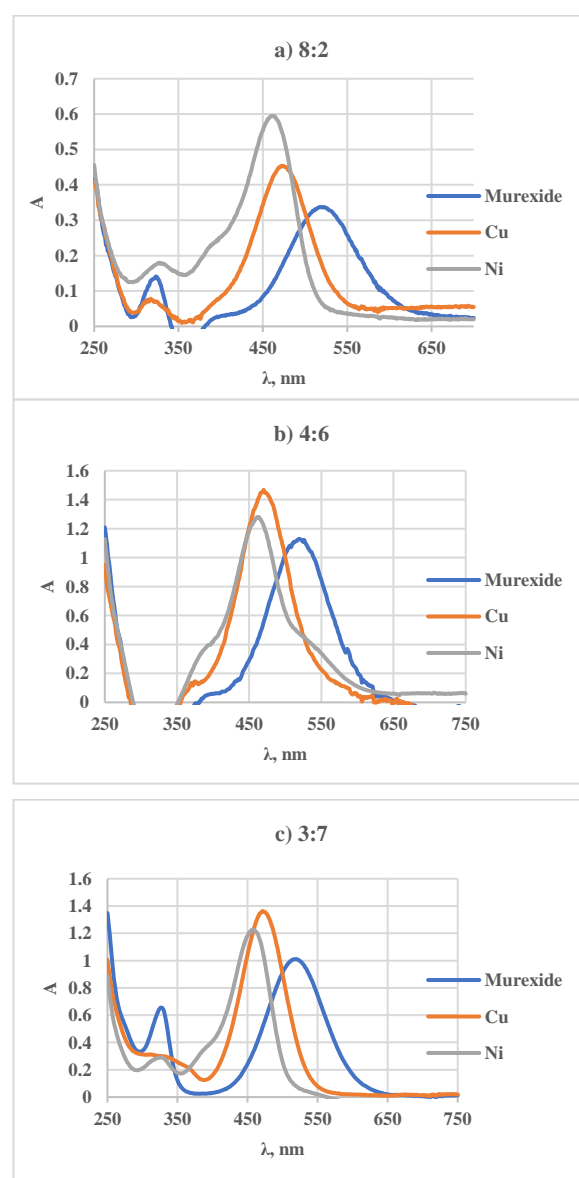


Figure (3). Absorption spectra of Cu-Murexide and Ni-Murexide complexes at various solvent proportions

3.3 Effect of pH on absorption maxima of metal-murexide complex at different proportions of water: isopropanol

One of the most critical factors influencing complex formation and stability is pH. Some complexes are stable in an acidic medium, some in a basic one, and still others in a neutral medium. Furthermore, all ligands are either weak acids or weak bases that ionize depending on the medium's pH. Murexide is classified as a weak acid since it contains four protons, as illustrated in Figure 4 (with very weak ionization constants, the protons ionize entirely in basic medium ($pK_{a1}=9.2$, $pK_{a2}=10.5$) (Winkler, 1972). Murexide dissociates into uramil and alloxan in a high acidic media (Ramaiah and Gupta, 1956; Viesca and Gómez, 2019).

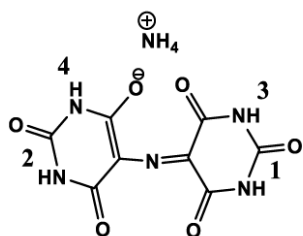


Figure (4). The four protons of murexide as a weak acid

Figure 5 displays graphical curves derived from studies investigating the effect of pH on metal ion complexes with murexide in the three investigated ratios. For Ni complex, it is noted that the complex in the three ratios have low absorption in the strong acidic medium ($pH < 3$) and high absorption in the range of (4-9). However, in the ratio (8: 2) Ni complex has low absorption in the strong alkaline medium ($pH > 9$) due to metal ion precipitation in the form of hydroxide. Otherwise; for Cu complex, it should be remarked that in the ratios (4:6) and (8:2), the complex exhibited weak absorption in acidic medium ($pH < 4$), whereas in the ratio (7:3), the complex displayed considerable absorption in strong acidic medium ($pH < 2$). However, in the case of the ratio (3:7), the complex was relatively stable over a wide pH range (2-8). At the ratio (8:2), where the Cu (II) ion precipitates as hydroxide, there is also a decrease in absorption in weak acid media ($pH > 6$). Table 9 shows the optimal pH values for the production of two complexes.

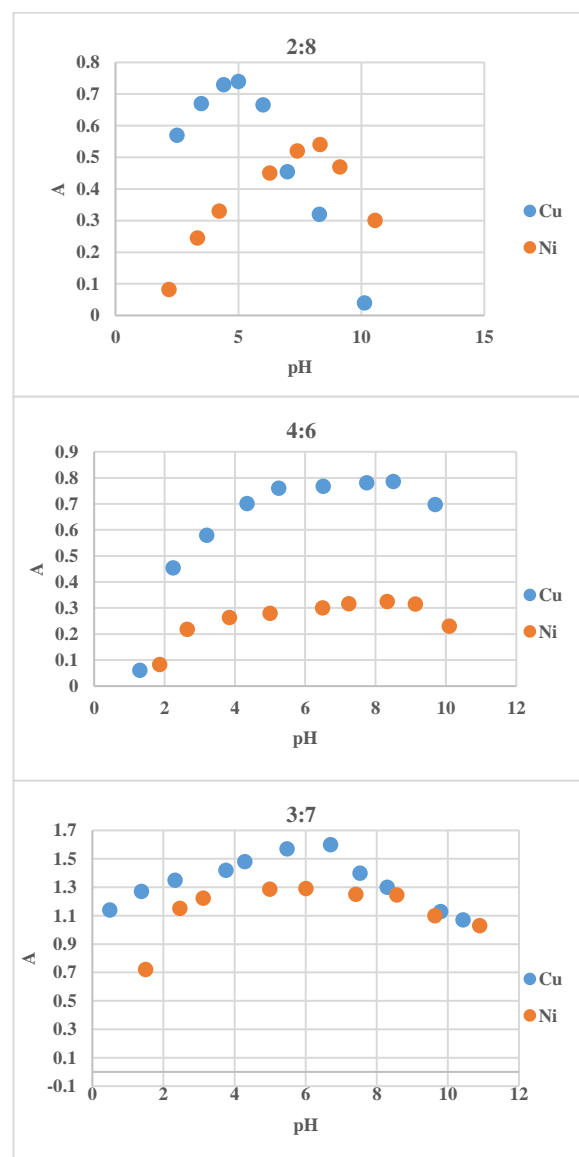


Figure (5). Effect of pH on metal-murexide complexes at different water: isopropanol proportions

3.4 Stability of metal-murexide complex over time at different proportions of water: isopropanol

Investigating the effect of time on complex stability have been gained more concern in order to recognize whether the complex reached its maximum stability or not, and to distinguish the stability duration of complex before it dissociates (Muneer et al., 2020). To demonstrate the effect of time on investigated murexide complexes stability; the change in absorbance of the complexes was measured for a period of 3 hours.

Figure 6 shows the change in absorbance versus time for Ni(II) complexes with murexide in the three mixed solvent proportions. It is observed that these complexes form quickly (the color changes immediately after addition), and they are still stable over the whole studied

time and it does not undergo any dissociation (except for 3:7 proportion which undergoes a slight dissociation). The same observed in the case of copper complexes in three studied proportions, where the complex is formed quickly and there is no remarkable dissociation (a slight dissociation is observed with the proportion of 4:6).

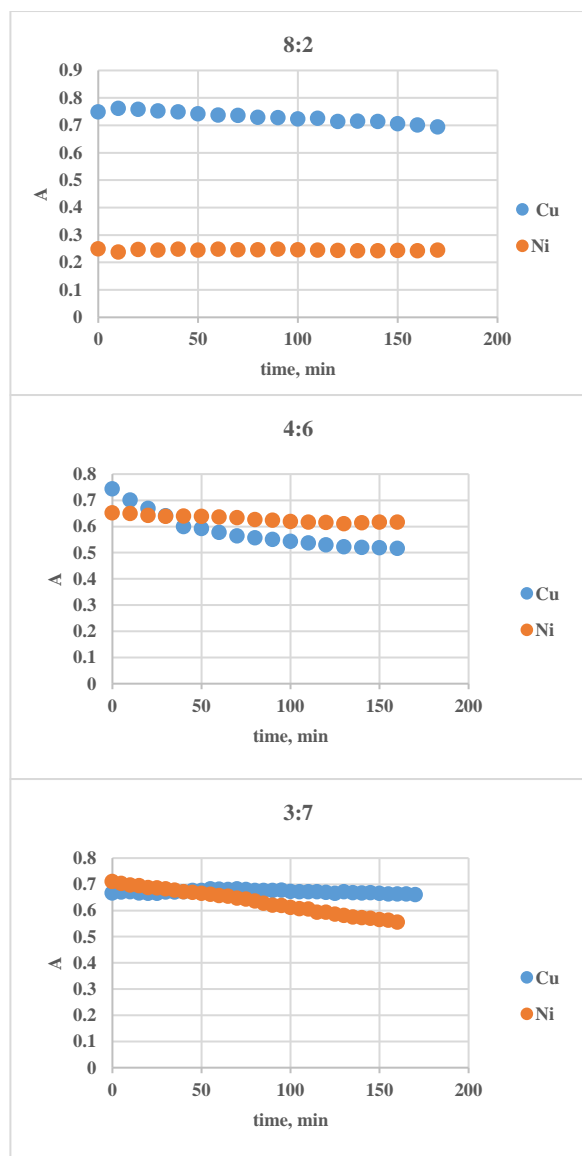


Figure (6). Effect of time on metal-murexide complexes at different water: isopropanol proportions

3.5 Stoichiometry and stability constant of metal-murexide complex at different proportions of water: isopropanol

Spectroscopic methods are one of the most important methods that are used to determine the stoichiometry and stability constant for complexes, especially if they are colored; as these complexes show clear and distinct absorption peaks in UV-VIS region. There are various spectroscopic methods, including the continues variation

method presented by Job and modified by Copper and Vosbury (AL-adilee and Hessoon, 2019).

The graphical Job curves developed for Ni(II) and Cu(II) complexes with murexide in the three examined proportions are shown in Figures 7 and 8. The absorbance versus mole fraction of the ligand relationship was displayed. The stoichiometry ratios for Ni (II) and Cu (II) complexes were determined from the Figures 7 and 8 as follows: The stoichiometry ratios were 1:1 (ML) for the (8:2) proportion and 1:2 (ML_2) for the (4:6 and 3:7) proportions. As the number of water molecules increases, they compete with ligand molecules for coordination with metal ions; however, as the number of water molecules decreases, the competition between water and the ligand decreases, allowing the metal ion to bind to more than one ligand.

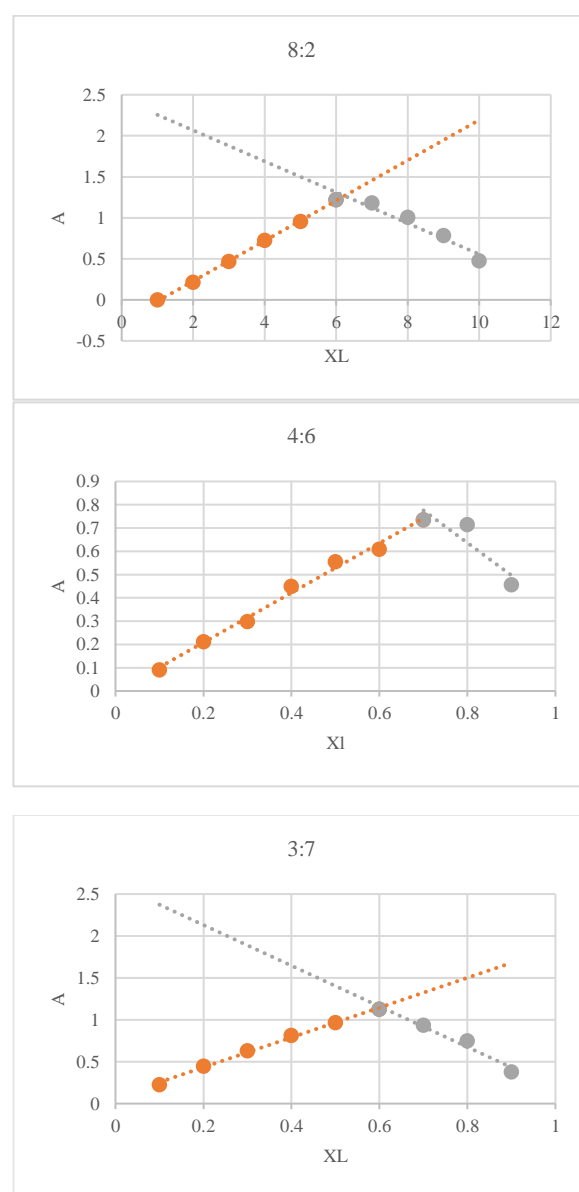


Figure (7). Job curves for Ni-murexide complexes in three mixed solvent proportions

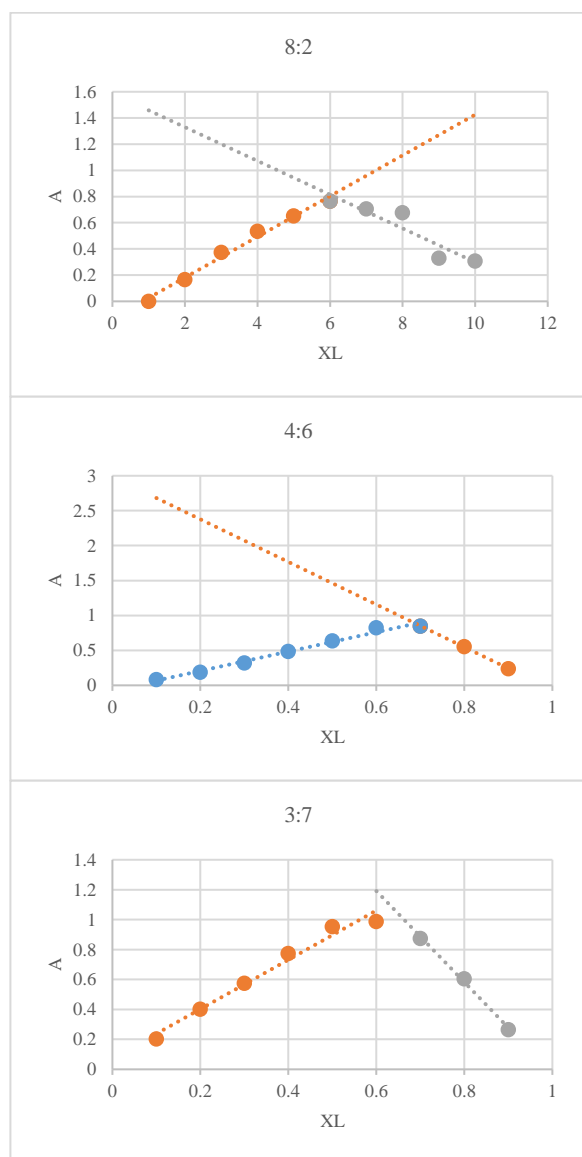


Figure (8). Job curves for Cu-murexide complexes in three mixed solvent proportions

Tables 2 and 3 present the values of the molar absorptivity and stability constants of the produced complexes in the three tested ratios. According to the values of the stability constants, the complexes generated in the ratio 8:2 were the least stable, while they were the most stable in the ratio 3:7, i.e. The percentage of water in the solvent mixture has an inverse relationship with stability (Fat'hi and Shamsipur, 1993).

The calibration curves of Ni(II) and Cu(II) complexes with murexide are shown in Figure 9, from which the molar absorbance values were derived.

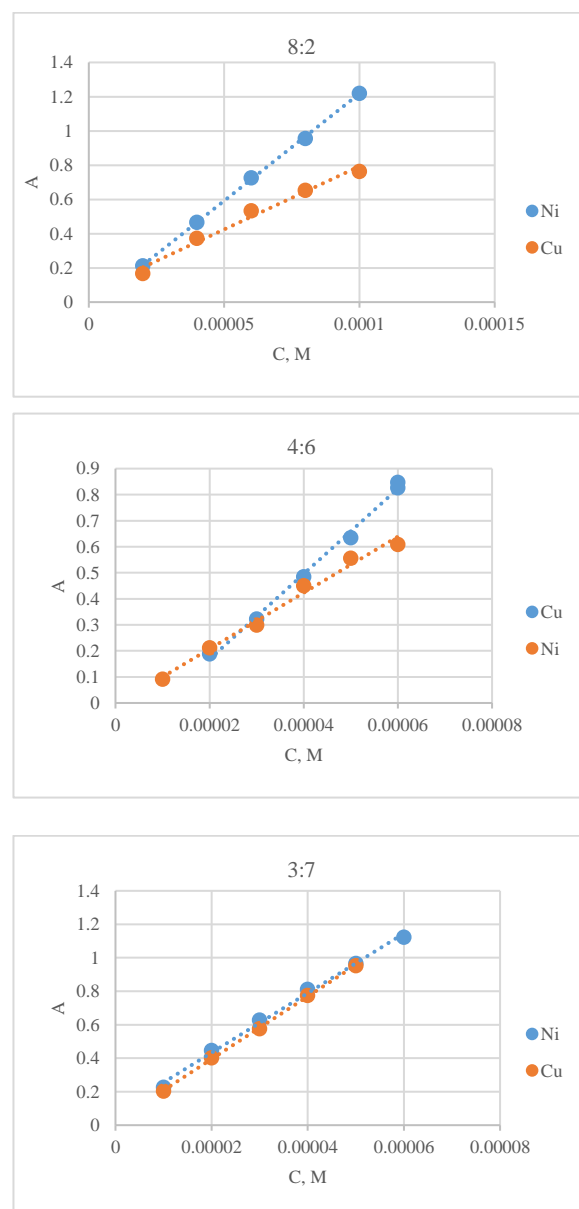


Figure (9). Calibration curves for murexide complexes in three mixed solvent proportions

Table (2). Parameters values of Ni-murexide complexes in three mixed solvent proportions

Ratio (w:Isopro.)	λ_{\max} (nm)	pH	L:M	ϵ $\text{l.mol}^{-1}\text{cm}^{-1}$	K_f
2:8	465	8.3	1:01	11720	5.06×10^6
4:6	462	10.1	2:01	10780	2.26×10^{12}
7:3	458	3.1	2:01	17800	4.33×10^{12}

Table (3). Parameters values of Cu-murexide complexes in three mixed solvent proportions

Ratio (w:Isopro.)	λ_{max} (nm)	pH	L:M	ϵ L.mol ⁻¹ cm ⁻¹	K_f
2:8	476	5.0	1:01	7370	3.24×10^6
4:6	472	8.5	2:01	14911	9.45×10^{11}
7:3	470	3.8	2:01	18700	9.80×10^{11}

3.6 Effect of interferences on metal-murexide stability at 3:7 water-isopropanol proportion

At the 7:3 ratio, the effect of some interfering ions on the stability of the synthesized complexes was investigated. The presence of particular ions enhances the probability of the ligand being displaced by a foreign ion (Nasir Uddin et al., 2013). Figure 10 depicts the influence of different salt concentrations (CH₃COONa, KCl, NaNO₃, and H₂SO₄) on the complex recovery (unaffected concentration by the presence of interfering ions). The figure shows that the complex recovery is uninfluenced by these salts at low concentrations levels, but falls dramatically at large concentrations; that is, these complexes are not stable at elevated concentrations of these salts.

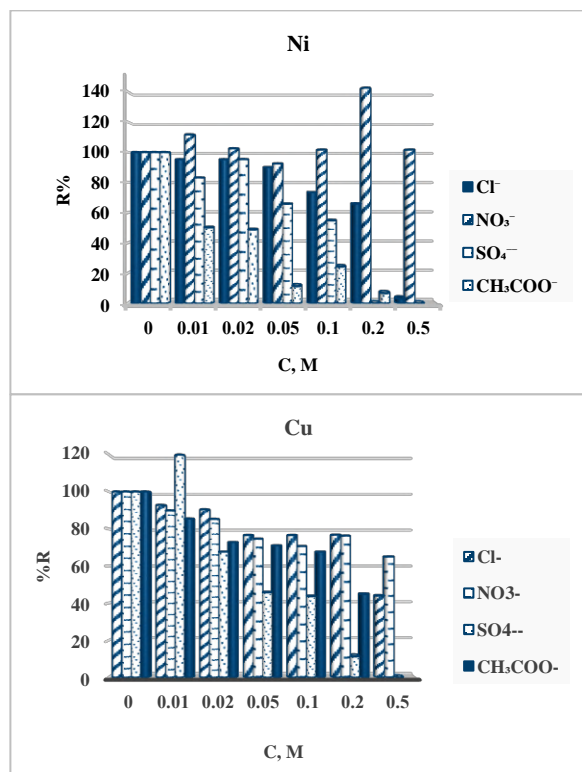


Figure (10). The effect of some interfering ions on complex stability

3.7 Determination of detection limits, quantification limits, and sensitivity

The ratio 3:7 was chosen for the evaluation of the spectrophotometric approach for the determination of Ni (II) and Cu (II) ions. The proposed spectroscopic method's sensitivity, detection limits, and quantification limits were all determined for this purpose. The sensitivity was calculated by plotting metal ion concentration in ppm versus absorbance (see Figure 11). The slope of the linear relationship is represented by the sensitivity. Table 4 shows the estimated linear range of concentrations at which Beer's law applies, as well as their correlation coefficient.

The detection limit (DL) and the quantification limit (QL) were estimated using the following equations (Elsherif et al., 2022):

$$DL = 3 \times SD \quad (1)$$

$$QL = 10 \times SD \quad (2)$$

Where: SD standard deviation of 10 Blanck's solution runs.

The obtained detection limits and quantification limits values are shown in Table 4.

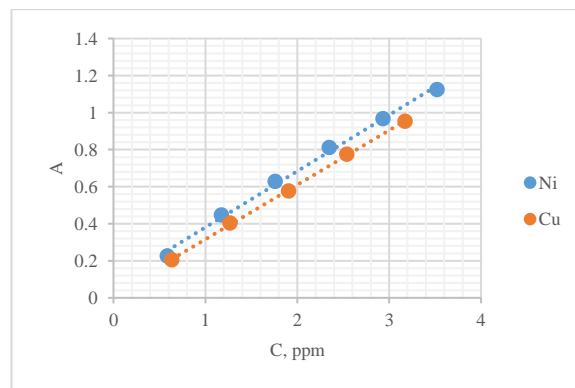


Figure (11). Sensitivity of the proposed method at 3:7 proportion

Table (4). Some calculated parameters for the proposed method

Metal ion	S (ppm ⁻¹)	DL (ppm)	QL (ppm)	Linear rang (ppm)	R ²
Ni	0.32	0.01	0.03	0.2-3.5	0.958
Cu	0.20	0.05	0.10	0.2-4.0	0.994

4 Conclusions

The coloring-developing reaction between murexide reagent and (Ni(II) and Cu(II)) was thoroughly explored in different proportions of water-isopropanol combination, as was the process for assaying Ni(II) and Cu(II) utilizing the complex coloring reaction in a 3:7 water-isopropanol mixture. When utilizing a UV-Vis. Spectrophotometer, maximum absorbance values were obtained at 458 nm and 470 nm for Ni-murexide and Cu-murexide complexes, respectively, and optimum circumstances at pH 3.1 & 3.8 and 0.2-3.5 & 0.2-4.0 ppm concentration for Ni and Cu, respectively. In comparison to other spectrophotometric approaches, this novel analytical method was comparatively simple, quick, and sensitive. In addition to the low detection limit of Ni and Cu, the analysis of a wide range of concentrations follows the Lambert- Beer's Law.

Acknowledgements

We would like to thank the Chemistry Department in Misurata University's at the Faculty of Science for providing the needed equipment to carry out this research.

Conflict of Interest: The authors declare that there are no conflicts of interest.

References

- Alabidi HM, Farhan AM, Al-Rufaie MM (2021) Spectrophotometric determination of Zn(II) in pharmaceutical formulation using a new azo reagent as derivative of 2-naphthol. *Curr. Appl. Sci. Technol.* 21:176-187.
- AL-adilee KJ, Hessoon HM (2019) Spectral properties and anticancer studies of novel heterocyclic azo dye ligand derived from 2-amino-5-methyl thiazole with some transition metal complexes. *J. Phys.: Conf. Series.* 1234. doi:10.1088/1742-6596/1234/1/012094
- Birghila S, Dobrinas S, Stanciu G, Soceanu A (2008) Determination of major and minor elements in milk through ICP-AES. *Environ. Eng. Manage. J.* 7:805–808.
- Cossee P (1964) Ziegler-Natta catalysis I. Mechanism of polymerization of α -olefins with Ziegler-Natta catalysts. *J. Catal.* 3:80-88.
- Elsherif KM, Hadidan Q, Alkariwi K (2022) Spectrophotometric determination of Zn(II) and Cu(II) in analytical sample using murexide reagent. *Prog. Chem. Biochem. Res.* 5:229-238
- Elsherif KM, Nabbra FM, Ewlad-Ahmed AM, Elkebbir NH (2020)a Spectrophotometric complex formation study of murexide with Nickel and Cobalt in aqueous solution. *To Chem. J.* 5:40-47.
- Elsherif KM, Zubi A, Najar A, Bazina E (2018) Complexation of 1,4-bis (3-(2-pyridyl) pyrazol-1-ylmethyl) benzene (1,4-PPB) with Cu (II), Co (II), and Ni (II): spectrophotometric studies in mixed solvent (EtOH-H₂O). *To Chem. J.* 1:214-223.
- Elsherif KM, Zubi A, Najar A, Bin Ghashir H (2021) Complexation of pyrazole based ligands with Ag (I): spectrophotometric studies in mixed solvent (EtOH-H₂O). *Arabian J. Chem. Environ. Res.* 8:236–246.
- Elsherif KM, Zubi A, Shawish HB, Abajja SA, Almelah EB (2020)b Spectrophotometric and conductometric study of formation constant and stoichiometry of Co(II)-salen type ligand complex. *Arabian J. Chem. Environ. Res.* 7:144–157.
- Elsherif KM, Zubi A, Shawish HB, Abajja SA, Almelah EB (2020)c formation of bis(salicylidene)ethylenediamine (salen type ligand) with copper(II) ions in different solvents: spectrophotometric and conductometric study. *Int. J. New Chem.* 7:1-13.
- Erkey C (2011) Supercritical fluids and organometallic compounds: from recovery of trace metals to synthesis of nanostructured materials. Elsevier.
- Esmaeili L, Perez MG, Jafari M, Paquin J, Ispas-Szabo P, Pop V, Andruh M, Byers J, Mateescu MA (2019) Copper complexes for biomedical applications: Structural insights, antioxidant activity and neuron compatibility. *J. Inorg. Biochem.* 192:87-97.
- Fat'hi MR, Shamsipur M (1993) Spectrophotometric study of zinc, cadmium, and lead complexes with murexide in binary ethanol-water mixture. *Spectrosc. Lett.* 26:1797-1804.
- Flett D, Melling J, Cox M (1983) Commercial solvent systems for inorganic processes. *Handbook of Solvent Extraction.*
- Huang G, Calvez G, Suffren Y, Daiguebonne C, Freslon S, Guillou O, Bernot K (2018) closing the circle of the lanthanide-murexide series: single-molecule magnet behavior and Near-Infrared emission of the Nd(III) derivative. *Magnetochemistry.* 4:44.
- Jeffery PG, Hutchison D (1981) Chemical methods of rock analysis. Elsevier. 3.
- Lum, CT, Wong AS-T, Lin MC, Che C-M, R. Sun W-Y (2013) A gold (III) porphyrin complex as an anti-cancer candidate to inhibit growth of cancer-stem cells. *Chem. Commun.* 49:4364- 4366.
- Masoud MS, Kassem TS, Shaker MA, Ali AE (2006) Studies on transition metal murexide complexes. *J. Therm. Anal. Calorim.* 3:549–555.
- Muneer ER, Al-Da'amy A, Kadhim SH (2020) Spectrophotometric determination of Cu(II) in analytical sample using a new chromogenic reagent (HPEDN) Indones. *J. Chem.* 20:1080– 1091.
- Nasir Uddin M, Abdus Salam M, Hossain MA (2013) Spectrophotometric measurement of Cu(DDTC)₂ for

- the simultaneous determination of zinc and copper. *Chemosphere*. 90:366–373.
- Ndagi U, Mhlongo N, Soliman ME (2017) Metal complexes in cancer therapy—an update from drug design perspective. *Drug Des., Dev. Ther.* 11:599-616.
- Ramaiah NA, Gupta SL (1956) Studies on the kinetics of the decomposition of murexide in acid solutions. *Proc. - Indian Acad. Sci., Sect. A.* 43:286-296.
- Shamsipur M, Alizadeh N (1992) Spectrophotometric study of cobalt, nickel, copper, zinc, cadmium and lead complexes with murexide in dimethylsulphoxide solution. *Talanta*. 39:1209-1212.
- Shamsipur M, Madaeni S, Kashanian S (1989) Spectrophotometric study of the alkali metal-murexide complexes in some non-aqueous solutions. *Talanta*. 36:773-776.
- Spessard G, Miessler G (1996) *Organometallic Chemistry*. PRENTICE-HALL.
- Viesca FS, Gómez R (2019) On the Mechanism of the murexide reaction. *World J. Org. Chem.* 1:14-18.
- Wahba O, Hassan AM, Naser A, Hanafi A (2017) Preparation and spectroscopic studies of some copper and nickel schiff base complexes and their applications as colouring pigments in protective paints industry. *Egypt. J. Chem.* 60:25-40.
- Warra A (2011) Transition metal complexes and their application in drugs and cosmetics-a Review. *J. Chem. Pharm. Res.* 3:951-958.
- Winkler R (1972) Kinetics and mechanism of alkali ion complex formation in solution. In *structure and bonding*. Springer. 1-24.



Assessment of Radioactivity in the Soil Samples from Al Bayda city, Libya, and its Radiological Implications

Salha D. Y. Alsaadi, Areej Hazawi and Ahmed S. A. Elmzainy

Physics Department, Science Faculty, Omar Al-Mukhtar University, Al Bayda, Libya.

DOI: <https://doi.org/10.37375/sjfsu.v3i1.1058>

A B S T R A C T

ARTICLE INFO:

Received: 25 February 2023

Accepted: 28 March 2023

Published: 17 April 2023

Keywords:

(NaI(Tl) detector, Radioactivity, radiological hazards, soil).

The radioactivity concentration of the terrestrial radionuclides (^{238}U , ^{232}Th , and ^{40}K) have been determined in soil samples collected from eight different locations around of Al Bayda city, Libya, using the sodium iodide (NaI) detector. Radioactivity concentrations for these elements were estimated and calculated at 0-10 cm depth, we found that an average values of 64.27 Bq/kg, 65.38 Bq/kg and 157.01 Bq/kg, respectively. As well as the radiological hazards were investigated at the same depth, it was found that the radium equivalent (R_{eq}) with an average value of 169.85 Bq/kg and the average values for external and internal hazard indices were 0.46 and 0.63, respectively. While, the average values for Gamma and Alpha indices were 0.32 and 0.60, respectively.

In addition, this study was conducted at a depth of 10-20 cm, and the average value of uranium was for ^{238}U , ^{232}Th and ^{40}K , were an average values of 63.76 Bq/kg, 57.89 Bq/kg, and 253.524 Bq/kg, respectively, and the radium equivalent (R_{eq}) with an average value of 166.06 Bq/kg, and the average values for external and internal hazard indices were 0.45 and 0.62, respectively. The values of Alpha and Gamma indices with average values of 0.32 and 0.59, respectively.

The average activity concentrations of the radionuclides were compared with Global average value where some values were higher than them. The radiological hazard indices of primitive radionuclides were also calculated and it was within the internationally permitted limits.

1 Introduction

Natural radioactivity in soil comes from the ^{238}U , ^{232}Th and natural ^{40}K series. The presence of this natural radioactivity in soil and building materials causes Internal and external exposure to the population. The accumulation of these natural radionuclides in the soil can lead to potential health risks [Agar *et al.*, 2014], [Amanjeet *et al.*, 2017], [Faheem *et al.*, 2008], [Rafique *et al.*, 2011].

Therefore, evaluation of the dose of gamma radiation from natural sources is of particular importance as natural radiation is the largest contributor to the external dose of the world's population. [Selçuk, 2019], [Ademola and Obed, 2010], [Tufail *et al.*, 2013]

Natural gamma dose rates vary depending on the concentration of the natural radionuclides, ^{238}U , ^{232}Th , their nascent products, and ^{40}K present in soil, sand,

and rock, which, In turn, it depends on local geological and geographical conditions. Several investigations of the natural radioactivity and the level of natural gamma radiation have been reported by in situ measurement or by analysis of the radionuclide concentration in soil samples [Elmzainy *et al.*, 2022], [Rangaswamy *et al.*, 2016], [Gamal *et al.*, 2013], [Jabbar *et al.*, 2010]

Thus, the evaluation of the natural dose rate behavior in this area is important to understand doses from natural radiation as well as establishing a baseline reference Assessment of normal radioactivity concentration In a group of sites across Al Bayda Measurements were made using a gamma ray spectrometer containing Sodium iodide reagent. Radium Equivalent and Exogenous Activities The radiation hazard index was evaluated and compared with National reports and guidelines proposed by United Nations Scientific

Committee on Antiquities Atomic radiation (UNSCEAR 2008).

2 Materials and Methods

2.1. Study area:

The city of Al Bayda is located in the north-east of Libya at the top of the Jabal Akhdar at the confluence of latitude 21°44' north with longitude 32°76' east and an area of 11429 km². It is bordered to the east by the city of Cyrene, to the west by the village of Massa, to the south by the village of Aslanta, and to the north by the Al-Wasita forests, which makes it in the middle of the Jabal Akhdar. The main rocky features of the area It consists of limestone and clay layer located in the study area.

2.2. Sample collection and sample preparation

Sixteen samples of eight sites were taken from a site around the city of Al Bayda, Libya. Coordinates of the collected samples are shown the figure 1. Each sample was collected by selecting a square area of 3 m² per site, and the top surface of any organic material or debris was cleaned. Three samples were taken from each square at a depth of 0-10 cm and 10-20 cm. Each of the three samples of the same site were well mixed together, We now have eight samples at a depth of 0-10 cm and eight other samples at a depth of 10-20 cm, then all the mixed samples were kept in plastic bags and sent to the laboratory for further treatment to proceed with the analysis. Directions and locations of samples as given in Table 1.

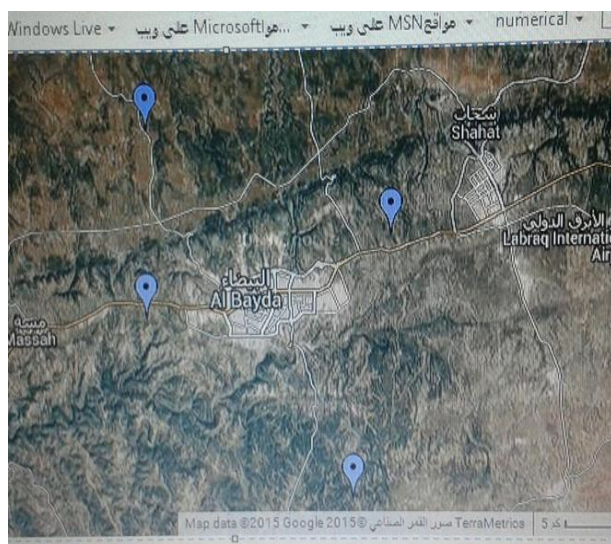


Figure 1. Map of the study area with sample collection points.

Table (1): Directions and locations of used samples:

Sample	Depth 0-10 cm and Depth 10-20 cm		
	Direction	Location((Latitude (N°))	Location ((Longitude (E°))
S1	South	32°49'31.2888	21°41'30.1272
S2	South	32°45'58.9213	21°43'28.2846
S3	North	32°49'15.7044	21°41'37.8276
S4	North	32°43'21.3132	21°48'11.1168
S5	West	32°45'35.9568	21°40'14.6496
S6	West	32°45'36.4320	21°40'14.9844
S7	East	32°48'21.9600	21°48'13.5072
S8	East	32°47'18.1824	21°49'3.6912

All soil samples were cleaned of stones and organic matter, then dried in an oven at a temperature 105 °C and after drying they were crushed and passed through a 2 mm sieve. Their weights were measured and then kept in plastic bags and carefully sealed to prevent Radon gas leakage from the sample. Then Stored for at least 4 weeks to allow time for ²³⁸U and ²³²Th to reach balance with their daughter radionuclides and then measured using the sodium iodide NaI (TI) detector.

2.3. Activity measurement

The activity concentrations of ⁴⁰K, ²³⁸U, and ²³²Th were measured in the prepared soil samples using gamma spectroscopy technology, which contains a sodium iodide NaI (TI) detector for radiation detection. The system was calibrated using two radioactive sources, cobalt ⁶⁰Co with two energies (1173KeV), (1332KeV) and cesium ¹³⁷C with energy (662KeV). Absolute efficiency was calculated. All measurements were carried out at the nuclear laboratory of Omar Al-Mukhtar University in Al-Bayda, Libya[13]. The measurement time was chosen two hour for all samples, were the activity concentrations all samples (Bq/Kg) were calculated by using the following formula [Alsaadi et al., 2018]:

$$A = \frac{A_R}{\varepsilon(E)tPW} \quad (1)$$

Where A is the activity level of a certain radionuclide expressed in Bq/kg dry weight, A_R is the net counting rate of the sample after subtracting background (counts/s), ε(E) is the counting efficiency of the detector at energy (E), t is the time for the measurement of the samples, P is the absolute transition probability of γ–

decay (Abundance (%)), and W is the dried sample weight expressed in kg.

2.4. Determination of radiation hazards

2.4.1 Radium equivalent dose (Ra_{eq}):

This is the common factor used to compare the radionuclides present in any material and this has been adopted in this present study for the purpose of comparing the measured radioactive concentration in the soil samples used. Radium equivalent activities were determined based on the estimation of 370 Bq/kg of Uranium-238, 259 Bq/kg of Thorium-232, and 4810 Bq/kg of potassium-40, respectively. Each of these radionuclides produces a gamma dose rate of Eq. (2) was used to estimate the radium equivalent activity of the samples [UNSCEAR, 2008], [Ali et al., 2021], [Antoaneta et al., 2010].

$$Ra_{eq} = A_U + 1.43A_{Th} + 0.077A_K \quad (2)$$

2.4.2. External hazard index (Hex).

The estimation of the external hazard assessment (Hex) associated with the gamma rays emitted from the soil sample was determined using equation (3) [Ali et al., 2021], [Beretka and Matthew, 1985].

$$H_{ex} = \frac{A_U}{370} + \frac{A_{Th}}{259} + \frac{A_K}{4810} \quad (3)$$

A_U, A_{Th} and A_K are the concentrations of activities in B/kg.

2.4.3. Internal hazard index (Hin):

Radon and its short-lived products are also dangerous for the respiratory organs. So the internal exposure to radon and its short-lived products is measured by the internal hazard index and expressed mathematically by equation (4). [Ali et al., 2021], [Beretka and Matthew, 1985]

$$H_{in} = \frac{A_U}{185} + \frac{A_{Th}}{259} + \frac{A_K}{4810} \quad (4)$$

Where Hin is the internal hazard index and A_U, A_{Th} and A_K are the activity concentration of ²³⁸U, ²³²Th and ⁴⁰K, respectively.

2.4.4. Gamma representative index (I_γ).

A representative gamma index is usually used to estimate the first risk associated with the occurrence of natural radionuclides in any particular material under study. The representation of the gamma index (I_γ) [Alsaadi et al., 2018], [Gbenuet et al., 2016] is estimated using Eq.(5).

$$I_{\gamma} = \frac{A_U}{300} + \frac{A_{Th}}{200} + \frac{A_K}{3000} \quad (5)$$

2.4.5. Alpha index representative (I_α).

The representative of the alpha index (I_α) is an important radiological hazard that has been developed in order to ensure the safety of the environment as a result of excessive exposure to radiation emitted from the ground that uses soil as a means of movement. Equation No. (6) was used to estimate. [Alsaadi et al., 2018], [Kriege, 1981]

$$I_{\alpha} = \frac{A_U}{200} \leq 1 \quad (6)$$

3 Results

The measured values of the activity concentrations of ²³⁸U, ²³²Th and ⁴⁰K radionuclides which obtained from soil samples at depths of 0-10 cm and 10-20 cm for eight different locations are presented in Table 2 and also in the Figure 2 and Figure 3.

Table (2): Activity concentration (Bq.kg⁻¹) for ²³⁸U, ²³²Th and ⁴⁰K at depth 0-10 cm and 10-20cm.

S.NO	Depth 0-10 cm			Depth 10-20 cm		
	²³⁸ U	²³² Th	⁴⁰ K	²³⁸ U	²³² Th	⁴⁰ K
S1	58.76	61.69	77.36	72.59	63.64	81.17
S2	52.76	82.69	263.82	39.36	97.37	78.46
S3	48.15	41.77	338.73	50.6	67.44	218.12
S4	53.07	64.00	55.73	68.67	31.39	553.01
S5	65.81	76.36	174.16	56.5	38.77	636.33
S6	64.57	77.34	93.57	73.28	37.36	130.78
S7	92.87	56.22	146.83	72.4	64.82	151.76
S8	78.14	62.96	105.85	76.65	62.30	178.56
Average	64.27	65.38	157.01	63.76	57.89	253.52

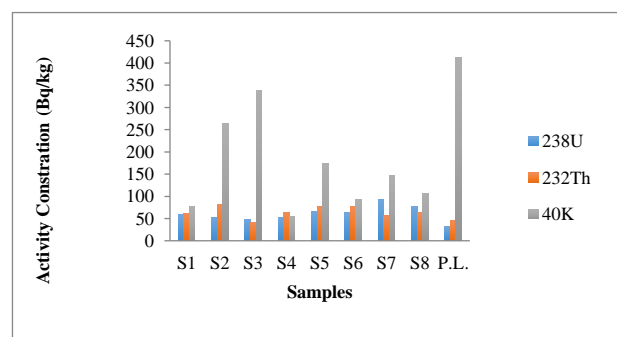


Figure 2: The activity of ²³⁸U, ²³²Th, ⁴⁰K, concentration for soil samples at Depth 0-10 cm.

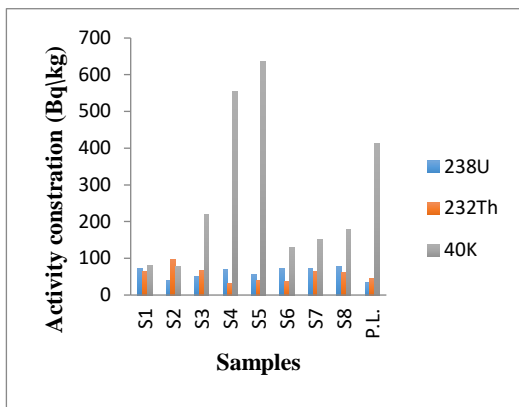


Figure 3: The activity of ²³⁸U, ²³²Th, ⁴⁰K, concentration for soil samples at Depth 10-20cm.

Radium Equivalent Activity (R_{aeq}) Due to Activity the concentration of the three natural radionuclides they are ²³⁸U, ²³²Th and ⁴⁰K from all eight locations difference shown in Table 3 and Figure 4.

Table (3): Radium equivalent dose (R_{aeq}) at depth 0-10 cm and 10-20cm.

S.NO	Depth 0-10 cm	Depth 10-20 cm
	R_{aeq}	R_{aeq}
S1	152.93	169.85
S2	191.32	184.64
S3	133.96	163.83
S4	148.88	156.14
S5	188.42	160.94
S6	182.37	136.77
S7	184.57	176.78
S8	176.32	179.49
Average	169.85	166.06

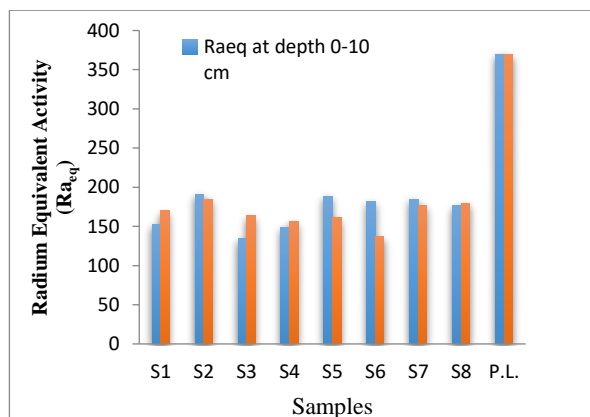


Figure 4: The Radium Equivalent Activity (R_{aeq}) for all samples.

The mean value of radiological hazard (Hex, Hin, I α and I γ). It is given in the following Table 4 and Figures 5 and 6 show the discrepancy in the values at the two depths from 0-10 cm and from 10-20 cm.

Table (4): The values of radiological hazard (Hex, Hin, I α and I γ) in the soil samples

Samples	Depth 0-10 cm				Depth 10-20 cm			
	Hex	Hin	I α	I γ	Hex	Hin	I α	I γ
S1	0.41	0.57	0.29	0.53	0.46	0.66	0.36	0.59
S2	0.52	0.66	0.26	0.68	0.5	0.61	0.2	0.64
S3	0.36	0.49	0.24	0.48	0.44	0.58	0.25	0.58
S4	0.4	0.55	0.27	0.52	0.42	0.61	0.34	0.57
S5	0.51	0.69	0.33	0.66	0.44	0.59	0.28	0.59
S6	0.49	0.67	0.32	0.63	0.37	0.57	0.37	0.48
S7	0.5	0.75	0.46	0.64	0.48	0.67	0.36	0.62
S8	0.48	0.69	0.39	0.61	0.49	0.69	0.38	0.63
Average	0.46	0.63	0.32	0.6	0.45	0.62	0.32	0.59

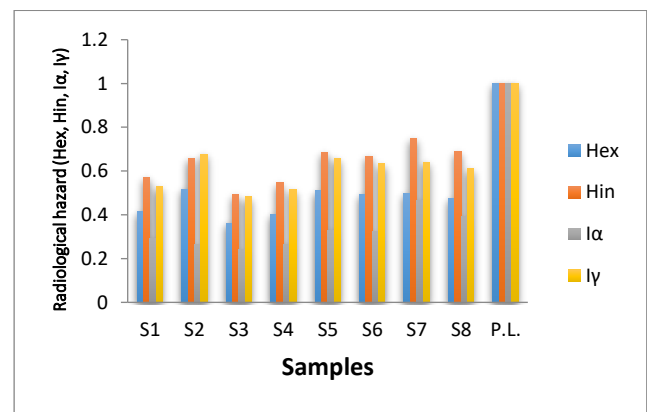


Figure 5: The Radiological Hazard at Depth 0-10 cm.

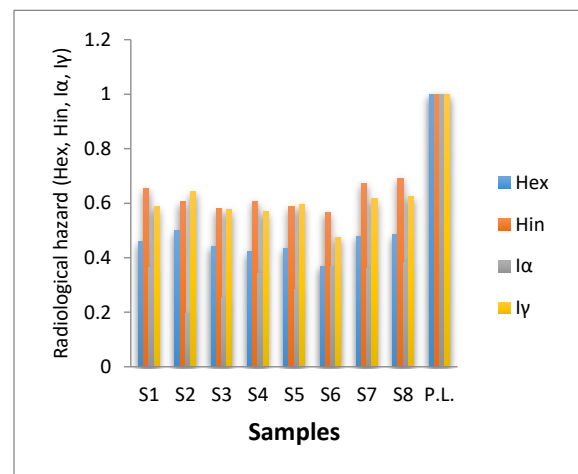


Figure 6: The Radiological Hazard at Depth 10-20 cm.

4 Discussion

Activity concentration ^{238}U , ^{232}Th and ^{40}K at depth 0-10 cm range from 48.15 to 92.87 Bq/kg, 41.77 to 82.69 Bq/kg, and 55.73 to 383.73 Bq/kg with an average value of 64.27, 65.38, and 157.01 Bq/kg, respectively. While the concentrations are at a depth of 10-20 cm range from 39.36 to 76.65 Bq/kg 31.39 to 97.37 Bq/kg, and 78.46 to 636.33 Bq/kg with an average value of 60.76, 57.89, and 253.52 Bq/kg, respectively.

Figure 2 illustrates the activity of uranium, thorium and potassium concentrations for soil samples that were studied at a depth of 0-10 cm. Where it was found that the highest value of uranium at sample No. 7 and the highest value of thorium at sample No. 2, while the highest value of potassium was at sample No. 3. While the lowest value for them was in samples No. 3, 3, and 4, respectively.

As for the depth of 10-20 cm, as shown in Figure 3, the highest value of uranium at sample No. 8 and the highest value of thorium at sample No. 2, while the highest value of potassium was at sample No. 5. While the lowest value for them was in samples No. 2, 4, and 2, respectively.

The Radium Equivalent Activity (R_{eq}) ranged from 133.96 to 191.32 Bq/kg at depth 0-10cm with average value 169.85 Bq/kg. While it is at a depth of 10-20 cm, a range from 136.77 to 184.64 Bq/kg at depth 10-20cm with average value 166.06 Bq/kg. As shown in Table 3. Figure 4 shows the radium equivalent, which was calculated from the concentrations of uranium, thorium and potassium obtained through equation No. 1, where it was found that its greatest value was at sample No. 2, while the lowest values were at sample No. 3 at a depth of 0-10 cm. As for the depth of 10-20 cm, the highest value was found in sample No. 2, while the lowest value was in sample No. 6.

From Table 4 it was found the external and internal hazard indices ranged from 0.36 - 0.52 and 0.49 - 0.75 respectively, and the average values for external and internal hazard indices were 0.46 and 0.63, respectively. While, the values of Alpha and Gamma indices ranged between 0.24 - 0.46 and 0.48 - 0.68, respectively, and the average values for Gamma and Alpha indices were 0.32 and 0.60, respectively.

As for 10-20 cm depth, the external and internal hazard indices ranged from 0.37 - 0.50 and 0.057 - 0.69, respectively, and the average values for external and internal hazard indices were 0.45 and 0.62, respectively.

The values of Alpha and Gamma indices ranged between 0.20 - 0.38 and 0.48 - 0.64, respectively, with average values of 0.32 and 0.59, respectively.

Figure 5 shows the radiological hazard (H_{ex} , H_{in} , I_{γ} and I_{α}). We note from the figure that the highest values were in sample No. 2 for (H_{ex} and I_{γ}), and sample No. 7 for (H_{in} and I_{α}). while the lowest value for them appears at sample No. 3, at a depth of 0-10 cm.

Figure 6 shows the radiological hazard (H_{ex} , H_{in} , I_{γ} and I_{α}). We note from the figure that the highest values were in sample No. 2 for (H_{ex} and I_{γ}), and sample No. 8 for (H_{in} and I_{α}). While the lowest value for them appears at sample No. 6 for (H_{ex} , H_{in} and I_{γ}) and sample No. 2 for I_{α} , at a depth of 10-20 cm.

5 Conclusions

The results showed that some values of the radioactivity levels of uranium, thorium and potassium in this study are relatively high compared to the internationally permitted limit. Due to the fact that the locations of the collected samples were not far from agricultural areas where chemical fertilizers are frequently used, this rise could be caused by fertilizers in the soil as well as transport factors such as wind and rain.

As for the radium equivalent (R_{eq}), and radiological hazard (H_{ex} , H_{in} , I_{α} and I_{γ}) at the sites studied in this study were within the internationally permissible limit.

References

- Ademola A. K., and Obed R. I. (2012). Gamma radioactivity levels and their corresponding external exposure of soil samples from Tantalite mining areas in Oke-Ogun, South-Western Nigeria. *Radioprotection*, 47, 243e252.
- Agar O., Boztosun I., Korkmaz M.E., and Ozmen S.F. (2014). Measurement of radioactivity levels and assessment of radioactivity hazards of soil samples in Karaman, Turkey. *Radiation Protection Dosimetry* 162 (4), 630–637.
- Ali J. M., Alsaadi S. D. Y. and Alkuwafi A. (2021). Assessment of Natural Radioactivity and Radiological Hazards in Ceramic Samples Imported for the Local Market in Benghazi-Libya. *Libyan Journal of Basic Sciences (LJBS)* Vol: 13, No: 1, P: 1-, 72-86. [https://ljbs.omu.edu.ly/eISSN 6261-2707](https://ljbs.omu.edu.ly/eISSN%206261-2707).
- Alsaadi S. D. Y., Younis A. M., Hazawi A. and Arhoma N. A. (2018). Characterization of ^{137}Cs in Soil from the Surrounding of Al Bayda City, Libya. *IOSR*

- Journal of Applied Physics (IOSR-JAP) e-ISSN: 2278-4861. Volume 10, Issue 5 Ver. II , 26-31. www.iosrjournals.org
- Amanjeet Kumar A., Kumar S., Singh J., Singh P., and Bajwa B. S. (2017) Assessment of natural radioactivity levels and associated dose rates in soil samples from historical city Panipat, India. *Journal of Radiation Research and Applied Sciences*, 10(3): 283–288.
- Antoaneta E., Alina B. and Georgescu L. (2010) Determination of heavy metals in soils using xrf technique". *Journal of Phys.*, Vol. 55, Nos. 7–8, pp. 815–820.
- Beretka J. and Matthew PJ. (1985) Natural radioactivity of Australian building materials, industrial wastes and by-products. *Health Phys*;48:87-95.
- Elmzainy A., Basil S. and Elbriki G., (2021) Evaluation of Natural Radioactivity and Radiological Hazards of Cement Available in Libyan Market, Libyan. *International Journal of Multidisciplinary Sciences and Advanced Technology Special Issue 1 (2021)*, 430–436.
- Elmzainy A., Basil S., Alsaadi S. D. Y., and Hazawi A., (2022). Measurement of natural radioactivity in the sediments of the beaches of the north east coast of Libya, Libyan. *Journal Science of Misurata*, 14, 38-46.
- European Commission, (EC). (1999). Report on Radiological Protection Principle concerning the natural radioactivity of building materials. Directorate-General Environment, Nuclear safety and civil protection. *Radiation Protection*, 112, 1e16.
- Faheem M, Mujahid SA, and Matiullah U. (2008) Assessment of radiological hazards due to the natural radioactivity in soil and building material samples collected from six districts of the Punjab province-Pakistan. *Radiation Measurements*, 43(8): 1443–1447.
- Gamal, H.E., Farid, A.M., Mageed, A.A., Hasabelnaby, M., and Hassanien, H.M., (2013). Assessment of natural radioactivity levels in soil samples from some areas in Assiut, Egypt. *Environ. Sci. Pollut. Res. Int.* 20, 8700–8708.
- Gbenu S.T., Oladejo O.F., Alayande O., Olukotun S.F., Fasasi M.K., and Balogun F.A. (2016). Assessment of radiological hazard of quarry products from southwest Nigeria, *Journal of Radiation Research and Applied Sciences* 9, 20 - 25, <http://www.elsevier.com/locate/jrras>.
- Jabbar A, Arshed W, Bhatti AS, Ahmad SS, Akhter P, Rehman SU, and Anjum MI (2010) Measurement of soil radioactivity levels and radiation hazard assessment in southern Rechna interfluvial region, Pakistan. *Environmental Monitoring and Assessment*, 169 (1–4): 429–438.
- Kriege V. R (1981). Radioactivity of construction materials. *BetonwerkFertigteil Technology*, 47: 468 - 473.
- Rafique M, Rehman H, Matiullah MF, Rajput MU, Rahman SU, and Rathore MH (2011) Assessment of radiological hazards due to soil and building materials used in Mirpur Azad Kashmir; Pakistan. *Iran J Radiat Res*, 9(2): 77–87.
- Rangaswamy DR, Srilatha MC, Ningappa C, Srinivasa E, and Sannappa J, (2016) Measurement of natural radioactivity and radiation hazards assessment in rock samples of Ramanagara and Tumkur districts, Karnataka, India. *Environmental Earth Sciences*, 75 (5): 1-11.
- Selçuk Zorer Ö (2019) Evaluations of environmental hazard parameters of natural and some artificial radionuclides in river water and sediments. *Microchemical Journal*, 145:762-766.
- Tufail M, Asghar M, Akram M, Javied S, Khan K, and Mujahid SA. (2013) Measurement of natural radioactivity in soil from Peshawar basin of Pakistan. *Journal of Radioanalytical and Nuclear Chemistry*, 298(2): 1085–1096.
- UNSCEAR (United Nations Scientific Committee on the Effects of Atomic Radiation) Sources. *Effects of Ionizing Radiation*. New York: United Nations; 2008.



Investigation of Medicinal Activity of Four Imported Trees to Libya Against Some Pathogens

Amani A. Abdurraziq¹, Sami M. Salih² and Ahmed A. Abdurraziq^{2*}

¹Public Health Department, High Institute of Medical Professions, El-Maraj, Libya.

²Biology Department, Education Faculty, Omar Al-Mukhtar University, Al-Bayda, Libya.

DOI: <https://doi.org/10.37375/sjfsu.v3i1.972>

A B S T R A C T

ARTICLEINFO:

Received: 10 February 2023

Accepted: 13 March 2023

Published: 17 April 2023

Keywords:

Imported trees, medicinal activity, human pathogenic bacteria, Plant-pathogenic fungi.

Many imported trees have been included in Libyan Flora data Base, but not all of its Bio-activity was studied, especially medical in a new environment. Therefore, this work was carried out to Investigate the medicinal activity of four imported trees (*Acaciasaligna*, *Acacia nilotica*, *Brachychiton populneus* and *Leucaena leucocephala*), and evaluate the activity of the aqueous extracts of leaves at a concentration 200mg/ml against four various types of human pathogenic bacteria (*Escherichia coli*, *Pseudomonas aeruginosa*, *Staphylococcus aureus* and *Proteus vulgaris*), and Plant-pathogenic fungi (*Aspergillus niger*, *Botrytis cinerea*, *Rhizopus microsporus* and *Fusarium solani*). The antibacterial activity was determined by disk diffusion, and the antifungal activity by poisoned food technique. The results showed the inefficiency of all imported trees leaves extracts against all bacteria types, while, was have good activity against most plant-pathogenic fungi tested, Commonly, *R.microsporus* was the most affected fungus for all the extracts tested, also, the results showed that *L.leuceana* extract is more effective as an antifungal than other extracts. Data in this study indicated the potential of using Imported trees as an environmentally friendly Fungicide.

1 Introduction

Most Arab countries import many ornamental trees, without attention to negative and positive effects (Salih and Abdurraziq, 2021). Efforts have been made to introduce many of these plants into Libyan flora both deliberately or accidentally, the introduced plants are represented by a total of 361species, 253 genera and 89families, Some are classified as toxic to humans and animals, while others are in fierce competition with native plants, as well as, twenty-nine species were classified as invasive, where these species are becoming established and part of Libyan flora (Alzerbi *et al.*, 2020; Mahklouf and Shakman, 2021). Although Several research centers have undertaken studies on the role of native medicinal plants in different fields, little information has been found about medicinal plants. Thus, Should be placed thorough inventory of all potential new medicinal plants in Libya (Agiel and Mericli, 2017; Louhaichi *et al.*, 2011). Importantly, if

new plant species are included in the import pharmacopeia without replacing native plants, this occupies a hitherto important unconsidered pharmacopoeial niche (Medeiros *et al.*, 2012). Fabaceae are one of the biggest families in Libya, represented by 37 medicinal species, 33 species of poisonous, and 9 species ornamental 9 species (Ali *et al.*, 2019).

Acacia saligna, *Acacia nilotica*, *Brachychiton populneus* and *Leucaena leucocephala* are among the introduced plants of this family, this species was introduced for a variety of purposes, including food, fodder, erosion control, and afforestation (Alzerbi *et al.*, 2020). Apart from that, This family contains chemical constituents of high medicinal value and ethnopharmacologically important, which act in the treatment and/or healing of various body systems (Macedo *et al.*, 2018), making an alternative to antibiotics in the treatment of many diseases pathogens

(Thabet *et al.*, 2017; El-Toumy *et al.*, 2010; Dzoyem *et al.*, 2014). Therefore, This study's objective of verifying the medicinal activity of four trees imported to Libya against some species of bacterial and fungal pathogens, in vitro.

2 Materials and Methods

The study was carried out in the Biology Department/Faculty of education / Omar Al-Mukhtar University. Dried leaves of four imported trees were grinded (*Acacia saligna*, *Acacia nilotica*, *Brachychiton populneus*, *Leucaena leucocephala*) by an electric grinder and saved for use.

2.1 Aqueous Extraction:

200 g of leaves dry powder was added to 1000 ml of sterile distilled water in a glass flask, for each type separately, separately. Hence, Put on a vibratory shaker for 24 hours at 35 ° C, then filter and shake in a centrifuge at 3000 rpm for 10 minutes. The next step was filtering with Whitman No.1 filter paper Filtration was carried out with filter paper on a Buckner funnel by using a vacuum pump. and dried in a Rotary evaporator to get dry powder at a weight of 2.8g (Jigna *et al.*, 2005). The concentration of 200 mg/ml was prepared by dissolving 2g of powder in 10 ml of distilled water.

2.2 Test organisms:

Escherichia coli, *Pseudomonas aeruginosa* and *Staphylococcus aureus*: Isolates predefined were obtained from patients reluctant to (Tiba, Alrazi and Altrahum Clinic) laboratories, Al-Bayda / Libya.

Proteus vulgaris: were provided by the bacterial collection, Department of Plant, Omar Al-Mukhtar University.

Fungal isolates (*Aspergillus niger*, *Botrytis cinerea*, *Rhizopus microsporus* and *Fusarium solani*) were provided by the fungal collection, Department of Plant Protection, Omar Al-Mukhtar University.

2.3 Antibacterial activity test:

The mediums were sterilized for 15 minutes in an autoclave at 121°C, bacteria were grown on Mueller-Hinton agar medium. For screening. Sterile filter paper disks (6 mm) impregnated with the extracts were placed on a surface of inoculated bacteria mediums, and used disks impregnated with water as control. The dishes were incubated for 18-24 hours at 37°C with three replications per dish, then a measure of diameters of inhibitory zones minus the diameter of the disc (Driscoll *et al.*, 2012).

2.4 Antifungal activity test:

The effect of plant extracts on pathogen growth was determined using poisoned food technique. A volume of 5 ml from each of leaves extracts with a concentration of 200 mg/ml was dispensed separately into 8.5 cm diameter Petri dishes and agitated gently with 45 ml of sterile media PDA. The medium was allowed to be solid and inoculated centrally with 5mm diameter of mycelia plugs of the tested fungi obtained from 7 days old cultures, using a sterile cork borer. Tested fungi were growing on PDA plates inoculated with sterile water that served as control. All cultures were incubated at 28°C and fungal colony diameters were measured daily for 7 days (Singh and Tripathi, 1999). Each experiment was replicated three times. Percentage inhibition as follows:

$$\text{Percentage inhibition} = \frac{N1 - N2}{N1} \times 100$$

Where, N1 = Radial diameter of fungus in control plates (PDA + Water);

N2 = Radial diameter of fungus in the presence of extracts (PDA + extracts).

3 Statistical Analysis:

The study experiences were designed according to the complete random design (CRD). Statistical analysis was performed using Minitab 17 program and ANOVA variance analysis tables. The averages were compared using Tukey's test at P < 0.05 (Abdulrazziq *et al.*, 2023).

4 Results

4.1. Effect of imported trees extract against bacteria.

The leaves extracts of four trees imported (*A.saligna*, *A.nilotica*, *B.populneus*, *L.leucocephala*) were tested against different human pathogenic bacteria (Table 1). The results showed no inhibition activity of all the tested tree leaves extracts against *E.coli* and *Ps.aeruginosa*. While *P.vulgaris* recorded weakened sensitivity to extracts *A.nilotica* and *B.populneus* at a diameter (0.7 and 1.0mm), respectively. On the other hand, the most sensitive type to extracts was *S.aureus*, although their sensitivity was weak with diameters ranging from (0.5-1.5mm).

Table (1): Effect of imported trees extract against human pathogens bacteria.

Bacteria \ Extract	<i>E.coli</i>	<i>S.aureus</i>	<i>Ps.aeruginosa</i>	<i>P.vulgaris</i>
<i>Acacia saligna</i>	-	1.2±0.2 ab	-	-
<i>Acacia noltica</i>	-	0.5±0.0 c	-	0.7±0.1 b
<i>Brachychiton populneus</i>	-	1.0±0.1 b	-	1.0±0.1 a
<i>leauceanaleucocephala</i>	-	1.5±0.0 a	-	-

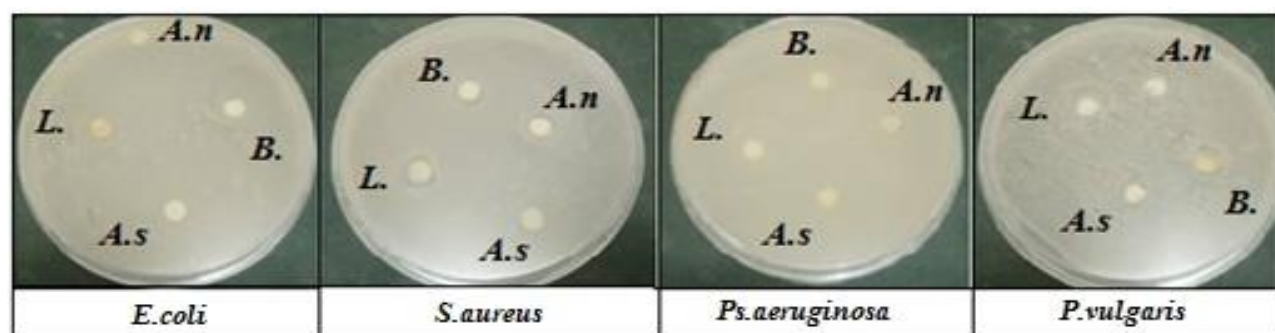


Figure (1): Effect of imported trees extract against types bacteria.

*A.n: *A.noltica*; A.s: *A.saligna*; B.: *B.populneus*; L.: *L.leucocephala*.

4.2. Effect of imported trees extract against fungi.

The leaves extracts of four trees imported (*Acacia saligna*, *Acacia nilotica*, *Brachychiton populneus*, *Leucaena leucocephala*) were tested against different plant pathogenic fungi. The results showed differential effects depending on the extract type and tested fungal species (Table 2). *A.saligna* extract showed no

inhibitory effect on the tested fungi except for *F.solani* (22%). While, *A.nilotica* extract showed inhibition rates (10 and 8%) against *A.niger* and *R.microsporus*, respectively. *B.populneus* extract showed inhibition rates (20, 12 and 16%) against *B.cinerea*, *R.microsporus*, and *F.solani*, respectively. moreover, *L.leucocephala* extract was the best effective against all tested fungi with inhibition rates (60, 55, 68 and 23%) against *A.niger*, *B.cinerea*, *R.microsporus* and *F.solani*, respectively.

Table (1): Effect of imported trees extract against plant pathogens fungi.

Fungi \ Extract	<i>Aspergillus niger</i>	<i>Botrytis cinerea</i>	<i>Rhizopus microsporus</i>	<i>Fusarium solani</i>
<i>Acacia saligna</i>	-	-	22.0±0.0 b	-
<i>Acacia noltica</i>	10.0±0.0 b	-	8.0±0.0 c	-
<i>Brachychiton populneus</i>	-	20.0±0.0 b	12.0±0.0 c	16.0±0.0 b
<i>leauceanaleucocephala</i>	60.0±0.0 a	55.0±0.0 a	68.0±0.0 a	23.0±0.0 a

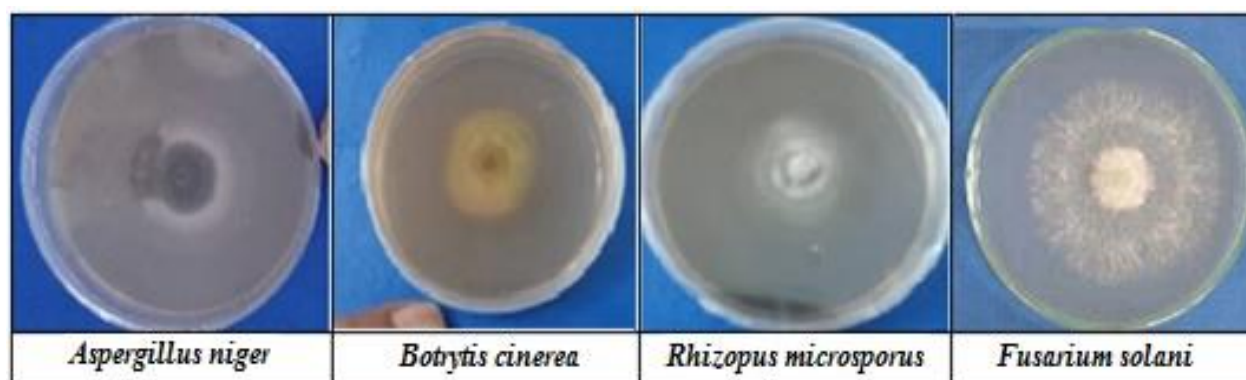


Figure (2): Effect of *Leucaena leucocephala* extract against plant pathogens fungi

5 Discussion

The new species may have the possibility of bioactive compounds, which requires many studies about its bioactivities (Guarim Neto and Morais, 2003). Thus, this study was conducted to commonly show that imported tree extracts possess did not have inhibitory activity against types of bacteria tested. This is evident from the high resistance for *E.coli* and *Ps.aeruginosa* and the weakness of the inhibition diameters, which ranged between (0.5-1.5) for *S.aureus* and *P.vulgaris*. disagree this result with (Vijayasanthi *et al.*, 2012; Al-Ramamneh *et al.*, 2022; Suparno *et al.*, 2018), who confirmed that this trees extracts are highly effective in control various types of bacteria. The sensitivity of *S. aureus* to *L.leucocephala* extract was the highest recorded result against bacterial species at an inhibition diameter (1.5mm), agrees this result with (Saptawati *et al.*, 2019), which recommended can be used as an ointment topical anti-*Staphylococcus*. In addition, the results indicate that extracts from these trees have good activity against phytopathogenic fungi, other studies reported good antifungal activity by applying some trees extracts (Banso, 2009; Salem *et al.*, 2014). *R.microsporus* was the most affected fungus for all the extracts tested. Finally, leaves extract from *L.leucocephala* showed strong fungicidal activity towards all fungal isolates, especially against *R.microsporus*, *A.niger* and *B.cinerea*, because has several bioactive compounds, which can act as a promising antimicrobial, this result agrees with (Elbanoby *et al.*, 2022).

In conclusion: it is easy to import many plants from their original habitat and cultivate them in the local environment for use in different agricultural fields, but the possibility of their exploitation in the medical field may be affected by new environmental factors, and thus become less efficient than it was.

6 Conclusions

This study concluded that the extracts of imported trees (*Acacia saligna*, *Acacia nilotica*, *Brachycton populneus*, and *Leucaena leucocephala*) had no antibacterial efficiency, on the other hand, they showed good medicinal activity against various types of phytopathogenic fungi. The best inhibition activity of *L.leucocephala* extracts against tested fungi, while, *R.microsporus* was the most affected fungus for all the extracts tested. Findings of this study indicated that the use of imported trees could be a valid alternative for bio-control of plant pathogenic fungi.

Acknowledgements

We extend our sincere thanks and appreciation to Tiba, Alrazi and Altrahum Clinic) laboratories, Al-Bayda / Libya and Plant Protection Department, Faculty of Agriculture, Omar Al-Mukhtar University

Conflict of Interest: The authors declare that there are no conflicts of interest.

References

- Abdulrazziq, A. A., Salih, S. M., & Ibrahim, N. (2023). Biological Effect of Oxalis per-carpes Extracts against Methicillin-Resistant Staphylococcus aureus (MRSA). *Pharmaceutical and Biosciences Journal*, 01-06.
- Agiel, N., & Mericli, F. (2017). A survey on the aromatic plants of Libya. *Indian J. Pharm. Educ. Res*, 51, 304-308.
- Ali, R. F., Dakeel, E. H., & Al-Wishish, F. M. (2019). Analysis and diversity of family Fabaceae in Flora of Libya. *Libyan Journal of Science & Technology*. 10(1):13-19.

- Al-Ramamneh, E. A. D. M., Ghrair, A. M., Shakya, A. K., Alsharafa, K. Y., Al-Ismail, K., Al-Qaraleh, S. Y., ... & Naik, R. R. (2022). Efficacy of *Sterculia diversifolia* leaf extracts: volatile compounds, antioxidant and anti-inflammatory activity, and green synthesis of potential antibacterial silver nanoparticles. *Plants*, 11(19), 2492.
- Alzerbi, A. K., Alaib, M., and Omar, N. O. (2020). Introduced species in Flora of Libya. *Libyan Journal of Science & Technology*. 11(2):65-72.
- Banso, A. (2009). Phytochemical and antibacterial investigation of bark extracts of *Acacia nilotica*. *J. Med. Plants Res*, 3(2), 082-085.
- Driscoll, A. J., Bhat, N., Karron, R. A., O'Brien, K. L., and Murdoch, D. R. (2012). Disk diffusion bioassays for the detection of antibiotic activity in body fluids: applications for the pneumonia etiology research for child health project. *Clinical Infectious Diseases* 54, S159
- Dzoyem, J. P., McGaw, L. J., & Eloff, J. N. (2014). In vitro antibacterial, antioxidant and cytotoxic activity of acetone leaf extracts of nine under-investigated Fabaceae tree species leads to potentially useful extracts in animal health and productivity. *BMC Complementary and Alternative Medicine*, 14, 1-7.
- Elbanoby, N. E., El-Settawy, A. A., Mohamed, A. A., & Salem, M. Z. (2022). Phytochemicals derived from *Leucaena leucocephala* (Lam.) de Wit (Fabaceae) biomass and their antimicrobial and antioxidant activities: HPLC analysis of extracts. *Biomass Conversion and Biorefinery*, 1-17.
- Jerab, J., Jansen, W., Blackwell, J., van Hout, J., Palzer, A., Lister, S., ... & De Briyne, N. (2022). Real-world data on antibiotic group treatment in European livestock: drivers, conditions, and alternatives. *Antibiotics*, 11(8), 1046.
- Jigna, P., Rathish, N., and Sumitra, C. (2005). Preliminary screening of some folklore medicinal plants from western India for potential antimicrobial activity. *Indian J. Pharmacol.* 37, 408.
- Louhaichi, M., Salkini, A. K., Estita, H. E., & Belkhir, S. (2011). Initial assessment of medicinal plants across the Libyan Mediterranean coast. *Advances in Environmental Biology*, 5(2), 359-370.
- Macêdo, M. J. F., Ribeiro, D. A., Santos, M. D. O., Macêdo, D. G. D., Macedo, J. G. F., Almeida, B. V. D., ... & Souza, M. M. D. A. (2018). Fabaceae medicinal flora with therapeutic potential in Savanna areas in the Chapada do Araripe, Northeastern Brazil. *Revista Brasileira de Farmacognosia*, 28, 738-750.
- Mahklouf, M. H., & Shakman, E. A. (2021). Invasive alien species in Libya. *Invasive Alien Species: Observations and Issues from Around the World*, 1, 173-195.
- Medeiros, P. M. D., Soldati, G. T., Alencar, N. L., Vandebroek, I., Pieroni, A., Hanazaki, N., & de Albuquerque, U. P. (2012). The use of medicinal plants by migrant people: adaptation, maintenance, and replacement. *Evidence-Based Complementary and Alternative Medicine*, 2012.
- Medeiros, P. M. D., Soldati, G. T., Alencar, N. L., Vandebroek, I., Pieroni, A., Hanazaki, N., & de Albuquerque, U. P. (2012). The use of medicinal plants by migrant people: adaptation, maintenance, and replacement. *Evidence-Based Complementary and Alternative Medicine*, 2012:11 pages.
- Neto, G. G., & De Moraes, R. G. (2003). Plantas medicinais com potencial ornamental: um estudo no cerrado de Mato Grosso. *Ornamental Horticulture*, 9(1): 89-97.
- Salem, M. Z. M., Ali, H. M., & Mansour, M. M. (2014). Fatty acid methyl esters from air-dried wood, bark, and leaves of *Brachychiton diversifolius* R. Br: Antibacterial, antifungal, and antioxidant activities. *BioResources*, 9(3), 3835-3845.
- Salih, S. M., and Abdulrazziq, A. A., (2021). Phytotoxicity test of *Acacia saligna* trees on germination seeds of some leguminous crops. *Bayan Journal*, Issue (9): 391-400.
- Saptawati, T., Dahliyanti, N., & Risalati, R. (2019). Antibacterial activity of *Leucaena leucocephala* leaf extract ointment against *Staphylococcus aureus* and *Staphylococcus epidermidis*. *Pharmaciana*, 9(1), 175-182.
- Singh, J., & Tripathi, N. N. (1999). Inhibition of storage fungi of blackgram (*Vigna mungo* L.) by some essential oils. *Flavour and Fragrance Journal*, 14(1), 1-4.
- Suparno, O., Panandita, T., Afifah, A., & Purnawati, R. (2018, March). Antibacterial activities of leave extracts as bactericides for soaking of skin or hide. In *IOP Conference Series: Earth and Environmental Science* (Vol. 141, No. 1, p. 012028). IOP Publishing.
- Thabet, A. A. Youssef, F. S. Korinek, M. Chang, F. Wu, Y. Chen, B. El-Shazly, M. Singab, A. B. and Hwang, T. (2018). Study of the anti-allergic and anti-inflammatory activity of *Brachychiton rupestris* and *Brachychiton discolor* leaves (Malvaceae) using in vitro models. *Complementary and Alternative Medicine*, 18:299.
- Vijayasanthi, M., Kannan, V., Venkataswamy, R., & Doss, A. (2012). Evaluation of the Antibacterial Potential of various solvent extracts of *Acacia nilotica* linn. *Leaves. Hygeia JD Med*, 4(1), 91-96.



Ground Water Quality Evaluation for Drinking Purposes in Sabratha City, Libya

Wafa A. Aldeeb^{1*} and Bashir M. Aldabusi²

¹Libyan Center for Studies and Research in Environmental Science and Technology, Libya.

²Chemical Engineering Department, Engineering Faculty, Sabratha University, Libya.

DOI: <https://doi.org/10.37375/sjfsu.v3i1.102>

A B S T R A C T

ARTICLE INFO:

Received: 27 November 2022

Accepted: 16 January 2023

Published: 17 April 2023

Keywords:

Canadian Council of Ministers of the Environment; Water Quality Index, Weighted Arithmetic Water Quality Index, Drinking purposes, Poor, Unsuitable.

The Water Quality Index reduces the large number of indicators used in the assessment to a simpler mathematical expression allowing easy interpretation of the monitoring data. The Canadian Council of Ministers of the Environment WQI (CCMEWQI) and the Weighted Arithmetic WQI (WAWQI) were used to assess the groundwater quality for drinking purposes in Sabratha City. Ten samples were collected from different sites of the study area. Eleven significant parameters were considered for calculating the WQI which are pH, total dissolved solids (TDS), calcium (Ca^{++}), magnesium (Mg^{++}), sodium (Na^+), potassium (K^+), Chloride (Cl^-), bicarbonate (HCO_3^-), Sulfate (SO_4^-), nitrate (NO_3^-) and Total Hardness (HD). The drinking water quality analysis by CCMEWQI and WAWQI shows that more than 60% of the samples described the groundwater quality in the study area as poor and unsuitable and cannot be used for drinking propose, only 20% of the samples was classified as suitable for direct consumption.

1 Introduction

Declining water quality has become a issue of concern due to unprecedented increase in population and rapid rate of urbanization as well as the intensification and expansion in agricultural practices. This has led to progressive and continual degradation of resources especially ground water (Adelagun *et al.*, 2021). The Water quality is characterized on the basis of water parameters (physical, chemical, and microbiological), the human health is at risk if those values exceed acceptable limits (WHO, 2012; Libyan standard, 1992). Water quality index (WQI) is considered as the most effective technique to assess the quality of water through a single value. Several parameters are included in a mathematical equation, that expresses the overall water quality (Uddin *et al.*, 2018; Uddin *et al.*, 2021; Gaytán-Alarcón *et al.*, 2022). Commonly, water quality index (WQI) is based on the following four steps: - selection of the parameters, - determination of the

quality function for each parameter, - calculation of the parameter weighting values and - aggregation through mathematical equation (Sutadian *et al.*, 2018; Abbasi and Abbasi, 2012).

The present study measures drinking water quality with the application of weighted arithmetic WQI and Canadian Council of Ministers of the Environment WQI methods based on some chemical and physical parameters.

2 Materials and Methods

The study area is in the north western part of Libya in Sabratha city, and is located between latitudes $32^{\circ}43'20.30''\text{N}$ to $32^{\circ}48'24.84''\text{N}$ North and Longitude $12^{\circ}19'27.00''\text{E}$ to $12^{\circ}31'26.83''\text{E}$, Table (1). The collected ten (10) boreholes of groundwater samples were selected randomly from both private and public water sources.

Table (1): Location of the study area.

Well	Latitudes	Longitude	Well	Latitudes	Longitude
1	32°47'59.41"N	12°26'50.93"E	6	32°47'13.11"N	12°28'36.04"E
2	32°44'15.63"N	12°25'52.43"E	7	32°48'24.84"N	12°25'12.51"E
3	32°43'20.30"N	12°19'27.00"E	8	32°46'24.64"N	12°31'26.83"E
4	32°43'21.50"N	12°19'27.77"E	9	32°48'7.31"N	12°23'51.76"E
5	32°44'4.81"N	12°29'15.85"E	10	32°45'1.62"N	12°28'21.05"E

At each borehole location, the sample bottles were washed and rinsed thoroughly with the sample water before being sampled. The boreholes were allowed to flow for about 5 minutes to ensure stable conditions before samples were collected. The water samples were analyzed for different drinking and agricultural parameters which include pH, electrical conductivity (EC), total dissolved solids (TDS), concentration of cations such as calcium, magnesium, sodium and potassium and concentration of anions such as Chloride, bicarbonate, Sulfate and nitrate. The concentration of Sodium and Potassium were measured using Flame photometer. The total hardness calcium and magnesium were determined by EDTA titrimetric method. The concentration of Chloride was determined

with silver nitrate titration. The concentrations of Carbonate and bicarbonate were determined by sulfuric acid. Whereas, the concentrations of sulfate and nitrate were determined using spectro-photometer. The Salinity refers to the amount of total dissolved solids (TDS) in the water and is frequently measured by electrical conductivity (EC). Waters with higher TDS concentrations will be relatively conductive. The general formula adopted to calculate the TDS (Kelly, 1946) is

$$TDS \left(\frac{mg}{L} \right) = 0.64 \cdot EC \left[\frac{\mu S}{cm} \right] \dots \dots \dots (1)$$

The statistical parameters and the major ion-concentrations (mg/L) in capering with the Libyan standard (1992), are tabulated in Table (2).

Table 2: Groundwater chemical analyses (mg/L).

Well	pH	TDS	Ca ²⁺	Na ⁺	Mg ²⁺	K ⁺	HCO ₃ ⁻	SO ₄ ²⁻	NO ₃ ⁻	Cl ⁻	HD
limit	7.5	1000	200	200	150	40	200	250	45	250	500
1	6.91	5094	737	862	149	46	129	731	13.3	2480	2453
2	6.86	8928	1291	1511	516	80	227	1599	23.2	4345	5343
3	7.52	1416	187	259	38	11.6	103	186	3.4	629	623
4	6.82	4563	422	796	286	23.8	173	843	7.4	2122	2228
5	6.83	8243	762	1438	261	45.2	131	1599	13.4	3833	2975
6	7.15	1766	163	308	110.6	7.9	128	281	2.9	822	861
7	7.3	6637	613	1158	415.7	36	106	1275	10.8	3086	3237
8	7.2	1670	154.5	291.5	104.6	7.3	126.6	259	2.7	777	815
9	7.2	1577	236	173	71.4	8	204	560	28.2	297	882
10	7.3	835	118	118.5	23.8	7.1	132	113	58.8	264	392

• **Water Quality Index Methods**

The water quality index reduces the bulk number of parameters used in an assessment and provides a single value of multiple water quality parameters into a mathematical equation that rates the health of water quality with number (Brown *et al.*, 1970). Most of the models employed eight to eleven water quality parameters. In this study, eleven important parameters were chosen to measures drinking water quality with the application of Canadian Council of Ministers of the Environment WQI (CCMEWQI) and Weighted Arithmetic WQI (WAWQI).

• **Canadian Council of Ministers of the Environmental WQI**

This method was formulated by the CCME (CCME, 1999; Khan, 2003). The calculation of CCME WQI can be obtained by using the following relation:

$$WQI_{CCME} = 100 - \left[\frac{\sqrt{F_1^2 + F_2^2 + F_3^2}}{1.732} \right] \dots \dots \dots (2)$$

F1: termed the ‘scope’, this is the percentage of the total parameters that do not meet with the specified objectives. It is expressed as:

$$F_1 = \left[\frac{\text{Number of failed variables (NFV)}}{\text{Total number of variables (TNV)}} \right] \times 100 \dots (3)$$

F2 represents the percentage of individual tests that do not meet standard.

$$F_2 = \left[\frac{\text{Number of failed tests (NFT)}}{\text{Total number of tests (TNT)}} \right] \times 100 \dots (4)$$

$$F_3 = \frac{nse}{0.01 \cdot nse + 0,01} \dots \dots \dots (5)$$

The number of times by which an individual concentration is greater or less than the objective is termed an “excursion” and is expressed as follows:

$$nse = \frac{\sum_1^n excursion_i}{\text{Total number of tests}} \dots \dots \dots (6)$$

When the test value must not exceed the objective

$$excursion_i = \frac{\text{Failed test value}_i}{\text{Objective}_i} - 1 \dots \dots \dots (7a)$$

For the other case when the test value must not fall below the objective

$$excursion_i = \frac{\text{Objective}_i}{\text{Failed test value}_i} - 1 \dots \dots (7b)$$

• **Weighted Arithmetic Water Quality Index**

Weighted arithmetic water quality index (WAWQI) method classified the water quality according to the degree of purity by using the most commonly measured water quality variables (Yisa and Jimoh, 2010; Tyagi *et al.*, 2014; Aldeeb and Algeidi, 2021). The method has been widely used by many scientists and the calculation of WQI was obtained by using the following equation:

$$WQI = \frac{\sum Q_n \cdot W_n}{\sum W_n} \dots \dots \dots (8)$$

The quality rating scale Q_n for each parameter is calculated by using this expression:

$$Q_n = \left[\frac{V_n - V_0}{S_n - V_0} \right] \cdot 100 \dots \dots \dots (9)$$

V_n Estimated concentration of nth parameter in the analyzed water

V₀ Ideal value of this parameter in pure water = 0 (except for pH =7.0)

S_n Recommended standard value of nth parameter

The unit weight W_n for each water quality parameter is calculated by using the following formula:

$$W_n = \frac{K}{S_n} \dots \dots \dots (10)$$

Where K, Proportionality constant and can also be calculated by using the following equation:

$$K = \frac{1}{\sum \frac{1}{S_n}} \dots \dots \dots (11)$$

Different levels of water quality index and their respective water quality status were given in Table (3). Various parameters with their standards and recommended calculation were summarized in Table (4). The rating of water quality according to this WQI is given below Table (1).

Table (3): Water Quality Rating.

WQI _{WA} Value	Rating	Grading
0-25	Excellent	A
26-50	Good	B
51-75	Moderate	C
76-100	Poor	D
Above 100	Unsuitable	E

(Aldeeb and Algeidi, 2021; Khan, 2003)

WQI _{CCME} Value	Rating
95-100	Excellent
80-94	Good
65-79	Fair
45-64	Marginal
00- 44	Poor

3 Results and Discussion

Water sample collected from Ten (10) different locations of Sabratha were tested to determine the Water Quality Index (WQI). To calculate desired WQI, each parameter was multiplied by weightage factors according to their relative importance in determining quality index as prescribed in WA and CCME index.

• Canadian WQI (CCMEWQI)

Calculation for Well 1 as example, in this case there is only one test for each Well. F1 represents the percentage of variables that do not meet their Objective or standard (failed variables), relative to the total number of variables measured and F2 represents the percentage of individual tests that do not meet standard

$$F_1 = \left[\frac{NFV = 7}{TNV = 10} \right] \times 100 = 70$$

$$F_2 = \left[\frac{NFT = 7}{TNT = 10} \right] \times 100 = 70$$

The test value must not exceed the objective

$$excursion_{TDS} = \frac{Failed\ test\ value_i}{Objective_i} - 1$$

$$= \frac{5094.4}{1000} - 1 = 4.0944$$

$$nse = \frac{\sum_1^n excursion_i}{Total\ number\ of\ tests} = \frac{21.08}{10} = 2.108$$

$$F_3 = \frac{nse}{0.01 \cdot nse + 0.01} = \frac{2.108}{0.01 \times 2.108 + 0.01} = 67.83$$

$$WQI_{CCME} = 100 - \left[\frac{\sqrt{70^2 + 70^2 + 67.83^2}}{1.732} \right] = 30.7$$

Well	pH	TDS	Ca ²⁺	Na ⁺	Mg ²⁺	K ⁺	HCO ₃ ⁻	SO ₄ ²⁻	NO ₃ ⁻	Cl ⁻	HD
limit	7.5	1000	200	200	150	40	200	250	45	250	500
1	6.91	5094	737	862	149	46	129	731	13.3	2480	2453

• Weighted Arithmetic WQI (WAWQI)

Calculation for Well 1 as example, the Proportionality constant K of 10 standard parameter S_n:

$$K = \frac{1}{\sum \frac{1}{S_n}} = \frac{1}{0.213222} = 4.689943$$

The quality rating scale Q_n and the unit weight W_n for each parameter were calculated and summarized in Table (4).

Table (4): Calculation of Q_n and W_n for well 1.

parameter	standard	experimental	W _n	Q _n	W _n · Q _n
pH	7.5	6.91	0.625326	18.00	11.256
TDS	1000	5,094.4	0.00469	509.4	2.389
Ca ⁺⁺	200	737	0.02345	368.5	8.641
Na ⁺	200	862	0.02345	431	10.106
Mg ⁺⁺	150	149	0.03127	99.3	3.106
K ⁺	40	46	0.11725	115	13.484
HCO ₃ ⁻	200	129.3	0.02345	64.65	1.560
SO ₄ ⁻	250	731.3	0.01876	292.5	5.488
NO ₃ ⁻	45	13.3	0.10422	29.56	3.080
Cl ⁻	250	2,480	0.01876	992	18.609
HD	500	2,453	0.00938	490.7	4.603
WQI					82.3

Analog calculations for the other wells for both, CCMEWQI and WAWQI are summarized in the Table (5). Different levels of water quality index (WQI_{CCME} & WQI_{WA}) and their respective water quality condition were given in Table (3). The drinking water quality analysis by CCMEWQI and WAWQI

shows that more than 60% of the samples described the groundwater quality in the study area as poor to unsuitable and cannot be used for drinking propose, only 20% of the samples was classified as good for direct consumption.

Table (5): Summarized WQIs for the 10 wells.

Well	CCME WQI	Rating	Well	AW WQI	Rating	Grading
1	30.7	Poor	1	82.3	Poor	D
2	12.6	Poor	2	151.4	Unsuitable	E
3	65.7	Fair	3	84.4	Poor	D
4	24.8	Poor	4	82.0	Poor	D
5	20.4	Poor	5	120.6	Unsuitable	E
6	56.3	Marginal	6	41.8	Good	B
7	28.4	Poor	7	123.2	Unsuitable	E
8	56.8	Marginal	8	46.8	Good	B
9	49.9	Marginal	9	51.4	Moderate	C
10	83.5	Good	10	62.0	Moderate	C

4 Conclusions

The groundwater of the study area in Sabratha region were evaluated for their chemical composition and suitability for drinking purpose using the water quality indices (CCMEWQI & WA). Groundwater samples were collected from ten (10) boreholes in Sabratha Libya at random. The drinking water quality analysis by WAWQI and CCMEWQI shows that 50% of samples described the groundwater quality in the study area as poor to unsuitable and 40% of samples described it as good to moderate water and can be used for direct consumption.

References

- Abbasi T., Abbasi S.A.; Water-Quality Indices Water Quality Indices, Elsevier (2012), pp. 353-356, [10.1016/B978-0-444-54304-2.00016-6](https://doi.org/10.1016/B978-0-444-54304-2.00016-6).
- Adelagun, Ruth Olubukola Ajoke, Etim, Emmanuel Edet and Godwin, Oko Emmanuel, Assessment of Water from Different Sources in Nigeria, Promising Techniques for Wastewater Treatment and Water Quality Assessment, 8, (2021), ISBN978-1-83881-901-9, DOI10.5772/intechopen.87732.

- Aldeeb W., Algeidi O.; Mitrid Groundwater Evaluation for Irrigation, Northern West Libya, Libyan Journal of Ecological & Environmental Sciences and Technology (LJEEST), Vol. 3 No. 2 Dec, 2021.
- Brown, R.M., McClelland, N.I., Deininger, R.A. and Tozer, R.G., (1970) "Water quality index-do we dare?", Water Sewage Works, 117(10). 339-343.
- CCME Canadian Council of Ministers of the Environment, "Canadian water quality guidelines for the protection of aquatic life: CCME Water Quality Index 1.0, Technical Report," In: Canadian environmental quality guidelines, 1999, Canadian Council of Ministers of the Environment, Winnipeg, Technical, 2001.
- Gaytán-Alarcón; Patricia Ana; González-Elizondo, M. Socorro; Sánchez-Ortíz, Eduardo & Alarcón-Herrera, María Teresa, Comparative assessment of water quality indices—a case study to evaluate water quality for drinking water supply and irrigation in Northern Mexico, Environmental Monitoring and Assessment, Volume 194, Article number: 588 (2022).
- Kelly, WP (1946), Permissible composition and concentration for irrigation waters. In: Proceedings of ASC, p: 607.

- Khan, A. A., Paterson, R., and Khan, H., "Modification and application of the CCME WQI for the communication of drinking water quality data in Newfoundland and Labrador," in 38th, Central Symposium on Water Quality Research, Canadian Association on Water Quality (February 10–11, 2003), 2003, vol. 867.
- Libyan National Center for Standardization & Metrology and Ministry of Commerce (LNCS&MC) "Libyan standard legislation for drinking water" No. 82, (1992).
- Sutadian A.D., Muttill N., Yilmaz A.G., Perera B.J.C.; Development of a water quality index for rivers in West Java Province; Indonesia. *Ecol. Indic.*, 85 (2018), pp. 966–982, [10.1016/j.ecolind.2017.11.049](https://doi.org/10.1016/j.ecolind.2017.11.049).
- Tyagi S, Singh P, Sharma B, Singh R. Assessment of water quality for drinking purpose in District Pauri of Uttarkhand India. *Appl Ecol Environ Sci*. 2014; 2(4):94–9.
- Uddin, M.G.; Moniruzzaman, M.; Quader, M.A.; Hasan, M.A.; (2018), Spatial variability in the distribution of trace metals in groundwater around the Rooppur nuclear power plant in Ishwardi, Bangladesh. *Groundw. Sustain. Dev.* <https://doi.org/10.1016/j.gsd.2018.06.002>.
- Uddin, Md. Galal, Nash, Stephen, Olbert, Agnieszka I., A review of water quality index models and their use for assessing surface water quality, *Environmental Science, Ecological Indicators* 122 (2021) 107218.
- World Health Organization (WHO). *Guideline for drinking water quality*. 2012.
- Yisa J, Jimoh T. Analytical studies on water quality index of river Landzu. *Am J Appl Sci*. 2010;7:453–8.



Formulate the Matrix Continued Fractions and Some Applications

Naglaa F. A. Elfasy

Mathematics Department, Higher Institute of Sciences, Alabyar, Libya.

DOI: <https://doi.org/10.37375/sjfsu.v3i1.1100>

A B S T R A C T

ARTICLE INFO:

Received: 26 February 2023

Accepted: 5 April 2023

Published: 17 April 2023

Keywords: *Continued Fractions, A Matrix Continued Fractions, Matrix Polynomials, Approximation of Irrational Numbers, Fibonacci Sequence.*

A matrix continued fraction is a matrix representation of a continued fractions, It has the following formula:

$$a_0 + \frac{1}{a_1 + \frac{1}{a_2 + \frac{1}{\dots + \frac{1}{a_n}}}}$$

The matrix can be used to convert a continued fraction to a rational number by using matrix multiplication to calculate the matrix product of the continuous fraction matrix and the vector [1, 0]. Additionally, it can be used to calculate the convergent of a continued fraction by using matrix multiplication to calculate the matrix product of the continuous fraction matrix and the vector [1, 1]. It can also be used to represent and calculate the solutions of some type of recursive equations. The use of matrix representation of continued fractions allows for efficient computation of continued fraction expansions using matrix multiplication, which can be easily parallelized in parallel computation algorithms. This can lead to significant speedup in the computation of continued fractions and can be useful in various fields such as computer graphics.

1 Introduction

Continued fractions have many important properties and applications in mathematics, including in number theory, Diophantine equations, and the theory of irrational numbers[1]. They can also be used to symbolize a variety of mathematical operations, such as the logarithm, trigonometric functions, and the Riemann zeta function. In matrix form, continued fractions are used in the study of linear recurrent sequences, which are sequences of numbers that are determined by a fixed set of initial conditions and a set of recurrence relations. They have many applications in areas such as statistics, physics, and control theory[2]. A matrix continued fraction is a type of representation for matrices, similar to how continued fractions represent real numbers. It is a method of approximating a matrix as the product of simpler matrices. The matrix continued fraction provides a way to decompose a given matrix

into a series of simple matrices that can be easier to work with[3, 4].

Some applications of matrix continued fractions include[5, 6]:

1. Solving linear equations: it is possible to resolve systems of linear equations using matrix continuing fractions.
2. Eigenvalue approximation: to roughly determine a matrix's eigenvalues, one can use matrix continued fractions.
3. Matrix inversion: you may quickly determine a matrix's inverse by using matrix continued fractions.

4. Matrix polynomials: matrix continued fractions can be used to represent matrix polynomials, which are polynomials in which the coefficients are matrices.
5. Control systems: matrix continued fractions can be used in the design of control systems, such as linear quadratic regulator (LQR) controllers.
6. Signal processing: matrix continued fractions can be used in digital signal processing to model linear systems.
7. Orthogonal polynomials: matrix continued fractions can be used to compute orthogonal polynomials, which have important applications in numerical analysis and computational mathematics.

Continued fractions and matrices are two important mathematical concepts with an extensive variety of usage scenarios across multiple fields. Continued fractions, by means of way of expressing numbers, have many properties and applications, particularly in number theory and irrational numbers. Matrices are a way to represent and manipulate large sets of data and equations, and have many applications in linear algebra, statistics, physics, and engineering [7].

1.1 Continued Fraction Formula

A continued fraction is a representation of the form [3, 4]:

$$a_0 + \frac{1}{a_1 + \frac{1}{a_2 + \frac{1}{\dots + \frac{1}{a_3}}}}$$

$a_0, a_1, a_2,$ and a_3 are all integers. This is a way of representing a rational number as the sum of an integer and a sequence of nested fractions.

It is also represented as $[a_0, a_1, a_2, a_3,]$

For example, the continued fraction representation of the number 2.5 (which is equal to 5/2) is [2, 2].

- Derive an Equation for Continued Fractions Formula

A type of expression that expresses a rational number as the combination of an integer and a series of fractional terms is called a Continued Fraction. We can derive a general equation for a continued fraction by breaking it down into its component parts.

Let us examine a type of continued fraction expressed as [5]:

$$a_0 + \frac{1}{a_1 + \frac{1}{a_2 + \frac{1}{\dots + \frac{1}{a_3}}}}$$

where the coefficients, a_0, a_1, a_2 and a_3 are integers.

$$a_0 + \frac{b_1}{a_1 + \frac{b_2}{a_2 + \frac{b_3}{\dots}}}$$

where a_1 and b_1 can be any complex numbers.

We can start by defining a sequence of nested fractions as:

$$\begin{aligned} f_1 &= a_1 \\ f_2 &= a_2 + \left(\frac{1}{f_1}\right) \\ f_3 &= a_3 + \left(\frac{1}{f_2}\right) \\ f_n &= a_n + \left(\frac{1}{f_{n-1}}\right) \end{aligned}$$

Here n is the sequence's number of terms.

Now we can substitute this sequence of nested fractions into the continued fraction equation:

$$a_0 + (1/f_1)$$

This is the general equation for a continued fraction.

Alternatively we can use the recursive relationship for the continued fraction, where:

$$a_n = p_n/q_n = p_{n+1} - q_n/q_{n+1},$$

where a_n and q_n are integers, so the equation becomes:

$$a_0 + \frac{1}{a_1 + \frac{1}{a_2 + \frac{1}{\dots + \frac{1}{a_n}}}}$$

This recursive relationship is useful for calculating the value of a continued fraction in the next step. The process is repeated until the remainder is zero and convergent.

For example, the number p_i can be represented as a continued fraction as follows:

$$\pi = 3 + \frac{1}{7 + \frac{1}{15 + \frac{1}{1 + \frac{1}{292 + \frac{1}{1 + \frac{1}{1 + \dots}}}}}}$$

To determine the Continued Fraction expression of a number, you can use the Euclidean algorithm to find the quotient and remainder at each step. The integer part of the quotient becomes the next term in the continued fraction, and the remainder is used as the numerator

Here is an example of how to determine the Continued Fraction expression of π through the use of the Euclidean Algorithm:

$$\pi = 3.14159265\dots$$

Start with the numerator as π and the denominator as 1.

$$\pi / 1 = 3.14159265\dots \text{ with a remainder of } 0.14159265\dots$$

Use the integer part of the quotient as the next term in the continued fraction, and the remainder as the numerator in the next step.

$$3 + 0.14159265\dots / 1 = 3 + 0.14159265\dots$$

Repeat the process with the new numerator and denominator.

$$0.14159265\dots / 1 = 0.14159265\dots, \text{ With a remainder of } 0.00159265\dots$$

Repeat the process until the remainder is zero.

$$+ 0.00159265\dots / 1 = 7 + 0.00159265\dots$$

The expression of π as a continued fraction is [3, 7, 15, 1, 292, ...]

Note that this is only an example of the first few steps to find the representation of π , and the exact representation can be infinite and not a finite number of terms. Other continued fraction expansions. Continued Fractions can also express other mathematical constants such as π and the square root of 2, along with certain irrational numbers. As an illustration, π has the Continued Fraction expansion [3; 7, 15, 1, 292, ...], while the square root of 2 is expressed as [1; 2, 2, 2, 2, ...]. These expressions can offer precise approximations for the values of these mathematical constants.

2. Materials and Methods

2.1 Applications of Continued Fractions

Continued fractions have many applications in mathematics and other fields. Some of the most notable applications include:

- Continued fractions provide accurate approximations of irrational numbers, particularly in computer arithmetic and numerical analysis. This is particularly useful in computer arithmetic and numerical analysis.
- Continued fractions can solve specific Diophantine equations, which are equations that seek integer solutions.
- Number theory: Continued fractions have been used to prove important theorems in number theory, such as the uniqueness of continued fraction expansions for certain numbers.
- Control theory: In control theory, continued fractions represent a system's transfer function, indicating its behaviour to varied inputs.
- Cryptography: Continued fractions have been used in the design of certain cryptographic systems, such as the RSA algorithm.
- Quantum Mechanics: Continued fractions can also be used to find the energy levels of a quantum mechanical system.
- Other fields: Continued fractions are also employed in fields including signal processing, dynamical systems, statistics, and probability theory.

2.2 The Set of Continued Fractions

2.2.1 Derivation of Equation of the Set of Continued Fractions

A group of related continued fractions is called a set of continued fractions due to their shared property or connection. The specific form of the equation for a set of continued fractions will depend on the specific property or relationship being considered. For example; let's consider the set of continued fractions that represent the square roots of integers. We can derive an equation for this set of continued fractions by starting with the equation for a general continued fractions [9]:

$$a_0 + \frac{1}{a_1 + \frac{1}{a_2 + \frac{1}{\dots + \frac{1}{a_3}}}}$$

If we let x be the square root of an integer, we can rewrite the equation as:

$$x = a_0 + \frac{1}{a_1 + \frac{1}{a_2 + \frac{1}{\dots + a_3}}}$$

We can now substitute the square root of an integer, x , into the equation:

$$\sqrt{n} = a_0 + \frac{1}{a_1 + \frac{1}{a_2 + \frac{1}{\dots + a_3}}}$$

where n is an integer.

Another example is the set of continued fractions that have convergent that form a Fibonacci sequence, and each convergence represents the relationship between two consecutive Fibonacci numbers. In general, the set of continued fractions can be represented by the recursive relationship for the continued fraction, where [10]:

$$a_n = p_n/q_n = p_{n+1} - q_n/q_{n+1},$$

and where p_n and q_n are integers, so the equation becomes:

$$a_0 + \frac{1}{a_1 + \frac{1}{a_2 + \frac{1}{\dots + a_n}}}$$

This recursive relationship is useful for calculating the value of a continued fraction and for finding its convergent.

An example of a set of continued fractions is the set of continued fractions that represent the square roots of integers. These continued fractions have the form:

$$\sqrt{n} = a_0 + \frac{1}{a_1 + \frac{1}{a_2 + \frac{1}{\dots + a_3}}}$$

Where n is an integer, and $a_0, a_1, a_2, a_3, \dots$ are integers that can be determined by the method of continued fraction.

For instance, this is how $\sqrt{2}$ is represented as a continuing fraction:

$$\sqrt{2} = [1, 2, 2, 2, \dots]$$

This can be expressed mathematically as:

$$\sqrt{2} = 1 + \frac{1}{2 + \frac{1}{2 + \frac{1}{2 + \frac{1}{2 + \dots}}}}$$

Another example is the continued fraction representation of $\sqrt{3}$:

$$\sqrt{3} = [1, 1, 2, 1, 2, \dots]$$

This can be expressed mathematically as:

$$\sqrt{3} = 1 + \frac{1}{1 + \frac{1}{2 + \frac{1}{1 + \frac{1}{2 + \frac{1}{1 + \dots}}}}}$$

$$\sqrt{3} = 1 + (1/(1 + (1/(2 + (1/(1 + (1/(2 + \dots))))))))$$

As you can see, both examples are infinite continued fractions, which is a good indication that the square roots of integers are irrational numbers.

Another example of set of continued fractions is the set of continued fractions that have convergent that form a Fibonacci sequence, where each convergent is the ratio of two consecutive Fibonacci numbers. The continuing fraction of the golden ratio is what these are called.

$$\varphi = [1, 1, 1, 1, 1, \dots] \quad [11]$$

This can be expressed mathematically as:

$$\varphi = 1 + \frac{1}{1 + \frac{1}{1 + \frac{1}{1 + \frac{1}{1 + \frac{1}{1 + \dots}}}}}$$

$$\varphi = 1 + (1/(1 + (1/(1 + (1/(1 + \dots))))))$$

As you can see, it never ends, which is a good indication that it is an irrational number.

2.3 Continued Matrix Formula

A number is mathematically represented as the sum of an integer and a series of nested fractions using a continuing fraction formula, also known as a continued fraction. Matrixes, a different kind of mathematical object utilized in linear algebra, are not directly related to it. A rectangular array of numbers arranged in rows and columns is known as a matrix. A matrix's elements are denoted by the letter a_{ij} where i stand for the row index and j for the column index. The specific form of

an equation for a matrix will depend on the operation or relationship being considered[10].

For example, the equation for matrix addition is:

$$C = A + B$$

Each element of the resulting matrix C is equal to the corresponding element of matrix A multiplied by the corresponding element of matrix B, where A, B, and C are all matrices of the same size.

The matrix multiplication equation, which is another illustration, is as follows:

$$C = AB,$$

where A and B are matrices, and C is the resulting matrix, this operation is only possible if the number of columns of the first matrix is the same as the number of rows of the second matrix. As you can see, there is no direct relationship between continued fractions and matrices; they are used in different fields of mathematics. The continued fraction expansion of a number can be represented using matrices. The matrix representation of a continued fraction is called a continued fraction matrix. The continued fraction matrix of a number x can be found by the following recursion: Let

$$A_0 = [1, x], \text{ and for } n > 0, \text{ let } A_n = [A_{n-1}, 0] * [0, 1; 1, (1/x)],$$

The continued fraction matrix of x is the matrix A_n , where n is the number of terms in the continued fraction expansion of x.

For example, let's say we want to find the continued fraction matrix of the number

$x = p_i$. The continued fraction expansion of p_i is [3; 7, 15, 1, 292, 1, 1, ...].

Using the recursion above, we can attain the continued fraction matrix of p_i is:

$$\begin{aligned} A_0 &= [1, p_i] A_1 \\ &= [A_0, 0] * [0, 1; 1, 1/(1/p_i)] \\ &= [1, p_i; 0, 3] A_2 \\ &= [A_1, 0] * [0, 1; 1, 1/(p_i - 3)] \\ &= [1, p_i; 0, 3; 0, 7] A_3 \\ &= [A_2, 0] * [0, 1; 1, 1/(p_i - 3 - 7/3)] \\ &= [1, p_i; 0, 3; 0, 7; 0, 15] \end{aligned}$$

The matrix A_n will be the matrix representation of the continued fraction of p_i . It should be noted that the above representation is a general formula, and that different types of continued fractions might have different matrix representation.

The prior quotient enables us to think about matrix continuing fractions for a family of p_q matrices called B_i .

$$\Pi_n = \frac{1}{B_1 + \frac{1}{B_2 + \frac{1}{B_3 + \frac{1}{\dots + B_n}}}}$$

Definition 1: If every element of B_k is satisfied, then the continued fractions are said to be true. $B_k > 0$. A continued fraction is called periodic if there exists a positive integer k such that $B_{k+p} = B_k$ for all $p > 0$, where p is a positive integer. In other words, a continued fraction is periodic if it has a repeating pattern in its terms[13].

- $b_{p,q}(z)$ is a polynomial of degree $sk \geq 1$;
- $b_{p,1}(z), \dots, b_{p,q=1}(z)$ and $b_1, q(z), \dots, b_{p=1}, q(z)$ are polynomials of degree smaller than $sk+1$; all $b_i, j(z), i=1, \dots, p-1; j=1, \dots, q-1$ are polynomials of degree smaller than $sk=2$.
- All $b_i, j(z), i=1, \dots, p-1; j=1, \dots, q-1$ are polynomials of degree smaller than $sk-2$.

Definition 2: A regular continued fraction is a true continued fraction where all sk equal 1. This continued fraction type is also known as a simple continued fraction. It is important to note that not all true continued fractions are regular continued fractions, as some may have numerator terms that are not equal to 1.

For a regular continued fraction, the $B_k(z)$ are of the following form, with $\delta, \gamma, \beta, \alpha$ constants, and nonzero [13]:

$$B_k(z) = \begin{pmatrix} 0 & 0 & \gamma_{k,1} \\ 0 & 0 & \gamma_{k,p=1} \\ \delta_{k,1} & \delta_{k,q=1} & \alpha_k z + B_k \end{pmatrix}$$

We will prove the considered functions always yield a true continued fraction, assumed to be regular.

2.4 Matrix-Valued Continued Fractions

Matrix-valued continued fractions (MVCF) are a generalization of matrix continued fractions, in which the matrices A_i in the continued fraction are not just scalar values, but are themselves matrix-valued functions. These functions can be defined on a domain, such as the complex plane, and the MVCF represents the matrix-valued function as a ratio of matrix-valued polynomials. MVCF have applications in the analysis of matrix-valued functions, such as in the study of matrix functions and operator theory. They can be used to represent solutions of certain matrix-valued differential

equations, and to approximate matrix functions in a numerically stable way.

The equation of a MVCF is similar to the one of matrix continued fraction, but the matrices A_i are matrix-valued function.

$$A(z) = A_0 + [A_1(z), A_2(z), \dots, A_n(z)]$$

Where $A(z)$ is the matrix-valued function being represented by the MVCF, A_0 is a matrix and $[A_1(z), A_2(z), \dots, A_n(z)]$

Is the matrix-valued fraction, also known as a matrix-valued continued fraction?

The matrix-valued fraction is defined recursively as:

$$[A_1(z), A_2(z), \dots, A_n(z)] = A_1(z) + A_2(z) * [A_3(z), A_4(z), \dots, A_n(z)]$$

Where $A_1(z)$ is a matrix-valued function, $A_2(z)$ is a matrix-valued function and $[A_3(z), A_4(z), \dots, A_n(z)]$ is a matrix-valued fraction.

2.5 The Algorithm

There are several algorithms that can be used to convert a real number into its continued fraction representation. One of the most common algorithms is the Euclidean algorithm.

The Euclidean algorithm for continued fractions proceeds as follows:

1. Start with a real number x .
2. Take the integer part of x , and call it a_0 .
3. Subtract a_0 from x to get the fractional part, and call it x_1 .
4. Invert x_1 to get $1/x_1$, and call it x_2 .
5. Take the integer part of x_2 , and call it a_1 .
6. Subtract a_1 from x_2 to get the fractional part, and call it x_3 .
7. Repeat steps 4-6 until a desired level of accuracy is reached.
8. The desired continued fraction representation of x is $a_0 + 1/(a_1 + 1/(a_2 + 1/(a_3 + \dots)))$
9. Alternate algorithm is the Stern-Brocot tree which is a binary tree in which the vertices are the continued fractions.
10. The algorithm for generating Stern-Brocot tree proceeds as follows:
11. Start with the two fractions $0/1$ and $1/0$.
12. At each step, two fractions are added to the tree, one where the numerator and denominator of the left fraction are added together, and another that is the sum of the numerator and denominator of the right fraction.

Repeat step 2 until a desired level of accuracy is reached.

The Stern-Brocot tree algorithm can be used to determine the best rational approximation of an

irrational number as well as the continuing fraction representation of any real number.

In summary, there are different algorithms that can be used to convert

2.5.1 Matrix-Valued Continued Fractions Algorithm

There are different algorithms to compute matrix-valued continued fractions. One of the most commonly used algorithms is the modified Lentz's algorithm. The basic idea of the algorithm is to recursively compute the matrix-valued fraction using the following steps:

1. Start with an initial approximation of the matrix-valued function, A_0 .
2. For $i = 1$ to n :
 - Compute the matrix-valued function $B_i(z) = A_i(z)A_{i-1}(z)$
 - Compute the matrix $C_i = B_i^{-1}(z)$
 - Compute the matrix-valued function $D_i(z) = C_i A_i(z)$
 - Update the approximation of the matrix-valued function $A_{i+1}(z) = D_i(z) + C_i A_0$
 - The final approximation of the matrix-valued function is $A_n(z)$

This algorithm is widely used as it has fast convergence properties and requires only matrix-vector multiplications and inversions of matrix-valued function.

It's worth noting that this algorithm has the assumption that the matrix-valued function $A_i(z)$ is invertible for all z in the domain, also the matrix-valued functions $A_i(z)$ should have the same dimensions.

Also, it is important to note that the above algorithm is a modified version of Lentz's algorithm that is suitable for matrix-valued functions. The original Lentz's algorithm was designed for scalar-valued functions.

2.5.2 Example Matrix-Valued Continued Fractions Algorithm [15]

Here is an example of how to use the modified Lentz's algorithm to compute a matrix-valued continued fraction for a matrix-valued function $A(z)$:

Let's assume that $A(z)$ is a 2×2 matrix-valued function defined on the complex plane and we want to approximate it using a matrix-valued continued fraction of order $n = 4$.

1. Start with an initial approximation $A_0 = I$, where I is the 2×2 identity matrix.
2. For $i = 1$ to 4 :
 - Compute the matrix-valued function $B_i(z) = A_i(z)A_{i-1}(z)$, where $A_i(z)$ is given.
 - Compute the matrix $C_i = B_i^{-1}(z)$, where $B_i(z)$ is given.

- Compute the matrix-valued function $D_i(z) = C_i A_i(z)$
- Update the approximation of the matrix-valued function $A_{[12]}(z) = D_i(z) + C_i A_0$

The final approximation of the matrix-valued function is $A_4(z)$

It's important to note that the above example is a simplified one and in practice, the matrix-valued function $A(z)$ and the matrices $A_i(z)$ are typically defined in terms of more complicated expressions and operations. Also, the values of z for which we want to approximate the matrix-valued function $A(z)$ have to be chosen carefully, taking into account the convergence properties of the algorithm.

Also, it's good to mention that, computing the inverse of a matrix-valued function can be computationally expensive and some approximations methods exist to overcome this problem.

2.6 The Properties of the Continued Fraction Matrix

A square matrix whose entries represent the coefficients of a continuing fraction expansion is known as a continued fraction matrix. These matrices have several properties, including:

1. They are triangular: The entries above the main diagonal are all zero.
2. They are invertible: Any continued fraction matrix can be inverted, and the inverse is also a continued fraction matrix.
3. They satisfy the matrix equation: $A = T_{n-1} A_0$, where T_n is the continued fraction matrix and A_0 is the initial matrix.
4. They have the property of semi-groups: The product of two continued fraction matrices is also a continued fraction matrix.
5. They are closely related to the Fibonacci sequence: The Fibonacci numbers can be calculated using a continued fraction matrix, and the continued fraction matrix can be calculated using the Fibonacci numbers.

Here are some properties of the continued fraction matrix:

1. Uniqueness: For a given real number, there is only one continued fraction representation.
2. Convergence: A real number converges to its continuing fractional representation
3. Periodicity: A continued fraction representation is periodic if and only if the number is a rational.

4. Monotonicity: The terms of the continued fractional representation of a number are monotonically decreasing in magnitude.
5. Inevitability: A number's continuing fraction expression can be inverted to get the number's decimal representation.
6. Continued fraction expansion: Using a procedure called the Euclidean algorithm; one can find the specific continued fraction approximation for each real integer.

2.6.1 A Numerical Example of the Properties of a Continued Fractions Matrix [18].

A numerical example of the properties of a continued fraction matrix can be demonstrated using the matrix $A = [a \ b; c \ d]$

Let's assume that the entries of this matrix are the coefficients of the continued fraction expansion of a real number.

1. Triangular property:

$$A = [a \ b; 0 \ d]$$

As you can see from the matrix A , the entries above the main diagonal are all zero.

2. Inevitability property:

$$A^{-1} = [d \ -b; -c \ a] / (ad-bc)$$

The inverse of matrix A is also a continued fraction matrix.

3. Matrix equation property:

$$A_1 = [a \ b; c \ d] * A_0$$

Where A_1 is the next matrix in the continued fraction expansion and A_0 is the initial matrix.

4. Semi-groups property:

$$A_3 = A_2 * A_1$$

The product of two continued fraction matrices is also a continued fraction matrix.

5. Fibonacci sequence property:

The Fibonacci numbers can be calculated using the continued fraction matrix, for example;

$$[F(n+1) \ F(n)], [F(n) \ F(n-1)] = [F(n+1) \ F(n)] * [1 \ 1; 1 \ 0] \quad [21]$$

The continued fraction matrix can also be calculated using the Fibonacci numbers.

Note that this is just an example; the entries of the matrix may vary depending on the continued fraction expansion you are working with.

Theorem 1: Every true continued fraction converges to some matrix [22].

Not all genuine continuing fractions reach matrices. Real numbers can be presented as an endless or finite sequence of rational numbers using continued fractions. While some real numbers can be defined by infinitely long continued fractions that do not converge to a single value, other real numbers can be represented by finite continued fractions.

However, certain types of continued fractions, such as regular continued fractions, do converge to a matrix. The properties of the continued fraction matrix can then be used to study the properties of the corresponding real number.

The proof typically starts by assuming that the continued fraction expansion has the form:

$$b_0 + 1 / (b_1 + 1 / (b_2 + 1 / (b_3 + \dots))),$$

where b_0, b_1, b_2, b_3 , are the coefficients in the continued fraction expansion.

The corresponding matrix for this continued fraction is defined as:

$$A = [b_0 \ b_1; 1 \ b_2],$$

$$T = [1 \ b_0; 0 \ 1],$$

$$T^2 = [1 \ b_0; 0 \ 1] * [1 \ b_0; 0 \ 1]$$

$$= [1 \ b_0 + 1; b_0 \ 1],$$

$$T^3 = [1 \ b_0 + 1; b_0 \ 1] * [1 \ b_0; 0 \ 1]$$

$$= [1 \ b_0 + b_1 + 1; b_0 + 1 \ b_2], \dots$$

By repeatedly applying the matrix equation, it can be shown that the matrix T^n converges to a specific matrix, as n approaches infinity. The value of the continuing fraction can sometimes be determined using this matrix, also referred to as the limiting matrix. The demonstration is successful because this matrix is distinct for just about any given continuing fraction. It's worth noting that for true continued fractions, the b_n are positive integers, this is the key to the matrix converges.

Theorem 2: Assuming that the continuation from (F) is a regular multi-index of size p , where $\bar{n}=(n_1, \dots, n_2)$,

$$(FQ_k - P_k) = O(1/z^{\bar{n}+1}), \quad i = 1, \dots, p$$

$$(FQ_k - P_k) = O(1/z^{\bar{n}+1}), \quad i = 1, \dots, p$$

Proof: The index describes also the regular index of size $q, \bar{m} = (m_1 - m_2)$, and because Q_k is expanded in the basis h_0, \dots, h_k , the amount i of Q_k is of degree at most m_i for $i=1, \dots, q$.

We have

$$(FQ_k - P_k) = (F - \Pi_k)Q_k$$

Using theorem

$$(F - \Pi_k)_{i,j} = O(1/z^{n_i^k+m_j^k+1})$$

With respect to z , it follows that, for $i=1, \dots, p$, $(FQ_k - P_k)(z) = \sum_{j=1}^q O(\frac{1}{z^{n_i+m_j+1}})z^{m_j} = O(\frac{1}{z^{n_i+1}})$

And from this, the weak approximation's conclusion is found.

Since this, the approximation of F is either Π_k or the two matrices Q_k and P_k ,

With $\Pi_k = P_k (Q_k)^{-1}$ satisfying

$$(F - \Pi_k)_{i,j} = O\left(\frac{1}{z^{n_i^k+m_j^k+1}}\right), \quad i = 1, \dots, p, \quad j = 1, \dots, q$$

$$FQ_k - P_k = O(1/z^{\bar{n}+1}),$$

a matrix with entries of type $1/z^*$ on the right-hand side of the second formula, where powers of $1/z$ are standard multi-indices on each row and column, reducing in the rows and rising in the columns, starting from \bar{n} indicated by k in the first column, i.e., writing only the power and authority of the matrix,

$$O\left(\frac{1}{z^{\bar{n}+1}}\right) \text{ we get, if } k = vp + \mu, \quad 0 \leq \mu < p$$

$$\begin{pmatrix} v+1 & \dots & v+1 & v+2 & \dots \\ v+1 & \dots & v+1 & v+2 & \dots \\ \cdot & \dots & \cdot & \cdot & \dots \\ v & \dots & v+1 & \cdot & \dots \\ v & v & v+1 & \cdot & \dots \end{pmatrix}.$$

A matrix Pade approximant of F is created as a result of the continuing fraction, and because P_k is a vector polynomial, it is necessarily the polynomial part of FQ_k .

$$i=1, \dots, p; \quad j=1, \dots, q,$$

$$f_{i,j} = \sum_{v=0}^{\infty} \frac{f_{i,j}^v}{z^{v+1}}, \quad \theta_{i,j}(x^v) = f_{i,j}^v$$

it respects, every functional acting on x , k defining (m_1, \dots, m_q) and $(P_k)_i$ be there the i th component of P_k

$$i=1, \dots, p, \quad (P_k)_i(z) = \sum_{j=1}^q \theta_{i,j}\left(\frac{(Q_k)_i(x)-(Q_k)_j(z)}{x-z}\right)$$

$$P_k(z) = \sum_{j=1}^q \theta\left(\frac{(Q_k)_i(x)-(Q_k)_j(z)}{x-z}\right), \quad \deg (P_k)_i = m_i - 1.$$

From this formula or from $P_k=P[FQ_k]$, the degree of the components $(P_k)_i$, $i=1, \dots, p$, is recognized: each $(Q_k)_j$ is of degree m_j for $j=1, \dots, q$, so $(P_k)_i$ is the summation of polynomials of degree correspondingly m_j+1 , and so is of degree lower than or equivalent to m_1+1 for all i among 1 and p .

Theorem 3: If and only if F is a weakly perfect matrix, the continuing fraction inferred from F is regular [24].

A weakly perfect matrix continued fraction is a specific type of matrix continued fraction that follows a specific pattern. A weakly perfect matrix continued fraction able to be signified as:

$$F = [A_0, A_1, A_2, \dots, A_n]$$

where A_0 is a scalar or matrix, A_1, A_2, \dots, A_n are matrices, and A_i^{-1} exists for all $i > 0$.

A regular matrix continued fraction is a matrix continued fraction that follows a specific pattern that is determined by the properties of the matrices A_i . A weakly perfect matrix continued fraction is regular because it follows a specific pattern that is determined by the properties of the matrices A_i . It follows that the continued fraction derived from F must be a weakly flawless matrix continued fraction in order for it to be true that now the continued fraction is regular.

An example of a weakly perfect matrix continued fraction is the following:

$$F = [A_0, A_1, A_2, A_3], \text{ where;}$$

$$A_0 = [1, 2], A_1$$

$$= [3, 4], A_2$$

$$= [5, 6], A_3$$

$$= [7, 8]$$

In this example, A_0 is a 2×2 matrix and A_1, A_2, A_3 are also 2×2 matrices. The inverse of A_1, A_2, A_3 exist, so the continued fraction is weakly perfect.

Since F is a weakly perfect matrix continued fraction, its continued fraction will be regular. It can be represented as:

$$F = [A_0; A_1, A_2, A_3]$$

$$= A_0 + 1/(A_1 + 1/(A_2 + 1/A_3))$$

This continued fraction can be used to represent solutions to certain types of matrix

Here is an example of a numerical matrix continued fraction that is both weakly perfect and regular:

$$F = [A_0, A_1, A_2, A_3]$$

$$\text{where } A_0 = [1, 2; 3, 4], A_1$$

$$= [5, 6; 7, 8], A_2$$

$$= [9, 10; 11, 12], A_3$$

$$= [13, 14; 15, 16]$$

In this example, A_0, A_1, A_2, A_3 are all 2×2 matrices and inverse of all matrices exist, it is a weakly perfect matrix continued fraction.

Thus the continued fraction is regular and can be represented as:

$$F = [A_0; A_1, A_2, A_3]$$

$$= A_0 + 1/(A_1 + 1/(A_2 + 1/A_3))$$

The continued fraction derived by F remains hence steady if and only if F is a weakly ideal matrix. The same is true in this instance.

2.7 Applications for Matrix Continued Fractions (MCF)

Matrix continued fractions (MCF) have a varied range of applications in several fields, such as control theory, signal processing, and computer science. Some of the most notable applications include:

1. Linear systems control: MCF can be used to represent systems of linear differential equations, which are commonly used in control systems. The MCF representation can be used to design controllers for linear systems, and to analyze the stability and performance of the system.
2. Signal processing: In the frequency domain, MCF may be used to represent signals and systems. This form can be used to create digital signal filters and examine the frequency response of a system.
3. Computer science: MCF can be used to represent systems of polynomials, which are commonly used in computer science. This representation can be used to analyze the properties of polynomial systems, and to design algorithms for solving polynomial equations.
4. Robotics: MCF can be used to represent systems of linear differential equations, which are commonly used in robotics. The MCF representation can be used to analyze the dynamics of robotic systems, and to design controllers for robotic systems.
5. Linear Algebra: MCF can be used to represent the matrix and its inverse; this representation can be used to explain linear systems and inversion of matrices.
6. Optimization: MCF can be used in optimization, MCF can be used to resolve linear least squares problem, and to find the maximum of a linear function subject to linear constraints.

It's worth noting that the application of MCF is not limited to these examples and it can be used in many other areas.

2.7.1 Solution of Matrix Equations by Branching Continued Fraction

The equation to solve matrix equations by branching the continuous fraction is called the "Matrix Fractional Description (MFD)". The general form of the MFD equation is [26]:

$$X = (A - BK)^{-1}(C + DK)$$

Where X is the unknown matrix, A , B , C , D , and K are known matrices and ${}^{(-1)}$ denotes the matrix inverse. This equation canister be used to find the optimal fundamental of the matrix equation by using the continuous fraction expansion. The optimal value of the matrix K can be found by iteratively solving the equation and updating the values of K .

Here is a simple example to illustrate the use of the Matrix Fractional Description (MFD) equation to solve a matrix equation:

Given the following matrix equation:

$$X = (A - BK)^{(-1)}(C + DK)$$

Where:

$$A = [[2, 0], [0, 3]]$$

$$B = [[1, 2], [3, 4]]$$

$$C = [[1, 0], [0, 1]]$$

$$D = [[1, 2], [3, 4]]$$

$$K = [[k_1, k_2], [k_3, k_4]] \text{ (unknown matrix)}$$

To find the solution for X , we need to find the optimal value of the unknown matrix K . We can do this by using the MFD equation and iteratively updating the values of K until a satisfactory solution is found.

Let's start with an initial guess for the values of K :

$$K = [[0, 0], [0, 0]]$$

Using the MFD equation, we can calculate the first iteration of X

:

$$X = (A - BK)^{(-1)}(C + DK)$$

$$= A - [[0, 0], [0, 0]]^{(-1)}(C + [[1, 2], [3, 4]])$$

$$= A^{(-1)}(C + D)$$

$$= [[0.5, 0], [0, 1/3]], [[1, 2], [3, 4]]$$

$$= [[2.5, 5], [9, 4]]$$

We can now use this updated value of X to update the values of K and repeat the process until the solution converges. This is just a simple example to show the basic idea of how to solve matrix equations using the MFD equation. In practice, the process can be more complex and multiple iterations may be required to achieve an optimal solution.

2.7.2 Matrix Representation of Continued Fraction and its Use in Parallel Computation Algorithms

Deduce the matrix representation equation for the continuous fraction and use it in parallel arithmetic algorithms. The matrix representation of a continuous fraction can be represented using the RATIONMATRIX formula, which is a 2×2 matrix. The equation for RATIONMATRIX is given by:

$$\text{RATIONMATRIX}(a, b, c, d) = \begin{vmatrix} a & b \\ c & d \end{vmatrix}$$

This matrix can be used in parallel arithmetic algorithms for fast computation of continued fractions. For example, the matrix representation can be used to estimate the value of a continued fraction in parallel, which can reduce the computational time compared to traditional sequential algorithms. In parallel arithmetic algorithms, the matrix representation of a continued fraction is multiplied with a vector of intermediate values to compute the final result in parallel. The intermediate values are then combined to get the final result. This approach is more efficient than traditional sequential algorithms as the computation can be done in parallel, reducing the overall time taken for computation.

Example for the matrix representation equation for the continuous fraction and use it in parallel arithmetic algorithms

Consider the continued fraction representation of a number as follows:

$$a_0 + 1/(a_1 + 1/(a_2 + 1/(a_3 + \dots)))$$

The matrix representation of this continued fraction can be given as:

$$R_0 = \text{RATIONMATRIX}(a_0, 1, 0, 1)$$

$$R_1 = \text{RATIONMATRIX}(a_1, 1, 0, 1)$$

$$R_2 = \text{RATIONMATRIX}(a_2, 1, 0, 1) \dots$$

The final matrix representation of the continued fraction can be calculated as the product of these matrices:

$$R = R_0 * R_1 * R_2 * \dots$$

This final matrix R can be used in parallel arithmetic algorithms to subtract the value of the continued fraction.

For example, a parallel algorithm can be implemented as follows:

1. Initialize a vector $v_0 = [1, a_0]$
2. Divide the intermediate matrices R_0, R_1, R_2, \dots into equal parts and assign each part to a different processing unit.
3. Each processing unit multiplies its assigned part of the intermediate matrices with the vector v_0 to get intermediate vectors v_1, v_2, \dots
4. The intermediate vectors are combined to get the final result $v = [x, y]$, everyplace x/y is the value of the continued fraction.

This parallel algorithm can significantly reduce the computational time compared to traditional sequential algorithms.

Consider a continued fraction representation of the number as:

$$a_0 + 1/(a_1 + 1/(a_2 + 1/(a_3 + 1/(a_4))))$$

$$= a_0 + 1/(a_1 + 1/(a_2 + 1/(a_3 + 1/a_4)))$$

The corresponding matrices for each term in the continued fraction can be given as:

$$R_0 = \text{RATIONMATRIX}(a_0, 1, 0, 1)$$

$$R_1 = \text{RATIONMATRIX}(a_1, 1, 0, 1)$$

$$R_2 = \text{RATIONMATRIX}(a_2, 1, 0, 1)$$

$$R_3 = \text{RATIONMATRIX}(a_3, 1, 0, 1)$$

$$R_4 = \text{RATIONMATRIX}(a_4, 1, 0, 1)$$

The intersection of these matrices yields the final matrix representation of something like the continuing fraction:

$$R = R_0 * R_1 * R_2 * R_3 * R_4$$

Let's say we have 4 processing units. The intermediate matrices R_0, R_1, R_2, R_3, R_4 can be divided into 4 parts and assigned to each processing unit as follows:

Processing Unit 1: $R_0 * R_1 * R_2$

Processing Unit 2: R_3

Processing Unit 3: R_4

The intermediate vectors can be calculated as:

Processing Unit 1: $v_0 * (R_0 * R_1 * R_2) = v_0 * R_0 * R_1 * R_2$

Processing Unit 2: $v_0 * R_3$

Processing Unit 3: $v_0 * R_4$

Finally, the intermediate vectors can be combined to get the final result $v = [x, y]$, and x/y is the continued fraction's value.

This example demonstrates how the matrix representation of a continued fraction can be used in parallel arithmetic algorithms for fast computation.

3. Results

A continuous fraction (CF) is a representation of a real number as an infinite sum of terms. A continuous fraction matrix is a matrix representation of a CF, where each element of the matrix is a fraction.

To formulate the CF matrix, first we complete a form with the CF.:

$$a_0 + \frac{1}{a_1 + \frac{1}{a_2 + \frac{1}{\dots + \frac{1}{a_3}}}}$$

Where $a_0, a_1, a_2, a_3, \dots$ are integers. The CF matrix is then formed by writing each fraction as a 2x2 matrix, with the numerator being the first element and the denominator being the second element.

Example: Consider the CF for the golden ratio $(1 + \sqrt{5})/2$.

The CF for the golden ratio is:

$$1 + 1/(1 + 1/(1 + \dots))$$

The CF matrix is then:

$$\begin{vmatrix} 1 & 1 \\ 1 & 0 \end{vmatrix}$$

This CF matrix can be used in different ways, such as:

1. Matrix exponentiation: The nth term of the CF can be calculated by raising the CF matrix to the power of n.
2. Fibonacci numbers: The nth Fibonacci number can be calculated using the CF matrix and the Fibonacci primary values $[F(0)=0, F(1)=1]$.
3. Converging to the golden ratio: The CF matrix can be used to approximate the golden ratio by repeatedly multiplying it with an initial vector. The result will converge to the golden ratio.

These are just a few examples of how the CF matrix can be used

4. Discussion

The use of continued fractions and their matrix representation allows for efficient computation of continued fraction expansions, which can be useful in a variety of applications. One important application is in the field of number theory, where continued fractions are used to find the best rational approximations of real numbers. This is important in many areas such as computer graphics, where approximating real numbers with rational numbers can improve the precision and accuracy of computations. Another application of continued fractions is in solving certain differential equations, however, in some circumstances, continuing fractions can be employed to achieve perfect answers.

5. Conclusions

Continued fractions have applications in cryptography, where they can be used for key generation and encryption/decryption. The use of matrix representation of continued fractions allows for efficient computation of continued fraction expansions using matrix multiplication, which can be easily parallelized in parallel computation algorithms.

This can lead to significant speedup in the computation of continued fractions and can be useful in applications such as computer graphics, cryptography, and scientific computing. To conclude, the use of continued fractions and their matrix representation allows for efficient and precise computation of real numbers, the continued fraction matrix can have practical uses across diverse fields.

Conflict of Interest: The authors declare that there are no conflicts of interest.

References

- Handley, H., *Continued Fractions: An Arithmetic and Analytic Study*, 2023.
- Cuyt, A.A., et al., *Handbook of continued fractions for special functions* 2008: Springer Science & Business Media.
- Frommer, A., K. Kahl, and M. Tsolakis, *Matrix functions via linear systems built from continued fractions*. arXiv preprint arXiv:2109.03527, 2021.
- Giscard, P.-L. and M. Foroozandeh, *Exact solutions for the time-evolution of quantum spin systems under arbitrary waveforms using algebraic graph theory*. Computer Physics Communications, 2023. **282**: p. 108561.
- Wall, H.S., *Analytic theory of continued fractions* 2018: Courier Dover Publications.
- Raïssouli, M. and A. Kacha, *Convergence of matrix continued fractions*. Linear Algebra and its applications, 2000. **320**(1-3): p. 115-129.
- Ibran, Z.M., E.A. Aljatlawi, and A.M. Awın, *On continued fractions and their applications*. Journal of Applied Mathematics and Physics, 2022. **10**(1): p. 142-159.
- Arnoux, P. and S. Labbé, *On some symmetric multidimensional continued fraction algorithms*. Ergodic Theory and Dynamical Systems, 2018. **38**(5): p. 1601-1626.
- Jenkinson, O. and M. Pollicott, *Rigorous effective bounds on the Hausdorff dimension of continued fraction Cantor sets: a hundred decimal digits for the dimension of E_2* . Advances in Mathematics, 2018. **325**: p. 87-115.
- Rao, S.S., *Vibration of continuous system*, s2019: John Wiley & Sons.
- Sorokin, V.N. and J. Van Iseghem, *Matrix continued fractions*. Journal of Approximation theory, 1999. **96**(2): p. 237-257.
- Yalkınoglu, B., *Knots and Primes: On the arithmetic of Toda flows*. 2022.



Evaluation of the Healthy of Workers in the Three Cement Factories of Expansion Badoush, New Badoush and Al-Rafidain in Nineveh Governorate

Aya A. H. Rasheed¹, Luay A. Al-Helaly², Ayad F. Qasim¹

^{1,3}Environment Science Department, Environment and Its Technologies College, Mosul University, Mosul, Iraq.

²Chemistry Department, Science College, Mosul University, Mosul, Iraq.

DOI: <https://doi.org/10.37375/sjfsu.v3i1.1169>

A B S T R A C T

ARTICLE INFO:

Received: 15 March 2023

Accepted: 21 March 2023

Published: 17 April 2023

Keywords:

Cement Factory, Pollution, Blood, Enzymes, Kidney, Antioxidants, Oxidative Stress.

The current study involved an assessment of the health of workers in three cement production plants and a comparison between them, as these factories were: Expansion Cement Factory, New Badoush cement factory, and Al-Rafidain cement factory in Nineveh Governorate, as blood samples were collected for a period from the beginning of August to the end of December (2022). The study include was (100) workers and for a control group (40), as the study aimed to know the effect of air pollutants on the workers by measuring (15) variables of different blood components (White blood cell (WBCs), red blood cell (RBCs), packed cell volume (PCV%), hemoglobin (Hb) concentration), platelet count (PLTs)), as well as measuring biochemical variables to evaluate kidney and liver functions, oxidants antioxidants status.

It was observed that there was an increase in the number of both WBC and PLTs Among the three cement workers, especially the Badoush cement factory workers, and there was a reduction in the number of RBC, Hb concentration and PCV% in all cement workers relative to the control group, decrease it was more severe on Badoush workers.

The results indicated a rise in the concentrations of urea and creatinine among the three cement workers, especially the Badoush cement factory workers, and less so among the Al-Rafidain workers, as well as an increase in the enzymes: CA, AST, ALT and ALP when compared with the control team.

It was observed that there was the rise on the state of oxidative stress for the workers in the three factories and it was the highest among the workers in Badoush, Al-Rafidain, and Expansion factories, respectively, as a result of a decrease in the levels of antioxidants and an increase in the levels of oxidants when compared with the control group.

In general, the study concluded that there is a clear Impact of cement pollutants on the workers' health in the three selected cement factories in Nineveh Governorate, and it was more affected by these pollutants on the workers of Badoush Cement, Expansion, and Al-Rafidain, respectively.

1. Introduction

Human health grows and becomes healthy in the degree of safety and hygiene of the environment in which it lives the more pollution in the environment in which it lives the more vulnerable it becomes. Environmental pollution, which is regrettably accelerating in our environment today and for many reasons jumps foremost in terms of technological

acceleration, excessive use of natural resources, and terrible emission of gases and vapors from factory towers, has caused significant pollution in the environment (Skalny et al., 2021).

The industry of cement is regarded as a vital, economic, and strategic industry all over the world because this industry is a pillar of the infrastructure of the states and also it meets the demand and needs for cement, which is so important in construction due to the

constant urban movement and development. However, at the same time, it is deemed an industry that causes pollution to the environment, particularly the air; inside the factory environment or outside in the environment that surrounds the factory due to the dust and gases emitted because these are released into the atmosphere from the quarries through all the production units at the factory, as a result handling the rocks and soil, which are the primary and raw materials. These are crushed and milled to be ready to enter the furnaces and these processes result in huge quantities of suspended materials. After the clinker from the kiln, comes the process of grinding causes which causes the generation of fine suspended dust and it followed by the cement filling process and loading it. The atmosphere in this unit involves high concentrations of fine suspended material produced (Al-Ahmady, and Obeed, 2015).

The pollution caused by suspended dust or suspended particles is one of the pollution aspects that is worthy to be paid attention as a result to the particles, particularly, those that can be easily inhaled, cause hazards to the environment, the atmosphere, and humans that are characterized by a diameter that is less than 10 microns can absorb toxic substances more compared to their coarse counterparts and get to the human body, then stay with stability in the lungs during the breathing process and they could cause many diseases that affect of the human respiratory system and can also cause cardiac diseases (Mahmmoud and Muwafaq, 2021; Al-Helaly, 2022).

Exposure to fine particulate matter (PM_{2.5}) air pollution originating from the combustion of fossil fuels is closely linked to the induction of both systemic inflammation and oxidative stress among the numerous air pollutants (Maciejczyk et al., 2021). The postulated mechanism is that fossil fuel particulate matter, particularly coal combustion PM_{2.5}, is high in both metals and sulfur which can produce oxidative stress, and sulfur, which causes acidity, increasing the bioavailability of reactive metals and causing systemic damage (Rosenbauer et al., 2016; Al-Helaly and Mahmood, 2019). The oxidative capacity of PM_{2.5} can be assessed by its ability to form hydroxyl radicals ($\bullet\text{OH}$) in the presence of hydrogen peroxide which in turn plays an active role in inducing oxidative stress (Ullah et al., 2021).

The human hemopoietic system knows to be highly sensitive to environmental effects due to quick synthesis and destruction of cells with consequent heavy metabolic demands, which makes it the best indicator in toxicological research (Scharf et al., 2020).

The study of (Al-Shamery and Jankeer, 2021) is among the studies in this domain, which is the effect of exposure to cement dust on the hematological variables in the workers of the new Badoush cement factory in Mosul City, Iraq. However, Al-Hayali and his

group (2012) study on the cement pollutants' effect on creatine and urea in the workers' blood serum as they work in the Hammam Al-Alil cement factory, which increases the concentration of urea and a decrease in the creatine concentration. Whereas Nwafor et al. (2019) study the effects of cement dust exposure on haematological indices, and heavy metal cases in the blood serum of rats, Results showed a significant increase in concentrations of calcium, silicon, manganese, iron, lead, and cadmium compared with unexposed animals. Significant reductions were observed in hematocrit values, and red and white blood cell counts after cement dust exposure.

Study the impact of some contaminants emitted by the cement labs in the Badoush region (Badoush Cement Expansion Plant, Badoush New Cement Plant, and Al-Rafidain Cement Factory) on workers' health, their impact on certain blood components and many biochemical variables in serum, and study the extent of oxidative stress events due to exposure of workers in these contaminants and compare compared to the health group.

2. Materials and Methods

The present study was conducted at the Northern State Company of Cement:

1-Study sites: The present study was performed at the Northern State Company for Cement Industry in Badoush Expansion Factory, Badoush New Factory, Al-Rafidain Factory (Old Badoush) that is located about 25 km north of Mosul city in Hamidat District. The study sites in these cement production plants are divided into five locations: Management Unit, Crusher Unit, Material Mills Unit, Furnace Unit, and Cement Packaging Unit.

2- Collection of Samples: Throughout this study, blood samples were taken from the employees for the period from the beginning of August until the end of December 2022. The employees are male workers who work in cement production plants (100) and the healthy group (40) (as the control group).

3-Blood tests: which included (White blood cells count (WBCs), red blood cells (RBCs) count, the concentration of hemoglobin (Hb), packed cell volume (PCV%), platelet count (PLTs) using a Sysmix coulter (Sysmex Corporation/Japanese), Principles of measurement Blood is sampled, and diluted, and moves through a tube which is thin enough that cells pass by one at a time. Characteristics of the cell are measured using lasers (Fluorescence flow cytometer) or electrical impedance, in addition to estimating the concentrations of some biochemical variables including evaluating kidney and liver functions (Urea, Creatinine, Albumin, Alanine aminotransferase (ALT), Aspartate aminotransferase (AST), Alkaline phosphatase (ALP)

using a FUJI NX500 device, It is made by from the Japanese company Fujifilm and respiratory functions enzyme activity (Carbonic anhydrase) using an ELISA device depends on the use of antibodies, the color change in identifying the presence of the enzyme in the sample, and assessment of antioxidant status by measuring the concentration of glutathione (GSH), Malondialdehyde (MDA), Peroxynitrite (ONOO-) nitrate in the serum of the blood using a Spectrophotometer were determined using manual methods (Table 1).

2.2: Statistical analysis

The he Statistical analysis was conducted by means of using the Statistical Package for Social Sciences (SPSS), Version 24. Data were demonstrated as arithmetic mean and standard error (mean \pm SE). The complete Randomized Design (C. R. D.) test was performed make a comparison between the groups and the value p-value of ≤ 0.05 as it is depended as the significance level.

Table 1: Methods used to determine biochemical parameters.

No.	Parameters measured	Method used
1	Urea	Depending on the enzymatic method (Friedman and Brandon, 2001)
2	Creatinine	(Jaffe method, 1886)
3	Albumin	Bromocresol green method (Doumas <i>et al.</i> , 1971)
4	Alanine aminotransferase (ALT)	BIOMERIEUX Company/France kit (Reitman and Frankel, 1957).
5	Aspartate aminotransferase (AST)	BIOMERIEUX Company/France kit (Reitman and Frankel, 1957).
6	Alkaline phosphatase (ALP)	BIOMERIEUX Company/France kit (Kind and King, 1954)
7	Glutathione (GSH)	Modified procedure utilizing DNTB reagent (Sedlak and Lindsay, 1968)
8	Malondialdehyde(MDA)	Thiobarbituric acid method (Janero, 1990)
9	Peroxynitrate (ONOO-)	Vanuffelen Method used (Vanuffelen <i>et al.</i> , 1998)
10	Carbonic anhydrase (CA)	Use of enzyme-related industrial adsorption technology (Enzyme – Linked Immuno sorbent ASSAY) (ELISA)

3. Results and Discussion

1. The effect of cement pollutants on the workers of the three cement factories on different blood components (Number of WBCs, RBCs, PLTs, and concentration of Hb, and PCV%):

Table (2) shows the effect of cement pollutants in the workers of the three cement factories on the components of the workers' blood at selected sites: Management Unit, Crusher Unit, Material Mills Unit, Furnace Unit, and Cement Packaging Unit (Badoush expansion, Badoush new and Al-Rafidain) in comparison to the control group.

Table (2): Comparison of blood component levels between the control group with workers in the three cement factories.

Blood components	Control group		Workers' Group (Badoush Expansion)		Workers' Group (new Badoush)		Workers' Group (Al-Rafidain)	
	Mean	SE	Mean	SE	Mean	SE	Mean	SE
Age (year)	33.5 a	1.16	35.28 a	1.93	33.32 a	1.75	35.04 a	2.58
BMI(kg/m ²)	25.8 a	1.05	26.47 a	1.059	26.37 a	1.059	26.97 a	1.44
WBC ($\times 10^3/L$)	8.01 a	0.79	8.65 b	0.403	9.13 c	0.19	8.67 b	0.33
RBCs($\times 10^6/L$)	4.56 d	0.33	3.59 c	0.18	2.21 a	0.202	2.89 b	0.21
Hb (gm/100ml)	14.86 d	0.50	13.32 c	0.47	12.22 a	0.27	13.02 b	0.64
PCV %	49.40 d	3.17	45.5 b	1.36	42.35 a	1.50	46.4 c	1.58
PLTs($\times 10^3/L$)	194.5 a	9.49	218.8 c	13.60	252.8 d	16.99	216.8 b	11.02

-Variation of letters (a, b, c, d) horizontally indicates that there is a significant difference at a lower probability level or equal to 0.05.

Results illustrate that there was a significant difference ($p \leq 0.05$) in terms of the numbers of WBCs, RBCs, PLTs, the concentration of Hb, and PCV%. It was noted that there is a significant decrease in three groups of workers and the highest WBCs at $9.13 (\times 10^3/L)$ and PLTs at $252.8 (\times 10^3/L)$ in the new cement Badoush plant and no significant difference between the cement Al-Rafidain plant and cement Badoush expansion plant was recorded in the number of WBCs at $8.6 (\times 10^3/L)$ compared to the control group in the number of WBCs by $8.01 (\times 10^3/L)$ and PLTs at $194.5 (\times 10^3/L)$.

The cause is thought to be an increased activity of phagocytic cells as a result of the occurrence of pulmonary infections after inhaling dust. This activity stimulates the bone marrow to release polymorphonuclear (PMN) is immature in large quantities that raise the numbers of WBCs (Losacco *et al.*, 2018).

The cause of platelet increase (PLT) in the current study is a lack of oxygen due to the reaction from cement dust irritating cells in the lung (Ewaid *et al.*, 2020). This result is consistent with the Poursafa researcher and others (2011), it was found an increase in the number of platelets after exposure to air pollutants in children and adolescents in the city of Isfahan.

While a significant decrease in number of RBCs, Hb concentration and PCV was observed in workers' groups and was the lowest concentration in the

workers of the new cement plant Badoush compared with control group (Number of RBCs at a rate of $4.56 (\times 10^6/L)$, Hb concentration at $14.86 (g/100 ml)$ and PCV at 49.40% , The reason for this may be attributed to the decrease in the number of red blood cells to the body's responses to irritation resulting from cement pollutants (Adeyanju and Okeke, 2019), as well as the decrease in the concentration of PCV% and Hb exposed to cement dust due to the negative correlation between the components of the blood and the exposure to pollutants, as the exposure is with chronic condition and the workers are exposed to substances that are toxic resulting from the silica cement components and these involve calcium oxide, aluminum oxide, and hexavalent chromium and they can result in various infections and thus lead to a decrease in hemoglobin production (Al-Shamery and Jankeer, 2021).

2. Effect of cement pollutants on the workers of the three cement factories on the levels of (CA, AST, ALT, ALP) enzymes, urea, and creatinine:

Table (3) shows the impact of cement contaminants on the workers of the three cement factories on the levels of (CA, AST, ALT, ALP) enzymes, urea, and creatinine at selected sites: Management Unit, Crusher Unit, Material Mills Unit, Furnace Unit and Cement Packaging Unit (Badoush expansion, new Badoush, and Al-Rafidain) compared with the control group.

Table 3: Comparison of levels of (CA, AST, ALT, ALP) enzymes, urea and creatinine between control group with workers in the three cement factories.

Blood components	Control group		Workers' Group (Badoush Expansion)		Workers' Group (new Badoush)		Workers' Group (Al-Rafidain)	
	Mean	SE	Mean	SE	Mean	SE	Mean	SE
Urea (mg/100ml)	19.97 a	1.48	29.16 c	1.41	30.11 d	1.08	28.07 b	1.92
Creatinine(mg/100ml)	0.713 a	0.08	0.902 c	0.031	0.97 d	0.024	0.81 b	0.03
CA (Pg/L)	75.21 a	3.2	100.9 c	5.53	108.3 d	3.76	95.65 b	3.51
AST (U/L)	21.32 a	1.10	27.87 c	2.42	29.62 d	1.47	26.40 b	1.87
ALT (U/L)	22.22 a	1.75	23.60 c	1.21	26.97 d	1.52	22.70 b	1.20
ALP (U/L)	73.66 a	3.03	102.3 d	7.7	81.76 b	4.17	90.54 c	6.38

- Variation of letters (a, b, c, d) horizontally indicates that there is a significant difference at a lower probability level or equal to 0.05.

Results showed that there is a significant difference ($p \leq 0.05$) in the concentrations of variables and high levels of urea and creatinine were observed

among cement workers in the three Factories in comparison to the control group, especially the workers of the new Cement Badoush plant, where the

concentration of urea was recorded at a rate (30.11 mg/100 ml) and the concentration of creatinine at a rate (0.97 mg/100 ml) and less Al-Rafidain workers had a urea concentration record at a rate (28.07 mg/100 ml). High concentration of urea in the serum of workers exposed to dust may be attributed to kidney effect and kidney inefficiency due to exposure to different contaminants and creatine concentration record at a rate (0.81 mg/100 ml) compared to the control group, the main reason for this is the low glomerular filtration rate of nitrogen, which impedes the flow of urine, i.e. dissolution outside the human body, resulting in the accumulation of metabolic waste (Kuraeiad and Kotepui, 2021).

It also recorded a significant rise of enzymes: CA at a rate of 108.3 pg/L and AST (29.62 U/L) and ALT (26.97 U/L) in the new cement Badoush plant and fewer Al-Rafidain workers had a CA concentration record at a rate (95.65 pg/L) and AST enzyme at (26.40 U/L) and ALT at (22.70 U/L), While the ALP enzyme at the cement Badoush expansion plant registered at a rate (102.3 U/L) and said the new cement Badoush workers had a rate (81.76 U/L). The cause of high CA levels is a result of its rise in cells lining pulmonary blood vessels such as epithelial tissue in identity vesicles, due to exposure to various air contaminants. The respiratory system is the only one in the body that is in contact with the air in the peripheral environment. Exposure to these contaminated substances will also lead to oxidative stress resulting from the increased production of oxidant compounds, which have an effect on the outer membrane of the tissue by raising the level of lipid peroxide as a result of the breakdown of cellular membranes in the lung resulting in a change in their susceptibility to selective permeability that frees large amounts of the CA enzyme out of the cell and

then into the serum as well as a lack of oxygen (Lakey et al., 2016).

On the other hand, the high level of ALP may be caused by the blockage of bile ducts resulting from exposure to cement dust, which may lead to bone deformation and bone cancer can occur as a result of exposure to various contaminants, all of which lead to a high increase in the effectiveness of this enzyme (Sanjel and Shim, 2020), There has also been a significant increase in the activity of the AST in the blood of persons exposed to the dust of the cement, which is likely to cause muscle dysmorphia or heart disorder due to increased blood content in the body, for example, high hemoglobin and PCV as a result of the large body's need for hemoglobin to transport oxygen and compensation for as a result of the presence of dust, all of which causes heart stress due to inhalation of contaminated air containing cement dust (Reda, et al., 2021).

The ALT is an indicator of the efficiency of the liver's work, as its increase means that the hepatic cells are destroyed decompose, or die in the event of the death of these cells. ALT is released into the bloodstream and its ratio rises. This increase can be clearly seen in the liver, leading to the release of the enzyme into the serum refers to this researcher (Abdu and Al-Bogami, 2019).

2. Effect of cement pollutants on the workers of the three cement factories on the levels of GSH, MDA, ONOO⁻ and Alb:

Table (4) shows the effect of cement contaminants on the three cement factories workers at GSH, MDA, ONOO⁻ and Alb levels at selected sites Badoush expansion, new Badoush, and Al-Rafidain compared with the control group.

Table 4: Comparison of GSH, MDA, ONOO⁻ and Alb levels between control group with workers in the three cement factories.

Blood components	Control group		Workers' Group (Badoush Expansion)		Workers' Group (new Badoush)		Workers' Group (Al-Rafidain)	
	Mean	SE	Mean	SE	Mean	SE	Mean	SE
GSH($\mu\text{mol/L}$)	11.08 d	0.62	4.55 b	0.97	2.30 a	0.44	5.78 c	0.90
MDA($\mu\text{mol/L}$)	3.98 a	0.35	5.14 b	0.72	6.93 d	1.08	5.68 c	0.73
ONOO-($\mu\text{mol/L}$)	56.37 a	3.89	59.04 b	2.92	72.29 d	2.51	68.68 c	2.16
Alb(gm/100ml)	3.81 a	0.21	4.22 c	0.14	4.39 d	0.17	4.06 b	0.25

* Variation of letters (a, b, c, d) horizontally indicates that there is a significant difference at a lower probability level or equal to 0.05.

The results indications of a significant decrease in GSH level at a probability ($p \leq 0.05$) in the workers compared with the control group where the highest concentration was recorded in the group of workers of the cement factory Badoush expansion (4.55 $\mu\text{mol/L}$), Next was the Al-Rafidain cement plant workers group

(5.78 $\mu\text{mol/L}$) and new Badoush cement plant workers group (2.30 $\mu\text{mol/L}$), while the highest concentration of control group was recorded at (11.08 $\mu\text{mol/L}$).

The reason for the low level of GSH is that it is a protective antioxidant that is involved in the deoxidation

because it can interact directly with radical ($\cdot\text{OH}$) or with hydrogen peroxide (H_2O_2) automatically through thiol group ($-\text{SH}$) containing it in its composition, as well as its use as a substrate in glutathione peroxidase. Therefore it has an important role in protecting cellular components from oxidation compounds (Hazra *et al.*, 2013), While it recorded a significant increase in the level of MDA, ONOO $^-$ and Alb in workers' blood where it recorded the highest concentrations in the new cement Badoush plant was the concentration of MDA at a rate ($6.93 \mu\text{mol/L}$), ONOO $^-$ at a rate ($72.29 \mu\text{mol/L}$) and Alb at a rate (4.39 g/100ml), Followed by cement workers Al-Rafidain and cement workers Badoush expansion respectively compared with the control group where MDA concentration ($3.98 \mu\text{mol/L}$), ONOO $^-$ concentration ($56.37 \mu\text{mol/L}$) and Alb concentration ($3.81 \mu\text{mol/L}$).

The increase of MDA may be reacted with deoxyadenosine and deoxyguanosine in DNA forming DNA adducts, primarily M1 G, which is mutagenic and may occur in workers in the future.

Recently, ROS have been recognized as important signaling molecules that control diverse signaling pathways involved in a variety of cellular responses such as programmed cell death, pathogen defense, and hormone signaling (Hwa Yun *et al.*, 2020). In addition, oxidative stress causes dramatic inhibition of the tricarboxylic acid cycle, glycolysis pathway, and pentose phosphate pathway (Al-Helaly and Ahmad, 2011).

Albumin is a major antioxidant component of plasma. In addition, albumin, one of the most important proteins in human plasma, is able to bind to Cu^{2+} tightly and with iron weakly. Copper bond to albumin is still effective in generating radicals species (Hydroxyl radicals) in the presence of hydrogen peroxide by Fenton reactions. Therefore, increasing it to protect humans from oxidants compounds formation (López-Tinoco *et al.*, 2011).

High ONOO $^-$ is caused by cellular destruction occurring under strong oxidation conditions when different contaminants are present and by increasing the formation of ONOO $^-$ participates in the destruction of DNA and the ineffectiveness of certain metabolic enzymes or ion pumps, damaging the cellular membrane (Ascenzi *et al.*, 2020).

3. Conclusions

In general, the study concluded that there was a clear impact of cement contaminants on the health status of the workers of the three selected cement factories in Nineveh governorate, and that they were further affected by those contaminants on the Badoush cement workers and its expansion, followed by Al-Rafidain, respectively.

Acknowledgements

The author would like to acknowledge those who always encourage and give their guidance, mom and dad.

References

- Abdu, S. B., & Al-Bogami, F. M. (2019). Influence of resveratrol on liver fibrosis induced by dimethylnitrosamine in male rats. *Saudi Journal of Biological Sciences*, 26(1), 201-209.
- Adeyanju, E., & Okeke, C. A. (2019). Exposure effect to cement dust pollution: A mini review. *SN Applied Sciences*, 1(12), 1572.
- Al-Ahmady, K. K., & Muhsin Obeed, H. (2015). Assessment of Air Particulate Pollution in New Badoosh Cement Factory/Iraq. *Al-Rafidain Engineering Journal (AREJ)*, 23(3), 123-135.
- AL-Hayali, H.L ; AL-Harbawi, M.K and Ali, s.y (2012) effect of cement pollution on creatinine and blood urea in haman AL-Alil factory workers. *College of Basic Education Researeners journal*, vol, 11. No 3.
- Al-Helaly, L. A., & Ahmad, T. Y. (2011, November). Oxidative Stress for X-Ray Diagnosis Workers in Mosul City. In *The Second Scientific Conference in Chemistry* (pp. 22-23).
- Al-Helaly, L. A., Mahmood, E. S. (2019). Studying of heavy and essential metals in the amniotic fluid for pregnant associated with high blood pressure. *Raf. Jour. Sci.* 22(1):53-68.
- Al-Helaly, L.A. (2022). *Mechanism of Toxic Substances Inside Living Organisms*, Dar Noun for Printing, Publishing and Distribution, Mosul, Iraq, ISBN: 978-9922-9818-5-7. Pp.167, 175. 194, 206, 213, 223, 220.
- Al-Shamery, H. A., & Jankeer, M. H. (2021, September). Study the effect o cement dust exposure on the hematological variables in the workers of new badoosh cement factory in mosul city, Iraq. In *Journal of Physics: Conference Series* (Vol. 1999, No. 1, p. 012030). IOP Publishing.
- Ascenzi, P., De Simone, G., Tundo, G. R., Platas-Iglesias, C., & Coletta, M. (2020). Ferric nitrosylated myoglobin catalyzes peroxynitrite scavenging. *JBIC Journal of Biological Inorganic Chemistry*, 25, 361-370.
- Doumas, B. T., Watson, W. A., & Biggs, H. G. (1971). Albumin standards and the measurement of serum albumin with bromocresol green. *Clinica chimica acta*, 31(1), 87-96.
- Ewaid, S.H.; Abed, S.A.; Al-Ansari, N.; Salih, R.M. (2020) Development and Evaluation of a Water Quality Index for the Iraqi Rivers. *Hydrology*, 7(3): 67.
- Fairley, T. L., Cardinez, C. J., Martin, J., Alley, L., Friedman, C., Edwards, B., & Jamison, P. (2006). Colorectal cancer in US adults younger than 50 years of age, 1998–2001. *Cancer*, 107(S5): 1153-1161.
- Friedman, M., & Brandon, D. L. (2001). Nutritional and health benefits of soy proteins. *Journal of agricultural and food chemistry*, 49(3), 1069-1086.
- Hazra, B., Sarkar, R., & Mandal, N. (2013). *Spondias pinnata* stem bark extract lessens iron overloaded liver toxicity due to hemosiderosis in Swiss albino mice. *Annals of Hepatology*, 12(1), 123-129.

- Hwa Yun, B., Guo, J., Bellamri, M., & Turesky, R. J. (2020). DNA adducts: Formation, biological effects, and new biospecimens for mass spectrometric measurements in humans. *Mass spectrometry reviews*, 39(1-2), 55-82.
- Jaffe, M. Z. (1886). Method for measurement of creatinine in serum. *Physiol Chem*, 10(391), 31.
- Janero, D. R. (1990). Malondialdehyde and thiobarbituric acid-reactivity as diagnostic indices of lipid peroxidation and peroxidative tissue injury. *Free radical biology and medicine*, 9(6), 515-540.
- Kind, P.R.N., and King, E.G., 1954. Estimation of Plasma Phosphate by Determined of Hydrolyzed Phenol with Amino Antipyrine. *J. Clin. Path.*, 7: pp.322-326.
- Kuraeiad, S., & Kotepui, M. (2021). Blood lead level and renal impairment among adults: A meta-analysis. *International journal of environmental research and public health*, 18(8), 4174.
- Lakey, P. S., Berkemeier, T., Tong, H., Arangio, A. M., Lucas, K., Pöschl, U., & Shiraiwa, M. (2016). Chemical exposure-response relationship between air pollutants and reactive oxygen species in the human respiratory tract. *Scientific reports*, 6(1), 16.
- Lopez-Tinoco C, Roca M, Garcia-Valero A, Murri M, Tinahones FJ, Segundo C, Bartha JL, Aguilar-Diosdado M. (2013) Oxidative stress and antioxidant status in patients with late-onset gestational diabetes mellitus. *Acta Diabetol.* 50:201–208.
- Losacco, C., & Perillo, A. (2018). Particulate matter air pollution and respiratory impact on humans and animals. *Environmental Science and Pollution Research*, 25, 33901-33910.
- Maciejczyk, P., Chen, L. C., & Thurston, G. (2021). The role of fossil fuel combustion metals in PM_{2.5} air pollution health associations. *Atmosphere*, 12(9), 1086.
- Mahmmoud, I. M., & Muwafaq, A. R. (2021). The Impact of Badoush Cements Factory Pollutant on the Health of Workers in It. *Annals of the Romanian Society for Cell Biology*, 14711-14724.
- Nwafor, P. C., Odukanmi, O. A., Salami, A. T., Owonikoko, M., & Olaleye, S. B. (2019). Evaluation of a cement dust generation and exposure chamber for rodents: blood heavy metal status, haematological variables and gastrointestinal motility in rats. *African Journal of Biomedical Research*, 22(1), 79-87.
- Poursafa, P., Kelishadi, R., Moattar, F., Rafiee, L., Amin, M. M., Lahijanzadeh, A., & Javanmard, S. H. (2011). Genetic variation in the association of air pollutants with a biomarker of vascular injury in children and adolescents in Isfahan, Iran. *Journal of Research in Medical Sciences: The Official Journal of Isfahan University of Medical Sciences*, 16(6), 733.
- Reda, F. M., El-Saadony, M. T., El-Rayes, T. K., Attia, A. I., El-Sayed, S. A., Ahmed, S. Y., ... & Alagawany, M. (2021). Use of biological nano zinc as a feed additive in quail nutrition: biosynthesis, antimicrobial activity and its effect on growth, feed utilisation, blood metabolites and intestinal microbiota. *Italian Journal of Animal Science*, 20(1), 324-335.
- Reitman, S., & Frankel, S. (1957). A colorimetric method for the determination of serum glutamic oxalacetic and glutamic pyruvic transaminases. *American journal of clinical pathology*, 28(1), 56-63.
- Rosenbauer, J., Tamayo, T., Bächle, C., Stahl-Pehe, A., Landwehr, S., Sugiri, D., & Rathmann, W. (2016). Re: ambient air pollution and early manifestation of type 1 diabetes. *Epidemiology*, 27(4), e25-e26.
- Sanjel, B., & Shim, W. S. (2020). Recent advances in understanding the molecular mechanisms of cholestatic pruritus: A review. *Biochimica et Biophysica Acta (BBA)-Molecular Basis of Disease*, 1866(12), 165958.
- Scharf, P., Broering, M. F., Oliveira da Rocha, G. H., & Farsky, S. H. P. (2020). Cellular and molecular mechanisms of environmental pollutants on hematopoiesis. *International Journal of Molecular Sciences*, 21(19), 6996.
- Sedlak, J., Lindsay, R. H. (1968). Estimation of total, protein bound and non-protein sulfhydryl groups in tissue with Ellman's reagent. *Anal. Biochem.* 25, 192-205.
- Skalny, A. V., Aschner, M., Bobrovnitsky, I. P., Chen, P., Tsatsakis, A., Paoliello, M. M., & Tinkov, A. A. (2021). Environmental and health hazards of military metal pollution. *Environmental Research*, 201, 111568.
- Ullah, I., Zahid, M., Jawad, M., & Arsh, A. (2021). Assessment of DNA damage and oxidative stress among traffic conductors and coal miners. *Pakistan Journal of Medical Sciences*, 37(2), 499.
- Vanuffelen, B.E.; J. Van der Zee, B.M. deKoster, J. VanSterinck and Elferink, J.G. (1998). Intracellular but not extracellular conversion of nitroxyl anion into nitric oxide leads to stimulation of human neutrophil migration. *Biochem. J.*, 330: 719-722.



Synthesis and Spectral Characterization of New Compounds Containing Benzotriazole Ring from 2 - chloro – N – (Substitutedphenyl) Acetamide

Ghazala Hashim¹, Nsreen Abdalfarg² and Hanan Bashir¹

¹Chemistry Department, Science Faculty, Omar Al-Mokhtar University, Libya.

²Chemistry Department, Science Faculty, Derna University, Libya.

DOI: <https://doi.org/10.37375/sjfsu.v3i1.837>

A B S T R A C T

ARTICLE INFO:

Received: 30 December 2022

Accepted: 07 March 2023

Published: 17 April 2023

Keywords:

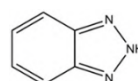
o - phenylene diamine, 2 - chloro - *N* - (substituted phenyl) acetamide, 1*H*-benzo[*d*] 1,2,3-triazole, synthesis.

A series of 2 – (1*H* – benzo[*d*] 1, 2, 3 – triazol -1 – yl) – *N* – (substituted phenyl) acetamide (3 -8) were synthesized by reacting 1*H* -benzo [d] 1, 2, 3 – triazole (2) and 2 - chloro – *N* – (substituted phenyl) acetamide (a1 - a6) in DMF in present K₂CO₃ was heated on water bath. 1*H* – benzo [d] 1, 2, 3 – triazole (2) is bicyclic heterocyclic system consisting of three nitrogen atoms and fused benzene ring, shows wide range of biological and pharmacological activities. Benzotriazole (2) can be synthesized by diazotization process using *o* -phenylene diamine with sodium nitrite and acetic acid. The synthesized compounds were isolated and purity was checked by TLC method. The structures of all new benzotriazoles derivatives were confirmed by melting point and spectroscopic methods (IR, ¹HNMR, ¹³CNMR, Mass spectrometry and elementary analysis). Furthermore, the purpose of this research is to synthesize some heterocyclic compounds that are of importance in the field of science and research. In addition, most of the studies based on benzotriazole derivatives possess wide spectrum of biological activities like including antibacterial, antifungal, antiviral, anti-inflammatory, antihypertensive, analgesic properties.

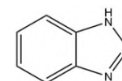
1 Introduction

A heterocyclic is an organic compound having a ring including at least one additional element, such as O, S, or N, and one or more carbon atoms. Since at least one heterocyclic component may be found in almost half of all known organic molecules, heterocyclic compounds are relatively common in nature. As they are essential to the metabolism of all living cells, their functions are frequently of basic relevance to living systems (Suma et al. 2011). Benzotriazole is a heterocyclic compound formed by the fusion of the benzene ring with the 4,5-positions of 1,2,3-triazole (Ram et al. 2019). It is also known as 1*H*-benzo[*d*]-1,2,3-triazole and Most of benzotriazole derivatives are prepared as a mixture of two isomers – the 2*H*- benzotriazole (1) and 1*H*-benzotriazole (2) isomers. In some instances, both isomers display a similar reactivity while in some

specific cases they display distinct reactivity profiles. A simple chromatography on silica gel usually suffices for their separation (Ueno et al. 2003).



(1)



(2)

Besides, benzotriazole is readily available in large quantities and is, most importantly, inexpensive. Anchored on molecular scaffolds, the benzotriazole moiety acts as an enabling group conveying its unique electronic, steric, and stereoelectronic properties to the surroundings. Four major properties of the benzotriazole fragment interplay and are responsible for the synthetic versatility of its derivatives: excellent leaving group ability, electron-donating or electron-withdrawing

character, stabilization of α -negative charges and stabilization of radicals. Most of benzotriazole derivatives are characterized by a long shelf-life, and their preparations are amenable to large scales (Alpana et al. 2020). Compounds containing benzotriazoles have been discovered to have a variety of uses in organic synthesis, such as biologically active systems, dye materials and fluorescent compounds, corrosion inhibitors, and photostabilizers in both medicine and industry (Uesaka et al. 2020). According to a review of the literature, the benzotriazole nucleus exhibits a variety of pharmacological properties, including anti-inflammatory (Jain et al. 2013), antibacterial (Jamkhandi et al. 2013), antifungal (Al-Omran et al. 2002), and anticancer (Noolvi et al. 2012) effects.

2 Materials and Methods

Melting point were decided in open capillary tube on VEEGO (VMP-D) softening point device and are uncorrected. IR spectro (KBr pellets) were recorded on a SHINADZU infrared spectrophotometer. The ^1H NMR spectra were determined in DMSO - d_6 at 300MHz on a BRUKER DP - X300NMR spectrophotometer using TMS as an internal standard. ^{13}C NMR were measured on Bruker 400MHz with internal reference TMS=0. Mass spectra were recorded at 70 ev with a GCMS - QP 1000 EX spectrometer.

Synthesis of 2-(1*H*-benzo[d]1,2,3 - triazol-1-yl) - *N*-(substituedphenyl) acetamide (3,4,5,6,7,8):

Equimolar quantity of 2 - Chloro - *N* - substituted phenyl) acetamide (**a1-a6**) (0.01mol) with 1*H*-benzo[d]1,2,3-triazole (**2**) (Bashir., et el. 2021) (0.01 mol) in present K_2CO_3 were dissolved in DMF, this mixture was heated on water bath for 24 hrs. The reaction was cooled at room temperature and poured into water (200 ml) with stirring for 15min, the solid obtained was filtrated and finally recrystallized from absolute ethanol.

2-(1*H*-benzo[d]1,2,3 -triazol-1-yl) - *N*-(4-methoxy-3 - nitrophenyl) acetamide (3):

Yield 70%, m.p. 203-204 $^\circ\text{C}$. IR ($\bar{\nu}_{\text{max}}$, cm^{-1}): 3323(NH), 3100 (CH- aromatic), 2921(CH- aliphatic) and 1689(CONH). ^1H NMR (DMSO, δH , ppm):3.8(s, 3H, OCH_3), 5.7(s, 2H, CH_2CO), 7.3 -8.1 (m, 7H, aromatic-H) and 10.7 (s, 1H, NH). M/S, m/z (%) = 327(M^+ , 5), 104(M^+ , $\text{C}_9\text{H}_9\text{N}_3\text{O}_4$, 100) and 76(M^+ , $\text{C}_9\text{H}_9\text{N}_5\text{O}_4$, 36). Anal. Calc. for $\text{C}_{15}\text{H}_{13}\text{N}_5\text{O}_4$ (327): C, 55.05; H, 4.00; N, 21.40; O, 19.55%, found: C, 55.15; H, 3.99; N, 21.60 %.

2-(1*H* - benzo[d]1,2,3 - triazol-1-yl) - *N*-(3-nitrophenyl) acetamide (4):

Yield 64%, m.p. 286-288 $^\circ\text{C}$. IR ($\bar{\nu}_{\text{max}}$, cm^{-1}): 3186(NH), 3012 (CH-aromatic), 2969(CH- aliphatic) and 1705(CONH). ^1H NMR (DMSO, δH , ppm): 5.8(s,

2H, CH_2CO), 7.4 -8.6 (m, 8H, aromatic-H) and 11.1(s, 1H, NH). M/S, m/z (%) = 297(M^+ , 2), 132(M^+ , $\text{C}_7\text{H}_5\text{N}_2\text{O}_3$, 35), 104(M^+ , $\text{C}_8\text{H}_7\text{N}_3\text{O}_3$, 2), 77(M^+ , $\text{C}_8\text{H}_8\text{N}_5\text{O}_3$, 100) and 78 (M^+ , $\text{C}_8\text{H}_9\text{N}_5\text{O}_3$,41). ^{13}C NMR: 50.049(1C),110.85(1C), 113.33(1C), 118.19(1C), 123.84 (2C), 125.13 (2C), 127.37 (1C), 130.21 (1C), 133.80 (1C), 139.42(1C), 145.03 (1C), 147.85 (1C) and 165.17(1C). Anal. Calc. for $\text{C}_{14}\text{H}_{11}\text{N}_5\text{O}_3$ (297): C, 56.56; H, 3.73; N, 23.56, found: C, 56.80; H, 3.99; N, 24.00%.

2 - (1*H* - benzo [d] 1,2,3 – triazol -1 – yl) – *N* - (2 - nitrophenyl) acetamide (5):

Yield 70%, m.p.195-197 $^\circ\text{C}$. IR ($\bar{\nu}_{\text{max}}$, cm^{-1}): 3316(NH), 3093 (CH-aromatic), 2929 (CH-aliphatic) and 1689(CONH). ^1H NMR (DMSO, δH , ppm): 5.8(s, 2H, CH_2CO), 7.4 -8.1 (m, 8H, aromatic-H) and 10.9(s, 1H, NH). M/S, m/z (%) = 297(M^+ , 1), 132(M^+ , $\text{C}_7\text{H}_5\text{N}_2\text{O}_3$, 61), 104(M^+ , $\text{C}_8\text{H}_7\text{N}_3\text{O}_3$, 17), 77(M^+ , $\text{C}_8\text{H}_8\text{N}_5\text{O}_3$, 100),78 (M^+ , $\text{C}_8\text{H}_9\text{N}_5\text{O}_3$,31) and 76(M^+ , $\text{C}_8\text{H}_7\text{N}_5\text{O}_3$, 23). Anal. Calc. for $\text{C}_{14}\text{H}_{11}\text{N}_5\text{O}_3$ (297): C, 56.56; H, 3.73; N, 23.56, found: C, 57.00; H, 3.84; N, 23.60%.

2 - (1*H* - benzo[d]1,2,3 – triazol-1-yl) – *N* - (4-nitrophenyl) acetamide (6):

Yield 78%, m.p. 269-271 $^\circ\text{C}$. IR ($\bar{\nu}_{\text{max}}$, cm^{-1}): 3314(NH), 3093 (CH-aromatic), 2938(CH- aliphatic) and 1697(CONH). ^1H NMR (DMSO, δH , ppm): 5.8(s, 2H, CH_2CO), 7.4 -8.1 (m, 8H, aromatic-H) and 11(s, 1H, NH). M/S, m/z (%) = 297(M^+ , 4), 132(M^+ , $\text{C}_7\text{H}_5\text{N}_2\text{O}_3$, 4), 104(M^+ , $\text{C}_8\text{H}_7\text{N}_3\text{O}_3$, 15), 76(M^+ , $\text{C}_8\text{H}_7\text{N}_5\text{O}_3$, 40), 77 (M^+ , $\text{C}_8\text{H}_8\text{N}_5\text{O}_3$, 100) and 78 (M^+ , $\text{C}_8\text{H}_9\text{N}_5\text{O}_3$,30). ^{13}C NMR: 50.50 (1C),110.86(1C), 118.86(1C), 120.27 (1C), 123.86 (2C), 124.97 (2C), 127.38(2C), 133.79 (1C), 142.51 (1C), 145.07 (1C) and 165.40(1C). Anal. Calc. for $\text{C}_{14}\text{H}_{11}\text{N}_5\text{O}_3$ (297): C, 56.56; H, 3.73; N, 23.56, found: C, 57.00; H, 3.84; N, 23.60%.

2 - (1*H* - benzo[d] 1, 2, 3 – triazol - 1-yl) – *N* - (3 - hydroxyphenyl) acetamide (7):

Yield 74%, m.p. 209-211 $^\circ\text{C}$. IR ($\bar{\nu}_{\text{max}}$, cm^{-1}): 3407(OH), 3360(NH), 3083 (CH-aromatic), 2935(CH- aliphatic) and 1667(CONH). ^1H NMR (DMSO, δH , ppm): 5.7(s, 2H, CH_2CO), 6.5 -8.1 (m, 8H, aromatic-H),9.4(s,1H, OH) and 10.5(s, 1H, NH). M/S, m/z (%) = 268(M^+ , 34), 133(M^+ , $\text{C}_7\text{H}_7\text{NO}_2$, 29), 104(M^+ , $\text{C}_8\text{H}_{12}\text{N}_2\text{O}_2$, 56), 76(M^+ , $\text{C}_8\text{H}_{12}\text{N}_4\text{O}_2$, 100) and 78 (M^+ , $\text{C}_8\text{H}_{14}\text{N}_4\text{O}_3$, 69). Anal. Calc. for $\text{C}_{14}\text{H}_{12}\text{N}_4\text{O}_2$ (268): C, 62.68; H, 4.51; N, 20.88; found: C, 63.01; H, 4.72; N, 21.00%.

2 - (1*H* - benzo[d] 1, 2, 3 – triazol - 1-yl) – *N* - (*p* -tolyl) acetamide (8):

Yield 80%, m.p. 244-246 $^\circ\text{C}$. IR ($\bar{\nu}_{\text{max}}$, cm^{-1}): 3276(NH), 3126 (CH-aromatic), 2979(CH- aliphatic) and 1688(CONH). ^1H NMR (DMSO, δH , ppm): 2.5(s,3H, CH_3), 5.7(s, 2H, CH_2CO), 7.1 -8.1 (m, 8H, aromatic-H) and 10.5(s, 1H, NH). M/S, m/z (%) = 266(

M+, 53), 132(M+, C₈H₈NO, 12), 104(M+, C₉H₁₀N₂O, 38), 76(M+, C₉H₁₀N₄O, 13), 78 (M+, C₉H₁₂N₄O, 32) and 77 (M+, C₉H₁₁N₄O,100). C¹³NMR: 50.42 (1C),110.88(1C), 118.97(1C), 123.79(2C), 127.25(2C), 129.2 (2C), 132.72 (1C), 133.83(1C), 135.88(1C), 145.04 (1C) and 164.06(1C). Anal. Calc. for C₁₅H₁₁N₄O (266): C, 67.65; H, 5.30; N, 21.04, found: C, 68.00; H, 5.44; N, 20.99%.

3 Results and Discussion

In the present work, 1*H*-benzo(*d*),1,2,3-triazole derivatives (**3,4,5,6,7,8**) (scheme1) obtained by reacting 1*H*-benzo(*d*),1,2,3-triazole (**2**) (Bashir, H., *et al* 2021) with 2-hloro-*N*-substituted(phenyl) acetamide (**a1 -a6**) in DMF in present K₂CO₃ on water bath for 24 hrs. The structure of compound (**3**) was confirmed by Elemental analysis and the IR spectrum. Which showed stretching bonds at 3323cm⁻¹ and 1689 cm⁻¹ corresponds (-NH-) and (-CO-) groups respectively. The ¹HNMR spectrum revealed the appearance of singlet single at 5.7 ppm attributed methylene protons, in addition to multiplet signals 7.3-8.1 ppm to seven aromatic protons and singlet signal at 10.7 ppm (-NH-). The mass spectrum of (**3**) showed molecular ion peak at m/z (327).

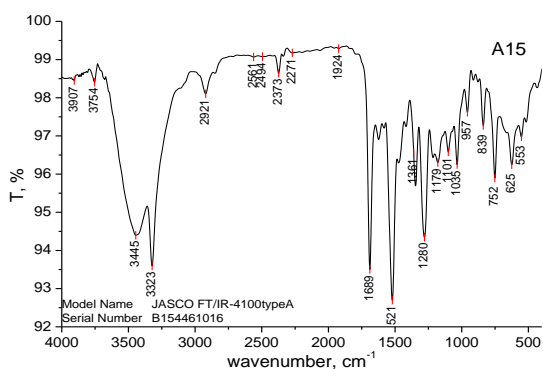


Figure: (1).IR spectrum (cm⁻¹) of compound (3)

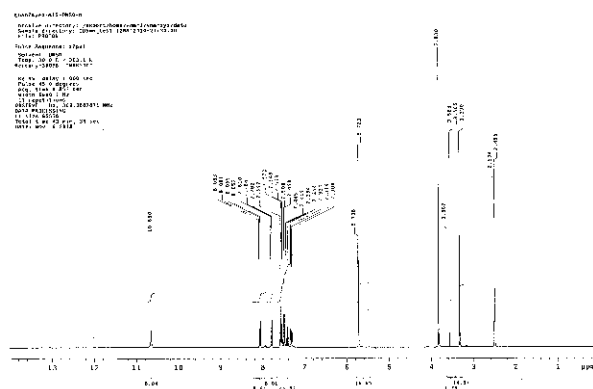


Figure: (2). ¹HNMR spectrum of compound (3)

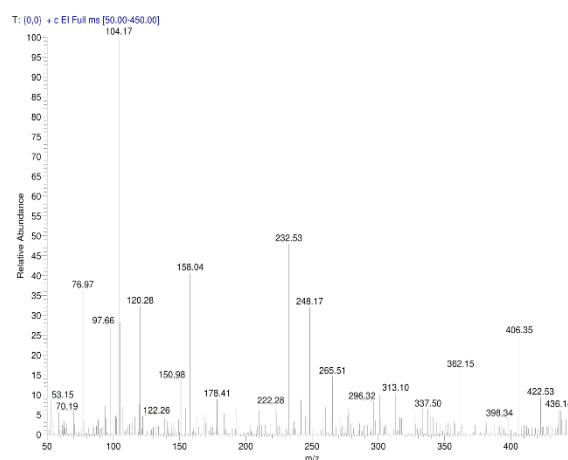


Figure: (3). Mass spectrum of compound (3)

The structures of compound (**4,5** and **6**) were characterized by the present of strong absorption bands of amidic carbonyl group at 1705cm⁻¹, 1689cm⁻¹ and 1697cm⁻¹ respectively, but absorption bands of (-NH-) group of compounds (**4,5** and **6**) appeared at 3186 cm⁻¹, 3316 cm⁻¹ and 3314cm⁻¹ respectively. The ¹HNMR spectrum of compound (**4,5** and **6**) showed singlet signals of (-NH-) group at 11.1ppm, 10.9 ppm and 11ppm respectively, also appeared singlet signal of (-CH₂-) group at 5.8 ppm of compound (**4, 5** and **6**). The mass spectrum of compounds (**4,5** and **6**) showed molecular ion peak at 286 that was consistent with the molecular weight of compounds. ¹³CNMR spectrum of compounds (**4**) and (**6**) appeared carbonyl group of amide (-CO-) at 165.17 ppm and 165.40 ppm respectively, in additional singles peak at 50.42 ppm and 50.50 ppm that indicated to (-CH₂-) group, respectively.

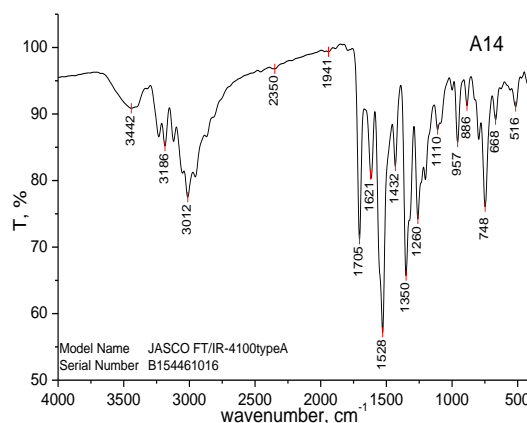


Figure: (4).IR spectrum (cm⁻¹) of compound (4)

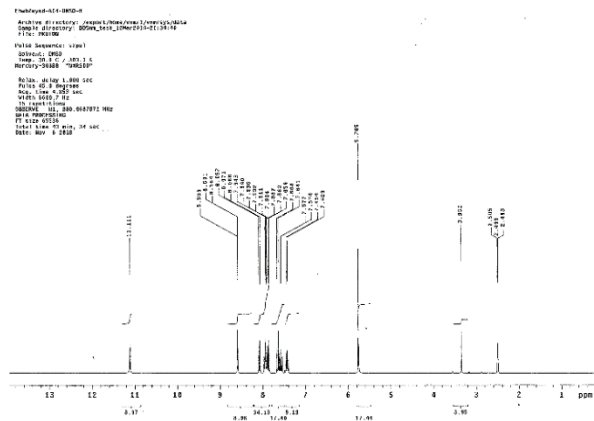


Figure: (5). ¹H NMR spectrum of compound (4)

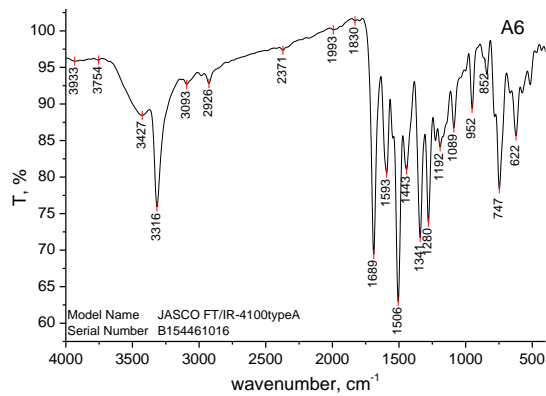


Figure: (8). IR spectrum (cm⁻¹) of compound (5)

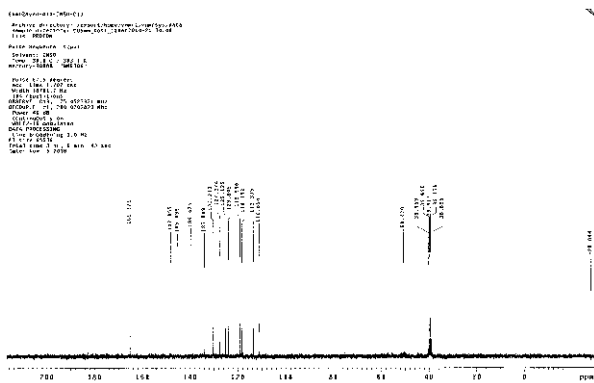


Figure: (6). ¹³C NMR spectrum of compound (4)

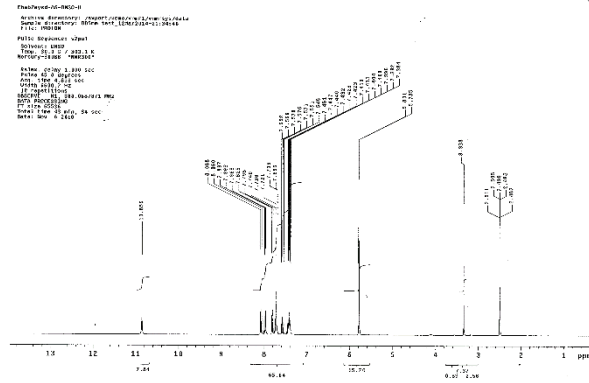


Figure: (9). ¹H NMR spectrum of compound (5)

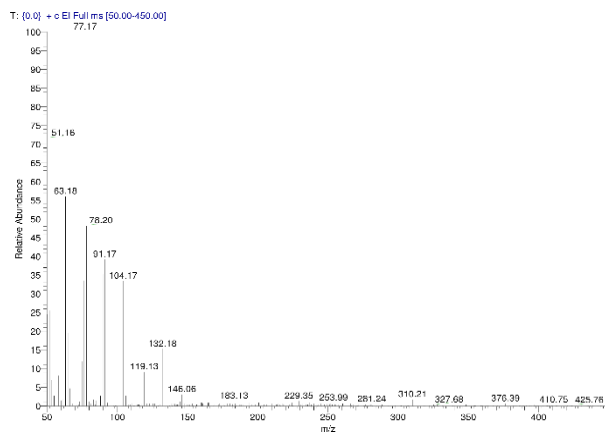


Figure: (7). Mass spectrum of compound (4)

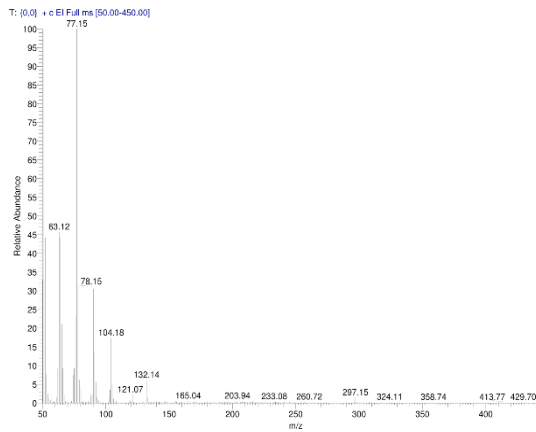


Figure: (10). Mass spectrum of compound (5)

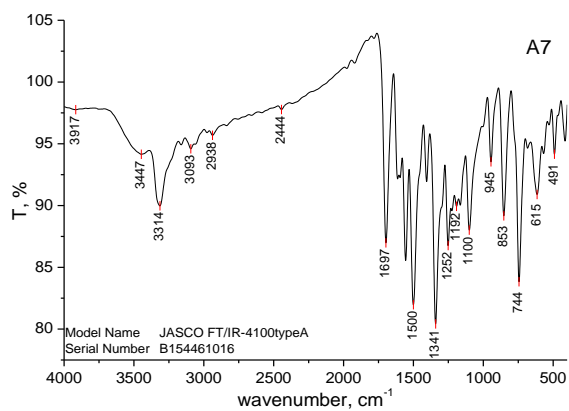
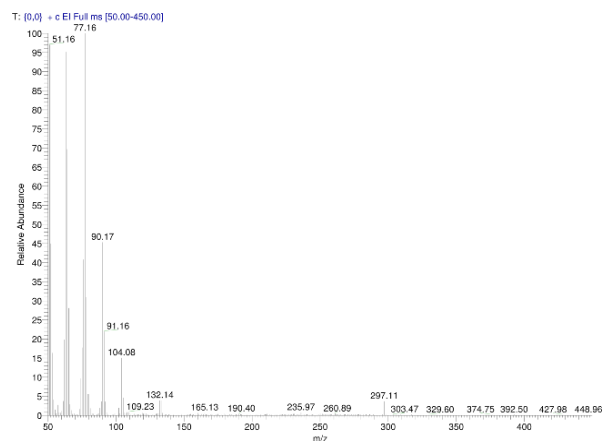
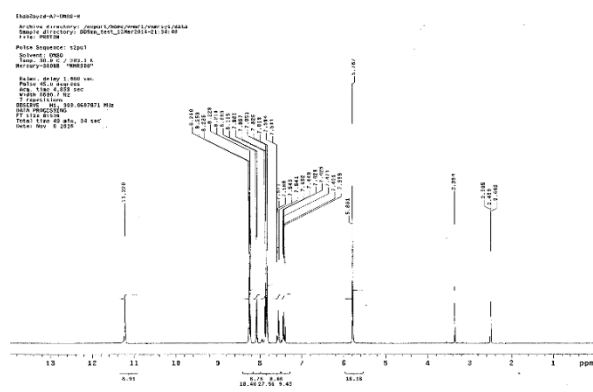
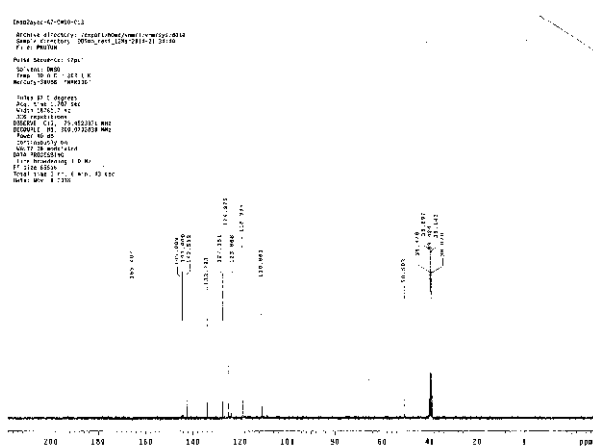
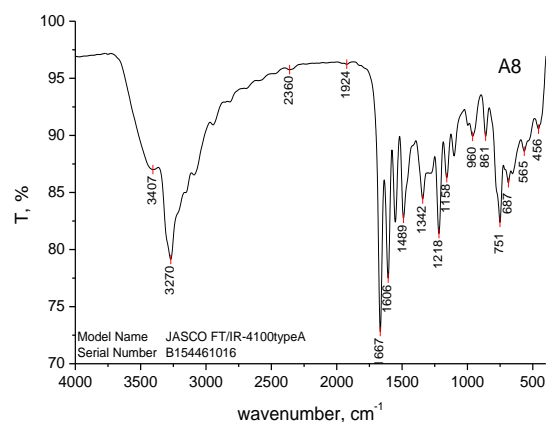
Figure: (11).IR spectrum (cm⁻¹) of compound (6)

Figure: (14). Mass spectrum of compound (6)

Figure: (12).¹H NMR spectrum of compound (6)Figure: (13).¹³C NMR spectrum of compound (6)Figure: (15).IR spectrum (cm⁻¹) of compound (7)

The structures of compound (7,8) were confirmed via ¹H NMR spectrum which revealed singlet signals of amidic groups at 10.5 ppm. also, singlet signal of (-OH) group at 9.4 ppm for compound (7). but its appeared singlet signal of compound (8) at 2.5 ppm. In other side its appeared methylene group of compound (7) and (8) at 5.7 ppm. IR spectrum of compounds (7) and (8) showed strong absorption bands of amidic group 1667 cm⁻¹ and 1688 cm⁻¹ respectively. The mass spectrum of compound (7) and (8) revealed m/z 268 and m/z 266 which corresponding to the molecular formula C₁₄H₁₂N₄O₂ and C₁₅H₁₄N₄O respectively. The ¹³C NMR spectrum of compound (8) appeared carbonyl group of amide (-CO-) at 164.03 ppm, also (-CH₂-) group observed at 50.42 ppm. We proposed a possible mechanism for the synthesis of substituted benzotriazoles from 1*H*-benzo(*d*)1,2,3-triazole (2) and 2 - Chloro - *N* - substituted phenyl acetamide (a1-a6) using K₂CO₃ as the catalyst (scheme 2)

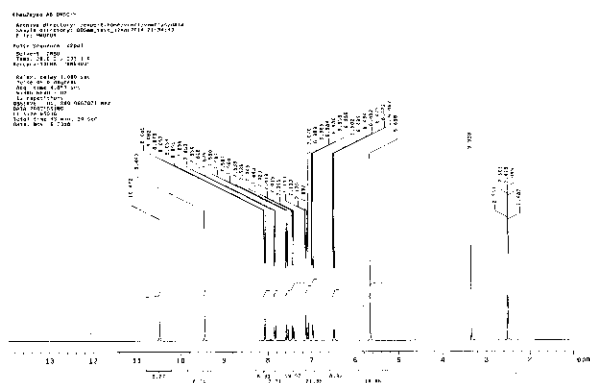


Figure: (16). ¹H NMR spectrum of compound (7)

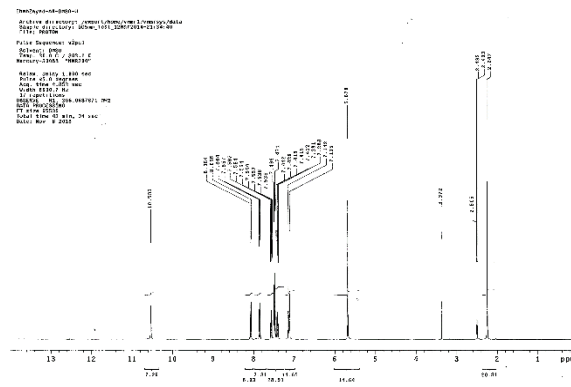


Figure: (19). ¹H NMR spectrum of compound (8)

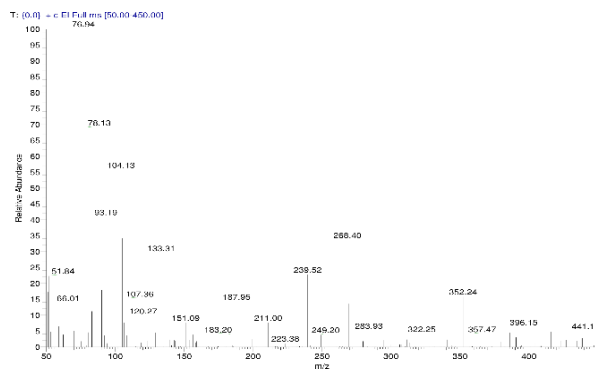


Figure: (17). Mass spectrum of compound (7)

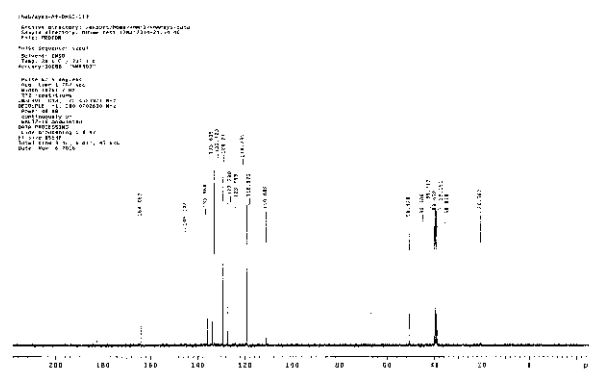


Figure: (20). ¹³C NMR spectrum of compound (8)

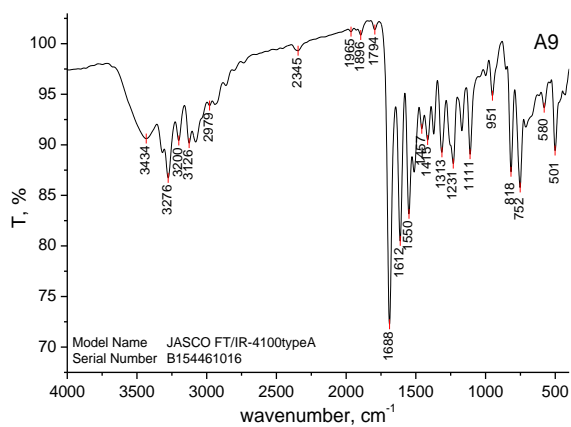


Figure: (18). IR spectrum (cm⁻¹) of compound (8)

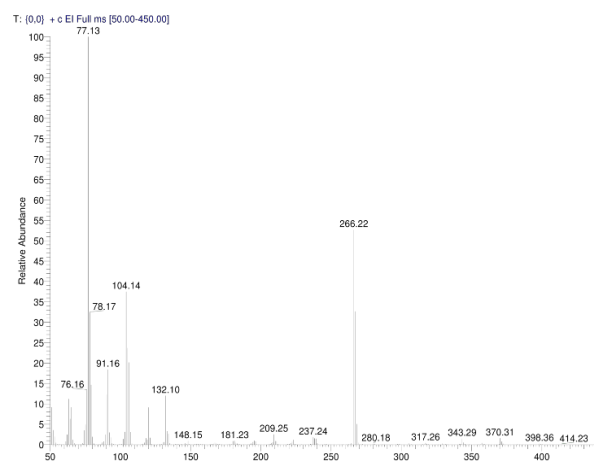
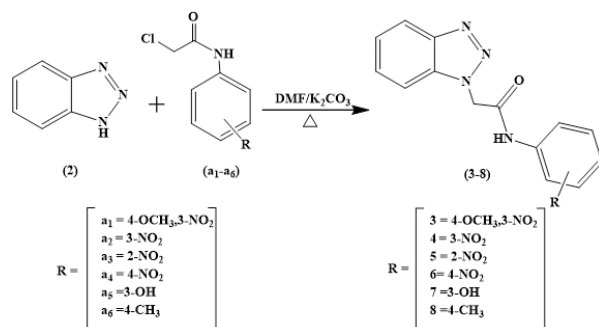
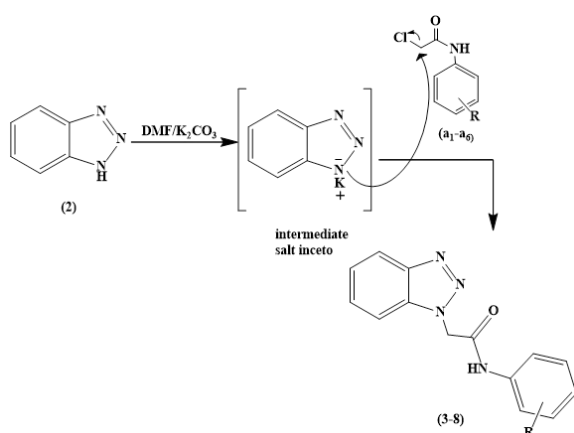


Figure: (21). Mass spectrum of compound (8)



Scheme 1



Scheme 2: proposed mechanism for the formation of compounds (3-8)

4 Conclusions

1*H*-benzo[d]1,2,3-triazole (**2**) is heterocyclic compound consisting of three nitrogen atoms and fused benzene ring. It is synthesized via diazotization process by treatment of *o*-phenylenediamine with sodium nitrite in glacial acetic acid. Which reacts with 2-chloro-*N*-(substituted phenyl) acetamide (**a₁** - **a₆**) in the presence of K_2CO_3 in DMF to give 2-(1*H*-benzo[d]1,2,3-triazol-1-yl)-*N*-(substituted phenyl) acetamide (**3-8**). Their structures were confirmed by infrared, 1H NMR, ^{13}C NMR and mass spectrometric analysis.

Acknowledgements

We thank the research committee and the Department of Chemistry of the University of Omar Al-Mukhtar for providing financial support.

Conflict of Interest: The authors declare that there are no conflicts of interest.

References

- Al-Omran, F., Mohareb, R. M., Abou El-Khair, A., (2002), synthesis and biological effects of new derivatives of benzotriazole as antimicrobial and antifungal agents, *J. heterocyclic chem*, 39, 877 – 883.
- Alpana, A., Shrikant, M., Pratyush, K., Abhibnav, B., Ruchita, T., (2020), Review on synthetic study of benzotriazole, *GSC biological and pharmaceutical sciences*, 11(02), 215 – 225. <https://doi.org/10.30574/gscbps.2020.11.2.0137>
- Bashir, H., Hashim, G. and Abdalfarg, N., (2021), Synthesis of Benzotriazole Derivatives, *international Invention of Scientific Journal*, 05 (3), 17-26. <https://doi.org/10.1016/j.ejmech.2012.05.028>
- Jain, N. P., Upassani, C. D., Kalkotwar, R. S., Jain, U. P., (2013), Synthesis and anti-inflammatory activity of *N*-(alkyl or aryl)-2-(1*H*-benzotriazol-1-yl)acetamide derivatives, *Research journal of pharmaceutical, biological and chemical sciences*, 4(3) 1470 -1480.
- Jamkhandi, C. M., Disouza, J. I., (2013), Synthesis and antimicrobial evaluation of 1*H*-Benzotriazol-1-yl {2-hydroxy-5-[(*E*) phenyldiazenyl] phenyl} methanone derivative, *international journal of pharmacy and pharmaceutical sciences*, 5(3)225 - 228.
- Noolvi, M. N., Patel, H. M., Kaur, M., (2012), Benzotriazoles: search for anticancer agents, *European journal of medicinal chemistry*, 54, 447-462.
- Ram, V. J., Sethi, A., Nath, M., Pratap, R., (2019), Five-membered heterocycles. In *The Chemistry of Heterocycles*, 149-478. Elsevier. <https://doi.org/10.1016/B978-0-08-1010334.00005-X>.
- Suma, B.V., Natesh, N. N., Madhavan, V., (2011), Benzotriazole in medicinal chemistry: An overview, *Journal of chemical and pharmaceutical research*, 3(6):375-381.
- Ueno, L. T., Ribeiro, R. O., Rocha, M.S., Suárez-Iba, M. E.V., Iba, K., Machado, F. B. C., (2003), About the benzotriazole tautomerism: An ab initio study, *Journal of Molecular Structure (theochem)*, 207-215. <https://doi.org/10.1016/j.theochem.2003.09.004>
- Uesaka, T., Ishitani, T., Sawada, R., Maeda, T., Yagi, S., (2020), Fluorescent 2-phenyl-2*H*-benzotriazole dyes with intramolecular *N-H...N* hydrogen bonding: Synthesis and modulation of fluorescence properties by proton-donating substituents, *Dyes and pigments*, <https://doi.org/10.1016/j.dyepig.2020.108672>



Air Pollution: Selected Fuel Stations in Benghazi City, Libya

Adel M. Najar*¹, Mohmed A. I Amajbary, Abduslam H. A. Awarfaly, Tahani Aeyad², Mona H. A. Bnhmad³, Naima Aeyad⁴, Aliaa M. M. Khalifa⁵

¹ School of Basic Science, Chemistry Department, Libyan Academy for Postgraduate Studies Benghazi, Libya.

^{2,3,5} Chemistry Department, Art and science Faculty, Al-Marj, Benghazi University, Libya.

⁴ Higher Institute of Science and Technology, Al-Marj, Libya.

DOI: <https://doi.org/10.37375/sjfsu.v3i1.299>

A B S T R A C T

ARTICLEINFO:

Received: 16 December 2022.

Accepted: 05 March 2023.

Published: 17 April 2023.

Keywords:

Fuel Stations, air pollution, Filling Station, Benzene, Xylene, VOCs, CO₂

This study aims to measure the amount of pollutants that might be present in the air of Benghazi city. Twelve refueling stations from different regions of Benghazi City in Libya were selected. The ambient air quality at all stations was investigated. Also, the evaporation of fuels from loosely closed underground tanks has been investigated for two fuel stations. Drager X-am7000 and MiniRAE-3000 Instruments were used to measure the concentration of CH₄, H₂S, CO, O₂, xylene, and benzene as pollutants in the atmosphere. The pollutant concentrations were within the range of the FEPA air quality standard in most stations; however, the measurement of these pollutants during tank refueling showed a high percentage in the surrounding area of the fuel tanks. Therefore, this study can contribute to understanding the air pollutants exposure and its effects on human health.

1 Introduction

At the local, national, and global levels, air pollution is seen as a serious issue today. Many nations have put restrictions on the amount of pollutants that can be released into the air. Many epidemiological studies have authenticated decrements in lung function and several additional health problems associated with long-time air pollution exposure (Aprajita et al., 2011). Many persuasive pieces of evidence exist for an association between air pollution and cardiovascular disease (Novikova et al., 2014). Air pollution consists of heavy metal or particles in the atmosphere that pose severe health and ecological threats. One of the main polluting compounds is benzene, a volatile chemical substance that with other substances constitutes gasoline. The health effect of vocational exposure to petroleum vapour and air pollution associated with vehicular sources have been thoroughly investigated among petrol-filing workers (Zamanian et al., 2018) (Spengler et al., 2011)(Qafisheh et al., 2021)(Rahimi Moghadam et al., 2019). It is well recognized that vehicular emitted air

pollution has a pernicious effect on health outcomes such as morbidity, mortality, and hospital admission. Furthermore, the economic costs could be great (Kingham et al., 2013). In addition to the spread of diseases among workers and neighbours, environmental problems can be caused by the activity of gas stations. For instance, the potential leakage of fuel and oil to the ground and groundwater, also distortion of the aesthetic face of the areas surrounding the gas station, especially when it is located in a crowded residential neighbourhood (Hazrati et al., 2016).

Given the complexity of factors influencing air quality and generally high uncertainty of the results of emission estimation and mathematical modelling, the most credible information about air pollution is estimated by direct measurement results. These are achieved by using reference measurement methods or methods recognized as equivalent to the reference (Parliament et al., 2008). The convenience of air quality monitoring stations for the performance of specific tasks can be assessed using various methods, depending mainly on the type of station (which is strongly dependent on its location), size

or specificity of the monitored area, and measurement range (Chan & Hwang, 1996) (Li et al., 2021). Essentially, in urban-industrial areas, there are three main types of monitoring stations: urban traffic stations, background stations and industrial stations. The measurement data acquired from these usually authorize the estimation of the average exposure to air pollution in the city, the impact of road transport and the impact of industry respectively. These impacts overlap each other depending on: the location of the station, the wind direction and the period assessed, which may reflect different types of emission sources in addition to the local and inflow background (Cyrus et al., 2012)(Oleniacz & Gorzelnik, 2021). The variability assessment of the pollutant concentration results in the air at various types of monitoring stations has been carried out, among other things, in research works (Kim et al., 2005)(Sówka et al., 2019). In some cases, it was achieved using cluster analysis or other statistical methods. Several applications of cluster analysis were described in (Govender & Sivakumar, 2020)(He et al., 2018). Moreover, the similarity assessment of air quality monitoring stations based on PM 2.5 concentrations enabled the detection of redundant stations while in diurnal concentration profiles of PM10 and black carbon were conducted. (Žibert & Pražnikar, 2012). Statistical significance tests were also conducted in air quality studies. For instance, in (Almeida-Silva et al., 2016), the Wilcoxon signed-rank test allowed for assessment of the statistical significance of the differences between indoor and outdoor PM10 concentrations (Battista et al., 2016). Used probability distribution, Poincaré sections, Skewness, Kurtosis, and cross-correlation of the different pollutants to estimate the level of air pollution in the city of Rome and the correlation of human activity sources with the pollutant release. Statistical analysis of spatiotemporal heterogeneity of the distribution of air quality index (using the Kruskal–Wallis rank-sum test method and the Wilcoxon signed-rank test) was also performed for urban zones by (Zhao et al., 2018). On the other hand, (Nikolopoulos et al., 2021) used statistical and entropy methods to investigate a 17-year PM10 time series that was recorded from air quality stations in Athens to delineate existing stochastic and self-organization trends.

This study aimed to estimate the harmful environmental effects that could result from the activities of gas stations in the city of Benghazi-Libya. The focus was placed on

the air quality near to these stations and the concentrations of some volatile organic compounds (VOCs) were determined. In general, the pollutant concentrations of these compounds were within the authorized percentage range.

2 Materials and Methods

In this paper, twelve different filling stations were studied. All stations were located in Benghazi city in Libya. However, the stations were located in different places within the city. The measurements of ambient air quality at all stations were measured once at one point which was in the center of each filling station. These one-point measurements aimed to investigate the concentrations of products of combustion and the volatile organic compounds that the workers and citizens are exposed to during working hours. The equipment used in the air quality monitoring and measurements are X-am 7000 and MiniRAE3000. The X-am 7000 particle gas Monitor was used in measuring the concentrations of the particulate matter. Each of the filling stations was visited, and the ambient air quality was measured at one point of the filling station. Moreover, some measurements have been taken during the supplying of the stations with fuel. Seven different air pollutants were measured, and their data was collected from each filling station. These pollutants include the suspended particulate matter (PM1, PM2.5, and TSP), CO, dinitrogen tetroxide (N₂O₄), sulphur dioxide (SO₂), hydrogen sulphide (H₂S), methane (CH₄), and volatile organic compounds. The data collected from each filling station were compared to the FEPA air quality standard (*Air Quality Guidelines for Europe*, 2000)(Garzón et al., 2015)(Colman Lerner et al., 2012) to determine whether the pollutant concentrations are within the permissible range.

3 Results and Discussions

Pollutant concentration measurements of the VOCs were determined three times. The average of these readings has been calculated. The concentrations of CO measured in our study in the (E) and (D) stations were slightly, but not significantly, higher than those of other stations at 34.67 and 35 ppm respectively, as shown in table-1 and figure-1.

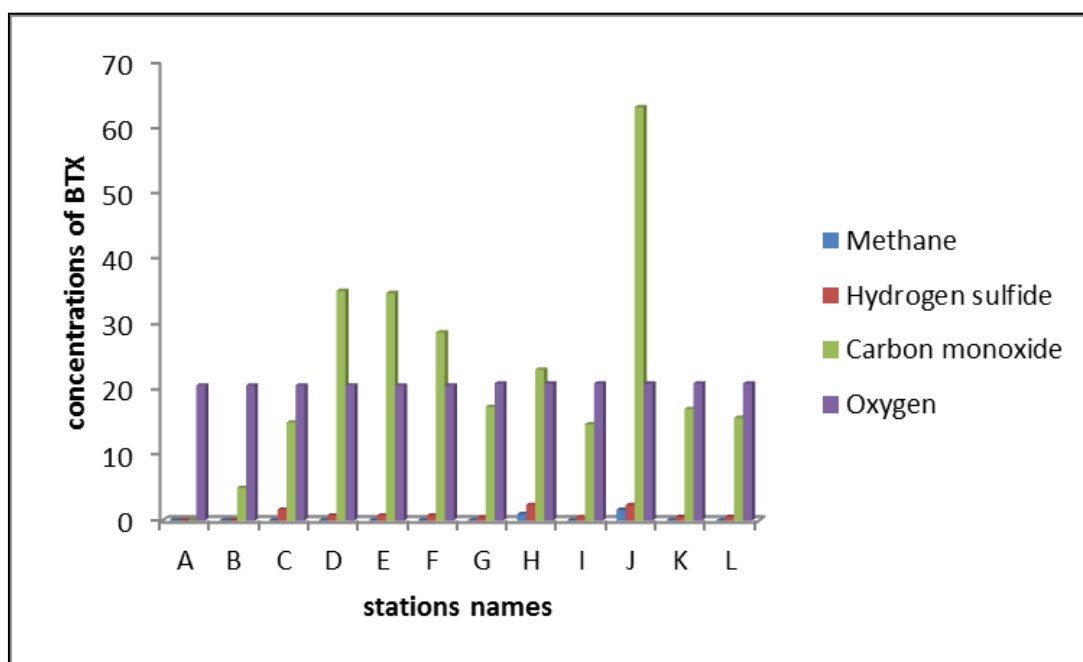


Figure 1: Concentration of VOCs

Table 1: Concentrations of methane, hydrogen sulfide, carbon monoxide and oxygen (VOCs)

Name of station	Methane CH ₄ LEL%	Hydrogen Sulfide H ₂ S ppm	Carbon monoxide CO ppm	Oxygen O ₂ Vol%
A	0	0	0	20.6
B	0	0	5	20.6
C	0	1.7	14.97	20.6
D	0	0.8	35	20.6
E	0	0.8	34.67	20.6
F	0	0.8	28.67	20.6
G	0	0.5	17.33	20.9
H	1	2.4	23	20.9
I	0	0.53	14.67	20.9
J	1.67	2.37	63	20.9
K	0	0.55	17	20.9
L	0	0.56	15.67	20.9

Average concentrations of toluene, benzene, and xylene (BTX) were measured. Their concentrations were significantly raised, the values obtained were 1544, and

2068 mg/m³ for benzene and xylene respectively in (E) station, and 1306 mg/m³ for toluene in (J) station as shown in (Table 2) and (Figure 2).

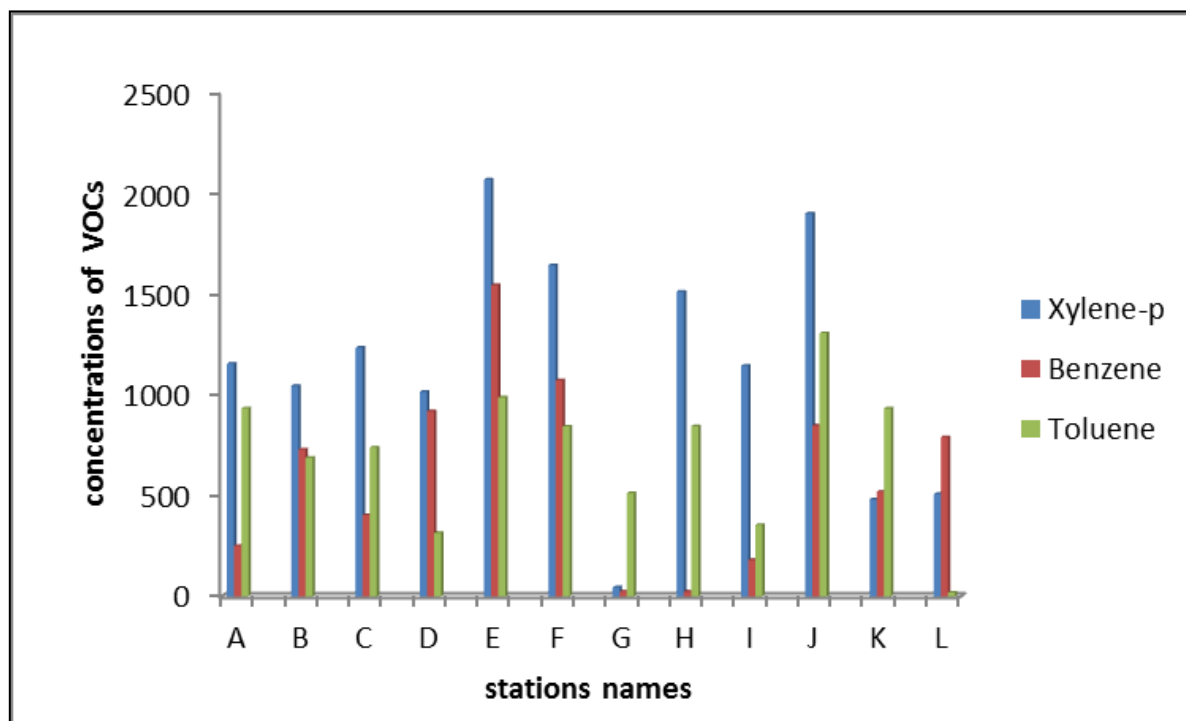


Figure 2: Concentration of BTX

Table 2: Concentrations of *P*-xylene (BTX), benzene, and toluene

Name of station	<i>P</i> -Xylene mg/m ³	Benzene mg/m ³	Toluene mg/m ³
A	1155	250.7	933.2
B	1044	729.4	687.9
C	1234	403.8	739
D	1015	918.2	315
E	2068	1544	987
F	1643	1072	843
G	46	25.4	511.9
H	1512	24.3	844.1
I	1145	180.7	354.5
J	1900	848.3	1306
K	481.6	519.3	932.1
L	508.8	790.2	19.4

(Table 3) shows the data obtained at fuel supply stations (C and J) near the tank nozzle of a station during refueling, where it was noted that the values were raised.

Table 3: Concentration of pollutants at the tank nozzle (during refueling).

Name of station	Carbon monoxide CO ppm	Oxygen O ₂ Vol%	H ₂ S ppm	Methane CH ₄ LEL%	Toluene mg/m ³	Benzene mg/m ³	<i>P</i> -Xylene mg/m ³
C	378	20.4	15.7	20	1047	802.7	3617
J	126	20.6	7.2	10	1447	2667	3096

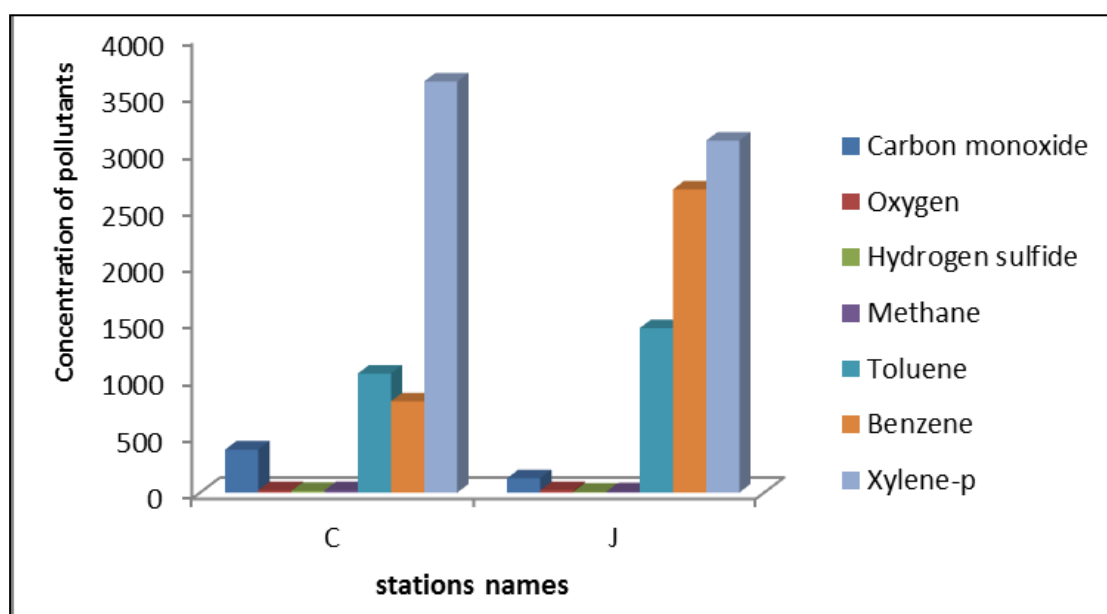


Figure 3: Concentration of pollutants at the tank nozzle (during refuelling).

In addition, table 4 shows high readings recorded at the (H) station. The high values recorded were concentrated near the station's washing machine. It appears that benzene was used as a cleaner.

Generally, BTX compound concentrations were acceptable in most of the stations, especially those that have a large area and good ventilation. However, the concentrations of BTX compounds were high, as well as the concentrations of methane, hydrogen sulphide, and carbon monoxide gas during the supply of stations with fuel, which led to the alarm of the measuring device sounding. It was also found in some stations that benzene was used as a cleaning substance without considering the dangers of this use and without any protection. Furthermore, liquid waste resulting from car wash centres and oil change workshops inside the stations are discharged to the municipal sewer networks without any treatment or restrictions.

Table 4. Concentration of pollutants near the station's washing machine.

Name of station	Toluene mg/m ³	Benzene mg/m ³	P-Xylene mg/m ³
H	3485	808	2033

4. Conclusion

In conclusion, the results show that the construction projects and operations of gas stations within the city of Benghazi are not subject to any monitoring or control, which led to the expansion of various activities within these stations, without considering the risks of such

activities to public health and the environment. Furthermore, this study has shown that the measured concentrations of polluting gases inside the stations were somewhat acceptable, except for those measured at the tank nozzle, which requires taking more means of protection for workers inside the station.

It is recommended that all filling stations and their activities are placed under inclusive control, in addition to locating them away from residential areas.

Acknowledgments

The authors would like to address thanks to Sirte Company for oil in Libya.

References

- Air Quality Guidelines for Europe, Second Edition., (2000). 91.
- Almeida-Silva, M., Faria, T., Saraga, D., Maggos, T., Wolterbeek, H. T., & Almeida, S. M. (2016). Source apportionment of indoor PM10 in Elderly Care Centre. *Environmental Science and Pollution Research International*, 23(8), 7814–7827. <https://doi.org/10.1007/s11356-015-5937-x>
- Aprajita, Panwar, N. K., & Sharma, R. S. (2011). A study on the lung function tests in petrol-pump workers. *Journal of Clinical and Diagnostic Research*, 5, 1046–1050.
- Battista, G., Pagliaroli, T., Mauri, L., Basilicata, C., & De Lieto Vollaro, R. (2016). Assessment of the air pollution level in the city of Rome (Italy). *Sustainability (United States)*, 8(9). <https://doi.org/10.3390/su8090838>

- Chan, C.-C., & Hwang, J.-S. (1996). Site Representativeness of Urban Air Monitoring Stations. *Journal of the Air & Waste Management Association*, 46(8), 755–760. <https://doi.org/10.1080/10473289.1996.10467510>
- Colman Lerner, J. E., Sanchez, E. Y., Sambeth, J. E., & Porta, A. A. (2012). Characterization and health risk assessment of VOCs in occupational environments in Buenos Aires, Argentina. *Atmospheric Environment*, 55, 440–447. <https://doi.org/https://doi.org/10.1016/j.atmosenv.2012.03.041>
- Cyrus, J., Eeftens, M., Heinrich, J., Ampe, C., Armengaud, A., Beelen, R., Bellander, T., Beregszaszi, T., Birk, M., Cesaroni, G., Cirach, M., de Hoogh, K., De Nazelle, A., de Vocht, F., Declercq, C., Dèdelè, A., Dimakopoulou, K., Eriksen, K., Galassi, C., ... Hoek, G. (2012). Variation of NO₂ and NO_x concentrations between and within 36 European study areas: Results from the ESCAPE study. *Atmospheric Environment*, 62,374–390. <https://doi.org/https://doi.org/10.1016/j.atmosenv.2012.07.080>
- Garzón, J. P., Huertas, J. I., Magaña, M., Huertas, M. E., Cárdenas, B., Watanabe, T., Maeda, T., Wakamatsu, S., & Blanco, S. (2015). Volatile organic compounds in the atmosphere of Mexico City. *Atmospheric Environment*, 119(722), 415–429. <https://doi.org/10.1016/j.atmosenv.2015.08.014>
- Govender, P., & Sivakumar, V. (2020). Application of k-means and hierarchical clustering techniques for analysis of air pollution: A review (1980–2019). *Atmospheric Pollution Research*, 11, 40–56.
- Hazrati, S., Rostami, R., Fazlzadeh, M., & Pourfarzi, F. (2016). Benzene, toluene, ethylbenzene and xylene concentrations in atmospheric ambient air of gasoline and CNG refueling stations. *Air Quality, Atmosphere & Health*, 9(4), 403–409. <https://doi.org/10.1007/s11869-015-0349-0>
- He, H., Li, M., Wang, W., Wang, Z., & Xue, Y. (2018). Prediction of PM_{2.5} concentration based on the similarity in air quality monitoring network. *Building and Environment*, 137, 11–17. <https://doi.org/https://doi.org/10.1016/j.buildenv.2018.03.058>
- Kim, E., Hopke, P. K., Pinto, J. P., & Wilson, W. E. (2005). Spatial variability of fine particle mass, components, and source contributions during the regional air pollution study in St. Louis. *Environmental Science & Technology*, 39(11), 4172–4179. <https://doi.org/10.1021/es049824x>
- Kingham, S., Longley, I., Salmond, J., Pattinson, W., & Shrestha, K. (2013). Variations in exposure to traffic pollution while travelling by different modes in a low density, less congested city. *Environmental Pollution*, 181, 211–218. <https://doi.org/https://doi.org/10.1016/j.envpol.2013.06.030>
- Li, F., Zhou, T., & Lan, F. (2021). Relationships between urban form and air quality at different spatial scales: A case study from northern China. *Ecological Indicators*, 121, 107029. <https://doi.org/https://doi.org/10.1016/j.ecolind.2020.107029>
- Nikolopoulos, D., Alam, A., Petraki, E., Papoutsidakis, M., Yannakopoulos, P., & Moustris, K. P. (2021). Stochastic and Self-Organisation Patterns in a 17-Year PM(10) Time Series in Athens, Greece. *Entropy (Basel, Switzerland)*, 23(3). <https://doi.org/10.3390/e23030307>
- Novikova, L. V., Stepanova, N. Y., & Latypova, V. Z. (2014). The human health risk assessment from contaminated air in the oil-producing areas (On the Example of Novoshehminsky Region of the Republic of Tatarstan). *Advances in Environmental Biology*, 109+.
- Oleniacz, R., & Gorzelnik, T. (2021). Assessment of the variability of air pollutant concentrations at industrial, traffic and urban background stations in Krakow (Poland) using statistical methods. *Sustainability (Switzerland)*, 13(10). <https://doi.org/10.3390/su13105623>
- Parliament, T. H. E. E., Council, T. H. E., The, O. F., & Union, P. (2008). 11.6.2008.
- Qafisheh, N., Mohamed, O. H., Elhassan, A., Ibrahim, A., & Hamdan, M. (2021). Effects of the occupational exposure on health status among petroleum station workers, Khartoum State, Sudan. *Toxicology Reports*, 8, 171–176. <https://doi.org/10.1016/j.toxrep.2020.12.025>
- Rahimi Moghadam, S., Afshari, M., Moosazadeh, M., Khanjani, N., & Ganjali, A. (2019). The effect of occupational exposure to petrol on pulmonary function parameters: A review and meta-analysis. *Reviews on Environmental Health*, 13(6), 732–738. <https://doi.org/10.1515/reveh-2019-0048>
- Sówka, I., Chlebowska-Styś, A., Pachurka, Ł., Rogul-Kozłowska, W., & Mathews, B. (2019). Analysis of Particulate Matter Concentration Variability and Origin in Selected Urban Areas in Poland. In *Sustainability (Vol. 11, Issue 20)*. <https://doi.org/10.3390/su11205735>

- Spengler, J., Lwebuga-Mukasa, J., Vallarino, J., Melly, S., Chillrud, S., Baker, J., & Minegishi, T. (2011). Air toxics exposure from vehicle emissions at a U.S. border crossing: Buffalo Peace Bridge Study. Research Report (Health Effects Institute), 158, 5–132.
- Zamanian, Z., Sedaghat, Z., & Mehrifar, Y. (2018). Harmful Outcome of Occupational Exposure to Petrol: Assessment of Liver Function and Blood Parameters among Gas Station Workers in Kermanshah City, Iran. *International Journal of Preventive Medicine*, 9, 100. https://doi.org/10.4103/ijpvm.IJPVM_296_16
- Zhao, X., Gao, Q., Sun, M., Xue, Y., Ma, R. J., Xiao, X., & Ai, B. (2018). Statistical analysis of spatiotemporal heterogeneity of the distribution of air quality and dominant air pollutants and the effect factors in Qingdao Urban Zones. *Atmosphere*, 9(4), 12–16. <https://doi.org/10.3390/atmos9040135>
- Žibert, J., & Pražnikar, J. (2012). Cluster analysis of particulate matter (PM10) and black carbon (BC) concentrations. *Atmospheric Environment*, 57, 1–12. <https://doi.org/https://doi.org/10.1016/j.atmosenv.2012.04.034>



Improvement the Germination Characteristics in Aged Seeds of *Hordeum vulgare* Plants by Some Invigoration Solutions

Rabha B. Hamad

Botany Department, Science Faculty, Omar Al Mukhtar University, Al bayda, Libya.

DOI: <https://doi.org/10.37375/sjfsu.v3i1.1015>

A B S T R A C T

ARTICLE INFO:

Received: 12 February 2023

Accepted: 27 March 2023

Published: 17 April 2023

Keywords:

Hordeum vulgare L, Aged seeds, growth parameters, carbohydrate constituents, KNO₃., ZnSO₄.

Seeds viability and seed vigour decline during storage, **The aim** of this research was the improvement of seed quality by treatment with KNO₃ and ZnSO₄ of *Hordeum vulgare* L. plants aged seeds. **Experiment** was on barley seeds storage for different periods of (1 year and 4 years) in open storage type and treatment these by using seeds invigoration solutions, 3% zinc sulfate (ZnSO₄), and 3% potassium nitrate (KNO₃) in addition to non primed seed (control) to know their effect on viability and vigour of seeds and determine the best one on them. **The results** showed that growth parameters, total available carbohydrate (TAC) content and starch (St) contents decrease under long storage, while total soluble sugars (TSS) increased. While at treatment by ZnSO₄ and KNO₃ there was an increase in total germination, mean germination time, radical and plumule lengths, seedling fresh and dry weight, and vigour index, also increasing in TSS, St, and TAC contents. However, the treatment with KNO₃ was the best compared with treatment by ZnSO₄. **Conclusions:** It can be concluded from this study that using invigoration solutions led to improve germination and vigour of barley seeds for all the seed storage.

1 Introduction

The most important factor affecting crop production is the quality of the seed. Seeds deteriorate during the period of prolonged storage. It is one of the most intriguing and challenging scientific problems of universal concern. (Raj *et al.*, 2013). (Abnavi and Ghobadi, 2012) studied the effects of seed storing on germination of two wheat cultivars, which is a loss in quality in terms of seed viability and vigour during seed storage. (Alam *et al.*, 2021) reported that the biochemical properties like amino acid, lipid, oil, soluble sugar and enzymatic activities are changed in aged seeds. The quality of the seeds has to be protected for a prescribed period of storage without quality deterioration until sowing. Seed deterioration is triggered by many biotic and abiotic factors such as temperature, relative humidity, seed

moisture content and storage pathogen & insects (Pallavi *et al.*, 2003). All these factors are directly or indirectly associated with lipid oxidation, a process that happens both through enzymatic and non-enzymatic pathways, that causes cell membrane disintegration and eventually causes seed death (Oenel *et al.*, 2017).

Different methods can be used to improve agricultural production while seed priming is the most suitable and simple technique to increase germination, emergence and yield (Dalil, 2014). Seed priming theory was proposed by (Heydecker *et al.*, 1973) it is a technique which is used before seed sowing, it includes seeds hydration to permit metabolic events prior to germination while preventing the emergence of radicals. (Adnan *et al.*, 2020) Improvement in metabolic events improves the speed of seed germination in vegetables, ornamental species and some small-seeded grasses. There are many

methods of seed priming such as halo priming, hydro priming, Osmo priming, and matrix priming. Seed priming is a simply easy, low-cost, highly effective and low-risk method. Halo priming is the soaking of seeds in salts (KNO₃, NaCl, CaSO₄ and CaCl₂) These techniques improves seed germination. (Khan *et al.*, 2009).

(Abnavi and Ghobadi , 2012) reported that the seed priming with potassium nitrate (KNO₃) gibberellins (GA₃), led to improve seeds germination and seedling growth s in Wheat plants.

Zinc is one of the most important nutrients that play a key role in all living organisms for their growth and development. It is an abundant trace element and acts as a co-factor for more than 300 enzymes, also plays a vital role in cell division, protein formation, and nucleic acid metabolism, and increases the chlorophyll contents (Cakmak, 2008).

Potassium is the third most important primary macronutrient, after Nitrogen (N) and phosphorus (P). It has a key role in many plant physiological processes such as the translocation of photo-assimilates stomata regulation, and enzymatic activation (Ahmed *et al.*, 2021).

Barley is number four in terms of the area cultivated in cereal grains in the world at 49.24 million hectares. The major uses of the barley grown are for malting and as a feed source own at a wide variety of locations. (Wolf *et al.*, 2019). Barley (*Hordeum vulgare* L.) has been a central and staple commodity crop in Libya. Barley's usages include its ground flour for making Bazine, a famous traditional Libyan cuisine and bread. Furthermore, barley grains and hay are used extensively for feeding livestock, and malting. Libya's production of barley was significantly low compared with other neighbouring countries' yields, 260 thousand tons in 2005, therefore, the country relies completely on importing barley seeds from the foreign markets, and Barley plays a major role in Libya's agricultural sector. It is considered a principal food grain in the daily life of the Libyan people (Elbeydi *et al.*, 2007). Storage is essential for food security or as a product bank for exchange into cash when required (Yusuf and He, 2011).

Seed quality reduces during the period of prolonged storage for this reason was the aim of this research improvement of seed quality by treatment with KNO₃ and ZnSO₄ aged seed of seedling *Hordeum vulgare* plants.

2 Materials and Methods

Seed Material

Barley (*Hordeum vulgare* verity Acsad 176) seeds obtained from the crops department, agriculture faculty, Omar Al-Mukhtar university, were employed in the current study for different periods of storage non-aged seed (1 year) , and aged seed, (4 years). The seeds were selected for uniformity of size, shape and color. Before germination, seeds were surface sterilized by soaking for two minutes in 4% (v/v) sodium hypochlorite, then washed several times with distilled water.

Priming Treatment

Before germination, each group of seeds (non-aged seed, and aged seed) was soaked in 8 ml of 3% KNO₃ 3 and 3% ZnSO₄n of solution (3 grams/100 ml) and kept at 20°C for 24 hours. In addition, to controlling (unprimed non-aged seed and aged seed), to know their effect on the viability and vigour of Seeds and determine the best one for them, after priming, seeds were washed with distilled water and then left to dry for 24 hours at room temperature between two filter papers. Then the seeds (control and treatment) were placed in 12 cm Petri dishes on a layer of filter paper. Ten seeds were placed in each Petri dish with 50ml distilled water. At 25°C, three replications in each treatment were measured parameter germination was calculated by recording some of germinated seeds in all treatments starting from the second day, on which the first germination occurred, germination criterion is the appearance of radical outside seed cover (Ganatsas, *et al.*, 2008): at end of the experiment took final results of following qualities'

Measured in this experiment were:

- Germination percentage (GP) is measured on the seventh day using the formula $GP (\%) = (\text{total number of germinated seeds} / \text{total seed}) \times 100$. (Ashraf and Abu-Shakra, 1978).

- Mean germination time (MGT) calculated according to the formula of (Ellis and Roberts, 1981):

$MGT = \sum (ni/di)$. With ni: number of germinated seeds and di: day of counting.

- Radical length (RL) in (mm), length (plumule PL) in (mm), radical and plumule lengths: The radical and plumule lengths were taken using a graduated ruler; the

averages were calculated by taking five seedlings from each plate.

- Seedling fresh weight (SFW) in mg, Seedling dry weight (SDW) in mg. Seedling's dry weights were measured after oven drying at 70°C for 72h of seedlings

- Vigour Index (VI) using the formula of (Abdul- Baki and Anderson, 1973).

$$VI = [TG (\%) \times \text{seedlings length (mm)}] / 100]$$

: Seedlings length= radical length + plumule length.

Extraction and estimation of carbohydrate constituents: Total available carbohydrate (TAC), total soluble sugars (TSS), and polysaccharides (starch).

Extraction method

This was done by the alcoholic extraction method as described by Younis (1963) in which an aliquot of oven-dry biomass (100 mg) was extracted twice (2x2h) with 80% ethanol in a reflux apparatus on a boiling water bath. The two alcoholic extracts and washings were added together, evaporated to few mls in an air-dry oven at 50°C and the residue taken in water and made to known volume.

Clarification of the extract

The common lead acetate method was done in which to an aliquot of the extract, basic lead acetate solution was added drop wise with continuous stirring until another drop of lead acetate gave no further turbidity. The deleading agent, disodium hydrogen phosphate (Na₂HPO₄) was added drop wise to the supernatant solution with continuous stirring until the precipitation of lead phosphate was completed. The solution was then centrifuged. The clear supernatant was neutralized to phenol red end point then made to known volume and used for the determination of soluble sugars.

Estimation of total available carbohydrate content (TAC)

This is usually referred to as the total available carbohydrate (TAC) since it does not include cellulose. This fraction was estimated by the procedure described by (Murata *et al.*, 1968), in which an aliquot (100 mg) of the finely powdered oven-dry plant material was introduced into a boiling tube. Ten ml of 0.7 N HCl were then added and the tube placed in a boiling water bath for 30 min. The hydrolyzed was neutralized to phenol red end point and made to known volume. An aliquot of hydrolyzes was assayed as glucose according the method described by (Dubois *et al.*, 1956). To two ml of sugar

extract one ml of 5% phenol was added then 5 ml of concentrated sulphuric acid were added rapidly. The tubes were allowed to stand for 10 min shaken gently and placed for 10-20 min in water bath at 30°C. Absorbance was read at 490 nm. A calibration curve using pure glucose was made from which the amount of sugar was calculated as mg g⁻¹ d.m.

Estimation of total soluble sugars (TSS)

An aliquot (5ml) of the purified sugar extract was mixed with 5ml of 1 N HCl in a boiling tube and placed in boiling water bath for 60 min and then the hydrolyzate was neutralized to phenol red end point and made to known volume. An aliquot (2 ml) was taken and assayed as glucose by the method described before.

Estimation of polysaccharides (St.)

This is referred mainly to starch content (St) and it was deduced from the differences between the total available carbohydrate and the total soluble sugars (TAC- TSS).

Statistical analysis:

Statistical analysis of the results was done using Excel 2007 in this study; ANOVA was used for comparison between independent samples. LSD was estimated $p \leq 0.05$.

3 Results

Changes of germination percentage (GP), and mean germination time (MGT):

The results showed that decrease in total germination (GP), under long storage conditions(control) where to reduce this value in (GP)from 77.4% in non-aged seed to 58.3% in aged seed , while at treatment by ZnSO₄ and KN03 for aged seed (4years old) there was increased in(GP)these values were 61.23%,84.45%

compared with control 58.3%. Figer. (1) Showed that decrease in germination (GP), in aged seed and compared to non-aged seed, and increase in GP after treatment.

Mean germination time (MGT) in seed *Hordeum vulgare* L. was reduce in aged seeds compared with non-aged seeds (control), where reduced these values from 1.34 to 0.77 seedlings. day⁻¹, while there was increasing in the mean germination time (MGT) in aged seed (4years old) at treatment with ZnSO₄ and KN03compared with control. The values were 1.65 seedlings. day⁻¹ and 2.82 seedlings.day⁻¹compared with control 0.77 seedlings.day⁻¹ compared to control Figer.2showed that decrease in

(MGT), in aged seed and compared to non-aged seed, and increase in MGT after treatment (figer.2).

Figure. (1). Changes in germination percentage:

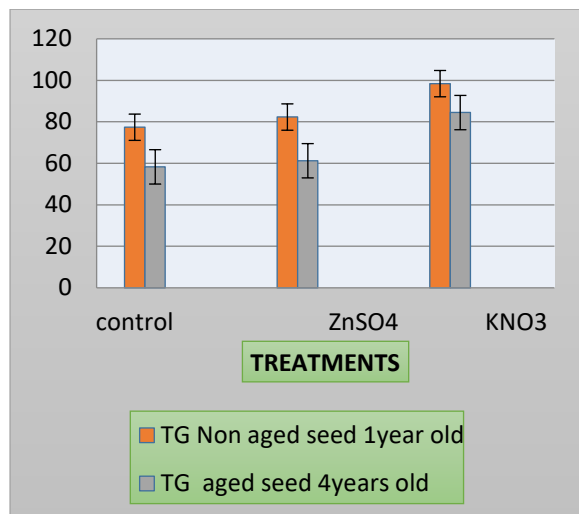
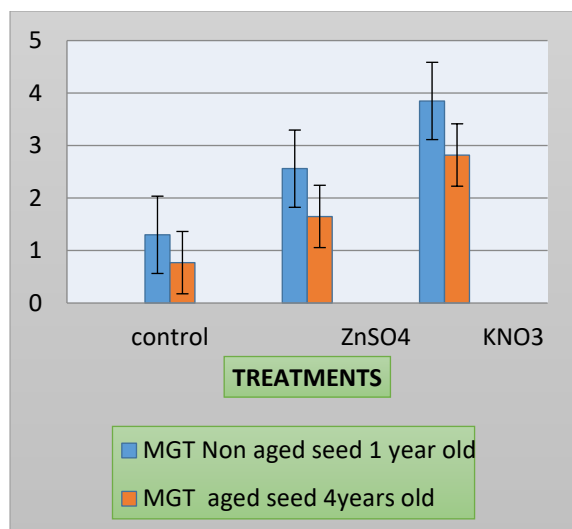


Figure. (2). Changes in Mean germination time:



Each datum indicates the mean value and vertical lines on top of the bars indicate the standard error of means.

Changes Radical length (RL) and a plumule length (PL):

(Table 2) showed that the radical length and plumule length of seedling barley plants significantly decreased in response to storage conditions. Where report these values of (RL) 49.3 mm and 26.4mm in aged seed and non-aged seed (control.) respectively. While the values of (PL) were 36.23mm, and 13.83 mm in aged seed and non-aged seed (control.) respectively (Table 1). But after treatment

by ZnSO4 and KN03 the results showed to increasing in radical length and plumule length in seedling of *Hordeum vulgare* L plants where the values of (RL) were 41.6 mm, 64.3mm compared to control 26.4mm. While (PL) report these values 33.52 mm, 46.56mm compared to control 13.83mm. The values in (Table1) showed to improve growth parameter of seedlings aged seed by invigoration solutions.

Table. (1). Changes of radical length (RL) in (mm) and plumule length (PL) in (mm) of seedlings barely plants.

Parameter	RL(mm)		PL(mm)	
	Non aged seed	Aged seed	Non aged seed	Aged seed
Control	49.3 ^d	26.4 ^f	36.23 ^c	13.83 ^f
ZnSO4	52.5 ^c	41.6 ^d	45.45 ^b	33.52 ^c
KNO3	79.7 ^a	64.3 ^b	62.47 ^a	46.56 ^b
P-Value	0.042		0.031	
LSD	18.45		16.08	

P-value: was considered significant at P≤0.05.

LSD: Mean indexed by different superscripts is significantly different at P≤0.05

Changes in seedling fresh weight (SFW), and Seedling dry weight (SDW) of seedling barley plants.

The results showed that decrease in seedling fresh weight (SFW) and Seedling dry weight (SDW) under long storage conditions, where reports these values were 2.13mg, 1.13 mg of (control) none aged seed and aged seed, respectively. While at treatment by ZnSO4 and KN03 for aged, seed (4years old) there was an increase in (SFW) these values were 1.45mg, and 2.68 mg compared with control 1.13mg. Seedling dry weight (SDW) of seedling barley plant was reduced in aged seeds compared with non-aged seeds (control), where reports these values were 0.34mg, 0.21mg of (SDW) in non-aged seed and aged seed, respectively. While there was increasing in Seedling dry weight (SDW) of aged seed(4 years old) the treatment with ZnSO4 and K N 03 compared with control these values were 0.23 mg, 0.47

mg compared with control 0.21mg. The data in (Table, 2) report a decrease in seedling fresh weight (SFW), and Seedling dry weight (SDW) in aged seed compared to non-aged seed and an increase in these values after treatment.

Table. 2. Changes of seedling fresh weight (SFW) and Seedling dry weight (SDW) of seedling barely plants.

Parameter	SFW(mg)		SDW(mg)	
	Non aged seed	Aged seed	Non aged seed	Aged seed
Control	2.13 ^c	1.13 ^f	0.34 ^c	0.21 ^d
ZnSO ₄	2.56 ^b	1.45 ^d	0.46 ^b	0.23 ^d
KNO ₃	3.83 ^a	2.68 ^b	0.66 ^a	0.47 ^b
P-Value	0.001		0.024	
LSD	0.27		0.15	

P-value: Was considered significant at $P \leq 0.05$

LSD: Mean indexed by different superscripts is significantly different at $P \leq 0.05$

Changes of Seedling Vigour Index (SVI) of seedling barley plants.

The results in (table 3) found a significant decrease in Seedling vigour index, in seed storage for 4 years compared to seed storage for 1years where this value reduce from 66.2 to 23.5. While vigour index of seedling was a significant increase at stored seeds for 4 years and treatment with ZNSO₄ (46) compared with seedlings from control seeds (23.5), and stored seeds for 4 years and treatment with KNO₃ was increasing significantly (93.6) compared with seedlings from control seeds (23.5). At (Table 3) showed that: the seedling vigour index (SVI) of barley plants significantly increased in response to treatment by KNO₃.

*Significant levels, in aged seeds (93.6)

**Very significant levels represented in non-aged seed (127).

Table.3. Changes of Seedling Vigor Index (SVI) of seedling barely plants.

Treatment	Aged seed	Non aged seed
Control	66.2 ^c	23.5 ^e
ZnSo ₄	80.6 ^b	46 ^d
KNO ₃	127 ^{a**}	93.6 ^{a*}
P-Value	0.006	
LSD	15.4	

P-value: Was considered significant at $P \leq 0.05$

LSD: Mean indexed by different superscripts is significantly different at $P \leq 0.05$

Changes of carbohydrate constituents

Data in Table 4 showed decreasing of total available carbohydrate (TAC) content and starch (St) contents, in radical of untreated plants of seed storage 4years compared to seed storage 1years the decrease of (St) and TAC was 15% and 1% respectively. **Table. (4a)**

Similarly, the results reported decreasing of starch (St) and (TAC) content in pulumela of seed storage 4years compared to seed storage 1years this reduce was 16% and 10%. **Table. (4b)**

Conversely, increase the TSS content in radical and pulumela of seed storage 4years compared to seed storage 1years was 1.28-, 1.3- fold. **Table. (4a & b)**

While during treatment by ZnSO₄ the increase of the TSS, St, and TAC content in radical and pulumela of barley plants.

Increased in TSS, St, and TAC content in radical (seed storage 4years) were 2.4-, 1.2 -, 1.5 - fold respectively compared to control. The corresponding values for pulumela were 1.9-and 1.3-, 1.4-fold, respectively (Table 4a & b).

Similarly. At treatment by KNO₃ the results report increasing of TSS, St, and TAC content in radical and pulumela, of seed storage 4years compared to control. The values in radical were 3.2-, 1.2-, 1.7-fold respectively compared to control. The corresponding values for pulumela were 2.3-, 1.4-, 1.5-fold, respectively (Table 4a & b). The content of total soluble sugar (TSS), total available carbohydrate (TAC) and starch (St) at treatment by KNO₃ was higher than treatment by ZnSO₄.

Table. (4a) Changes of carbohydrate constituents of seedling barley plants.

Seeds old & Treatments		Radical		
		TSS	ST	TAC
1y	Control	10.54 ^d	39.48 ^b	50.02 ^d
	ZnSO ₄	29.06 ^c	41.51 ^a	70.57 ^b
	KNO ₃	41.53 ^a	47.90 ^a	89.43 ^a
4y	Control	13.44 ^d	33.71 ^b	47.15 ^d
	ZnSO ₄	32.86 ^b	38.97 ^b	71.83 ^b
	KNO ₃	43.14 ^a	39.26 ^b	82.40 ^a
P-Value		0.031*	0.001*	0.001*
LSD		4.16	6.1	7.2

P-value: was considered significant at $P \leq 0.05$.

LSD: Mean indexed by different superscripts is significantly different at $P \leq 0.05$.

Table. (4b) Changes of carbohydrate constituents of seedling barley plants.

Seeds old & Treatments		Plumule		
		TSS	ST	TAC
1y	Control	10.26 ^d	74.95 ^c	85.21 ^b
	ZnSO ₄	22.66 ^b	83.43 ^a	106.09 ^a
	KNO ₃	29.23 ^b	94.27 ^a	123.50 ^a
4y	Control	13.56 ^d	63.04 ^c	76.60 ^c
	ZnSO ₄	25.28 ^b	79.19 ^b	104.47 ^a
	KNO ₃	31.19 ^a	85.26 ^a	116.45 ^a

P-Value	0.008*	0.0001*	0.001*
LSD	4.50	6.5	7.1

P-value: was considered significant at $P \leq 0.05$.

LSD: Mean indexed by different superscript is significantly different at $P \leq 0.05$

Discussion

Seed characteristics decrease under long storage conditions due to ageing. It is the reason of declining in germination, emergence and seedling growth (Soltani *et al.*, 2016). The results in this study showed that Seed characteristics decrease under long storage, including germination percentage (GP); mean germination time (MGT), Plumule length (PL), Radical length (RL), fresh and dry weight of seedling, and seedling vigour index of barely plants. **Table 1, 2 and 3)**

Following these results, other studies reported a decline of growth parameters during the storage of seed the other plants such as (Pallavi *et al.*, 2003) on sunflower plants and (Yousif, 2010) on sorghum.

Exposure of seeds to high temperatures and relative humidity during storage cause the reactive oxygen species to accumulate in the bilayer phospholipid membrane. Reactive oxygen species have been widely recognized as the main factor of seed ageing causing seed deterioration (Laloi *et al.*, 2004). The species include free radicals like superoxide anion ($O_2^{\bullet-}$), hydroxyl radical ($\bullet OH$); non-radical molecules like hydrogen peroxide (H_2O_2), and singlet oxygen (1O_2), (Sharma *et al.*, 2012). (Kibinza *et al.*, 2006) reported the loss of viability in sunflower seeds during ageing was associated with the decline of antioxidant enzyme activity caused by the accumulation of free radicals hydrogen peroxide and lipid peroxidation. Once the seeds are imbibed in the water, enzymatic mechanisms in the seeds initiate the production of reactive oxygen species, especially in the mitochondrial respiratory chain of the metabolically active seeds (Bailly, 2004). Excess of ROS oxidised and denatured protein structures in the cells, caused cellular membrane starts to disorganize, and gradually lose its integrity and selectivity, leading to the rapid increment of water imbibition in the cells and affecting embryo viability (Kapoor *et al.*, 2011; Peng *et al.*, 2011).

Seed invigoration techniques with, chemicals, are used to reduce a seed deterioration (Duraimurugan *et al.*,

2011) in the present study, using invigoration solutions KNO₃ and ZnSO₄ led to increase of the growth parameters including total germination (TG), mean germination time (MGT), Seedling length (SL), Radicle length (RL), fresh and dry weight of seedling, and vigour index, for all the seed storage. At (Table 3) showed that: the seedling vigour index (SVI) of barley plants significantly increased in response to treatment by KNO₃. Potassium plays vital roles in most the biochemical and physiological processes as enzyme activation, protein synthesis, photosynthesis is, movement, energy transfer, phloem transport, and stress resistance (Meharg, 2011).

The results of this study contribute to the understanding of germination seeds through the carbohydrate metabolism in seeds during storage, total available carbohydrate content in radical and pulumela were declined. (Table 4 a & b) Of barley seeds storage for different periods of (1 year and 4 years) this was accompanied with increasing of total soluble sugars reflecting their roles as regulators. (Alam *et al.*, 2021). during storage, biochemical properties like, carbohydrate, and soluble sugar are changed. The process of seed deterioration is most pronounced. In carbohydrate rich seeds the processes are described by the degree of concentration of soluble sugar. Generally, it is known that total carbohydrate declines with seed ageing Bernal-Lugo and Leopold, (1992). reported that the soluble sugars present in embryo may serve as important components of protection or may contribute to the deteriorative changes occurring during seeds storage. Examination of the changes in sugars during accelerated aging of seeds with a marked decline in mono saccharides and in raffinose Sucrose content remains relatively stable.

Using invigoration solutions KNO₃ and ZnSO₄ led to an increasing of all carbohydrate constituents in barely plants compared to those untreated plants. Increase in germination of KNO₃ primed seeds recorded over control. This increase in germination may be due to the activity of α -amylase due to osmopriming. Amylases are key enzymes that play a vital role in hydrolyzing the seed starch reserve, thereby supplying sugars to the developing embryo Abnavi, and Ghobadi, (2012).

4 Conclusions

Conclusions: It can be concluded from this study that using invigoration solutions led to improve germination

and vigour of barley seeds for all the seed storage duration. In addition, stored barley seed treatment by KNO₃ was the best compared treatment by ZnSO₄. The priming may be an effective method to meet the demands of farmers during the culture in the field for this reason, further studies are needed to use invigoration solutions to assess the efficacy during the later stages of plant growth.

Acknowledgements

The author wishes to express his gratitude to the Department of Botany, Faculty of Science, University of Omar Al Mukhtar. I would also like to thank the Agriculture faculty, at Omar Al-Mukhtar University for providing seeds.

Conflict of Interest: The author declares that there are no conflicts of interest.

References

- Abdul-Baki, A. A., & Anderson, J. D. (1973). Vigor determination in soybean seed by multiple criteria 1. *Crop science*, 13(6), 630-633
- Abnavi, M. S., & Ghobadi, M. (2012). The effects of source of priming and post-priming storage duration on seed germination and seedling growth characteristics in wheat (*Triticum aestivum* L.). *Journal of Agricultural Science*, 4(9), 256.
- Adnan, M., Rehman, H. A., Asif, M., Hussain, M., Bilal, H. M., Adnan, M., & Khalid, M. (2020). Seed priming; an effective way to improve plant growth. *EC Agriculture*, 6(6), 01-05.
- Ahmad, I., G. Zhou, G. Zhu, Z. Ahmad, X. Song, G. Hao, Y. Jamal and M.E.H. Ibrahim. (2021). Response of leaf characteristics of BT cotton plants to ratio of nitrogen, phosphorus, and potassium. *Pak. J. Bot.*, 53(3): 873-881.
- Alam, A. T. M. M., Haque, M. M., Rasul, M. G., Khan, M. A. A., & Karim, M. A. (2021). Changes of Jute Seed Qualities under Ambient Storage Condition. *Annals of Bangladesh Agriculture*, 25(1), 79-87.
- Ashraf, C. M., & Abu-Shakra, S. (1978). Wheat seed germination under low temperature and moisture stress. *Agronomy Journal*, 70(1), 135-139.

- Bailly, C. (2004). Active oxygen species and antioxidants in seed biology. *Seed science research*, 14(2), 93-107.
- Baill, C., El-Maarouf-Bouteau, H., & Corbineau, F. (2008). From intracellular signaling networks to cell death: the dual role of reactive oxygen species in seed physiology. *Comptes rendus biologies*, 331(10), 806-814
- Bernal-Lugo, I., & Leopold, A. C. (1992). Changes in soluble carbohydrates during seed storage. *Plant physiology*, 98(3), 1207-1210.
- Cakmak, I. (2008). Enrichment of cereal grains with zinc: Agronomic or genetic biofortification? *Plant and Soil*, 302(1): 1-17.
- Dalil, B. (2014). Response of medicinal plants to seed priming: a review. *International Journal of Plant, Animal and Environmental Sciences*, 4(2), 741-745
- Duan HM, Ma YC, Liu RR, Li Q, Yang Y, Song J (2018) Effect of combined water logging and salinity stresses on halophyte *Suaeda glauca*. *Plant Physiol. Biochem.* 127:231-237.
- Dubois, M., Gilles, K.A., Hamiton, J.K., Rebers, P.A. and Smith, F. (1956). Phenol sulphuric acid colourimetric method. In "Methods in Carbohydrate Chemistry", ed. Whistler, R. L. and Wolfrom, M. L. Academic press, New York, 388-389.
- Duraimurugan, P., Raja, K., & Regupathy, A. (2011) An eco-friendly approach for management of pulse beetle, *Callosobruchus maculatus* through neem formulations assisted with pitfall trap. *Journal of Food Legumes*, 24(1), 23-27.
- Ellis, R. H., & Roberts, E. H. (1981). The quantification of ageing and survival in orthodox seeds. *Seed Science and Technology* (Netherlands).
- Elbeydi, K. R., Aljdi, A. A., & Yousef, A. A. (2007). Measuring the supply response function of barley in Libya. In *African Crop Science Conference Proceedings* (Vol. 8, pp. 1277-1280).
- Ganatsas, P., Tsakalimi, M., and Thanos, C., (2008). Seed and cone diversity and seed germination of *Pinus pinea* in Strofylia Site of the Natura 2000 Network Biodiversity and Conservation, 17: 2427-2439
- Heydecker, W., Higgins, J., & Gulliver, R. L. (1973). Accelerated germination by osmotic seed treatment. *Nature*, 246(5427), 42-44.
- Kapoor, N., Arya, A., Siddiqui, M. A., Kumar, H., & Amir, A. (2011). Physiological and biochemical changes during seed deterioration in aged seeds of rice (*Oryza sativa* L.). *American Journal of Plant Physiology*, 6(1), 28-35.
- Khan, H. A., Ayub, C. M., Pervez, M. A., Bilal, R. M., Shahid, M. A., & Ziaf, K. (2009). Effect of seed priming with NaCl on salinity tolerance of hot pepper (*Capsicum annuum* L.) at seedling stage. *Soil and Environment*, 28(1), 81-87.
- Kibinza, S., Vinel, D., Côme, D., Bailly, C., & Corbineau, F. (2006). Sunflower seed deterioration as related to moisture content during ageing, energy metabolism and active oxygen species scavenging. *Physiologia Plantarum*, 128(3), 496-506.
- Krishnan, A., Venkataraman, V., Fik-Rymarkiewicz, E., Duda, T., & Sharma, R. K. (2004). Structural, biochemical, and functional characterization of the calcium sensor neurocalcin δ in the inner retinal neurons and its linkage with the rod outer segment membrane guanylate cyclase transduction system. *Biochemistry*, 43(10), 2708-2723.
- Laloi, C., Apel, K., & Danon, A. (2004). Reactive oxygen signalling: the latest news. *Current opinion in plant biology*, 7(3), 323-328.
- Marthandan, V., & Jerlin, R. (2017). Effects of Seed Storage Conditions on Biochemical Changes of Freshly Harvested High Moisture Undried Rice Seeds cv. CO 51. *Int. J. Curr. Microbiol. App. Sci*, 6(12), 2807-2813.
- Meharg, A (2011). *Marschner's Mineral Nutrition of Higher Plants*. Edited by P. Marschner. Amsterdam, Netherlands: Elsevier/Academic Press, pp. 684, US \$124.95. ISBN 978-0-12-384905-2. *Experimental agriculture* 48, 305-305 (2012)
- Murata, T., Akazawa, T. and Shikiko, F. (1968). Enzymic mechanism of starch breakdown in germinating rice seeds. *Plant Physiol.*, 43: 1899-1905
- Oenel, A., Fekete, A., Krischke, M., Faul, S. C., Gresser, G., Havaux, M., & Berger, S. (2017). Enzymatic and non-enzymatic mechanisms contribute to lipid oxidation during seed aging. *Plant and Cell Physiology*, 58(5), 925-933
- Pallavi, M., Kumar, S. S., Dangi, K. S., & Reddy, A.V. (2003). Effect of seed ageing on

- physiological, biochemical and yield attributes in sunflower (*Helianthus annuus* L.) cv. Morden. SEED RESEARCH-NEW DELHI-, 31(2), 161-168.
- Peng, B., Li, Y., Wang, Y., Liu, C., Liu, Z., Tan, W., & Li, Y. (2011). QTL analysis for yield components and kernel-related traits in maize across multi-environments. *Theoretical and applied genetics*, 122, 1305-1320.
- Raj, D. E. S. H., Dahiya, O. S., Arya, R. K., Yadav, A. K., & Kumar, K. (2013). Improvement in germination characteristics in artificially aged seeds of okra (*Abelmoschus esculentus*) by osmoconditioning. *Indian Journal of Agricultural Sciences*, 83(7), 699-702.
- Sharma P, Jha AB, Dubey RS, Pessaraki M (2012). Reactive oxygen species, oxidative damage, and antioxidative defense mechanism in plants under stressful conditions. *J. Bot.* pp. 1-26.
- Sultana, N., Md. Y. Ali, Md. S. Jahan and S. Yasmin. (2016). Effect of storage duration and storage devices on seed quality of Boro rice variety BRRI dhan47, *Journal of Plant Pathology and Microbiology*, 8(1): 2-6.
- Thirusenduraselvi, D., & Jerlin, R. (2010). Effect of pre-germination treatments on the emergence percentage of bitter melon cv. CO 1 seeds. *Tropical Agricultural Research and Extension*, 10.
- Wolf, P., Moon, D., & Mason, R. E. (2019). Determination of optimum harvest date for winter malting quality barley in Northwest Arkansas. *Discovery, the Student Journal of Dale Bumpers College of Agricultural, Food and Life Sciences*, 20(1), 86-93.
- Yousif, A. A. (2010). Effect of seed age, size and moisture content on seed quality of sorghum (*Sorghum bicolor* L. Moench). *Research Journal of Agriculture and Biological Sciences*, 6(4), 522-529.
- Yusuf, B. L., & He, Y. (2011). Design, development and techniques for controlling grain post-harvest losses with metal silo for small and medium scale farmers. *African Journal of Biotechnology*, 10(65), 14552-14561.
- Younis, M.E. (1963). Organic acid metabolism in storage organs. M.Sc. Thesis, Faculty of Sci. Mansoura Univ. Mansoura, Egypt.



Assessment of the Cytological and Chemical Changes of Some Varieties of Potato Tissues (*Solnum tubersum* L.) under Salt Stress

Ghada Elrgaihy¹, Adel Elmaghrabi¹, Said Abojreeda¹, Huda Abugnia² and Elmundr Abugnia¹

¹ Libyan Biotechnology Research center Department tissue culture plant.

² Education Faculty, Tripoli University, Libya.

DOI: <https://doi.org/10.37375/sjfsu.v3i1.937>

ABSTRACT

ARTICLE INFO:

Received: 09 February 2023

Accepted: 26 March 2023

Published: 17 April 2023

Keywords:

In vitro, *Solnum tubersum*, salinity and Sodium Chloride.

In vitro culture can provide a controlled and uniform system for studying the morphological and chemical effects of salt stress at the tissue development level. Explants cultured under a biotic stresses such as salinity has been examined through morphological and chemical analyses. This has led to much information through studies of plants subjected to salt treatments. The aim of the work reported in this study, was to evaluate two varieties of Potato (Spunta and Agria) for their competence for Sodium Chloride (NaCl) Within the (0, 10, 20, 40, 60, 80 mmol) tolerance and tissues developments. Data reported in this study are summarized as follows:

Increase salinity levels in MS medium to a decrease the number of leaves, number of branches and plant length of each explant. Plantlets established from two varieties potato and developed on MS medium supplemented with NaCl proved to be tolerant to and 80 mmol NaCl, in addition to the control treatment.

1 Introduction

Plant tissue culture

Plant tissue culture technique to produce plant by using plant tissue, considered as one of the most important methods being used in plant propagation, while the produced plant often identical to the mother plant which being taken to establish the primary tissue cultures (AL-Baher *et al.*, 1999). Plant tissue culture was defined as a science containing several methods used to grow plant tissue or cells on artificial media under controlled growth conditions (Abugnia *et al.*, 2013).

Using plant tissue culture rather than conventional agriculture the produced plants number will be largely increased with homogeneity in the physiological composition and usually resulted free- disease plants through plant micro propagation seedlings which will be available throughout the year specially those plants in their dormancy period (Arias, 1992). Recently significant development has been found in the field of

plant propagation using plant tissue culture method which called plant Micropropagation while this technique has become one of the most important applications on both scientific and economic levels (Albaher *et al.*, 1999).

Plant potato (*Solnum tubersum* L.)

Taxonomic classification.

Potato in the rank fourth as strategic and economic crop after rice, wheat and corn (Bowen, 2003). Furthermore potato is daily food for more than 75-90% world population (Santamaria and Elia, 1997). The target plant in this study is potato plant, which is known in some Arab countries as the potato and the scientific name is (*Solnum tubersum* L.) follows the Solanaceae family which include about 90 species and 2000 variety, while the formations of tubers are only from specie which potato belong to *S. tubersum* and seven other cultivated species as well as 154 wild species on the other hand potato considered as one of the most

important and most used vegetable crop, moreover potato crops tops the list of tuberous (Hassan, 1999). Solanaceae family includes 24 species resistant to salinity (David and Nilsen, 2000). while potatoes are generally moderately sensitive to temperate salts, (Maas and Hoffman, 1976; Katerjietal., 2000).

Status of potato plant in Libya

At the local level potato crop is an important vegetable crop in terms of agriculture and consumption and there are two variety which are Spunta and Arinda the most important cultivars cultivated in Libya.

The imported potato cultivars are planted in Libya in two period during the year, the first one cultivated in autumn time which starts in September and second one cultivated in spring time which growing in January and February on the other hand potato production depends on seeds breeding the tuber must be imported tubers from abroad every year. Potato seeds are imported during July and August to be ready for agriculture in autumn while farmers reserve part of the production of the autumn season to grow it in spring season, planted in spring season usually decreased in both quality and quantity due to that potato plant is propagated by vegetative way which let the tuber infected by bacterial and viral disease (Abughnia et al., 2013). As well-known potato *S. tuberosum* propagated by traditional methods but on the other hand many attempts have been made to develop methods of propagation specially by plant tissue culture to provide disease-free seeds in a relatively short time compared to traditional methods (Miller and 1984; Wang and Hu, 1985; Dodds et al., 1992). Moreover, the easiest and fastest method to propagate potato which provide free-disease plants and tubers specially virus disease is plant tissue culture method (Khosrarifaret al., 2008).

Soil salinity

Soil salinity considered as one of the historical problems facing agricultural production for many years ago and even now days because it has an effect on plant growth through its effect on water and essential nutrients uptake by plants (Zubaidi, 1989). Furthermore salinity is one of the most important major stress affecting plant species and their productivity, particularly in arid and semi-arid areas, while salinity significantly reduces the production of many plant species also due to salinity problems world loses about 10 million hectares of arable land annually and lands with salinity problems has reached

594 million hectares (Munns, 2010). There fore researchers studied effect of salinity on plant growth and development, thus the study the effect of salinity on the plant depends on putting plants in different levels of salt concentrations by controlling salt quantity knowing that effect of salinity on plant depends on stress severity time it occurs, length exposure period and stage of plant growth (Sinhabab and Kumar, 2003).

Plants require the presence of some salts in the root zone for their growth and development but the optimal concentration of these salts is usually low for many plant species 10^3 mmol or less, The higher concentrations (100-150 mmol) even for the salt necessary, causes a state of salt stress which can reduce the growth, development and productivity of plants moreover effective of salinity on plants depending on the type of salts, their concentration, plant species, variety and growth stage of the plant (Chapman and Nieman, 2000).

Salt stress happens as a result of high concentration of sodium and potassium hydroxide, which negatively effects the rate of the water absorption by plant roots in addition salinity affects most aspects of plant growth and development also involves morphological changes (Flowers, 2001; Sheldon et al., 2004).

The main aim of this study is to determine the sensitively of the embryos to sodium chloride toxicity for two potato variety Spunta and Agria. The study was carried out at the plant tissue culture laboratory which belong to Biotechnology Research Center located in Tajoura region to determine the best level of tolerance of the potato tuber buds for sodium chloride salt.

2 Materials and Methods

Agria variety

Agria variety measured as Semi-late maturing, Its tubers are very large, oval longitudinal, outer color yellow and interior dark yellow, soft, superficial eyes, high in dry matter content, suitable for the manufacture of chips, thick stem standing, color crimson light, large leaves, big white flower, resistant to virus A, immune against virus X and resistant to gold nematodes,. (Khosrarifaret al., 2008).

Spunta variety

Spunta is Dutch variety characterized by medium early maturing, very low in dry matter ratio, drought

resistance, resistance to virus Y, immune to virus A, many stems spread over side with crimson color at base and leaf hubs. The leaves are relatively small and drooping, flowers are white and small while the tubers are large, long, slightly curved, somewhat pointed of its top, soft, its outer color is pale yellow, its interior color is light yellow and the buds are very superficial. Agria is among the best five varieties in terms of high productivity. (Khosrarifar et al., 2008).

Sample collection

Tubers of Spunta and Agria varieties have been taken after were imported from Netherlands during the season 2015 by Libyan agricultural marketing company.

First stage

1. Buds induction

After the tubers were cleaned with soap and water then dried on filter paper at the room temperature, placed in a dark place to induce them to produce buds (Figure.1)



Figure. (1) Potato tubers placed in a dark place to induce them to produce buds

After growing buds and reaching 1-2 cm during 4-6 weeks (Figure .2) the selected shoots were taken and surface sterilization was performed.



Figure. (2): Tuber buds of Spunta and Agria varieties.

Surface sterilization of potato tubers buds.

The vegetative parts (potato tubers buds) were collected from the plant and cut into parts of suitable lengths then placed in under running water for 30 minutes to remove surface contaminants from soil and insect residues ,after wards samples were transferred to the laminar airflow cabinet for sterilization by using ethanol with 70% concentration for two minutes then samples were sterilized by sodium hypochlorite (Clorox) with concentrations 2%, 2.5% and 3% for 20 minutes with keeping stirring of the samples time to time for sterilization from bacteria and fungus. finally samples were washed by using sterilized distill water for three times for five minutes each time to remove the toxic effect of sodium hypochlorite.

Media preparation

prepared MS media for the purpose of obtaining culture media (Murashige and Skoog, 1962), which mainly containing, 3% sucrose and 0.7% agar before adjusting the pH on level of 5.7 to 5.8 the prepared cutter media MS was placed in sterilized 250ml with value of 25ml in each jar and prepared media sterilized in autoclave at 121C and air pressure 1.02bar for 15min.

Buds development *in vitro* culture

The buds of the potato samples were sterilized while the culture operation started by planted the selected buds in containers supplemented with MS media however one bud placed in each container for the purpose of obtaining tissue cultures free of pathogens (Fig.3) afterwards samples were incubated in growth chamber at 16 hour light /day and 8 hour dark/day while the light intensity was $400\mu\text{mol}^{-1}\text{m}^{-2}\text{sec}^{-1}$ photon flux density and, temperature $25\pm 2\text{C}^\circ$ and 40% humidity, while all the conditions were under control and the samples incubated for four weeks.



MS media under the seam conditions for another four weeks. **Figure. (3)**

Second stage Subculture process

After four weeks of growth and a whole plants being obtained through tissue culture technique Fig. (4). Subculture stage started by transfer the single nodes on MS media under the seam condition for another four weeks (Fig. 5)



Figure. (4) plants obtained through tissue culture



Figure. (5) plant single nodes.

While sodium chloride was added to the culture media with different concentrations determined according to several studies (**Hatami *et al.*, 2010; Upreti and Murti, 2010**). Whereas, the used treatments in this study were prepared by using MS Media supplemented with sodium chloride as follows (0, 10, 20, 40, 60, 80 mmol) for purpose of study the effect of salinity on used potato varieties in the study, while each treatment contains ten replicates and only two plant was planted in each jar then all plant samples incubated in the growth chamber under the same pressure conditions.

Experimental design.

The experiment was designed by using completely randomized design (CRD) system, the LSD were calculated at significant differences at 5%. The main factors were measured and recorded of this experiment, explains after passed two of time under NaCl stress plant length, number of branches, number of roots, number of leaves, Na⁺ accumulation and osmolality.

3 Results and discussion

Surface sterilization process

one of objectives in this experiment is to determine the best concentration of sodium hypochlorite (Clorox) used to sterilize the plant samples a plants during the experiment. The results showed that the best concentration of sodium hypochlorite was 3% which led to an increase in the percentage of contamination-free explants to 92% and 89% for Spunta and Agria respectively, however the concentration of 2.5% showed a proportion of explants free of contamination 82% and 70% for spunta and Agria respectively while the use of Clorox 2% showed the lowest proportion of contamination- free plants which was 65% and 58% for Spunta and Agria (Fig. 6). These results are consistent with the result of (**Abughnia *et al.*, 2013**) when the researchers found that the best concentration of Clorox is 3% for 20 minutes.

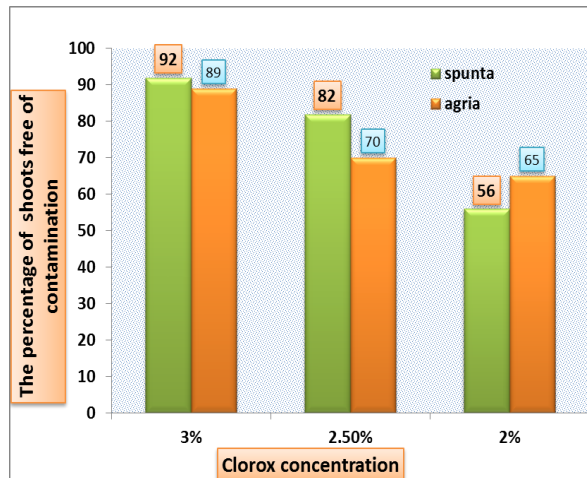


Figure. (6) Percentage of the uncontaminated a shoots under different concentrations of Clorox for spunta and Agria varieties.

Effect of adding sodium chloride on plant improve Spunta variety

After obtaining uncontaminated explants through using of plant tissue culture technique from Spunta variety. The obtained planted from tissue culture were replanted in MS media supplemented with different concentration of sodium chloride which are (0, 10, 20, 40, 60 and 80 mmol). The results (Fig. 7). showed that the number of leaves for obtained planets there was no significant difference between all treatments after 30 days of planting, while the treatment of control characterized among the other treatments after 75 days of planting exceeded the average of 24 leaves followed by the treatment of 10 mmol which exceeded the rest of the remaining treatments and recorded an average of 22.6 leaves, whatever from these results the number of leaves non significantly affected by the toxicity of sodium chloride salt until arriving to 75 days since day of culture or after which mean that the number of leaves poorly estimate these results were agree with (Wang et al 2007; Hasegawa et al, 2000; Munns, 2010). the effect of sodium chloride due to that there was no clear different between the treatments.

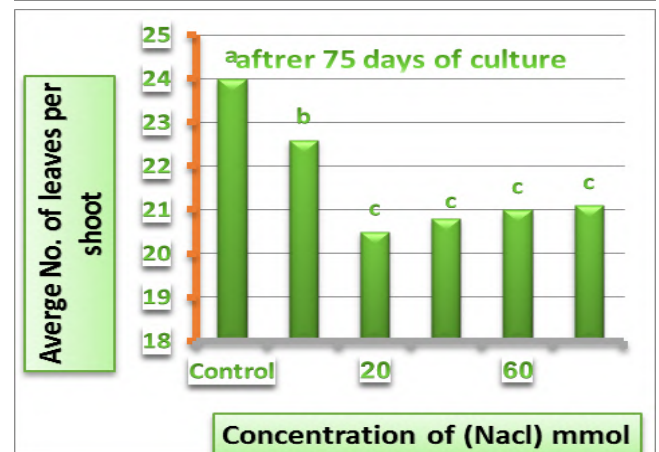
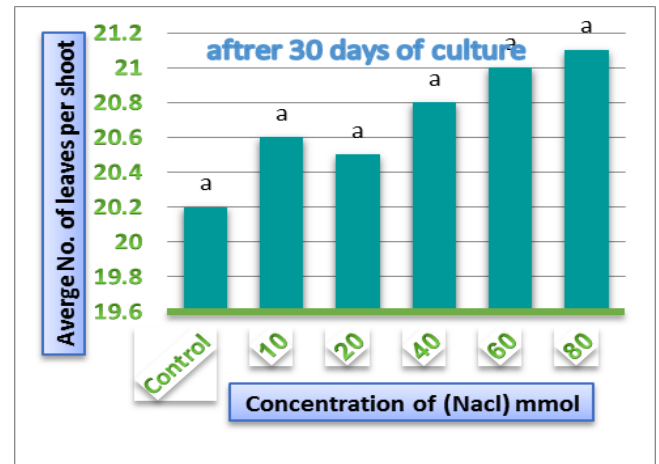
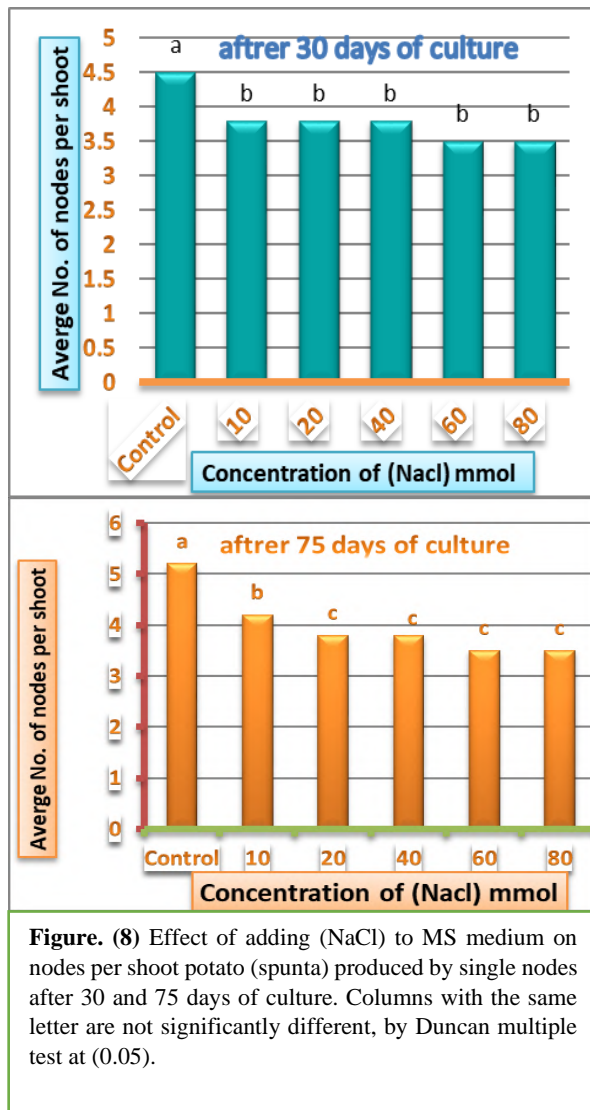


Figure. (7): the effect of adding (NaCl mM) to MS medium on leaves per shoot of potato (spunta) produced by single nodes after 30 and 75 days of culture.

Either by number of nodes shown in (Fig. 8), while culture of plant single nodes in MS media supplemented with different concentrations of sodium chloride salt was directly affected and the results showed that the control treatment gave the highest significant number of nodes compare with the other treatments and it was superiority on the other treatments after 30 days of planting, while the average of the number of nodes in control treatment was 4.5 branches while no more than 3.8 branches in the rest of the other treatments, in a related when reading the results after 75 days continued to exceed the treatment of control on the rest of the treatments recording an average of 5.2 branches followed by the treatment of 10 mmol of NaCl which recorded an average of 4.2 nodes while the other treatments did not pass the average of 3.8 nodes. These results were agree with (Wang et al 2007; Hasegawa et al , 2000; Munns, 2010).



Results (Fig. 9) that there was non significant different of 10mmol NaCl which main the planted did not affect by salt stress get also the was no different among treatments of (10,20mmol) NaCl and treatments of (20mmol) NaCl and treatments of (40,60,80mmol) NaCl finally we observe that the planted plants clearly affected by the in increasing of salt concentration. (Wang *et al.*, 2007; Hasegawa *et al.*, 2000; Munns, 2010).

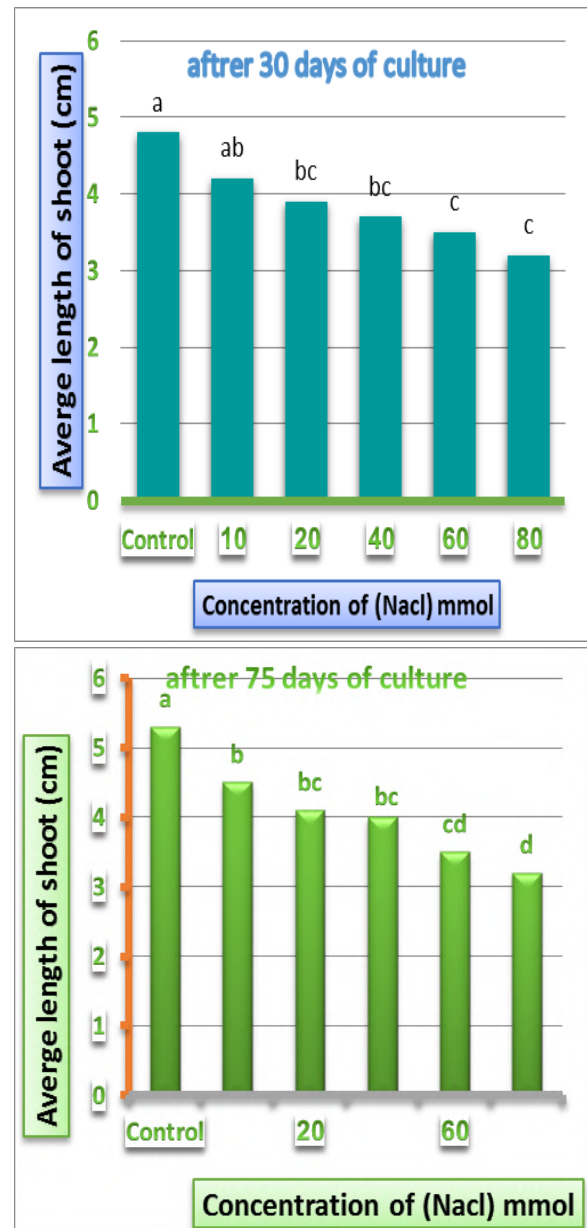
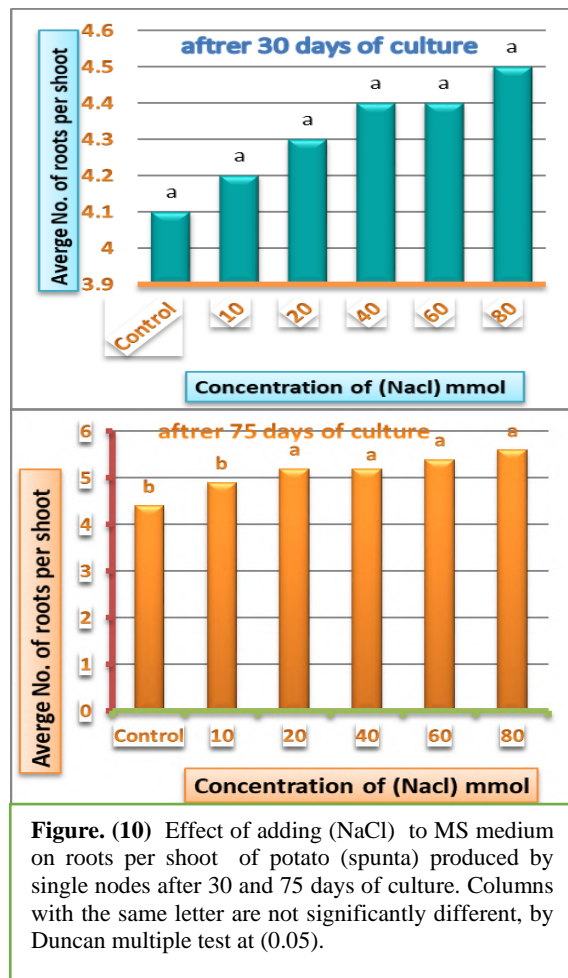


Figure. (9) Effect of adding (NaCl) to MS medium on shoot length of potato (spunta) produced by single nodes after 30 and 75 days of culture. Columns with the same letter are not significantly different, by Duncan multiple test at (0.05).

while for the number of roots the results showed that there were no significant differences between all the treatments (Fig. 10) even after 30 days of planting there was no significant effect of NaCl on the number of roots but after observation the results at or after 75 days there are significant effect in control and 10mmol Nacl from other treatments and the data changed and significant differences were found among the treatments, while the treatments of (20, 40, 60 and 80 mmol) were distinguished on the other rest treatments and recorded average of (5.2, 5.2, 5.4 and 5.6) respectively, moreover the results indicated that increased salt concentration increase number of roots and exceeded them even on the treatment of control . these results were agree with (Jorge and Susana, 2007).



In general results of these experiment explained that increase concentration of sodium chloride led to decrease the number of leaves, number of branches and plant length and these results were agree with (Wang et al., 2007; Hasegawa et al., 2000; Munns, 2010). The results also showed that increase concentration of sodium chloride led to increase number of roots which in combine with results as (Jorge and Susana,2007).

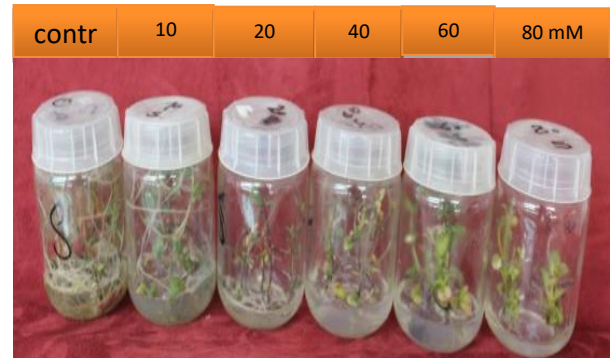


Figure. (11) Effect of adding (NaCl) to MS medium on roots per shoot of potato (spunta) produced by single nodes after 75 days of culture.

Agria variety

After obtaining non-contaminated tissue cultures the obtained plants were replanting in MS media supplemented with several concentrations of sodium chloride salt (0, 10, 20, 40, 60, 80 mmol), while the results for this variety described in (Fig.12) . Beginning from plant length factor the results showed that plant length in treatments (0, 10, 20 mmol) was recorded significantly higher than the other treatments which are (40, 60, 80mmol) which main that plant length significant superiority of treatments (0, 10 and 20 mmol) on the other treatments and their recording of the mean (4.9, 4.6 and 4.4cm) respectively after 30 days of planting and this superiority continued even after 75 day of planting followed by the treatment of 40Mm which recorded an average of 5.2 cm, furthermore the toxicity effect of sodium chloride salt there was non-significant different among on treatments of (60, 80 Mm). NaCl specially during period of 75 days of planting for the plant length factor these results were agree with (Bsharaa et al., 2013),

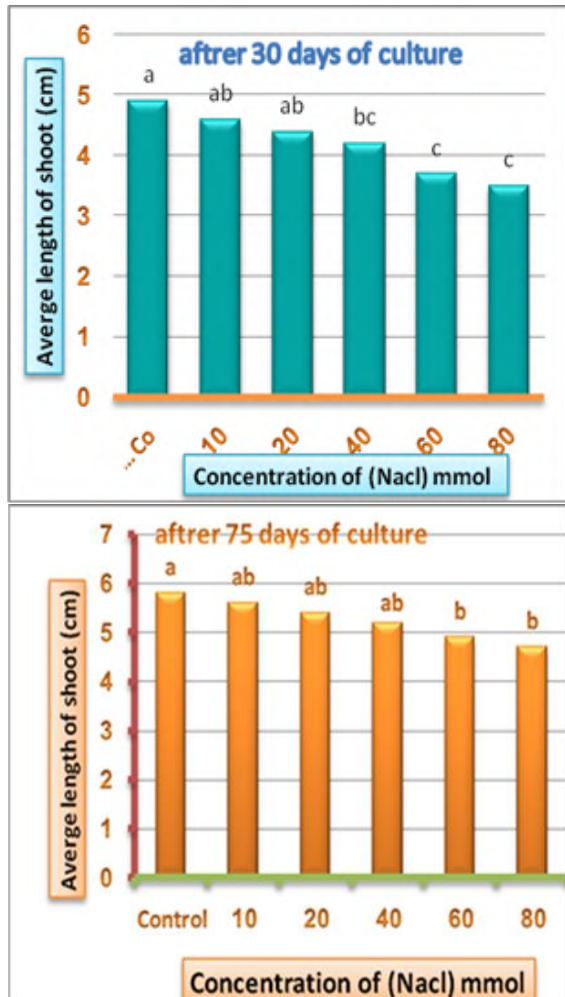


Figure. (12) Effect of adding (mmol NaCl) to MS medium on shoot length of potato (Agria) produced by single nodes after 30 and 75 days of culture. Columns with the same letter are not significantly different, by Duncan multiple test at (0.05)

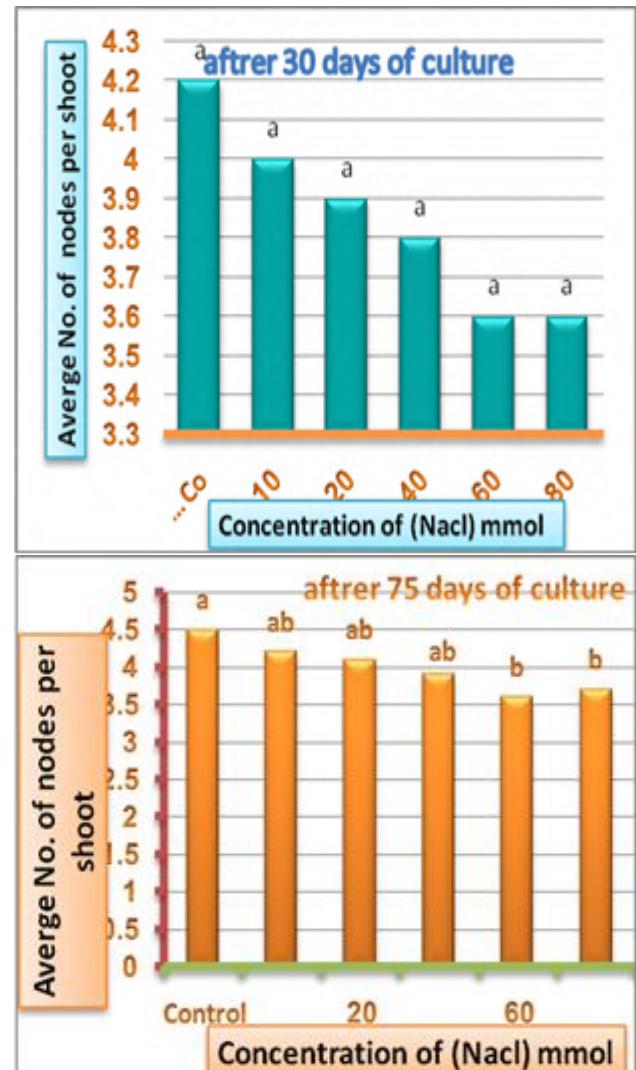


Figure. (13) Effect of adding (mmol NaCl) to MS medium on nodes per shoot potato (Agria) produced by single nodes after 30 and 75 days of culture. Columns with the same letter are not significantly different, by Duncan multiple test at (0.05)

Either by number of branches the results described in (Fig. 13), while planting single nodes in MS media supplemented with different concentration of sodium chloride salt grown plants were not affected by toxicity of NaCl after 30 days of grown even after 75 days of culture all the treatments were not affected except for the treatment of 60 and 80mmol with an average of 3.6 and 3.7 branches respectively these two treatments directly affected by added NaCl which led the other treatments to had significant superiority in compare with treatments of 60, 80 mmol NaCl. these results were agree with (Munns, 2010),

Followed by number of leaves factor the results explained in (Fig. 14) in which the treatments of 0 and 10Mm exceeded the other treatments by recording the averages (19.7 and 19.2 leaves) respectively. While the effect of sodium chloride salt toxicity being occurred on the other treatments after 30 days of planting and exceeded of 0 and 10 mmol NaCl treatments continued even after 75 days of grown. The toxicity effect of sodium chloride salt continued on the other treatments started from treatment of 20mmol which exceeded the average of 19.9 leaves until reaching an average of 19.1 leaves for the treatment of 40mmol NaCl these results were agree with (Munns, 2010).

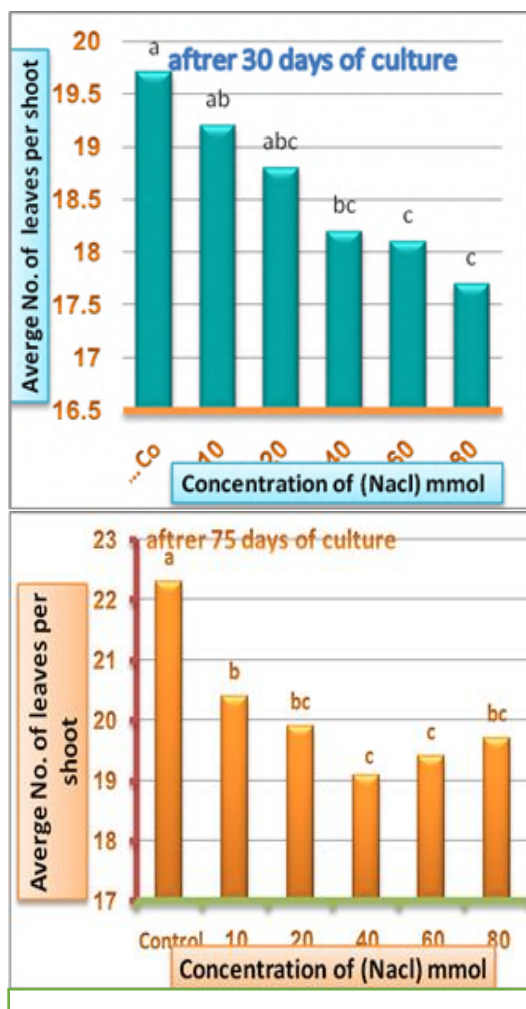


Figure. (14) Effect of adding (mmol NaCl) to MS medium on leaves per shoot of potato (Agria) produced by single nodes after 30 and 75 days of culture. Columns with the same letter are not significantly different, by Duncan multiple test at (0.05)

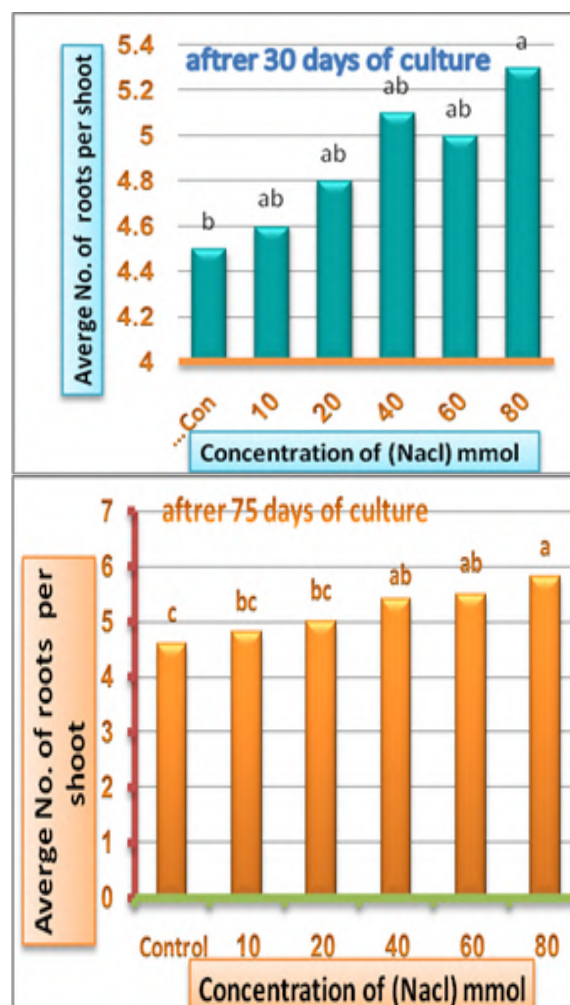


Figure. (15) Effect of adding (mmol NaCl) to MS medium on roots per shoot of potato (Agria) produced by single nodes after 30 and 75 days of culture. Columns with the same letter are not significantly different, by Duncan multiple test at (0.05)

As for number of roots character the results which shown in (Fig. 15) the results showed that the increase sodium chloride salt concentration increase the number of roots, this was proved in the treatment of 80 mmol which recorded an average of 5.3 root after 30 days of planting and this prove continued even after 75 days of culture while treatment of 80mmol recorded an average of 5.8 root, although it did not significantly exceed the other treatments except treatments of 0, 10 and 20 which recorded an average of (4.6, 4.8 and 5 root) respectively. (Jorge and Susana, 2007).

Increasing the concentration of sodium chloride salt leads to a decrease in the leaf area which represented in the number of leaves, number of branches and length of the plant and these results were agree with (Munns, 2010), also increase the salt concentration leads to decrease the plant length and this result corresponds to what was found by (Bsharaa et al., 2013).

In general through the results the ability to tolerate salt stress by plant depends on the ability of the variety to maintain the intracellular effort of fullness in the plant cell, also related to the efficiency of the variety to absorption control, this is consistent with it found by

(Khretdiev, 2000). Whatever the case it has been proven that Agria variety was one of the best varieties to tolerate high levels of salinity when compared to Spunta variety while Spunta variety considered as one of best varieties capable to tolerating high levels of salinity (Bsharaa et al., 2013).



Figure. (16) Effect of adding (mmol NaCl) to MS medium on roots per shoot of potato (Agria) produced by single nodes after 75 days of culture

4 Conclusion

The best method to sterilize the surface of potato explants use commercial Clorox solution at a concentration of 3% for 20 minutes, which gave the highest proportion of tissue cultural free of contamination.

Increase salinity levels leads to a decrease in the number of leaves and number of nodes. Plant length for each of the two potato varieties. Increase the number of roots for a specific period of time .Possibility of plant tissue.

growth for the two varieties Agria and Spunta without any effect of the concentration of salinity stress which reached a maximum concentration of 80 mmol NaCl after 30 days of planting. The significant impact of potato tissues after 75 days of explants were cultured under stress at the concentration of 80mmol NaCl.

The ability of salt tolerance depends, on the ability of the variety of maintain the osmotic adjustment in the cell. Agria variety considered as one of the best varieties to tolerate of high levels of salinity when compared with Spunta variety.

References

- Abughnia, E. Saleh, A. Hamud, S. and Apocnina, M. (2013). Production Microtubers of Potato var. Spunta free virus using meristem tip culture 6th National Conference of the biotechnology- Misurata – Libya. P. 42-53.
- Al Baher, M., A. Fouad, and S.Mahmoud. (1999). Plant Biotechnology Tissue Culture and genetic engineering .Arab Company for Publication and Distribution 1st ed. Cairo Egypt.
- Arias, O. (1992). Commercial Micropropagation of Banana In Biotechnology Applications for Banana Costa Rico. P.139-142.
- Bowen, W.T. (2003). Water productivity and potato cultivation. P 229 - 238. In J.W. Kijhe, R. Barke, and D. Molden. Water productivity in Agriculture: limits and opportunities For improvement CAB. International 2003.
- Bsharaa, S., Hadad.S and lawand.S. (2013). Physiological study of salinity stress in some potato varieties (*Solanum tuberosum*). J. Agric. Damascus. Univ. 29 (3): 165-180.
- Chapman, D. Q. and Nieman, M. L. (2000). Development of genetic fingerprinting strategy for the Maine potato breeding program, frontiers in plant science. 7(2): 6-14.
- David, M. O. and E. T. Nilsen .(2000) . The Physiology of Plant Under Stress. John Wiley & Sons , Inc.
- Dodds, J. H. D. Silvia-Rodrigures, and P. Tovar.(1992). Micropropagation of *Solanum tuberosum* L. In: Biotechnology in Agriculture and Forestry, Vol, 19. High Tech and Micropropagation III, Y.P.S. Bajaj, Ed., pp. 91-106. Springer-Verlag, New York.
- Flowers, T. N. (2001). Mapping and characterization of new EST –derived microsatellites for potato (*Solanum tuberosum* L.)
- Hasegawa P. M., Bressan R. A., Zhu J. K., Bohnert H. J. (2000). Plant cellular and molecular responses to high salinity. Annu. Rev. Plant Biol. 51, 463–499. 10.1146/annurev.arplant.51.1.463.
- Hassan,A. Abdel Moneim. (1999). Potato Production. Vegetable crops series. Arabic Publishing House. Egypt.
- Hatami, E., M. Esna-Ashari and T. Javadi.(2010). Effect of Salinity on Some Gas Exchange Characteristics of Grape (*Vitis vinifera*) Cultivars, Int. J. Agric. Biol.. 12: 308–310.
- Jorge T., and Susana P. (2007). High salinity and drought act on an organ-dependent manner on potato glutamine synthetase expression and accumulation. Environmental and Experimental Botany 60 : 121–126.
- Katerji N., Van-Hoorn J., Hamdy A. and Mastrorilli M. (2000). Salt tolerance classification of crops according to

- soil salinity and to water stress day index. Agric. Water Manage. 43, 99–109.
- Khosrarifar, S. yarnia, M. KhorshidiBenam, M.B. and Hosseinzadehmoghgheli A.H.(2008). Effect of potassium on drought tolerance in potato c.v. Agria. Journal of agriculture and Environment vol.6(3&4), 236-241.
- khrediv, A. (2000). Studies on salt tolerance and its mechanism in potato. Jiangsu J. Agric.Sci., 9(1): 8-12.
- Maas, E and G. Hoffman. (1976). Evaluation of existing data of crop salt tolerance. Proceedings of the International Salinity conference, Texas, USA(187 – 198).
- Miller, S. A. and L. Lipschultz.(1984). Potato In; Handbook of Plant Cell Culture.
- Munns, R. 2010. Salinity and Plant Tolerance. Electronic Publishing, Utah State University. Extensio.
- Murashige, T. and F. Skoog.(1962). A revise for rapid growth and bioassays with tobacco cultures. Physiol. Plant. 15: 473–497.
- Santamaria, P. and A. Elia.(1997). Producing nitrate-free endive heads: Effect of nitrogen form on growth yield and ion composition of endive: J Amersoc Hort. Sci 122. 140-145.
- Sheldon, A., Menzies, N. W. So, H.B and Dalal, R. C.(2004). The effect of salinity on plant available water, In: B. Sing 3rd Australian New Zealand Soils Conference, University of Sydney, 5-9 December 200.
- Sinhabab, K. and H. Kumar.(2003). The effect of salt stress on photosynthetic electron transport, 38(4): 481-485.
- Upreti, K.K and G.S.R. Murti.(2010). Response of grape rootstocks to salinity: changes in root growth, polyamines and abscisic acid. Biologia Plantarum. 54 (4): 730-734.
- Wang Z. Q., Yuan Y. Z., Ou J. Q., Lin Q. H., Zhang C. F. (2007). Glutamine synthetase and glutamate dehydrogenase contribute differentially to proline accumulation in leaves of wheat (*Triticum aestivum*) seedlings exposed to different salinity. J. Plant Physiol. 164, 695–701.
- Wang, P. J., Hu, C. (1985). Potato Tissue Culture and Its Application in Agriculture. Potato Physiology. New York: Academic Press; 504-599.
- Zubaidi, Ahmed Haidar. (1989) Soil Salinity Theory Application. Faculty of Agriculture, University of Baghdad, Iraq.



Growth and Yield of Triticale (*×Triticosecale Wittmack*) as Influenced by Different Sowing Dates

Amal Ehtaiwesh* and Munira Emsahel

Plant Science Department, Science Faculty, Zawia University, Libya.

DOI: <https://doi.org/10.37375/sjfsu.v3i1.324>

A B S T R A C T

ARTICLE INFO:

Received: 28 January 2023

Accepted: 2 April 2023

Published: 17 April 2023

Keywords:

Growth; sowing dates; Triticale (*×Triticosecale Wittmack*); yield component;

Pot experiment involving three sowing dates was conducted for studying the response of triticale (*×Triticosecale Wittmack*) to sowing dates. Triticale grains were sown at three different times October 15, November 15, and December 15. The current outcomes revealed that there is a significant difference between sowing dates on plant growth and yield attributes. The most effective in this regard was 15th October followed by 15th November and then 15th December. The greatest values of plant height (95.5 cm), flag leaf area (37.5 cm²), tiller number plant⁻¹ (9.5 tillers), spike length (18.5 cm), grain number spike⁻¹ and spike weight (3.8 g), were recorded within the 1st sowing date (15th October). Additionally, the lowest values of grains and biological yield was recorded under the 3rd sowing date (Dec 15). It is concluded from this study that the best date for triticale sowing falls within the period between late October and the middle of November.

1 Introduction

Triticale (*×Triticosecale Wittmack*) is an anthropogenic cereal designed to incorporate the functionality and high yield of wheat (*Triticum* spp. L.) and the durability of rye (*Secale cereale* L.) (McGoverin et al., 2011; Abdelaal et al., 2019). Triticale is a new promising grain crops worldwide due to its ability to grow well in low-fertility soil and high resistance to biotic and abiotic stresses (Randhawa et al., 2015; Khoshkharam and Shahrajabian, 2021, Ehtaiwesh, 2022). The importance of triticale comes from its high protein content and their constituents, i.e., it contains the most important amino acids in the nutrition of living organisms (Neuweiler et al., 2021). So far triticale is grown generally as a feed grain, green forage, cover crop, as well as for biogas production (Wójcik-Gront and Studnicki, 2021; Coblentz et al., 2022). Nevertheless, with the integration of new breeding tools and enabling technologies such as doubled haploid, marker-assisted selection, genomics selection, transgenic, and targeted genome editing, with conventional plant breeding approaches, triticale has the prospective to be a

successful future crop (Randhawa et al., 2015). The world area cultivated with triticale was about 3.830.794 hectares and worldwide yield production reached 38755 hectogram per hectare (FAO, 2022). However, cereal production for both forage and grain is strongly influenced by environmental conditions and farming practices such as, spacing, fertilization, seeding rate, and sowing date (Khoshkharam and Shahrajabian, 2021) Global warming drastically reduced cereal crop yield by hampering germination capacity and seedling establishment associated with reduced crop productivity, therefore sowing dates adjustment is a critical measure to alleviate and adapt to global warming (Xiao et al., 2017; Ali et al., 2021). Sowing time is the key to successful wintering and ensures efficient use of resources (Salmon et al., 2004; Santiveri et al., 2004; Bielski et al., 2020). Many studies have indicated that inappropriate planting dates affected wheat grain yield, plant height, number of grains per spike, and the weight of wheat grains (Ali et al., 2010; Ahhmed, 2015; Tahir et al 2019). Earlier sowing time contributed to intensive tillering, and strong growth, which may cause plant death and lower yields

(Pomortsev et al., 2019). Sowing date significantly affected the grain yield of triticale plants as reported in some studies. For example, sowing triticale seed on November 1 was significantly superior and gave the highest values of plant height, spike length, and number of spikes^{m²}, number of grains per spike, grain yield, and the biological yield, while sowing triticale seed in the middle of November gave the highest average of 1000 grains (Noaema et al., 2020). The use of triticale is still limited now in Libya, and there are few studies on the seeding rates, the appropriate varieties, the date of planting and the environmental conditions that may have an impact on triticale growth and yield. Therefore, the aim of this study was to highlight the effect of sowing times on the growth and yield component of triticale plant.

2 Materials and Methods

Plant Material

Grains of triticale plants were obtained from the Libyan National Gen-Bank in Tripoli, Libya

2.1 Experimental and treatment conditions

The pot experiment with a completely randomized design (RCD) was done within the 2021/2022 winter season to highlight the effect of sowing date (15th October, 15th November, and 15th December) on growth and yield trials of triticale. The plastic pots (20 x 25 cm) were filled with 10 kg of homogeneous sandy soil, and then 10 grains were cultivated in each pot.

After seedling establishment, seedlings were thinned to four seedlings per pot, which was kept until harvesting. From the sowing date until harvesting, the triticale plants were irrigated with fresh water as needed to ensure germination, growth and yield processes naturally. Fertilizer (N. P. K 20, 20, 20) was added at different plant growth stages at a rate of 5g pot⁻¹ was added, at tillering, booting, and flowering stages, Diammonium phosphate (DAP) (NH₄)₂HPO₄ NP 18:46 was also added around emergence.

Data collection

At maturity, four plants from each replicate were hand-harvested by cutting them at the soil level. Data on plant height (cm), number of tillers plant⁻¹, and number of spike plant⁻¹ was recorded on the day of harvesting. Plant height was determined as the distance between the bases of the plant to the tip of the main stem spike including awns. Tiller number plant⁻¹ contained both fertile (with spikes) and non-fertile tillers (without spikes). Flag leaf area (cm²) was measured according to the equation of Aldesuquy et al., (2014) as indicated leaf area =Length * Breadth * 0.75. After drying for 7 days in the air oven at

40°C, the main spike of each replicate was weighted (g), and spikelet numbers spike⁻¹ were counted. Then the main spikes were hand threshed to separate grains, and grain number spike⁻¹ was counted manually. Grain yield for the main spike, per plant, and 1000-grain weight were calculated. The harvest index was calculated as the ratio of grain yield plant⁻¹ to the total vegetative dry weight for each replicate.

2.2 Experiment design and data analysis

Data were analyzed using GLM procedure in statistical software SAS 9.4 (SAS Institute Inc., Cary, NC, USA) for mean and standard error estimation. Separation of means was carried out using the least significant differences (LSD; $P < 0.05$).

3 Results

The data presented in table 1 show the effect of different sowing dates on the growth and yield traits of triticale. The results showed that the effect of sowing dates was highly significant ($P < 0.01$) on tiller number plant⁻¹, spike number plant⁻¹, spike length, and grain yield plant⁻¹. In addition, the result indicated that the effect of sowing dates was significant ($P < 0.05$) on other traits included in this study Table 1.

Table: (1). Probability values of the effects of sowing date on various growth and yield traits of triticale plant.

Traits	Treatment
Plant height (cm)	0.0491
Leaf area (cm ²)	0.0497
Dry weight plant ⁻¹ (g)	0.0419
Tiller number plant ⁻¹	0.0098
Spike number plant ⁻¹	0.0088
Spikelet number spike ⁻¹	0.0475
Spike length (cm)	0.0179
Spike weight (g)	0.0485
Grain number spike ⁻¹	0.0485
1000 grain weight (g)	0.0496
Grain yield plant ⁻¹ (g)	0.0096
Harvest index (%)	0.0442

The results indicate that there was a significant increase in growth and yield traits in triticale plants when triticale sowed in the period between October 15th and November 15th compared to late sowing (December 15).

The results shown in Figure 1a pointed out that planting dates significantly affected plant height (cm). The first

sowing date provided the highest average of plant height, where triticale plant height reached to 95.5 cm, while the third sowing time recorded the lowest plant height, which was 75 cm (Figure 1a). In addition, the result showed the advantage of the first sowing date of triticale as it averaged in the highest of flag leaf area of triticale with almost 37.5 and 37 cm² in the first and second date of sowing. However, this result varied significantly with the third sowing date, which recorded the lowest in flag leaf area (30.5 cm²) as observed in Figure 1b. As for total plant dry weight, the result indicated that both early first and second sowing dates resulted in higher accumulations of above*ground biomass which account for total plant dry weight. However, plant dry weight did not vary significantly between the first and second date of sowing, which gave about 34 and 35 g of plant dry weight, while the third sowing date recorded the lowest value of plant dry weight 25g) as observed in Figure 1c.

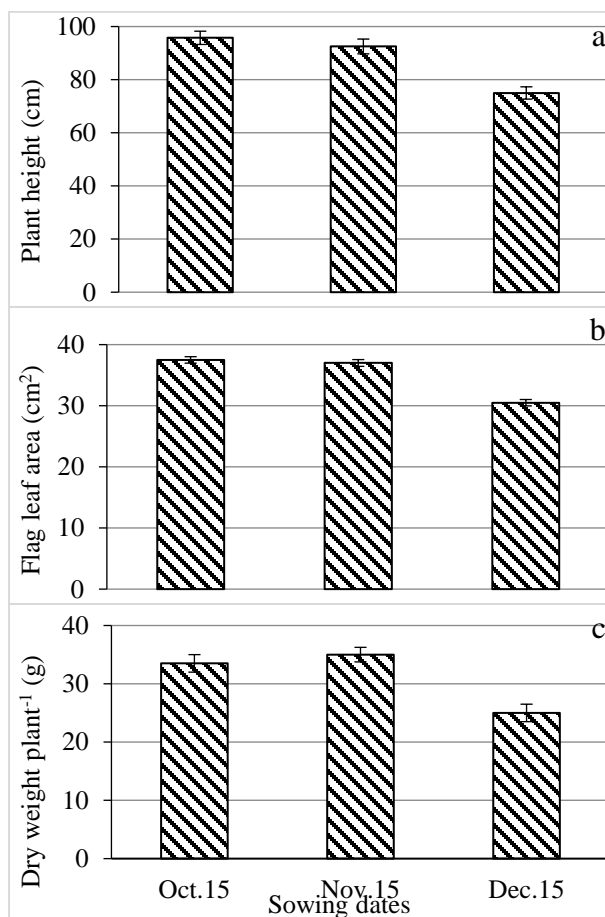


Figure: (1). The effect of sowing dates on (a) plant height (cm), (b) leaf area (cm²) and (c) dry weight (g) plant⁻¹ of the triticale plant. Each datum indicates the mean value and vertical lines on top of the bars indicate the standard error of means (n = 4).

The same trend was found with the number of tillers plant⁻¹ of triticale plants, which is considered as one of the important indicators in plant growth and it has a great impact and prompting yield. Either first and second

sowing dates gave the highest tillers number of 9.5 and 9 tillers plant⁻¹ respectively as compared with the third sowing date that recorded 6 tillers plant⁻¹ (Figure 2a). The results also indicated that there was a significant effect of sowing dates on the number of spikes plant⁻¹. Figure 2b showed that the second date of sowing gave the highest average number of spikes plant⁻¹ (8.7 spikes plant⁻¹) followed by the first sowing date (8.5 spikes plant⁻¹), which significantly altered in the third sowing date that gave the lowest average of spikes plant⁻¹ (5.5 spikes plant⁻¹) as seen in Figure 2b. Triticale yield is also effected by the sowing date in terms of the number of spikelet spike⁻¹. The result herein indicated that the second sowing date averaged with 27.5 spikelet number spike⁻¹, which was close to the average of the first sowing time that gave 27 spikelet number spike⁻¹. Conversely, the spikelet number spike⁻¹ was significantly reduced by the third sowing date, which averaged with 21 spikelet number spike⁻¹ as observed in Figure 2c.

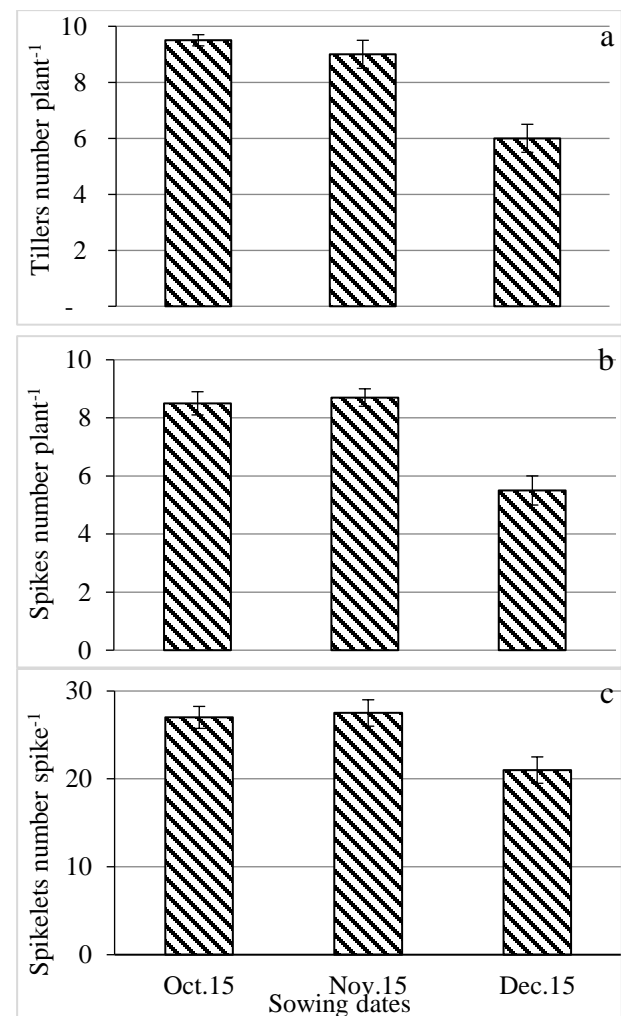


Figure: (2). The effect of sowing dates on (a) the number of tillers plant⁻¹, (b) the number of spikes plant⁻¹, and (c) the number of spikelet spike⁻¹ of the triticale plant. Each datum indicates the mean value and vertical lines on top of the bars indicate the standard error of means (n = 4).

Moreover, spike length (cm) and spike weight (g) of triticale significantly altered with the sowing date. Yet the third sowing date negatively affected both parameters. In the first and second sowing dates, the average length of the spikes was 18.5 and 18 cm respectively and was 13 cm in the third sowing date (Figure 3a). The same trend was found in spikes weight (g). The result revealed that in the first, the second and the third sowing dates the average weight of the spikes were 3.8, 3.7, and 3 g respectively as observed in Figure 3b. The number of grains spike⁻¹ was significantly affected by the sowing date. As the results showed that the first and second sowing dates gave the highest average number of grains spike⁻¹ with 62 and 61 grains spike⁻¹, whereas the third sowing date significantly differ from the first and second sowing dates and gave 49 grains spike⁻¹ as observed in Figure 3c.

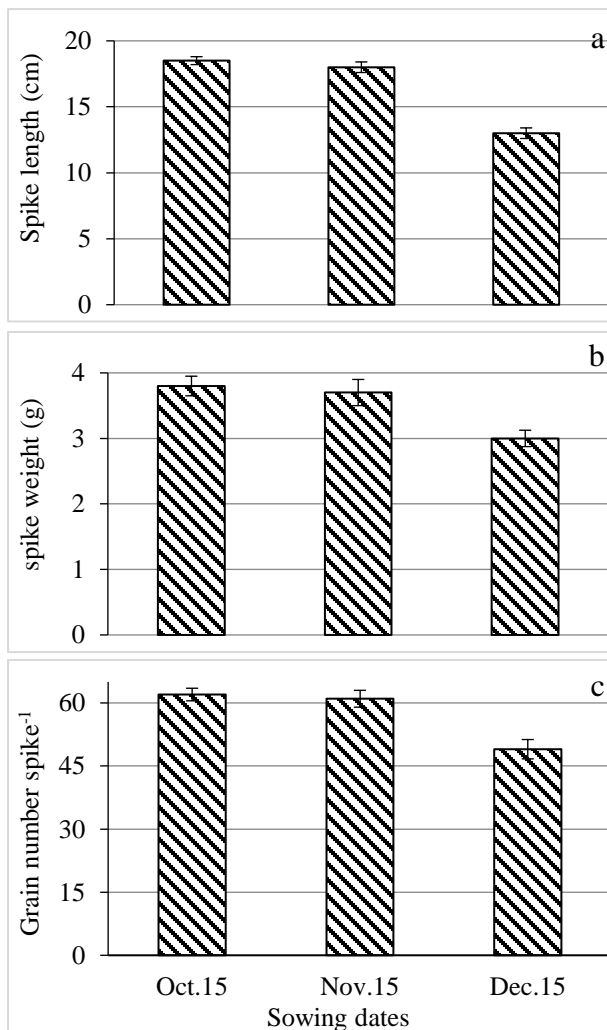


Figure (3). The effect of sowing dates on (a) spike length (cm), (b) spike weight (g) and (c) the number of grains spike⁻¹ of the triticale plant. Each datum indicates the mean value and vertical lines on top of the bars indicate the standard error of means (n = 4).

Furthermore, the results revealed a significant effect of sowing dates on 1000 grains weight of triticale. Figure 4a showed that the 1000-grain weight of the first and second sowing date surpassed third sowing dates by giving the highest average weight of 1000 grains amounting to 51.5 and 53g respectively, whereas the third sowing date gave an average of 44g for 1000 grains weight as seen in Figure 4a. With the regard to the grain yield plant⁻¹, which is considered the final outcome of yield components that include the number of spikes plant⁻¹, grains yield spike⁻¹ and the weight of 1000 grains, the results showed a significant effect of sowing dates. The first and second sowing dates gave the highest average of grains yield of 27.5 and 28.05 g plant⁻¹ respectively while the third sowing date recorded the lowest average of grain yield of about 17g plant⁻¹ (Figure 4b). Moreover, the result illustrated that there was no difference between the first and second sowing dates in terms of harvest index parameters both sowing dates recorded the highest harvest index of 0.80 %. However third sowing date significantly affected the harvest index which recorded the lowest harvest index of 0.69% as seen in Figure 4c.

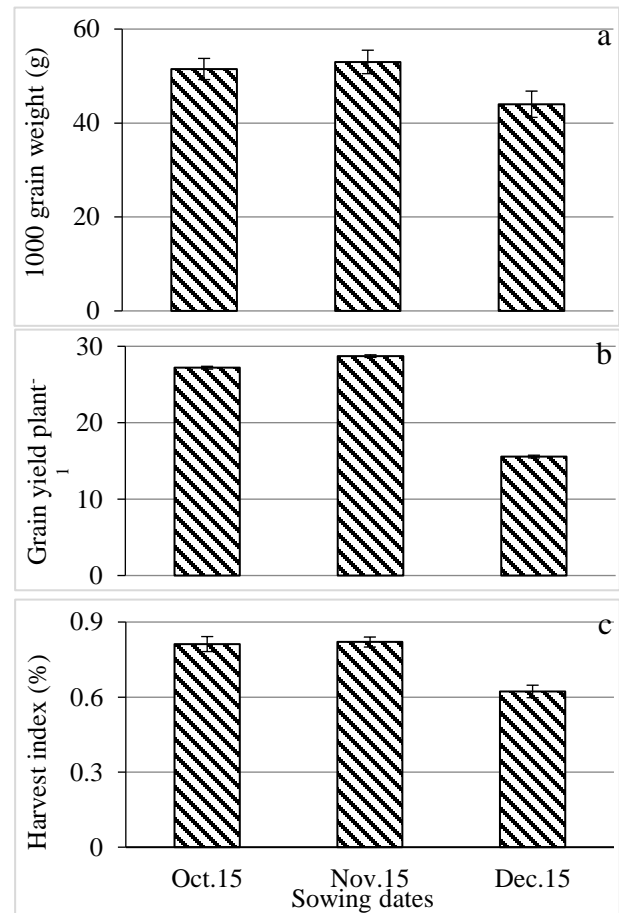


Figure (4). The effect of sowing dates on (a) 1000 grain weight (g), (b) grain yield plant⁻¹, and (c) harvest index of the triticale plant. Each datum indicates the mean value and vertical lines on top of the bars indicate the standard error of means (n = 4).

4 Discussion

The aim of this study was to evaluate growth and yield traits of triticale x *Triticosecal Wittmack* as affected by sowing dates. The results pointed out that sowing dates significantly affected the growth and yield traits of triticale, which agreed with many previous studies (Alam et al., 2020; Ding et al., 2020). The result showed that grain yield and plant biomass production of triticale plants sowed at the first and second sowing date gave the highest average of grain yield traits, while the third sowing date gave the lowest average of the same traits. The reason for this disparity in plant height is due to the reduction in plants growth at elongation stage, which could be due to the restriction of needed days for plant growth. Ramos et al. (1993) reported a reduction in forage yield by 22 to 44%, grain yield by 12 to 60%, and total useable biomass (i.e., forage + grain) by to 52%. In addition, the result showed that the third sowing date recorded the shortest spike length as compared with the first and second dates of sowing. The reason for the reduction in spike length because of the increased of temperature which resulted in the hastening of plant growth and shortening of time needed for spike growth at the period in which enough time is important in determining the length of the spike. This result was similar to previous findings (Tomple and Jo, 2019; Prasun et al., 2021). This study conclude that depending on the sowing dates, tiller number was between 9.5 and 6 tillers plant⁻¹, spikes number between 8.7 and 5.5 spikes plant⁻¹, dry weight was between 35 and 25 g plant⁻¹, and grain yield was between 28.7 and 15.6 g plant⁻¹. This result was comparable to other studies that reported the impact of delayed sowing date was significant in triticale as it diminished grain-filling duration by 13%, final grain weight by 16%, grain volume by 15%, and embryo area by 8% (Royo et al., 2000, Ganvit et al., 2019). Moreover, the results pointed out that there was a significant effect of sowing dates on the number of spikes plant⁻¹. Both first and third sowing dates gave the lowest mean of spikes plant⁻¹. The reason for this decrease may be due to the short time required for the growth and formation of sprouts, which was reflected negatively in the number of spike plant⁻¹. Similar results were obtained in an earlier study (Tahir et al., 2009). The study indicated a decrease in the number of grains spike⁻¹ at the third sowing date. This could be due to the effect of high temperature during grain formation, which caused a reduction in grain numbers spike⁻¹. An early study indicated a similar result (Noaema et al., 2020). Likewise, the result of this study reported a decrease in 1000-grain weight at the third sowing date, which could be because of the adverse effect of high temperatures that accelerate the growing of plant and reduce the length of a period of grain filling to the

extent that negatively affected the weight of grains. This result is consistent with what was reported by another study (Shah et al., 2006). In fact, temperature and light are considered among the factors that affect most of the physiological processes of the plant that may influence plant growth and yield traits. The study indicated that grain yield traits are significantly affected by sowing dates. These conclusions were also seen in early studies of different plant species including triticale (Koppensteiner et al., 2021), corn (Van Roekel and Coulter, 2011, Maresma et al., 2019), wheat (Kabir et al., 2019; Tahir et al., 2019), rice (Patel et al., 2019) and barley (Amarjeet et al., 2020; Moustafa et al., 2021).

5 Conclusions

In Libya there has not been sufficient enough work conducted on evaluating the response of triticale plants to different agricultural practices such as sowing dates. This study designated that November 15 sowing date exceeded other sowing dates in spike number plant⁻¹, spikelet number spike⁻¹, the weight of 1000 grains, total dry weight plant⁻¹, grain yield plant⁻¹ and harvest index. Therefore, the study concludes that the best balance for forage and grain production in this environment was achieved by sowing during the last week of October or the first week of November. Sowing after this period may reduce growth and yield traits. However, this important crop still needs further research to understand the factors that affect its productivity characteristics under the environmental conditions of Libya.

Acknowledgments

The authors would like to thank Libyan National Gen-Bank for providing seeds of triticale. The authors are also grateful to the plant science department, the University of Zawia for providing the equipment used for the study.

Conflict of interest: The authors declare that there are no conflicts of interest.

References

- Abdelaal, H. K., Bugaev, P. D., & Fomina, T. N. (2019). Nitrogen fertilization effect on grain yield and quality of spring triticale varieties. *Indian Journal of Agricultural Research*, 53(5), 578-583.
- Ahmed, M. (2015). Response of spring wheat (*Triticum aestivum* L.) quality traits and yield to sowing date. *PLoS one*, 10(4), e0126097.
- Aldesuquy, H., Baka, Z., & Mickky, B. (2014). Kinetin and permire mediated induction of salt tolerance in wheat plants: Leaf area, photosynthesis and chloroplast ultrastructure of flag leaf at ear emergence. *Egyptian journal of basic and applied sciences*, 1(2), 77-87.

- Alam, M. J., Ahmed, K. S., Nahar, M. K., Akter, S., & Uddin, M. A. (2020). Effect of different sowing dates on the performance of maize. *Journal of Krishi Vigyan*, 8(2), 75-81.
- Ali, K. A., Amin, S. M., & Abdullah, R. A. (2021). Late sowing date influence on wheat and triticale crop yields as a draught management tool. *Journal of the Saudi Society of Agricultural Sciences*, 20(6), 353-358.
- Ali, M. A., Ali, M., Sattar, M., & Ali, L. (2010). Sowing date effect on yield of different wheat varieties. *J. Agric. Res*, 48(2), 157-162.
- Amarjeet, A., Singh, B., Kumar, J., Kumar, M., Sharma, R., & Kaushik, P. (2020). Effect of sowing date, seed rate and row spacing on productivity and profitability of barley (*Hordeum vulgare*) in north India.
- Bielski, S., Romaneckas, K., & Šarauskis, E. (2020). Impact of nitrogen and boron fertilization on winter triticale productivity parameters. *Agronomy*, 10(2), 279.
- Coblentz, W. K., Ottman, M. J., & Kieke, B. A. (2022). Effects of Harvest Date and Growth Stage on Triticale Forages in the Southwest USA: Agronomic Characteristics, Nutritive Value, Energy Density, and In Vitro Disappearance of Dry Matter and Fiber. *Journal of Animal Science*.
- Ding, Y., Wang, W., Zhuang, Q., & Luo, Y. (2020). Adaptation of paddy rice in China to climate change: The effects of shifting sowing date on yield and irrigation water requirement. *Agricultural Water Management*, 228, 105890.
- Ehtaiwesh, A. F. A. (2022). Study of germination traits and seedlings growth of Wheat (*Triticum aestivum*) Barley (*Hordeum vulgare*) compared with Triticale (*x Triticosecale Wittmack*) under salinity stress. *Journal of Misurata University for Agricultural Sciences*.3 (2): 63-83.
- FAO. (2022). FAOSTAT Database Agricultural Production. Available at <http://apps.fao.org>. Food and Agricultural Organization of the United Nations.
- Ganvit, J. B., Sharma, S., Surve, V. H., & Ganvit, V. C. (2019). Effect of sowing dates and crop spacing on growth, yield and quality of linseed under south Gujarat condition. *Journal of Pharmacognosy and Phytochemistry*, 8(1), 388-392.
- Kabir, M. E., Sarker, B. C., Ghosh, A. K., Mainuddin, M., & Bell, R. W. (2019). Effect of sowing dates on yield of wheat grown in excess water and salt affected soils in southwestern coastal Bangladesh. *Journal of the Indian Society of Coastal Agricultural Research*, 37(2), 51-59.
- Khoshkharam, M., & Shahrajabian, M. H. (2021). Growth and Yield Parameters of Triticale as Influenced by Methanol Foliar Application Under Water Stress. *Journal of Stress Physiology & Biochemistry*, 17(3), 13-22.
- Koppensteiner, L. J., Obermayer-Böhm, K., Hall, R. M., Kaul, H. P., Wagentristl, H., & Neugschwandtner, R. W. (2021). Autumn sowing of facultative triticale results in higher biomass production and nitrogen uptake compared to spring sowing. *Acta Agriculturae Scandinavica, Section B—Soil & Plant Science*, 71(9), 806-814.
- Maresma, A., Ballesta, A., Santiveri, F., & Lloveras, J. (2019). Sowing date affects maize development and yield in irrigated mediterranean environments. *Agriculture*, 9(3), 67.
- McGoverin, C. M., Snyders, F., Muller, N., Botes, W., Fox, G., & Manley, M. (2011). A review of triticale uses and the effect of growth environment on grain quality. *Journal of the Science of Food and Agriculture*, 91(7), 1155-1165.
- Moustafa, E. S., El-Sobky, E. S. E., Farag, H. I., Yasin, M. A., Attia, A., Rady, M. O., ... & Mansour, E. (2021). Sowing date and genotype influence on yield and quality of dual-purpose barley in a salt-affected arid region. *Agronomy*, 11(4), 717.
- Neuweiler, J. E., Maurer, H. P., & Würschum, T. (2021). Genetic architecture of phenotypic indices for simultaneous improvement of protein content and grain yield in triticale (*x triticosecale*). *Plant Breeding*, 140(2), 232-245.
- Noaema, A. H., Abdul-alwahid, M. A. A., & Alhasany, A. R. (2020). Effect of planting dates on growth and yield of several european varieties of triticale (*x-ticosecale wittmack*) under environmental conditions of al-muthanna district, IRAQ. *Int. J. Agricult. Stat. Sci. Vol*, 16(1), 1261-1267.
- Patel, A. R., Patel, M. L., Patel, R. K., & Mote, B. M. (2019). Effect of different sowing date on phenology, growth and yield of rice—a review. *Plant Archives*, 19(1), 12-16.
- Pomortsev, A. V., Dorofeev, N. V., Zorina, S. Y., Katysheva, N. B., & Sokolova, L. G. (2019). The effect of planting date on winter rye and triticale overwinter survival and yield in Eastern Siberia. In *IOP Conference Series: Earth and Environmental Science* (Vol. 315, No. 4, p. 042031). IOP Publishing.
- Prasun, A., Reuter, T., & Trautz, D. (2021). The influence of sowing date, row width and seed rate on organic winter triticale (*x triticosecale*) development and weed growth in autumn in north-west germany. Osnabrück University of Applied Sciences, Germany. *Measurements*, 11.
- Ramos, J. M., Garcia Del Moral, M. B., Marinetto, J., & Garcia Del Moral, L. F. (1993). Sowing date and cutting frequency effects on triticale forage and grain production. *Crop science*, 33(6), 1312-1315.
- Randhawa, H. S., Bona, L., & Graf, R. J. (2015). Triticale breeding—Progress and prospect. In *Triticale* (pp. 15-32). Springer, Cham.
- Royo, C., Abaza, M., Blanco, R., & Del Moral, L. F. G. (2000). Triticale grain growth and morphometry as affected by

- drought stress, late sowing and simulated drought stress. *Functional Plant Biology*, 27(11), 1051-1059.
- Salmon, D. F., Mergoum, M., & Gomez-Macpherson, H. (2004). Triticale production and management. *Triticale improvement and production*, 179, 27-32.
- Santiveri, F., Royo, C., & Romagosa, I. (2004). Growth and yield responses of spring and winter triticale cultivated under Mediterranean conditions. *European journal of agronomy*, 20(3), 281-292.
- Shah, W. A., Bakht, J., Ullah, T., Khan, A. W., Zubair, M., & Khakwani, A. A. (2006). Effect of sowing dates on the yield and yield components of different wheat varieties. *Journal of Agronomy*.
- Tahir, M., Ali, A., Nadeem, M. A., Hussain, A., & Khalid, F. (2009). Effect of different sowing dates on growth and yield of wheat (*Triticum aestivum* L.) varieties in district Jhang, Pakistan. *Pak. j. life soc. sci*, 7(1), 66-69.
- Tahir, S., Ahmad, A., Khaliq, T., & Cheema, M. J. M. (2019). Evaluating the impact of seed rate and sowing dates on wheat productivity in semi-arid environment. *Int. J. Agric. Biol*, 22(1), 57-64.
- Tomple, B. M., & Jo, I. H. (2019). Effects of the autumn sowing date on grain yield and feed value of winter triticale (*X. Triticosecale* Wittm.) in the southeast of the Gyeongbuk province. *Korean Journal of Agricultural Science*, 46(3), 439-449.
- Van Roekel, R. J., & Coulter, J. A. (2011). Agronomic responses of corn to planting date and plant density. *Agronomy Journal*, 103(5), 1414-1422.
- Wójcik-Gront, E., & Studnicki, M. (2021). Long-term yield variability of triticale (\times *Triticosecale* Wittmack) tested using a CART model. *Agriculture*, 11(2), 92.
- Xiao, D., Cao, J., Bai, H., Qi, Y., & Shen, Y. (2017). Assessing the impacts of climate variables and sowing date on spring wheat yield in the Northern China. *Int. J. Agric. Biol*, 19, 1551-1558.



Aqueous Extract of Winter Jasmine Leaves Mediated Biosynthesis of Silver Nanoparticles

Kawther E. Adaila^{1*}, Samia S. E. Elraies¹, Abdounasser A. Omar¹, Eman J. Ben Younis², Hiba A. Alhaj², Salsabel A. Shlebek² and Sara N. Ali²

¹Chemistry Department, Science-Gharyan Faculty, Gharyan University, Gharyan, Libya.

²Undergraduate Student, Chemistry Department, Science-Gharyan Faculty, Gharyan University, Gharyan, Libya.

DOI: <https://doi.org/10.37375/sjfsu.v3i1.1139>

A B S T R A C T

ARTICLE INFO:

Received: 06 March 2023

Accepted: 03 April 2023

Published: 17 April 2023

Keywords:

Silver Nitrate, Silver Nanoparticles, Winter Jasmine, Biosynthesis.

This study reports a rapid and eco-friendly green method for the synthesis of silver nanoparticles from silver nitrate solution using winter jasmine leaves extract as a reducing agent of Ag^+ to Ag^0 . A visible Absorption Spectrophotometer was used to monitor the formation of silver nanoparticles (AgNPs). The visible spectrum showed an absorption peak at 420 nm which reflects the surface plasmon resonance (SPR) of AgNPs. In addition to that, the synthesis of AgNPs was confirmed by the color change of the solution. By studying the most important factors affecting the formation of AgNPs, it was noted that the productivity of AgNPs in the solution increased by increasing the pH of the solution, and the basic medium was the appropriate medium for the synthesis process. Also, the amount of produced AgNPs increased with the increase in temperature, volume of extract, reaction time, the extract volume ratio of the winter jasmine leaves, and silver nitrate concentration. In conclusion, the aqueous extract of winter jasmine leaves represents a suitable material for the biosynthesis of AgNPs, and large amounts of AgNPs with appropriate sizes may be obtained by controlling the parameters that affect the synthesis process.

1 Introduction

Silver nanoparticles (AgNPs) have sparked the interest of researchers in recent years due to their wide range of applications, such as antibacterial agents [Le Ouay et al., 2015, Franci et al., 2015], antifungal agents [Elgorban et al., 2016, Medda et al., 2015], antioxidant agents [Keshari et al., 2020, Khorrami et al., 2018], antitumor agent [Hashemi et al., 2020, He et al., 2016] and in dye degradation [Albeladi et al., 2020, David et al., 2020]. AgNPs have been synthesized using a number of physical and chemical methods. The physical methods include evaporation-condensation and laser ablation, whereas the

chemical methods include chemical reduction, and electrochemical techniques [Irvani et al., 2014]. However, adopting such approaches to synthesize AgNPs has a number of disadvantages, including high cost, excessive energy consumption, and pollution of the environment [Borah et al., 2020, Omar et al., 2018]. Biosynthesis has lately been proposed as an alternative to those conventional methods since it is simple, cost-effective, and an environmentally beneficial approach. Through this route, AgNPs could be produced by bacteria, fungi, and plants, which contain constituents that act as reducing and capping agents for synthesizing

AgNPs [David *et al.*, 2020, Omar *et al.*, 2021]. These constituents include proteins, polysaccharides, polyphenols, and vitamins [Hashemi *et al.*, 2020, David *et al.*, 2020]. Many researchers have reported biosynthesis of AgNPs using the extract of many plants, such as *Ocimum tenuiflorum*, *Solanum tricoloratum*, *Syzygium cumini*, *Centella asiatica*, and *Citrus sinensis* [Logeswari *et al.*, 2015], *Berberis vulgaris*, *Brassica nigra*, *Capsella bursa-pastoris*, *Lavandula angustifolia*, and *Origanum vulgare* [Salayová *et al.*, 2021], *Salvia spinosa* [Pirtarighat *et al.*, 2019], *Moringa oleifera* [Moodley *et al.*, 2018], *Cleome viscosa* [Lakshmanan *et al.*, 2018].

This study aimed to biosynthesize AgNPs using the aqueous extract of winter jasmine leaves, and silver nitrate as a precursor for silver. In addition to that, the effect of pH, reaction time, silver nitrate concentration, temperature, and the volume ratio of winter jasmine leaves was investigated.

2 Materials and Methods

2.1 Chemicals

Silver nitrate solution with a concentration of 0.1 M (Winlab, UK), was used to prepare all diluted solutions, which were required to work as a source of silver ions. Sodium hydroxide and hydrochloric acid (BDH) were used to prepare solutions with 0.1 M concentration to adjust the pH of the reaction medium.

2.2 Preparation of the aqueous extract of winter jasmine leaves

In September 2022, a sample of winter jasmine leaves was collected from the Faculty of Science - Gharyan and transferred to the lab in a nylon bag. These leaves were washed thoroughly with deionized water and dried in the open air, away from sunlight, then cut by hand into small pieces, in order to increase the surface area of these leaves. A quantity of winter jasmine leaves was added to a volume of deionized water in a ratio of 1g: 4 mL in a clean, dry beaker. After heating the mixture for 10 minutes, it was cooled by washing the outside of the beaker with tap water. Then the solution was filtered using Whatman No. 1 filter paper, and the filtrate was collected for later use in the biosynthesis of silver nanoparticles.

2.3 Biosynthesis of silver nanoparticles

The aqueous extract of winter jasmine leaves was added to a solution of silver nitrate with a concentration of 1 mM at a v/v ratio of 1:9, then the pH of the mixture was adjusted to 9 using sodium hydroxide solution before being kept at room temperature for 30 min. After that, the color change was observed, and the visible spectrum was recorded using a visible spectrophotometer (Jenway 6300 spectrophotometer, Staffordshire, UK).

2.4 Effect of pH

To 5 beakers, 1.5 mL of winter jasmine leaf extract and 8.5 mL of silver nitrate solution (1 mM) were added, in which the pH of the solution was initially 6. One of these solutions was left untreated and was among the readings that were monitored by the visible spectrophotometer. To the remaining four solutions, drops of sodium hydroxide solution (0.1 M) were added to obtain the following pH of 7, 8, 9, and 10. Hydrochloric acid (0.1 M) was used to reduce the pH when appropriate. All solutions were kept at room temperature for 30 min, then the color change of the previous solutions was observed, and the visible spectrum of each solution was recorded.

2.5 Effect of reaction time

Fifty mL of silver nitrate solution (1 mM) was transferred to a clean beaker, to which 5 mL of winter jasmine leaf extract was added. By adding drops of sodium hydroxide solution (0.1 M), the pH was adjusted to 9. After 5, 60, 120, and 180 min and 24 hours, 2 mL of the solution was withdrawn, and then the visible spectrum was recorded for each solution to monitor the effect of the time.

2.6 Effect of silver nitrate concentration

Two mL of winter jasmine leaf extract were added to 5 sample bottles, each of which contained 8 mL of silver nitrate solution with different concentrations: 0.5, 1, 2.5, 5, and 10 mM. The pH of each solution was adjusted to 9 by adding drops of sodium hydroxide solution, then all solutions were kept at room temperature for 30 min. After that, the visible spectrum for each solution was recorded.

2.7 Effect of extract volume ratio

To 6 sample bottles, different volumes of winter jasmine leaf extract were added to different volumes of silver nitrate solution (1 mM) provided that the total volume was 10 mL and the volume percentage of the extract in these solutions was 5, 10, 15, 20, 25 and 30%. The pH of each solution was adjusted to 9 using sodium hydroxide solution (0.1 M), and all solutions were kept at room

temperature for half an hour, then the visible spectrum of each solution was recorded.

2.8 Effect of temperature

One mL of the extract and 9 mL of silver nitrate solution (1 mM) were added to 5 sample bottles. Each solution's pH was adjusted to 9, and the solutions were heated for 20 min at different temperatures, namely 20, 30, 50, 60, and 70° C. Then the visible spectrum of each solution was recorded.

3 Results and Discussion

3.1 Confirmation of biosynthesized AgNPs

The color of the reaction medium changed rapidly from yellow to brown, as shown in Figure (1), when 1mL of aqueous extract of winter jasmine leaves was added to 9mL of 1mM AgNO₃ solution. The brown color was obtained by the excitation of surface plasmon vibrations, which are characteristic of AgNPs [Omar et al., 2018, Tripathy et al., 2010].

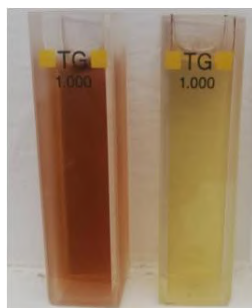


Figure. (1): Color change due to AgNPs formation

The visible spectrum of the reaction medium was used to monitor the bioreduction of pure Ag⁺ ions to Ag⁰. The surface plasmon resonance (SPR) of AgNPs produced a peak with a wavelength of around 420 nm, which was not shown in the winter jasmine extract's visible spectrum as depicted in Figure (2). The appearance of this peak confirmed the formation of AgNPs.

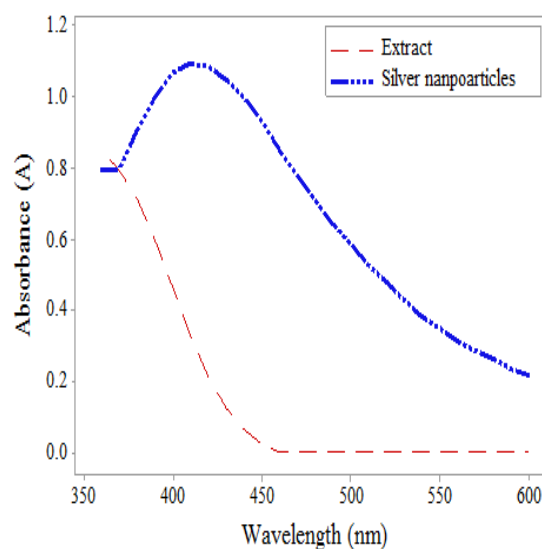


Figure. (2): Visible spectrum of winter jasmine extract and AgNPs solution

Several studies have found that polyphenols and flavonoids (One of the active biochemical components of the winter jasmine plant under investigation) appear to be responsible for the bioreduction of silver ions and the formation of AgNPs. [Iravani et al., 2014, Omar et al., 2018, Awwad et al., 2012, Shahmoradi et al., 2018].

3.2 Effect of pH

The absorbance of (SPR) peak was found to gradually increase with increasing pH as shown in Figure (3), and the color of solutions became darker (Figure (4)), implying that the rate of formation of AgNPs is more rapid in the basic pH than in acidic pH. Several previous studies have reported that the formation of AgNPs occurs rapidly in neutral and basic pH [Omar et al., 2018, Vivek et al., 2012], and this may be due to the ionization of the phenolic group present in the extract of winter jasmine leaves. The slow rate of formation and aggregation of AgNPs at acidic pH could be related to the electrostatic repulsion of anions present in the reaction solution [Omar et al., 2018, Vivek et al., 2012]. It should also be mentioned that Ag⁺ ions cannot hydrolyze in an acidic medium, whereas at pH values above 8, Ag⁺ ions partially hydrolyze to form bio-organic Ag complexes [Ag(OH)_x] on the surface of the particles and AgOH and Ag₂O colloid in the medium, hence the degree of hydrolysis and colloid formation increases with increasing pH of the solution. As a result of this impact, no significant changes in the values of the wavelength at the highest absorbance (λ_{max}) were detected in the extremely alkaline region, and a large number of

functional groups were available for silver binding at higher pH. On the other hand, they facilitated the binding of a larger number of silver nanoparticles, resulting in a large number of nanoparticles with smaller diameters [Tripathy et al., 2010, Vivek et al., 2012, Veerasamy et al., 2011].

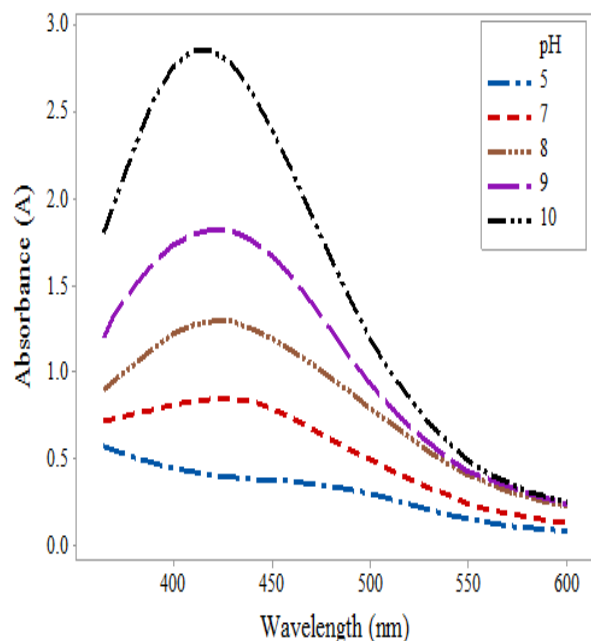


Figure. (3): Absorbance of (SPR) peak increased with increasing pH values



Figure. (4): The color of solutions became darker with increasing pH values

3.3 Effect of reaction time

Figure (5) shows the visible spectra of AgNPs obtained during varying periods (5 minutes to 24 hours), the absorbance of the SPR peak increased with increasing interaction time from 5 min to 24 h and the value of λ_{\max} shifted from 420 to 450 nm, indicating a redshift. The red shift was most likely produced by the SPR being

suppressed by the combined effects of increased silver nanoparticle particle size in colloidal solution and anisotropy in their morphologies [Tripathy et al., 2010]. After 24 hours, there was no significant change, and this reflects the stability of the yield. The active organic compounds in the extract of the winter jasmine leaves prevented the nucleation and growth of silver nanoparticles when they exceeded the required size, which is consistent with the results of a previous study [Tripathy et al., 2010].

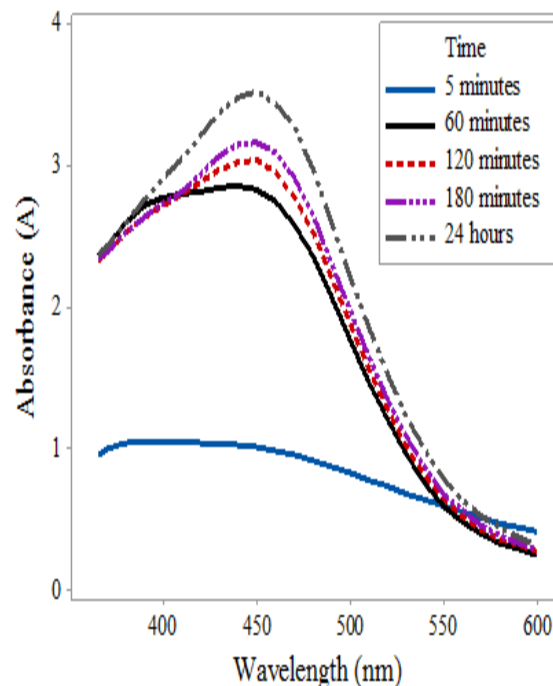


Figure. (5): The absorbance of (SPR) peak increased with increasing interaction time.

3.4 Effect of silver nitrate concentration

The results revealed that the higher the silver nitrate concentration, the higher the (SPR) peak values, as represented in Figure (6) when varied concentrations of silver nitrate solution (0.5, 1, 2.5, 5, 10 mM) were utilized. With increasing concentrations of silver nitrate, the (SPR) peak of AgNPs became increasingly evident. Due to the obvious abundance of silver ions in the reaction media, more silver particles are synthesized. All five (SPR) peaks produced a narrow and sharp peak with good symmetry, indicating a homogeneous and approximate size distribution of spherical AgNPs, and these results are consistent with previous research [Rao et al., 2017]. Additionally, figure (7) shows that when the concentration of silver nitrate increased, the color of the silver nanoparticle solution darkened, which was another proof of forming more of AgNPs.

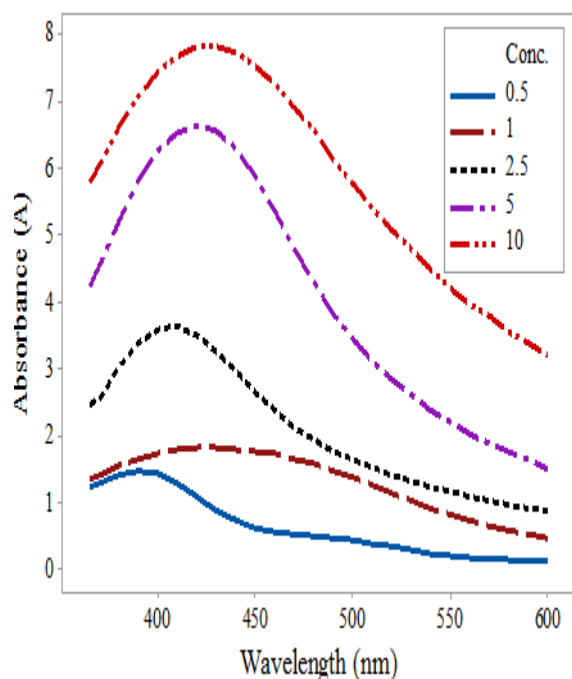


Figure. (6): Effect of silver nitrate concentration

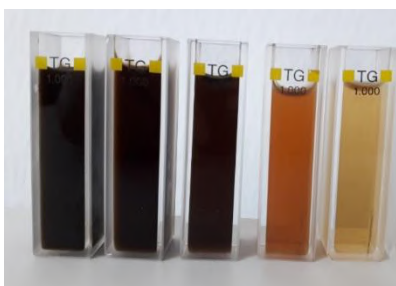


Figure. (7): How the color of the reaction mixture darkened as the concentration of silver nitrate increased

3.5 Effect of extract volume ratio

While fixing the rest of the parameters (time, temperature, AgNO_3 concentration, and pH), the different volume percentages of winter jasmine extract were utilized, and when the visible spectrum of these several solutions was scanned it was observed that as the volume percentage of the extract increased, the absorbance values increased as well, as shown in figure (8), this was due to an increase in the amount of bioactive compounds in the extract that is responsible for reducing silver ions and turning them into AgNPs as it has been evidenced by comparable research [Kiruba et al., 2013]. When using a small volume percentage of the extract to react with silver nitrate, the process of forming silver nanoparticles was very slow, but when the volume

percentage of the extract was increased, the reaction speed increased, which was a sign of the formation of larger amounts of silver nanoparticles in the solution, as evidenced by the increase in the (SPR) absorption peak (figure (8)) and the darkening of the solution's color as shown in figure (9).

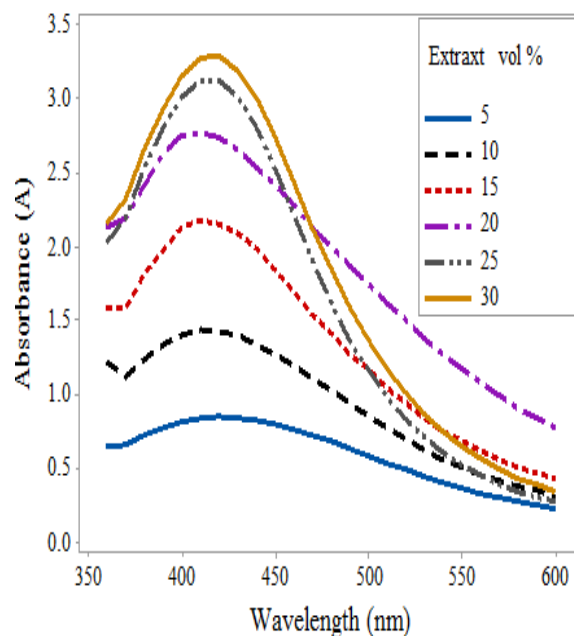


Figure. (8): Effect of extract volume percentage (%) on the synthesis of AgNPs.

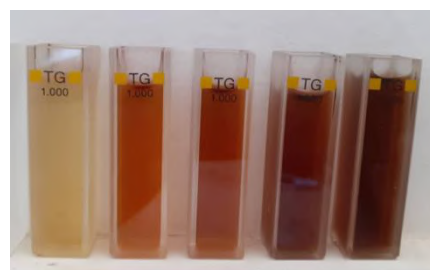


Figure. (9): The darkening of the color of the solution increases as the volume of the extract increases

3.6 Effect of temperature

When different temperatures were utilized in the synthesis process, it was revealed that the greater the temperature of the AgNPs solution, the higher the absorbance value of the (SPR) peak, specifically at 60 and 70 °C as shown in Figure (10). Furthermore, the (SPR) peak became sharper as the temperature increases, suggesting the synthesis of a significant number of similar-sized AgNPs. A previous study has noted the same observations [Singh et al., 2021].

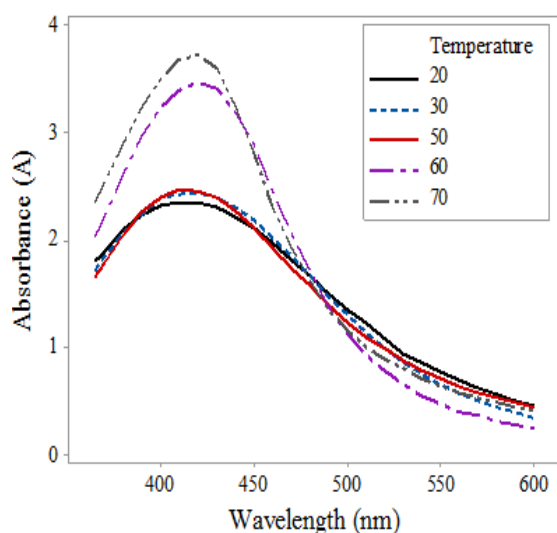


Figure. (10): effect of temperature on the synthesis of AgNPs.

4 Conclusions

Through its interaction with silver nitrate solution, the aqueous extract of winter jasmine leaves represents a suitable material for the biosynthesis of AgNPs, and large amounts of AgNPs with appropriate sizes may be obtained by controlling the parameters that affect the synthesis process (pH, reaction time, extract volume ratio, temperature, and silver nitrate concentration). It was determined that increasing the pH of the solution enhanced the productivity of AgNPs in the solution and that the basic medium was the best medium for the synthesis process. The amount of AgNPs produced increased as the temperature, volume of extract, reaction time, the extract volume ratio of the winter jasmine leaves, and silver nitrate solution concentration increased.

Characterization of AgNPs synthesized by the aqueous extract of winter jasmine leaves would require additional research, as well as using winter jasmine plant extract to synthesize gold, copper, and zinc nanoparticles.

5 Limitations of the Study

The shape and size of the silver nanoparticles that formed have not been characterized, which would have offered useful information.

Conflict of Interest: The authors declare that there are no conflicts of interest.

References

- Albeladi, S. S. R., Malik, M. A., & Al-thabaiti, S. A. (2020). Facile biofabrication of silver nanoparticles using *Salvia officinalis* leaf extract and its catalytic activity towards Congo red dye degradation. *Journal of Materials Research and Technology*, 9(5), 10031-10044.
- Awwad, A. M., Salem, N. M., & Abdeen, A. O. (2012). Biosynthesis of silver nanoparticles using *Olea europaea* leaves extract and its antibacterial activity. *Nanoscience and Nanotechnology*, 2(6), 164-170.
- Borah, D., Das, N., Das, N., Bhattacharjee, A., Sarmah, P., Ghosh, K., ... & Bhattacharjee, C. R. (2020). Alga-mediated facile green synthesis of silver nanoparticles: Photophysical, catalytic and antibacterial activity. *Applied Organometallic Chemistry*, 34(5), e5597.
- David, L., & Moldovan, B. (2020). Green synthesis of biogenic silver nanoparticles for efficient catalytic removal of harmful organic dyes. *Nanomaterials*, 10(2), 202.
- Elgorban AM, El-Samawaty AE, Yassin MA, Sayed SR, Adil SF, Elhindi KM, Bakri M, Khan M. (2016). Antifungal silver nanoparticles: synthesis, characterization and biological evaluation. *Biotechnology & Biotechnological Equipment*. 2;30(1):56-62.
- Franci, G., Falanga, A., Galdiero, S., Palomba, L., Rai, M., Morelli, G., & Galdiero, M. (2015). Silver nanoparticles as potential antibacterial agents. *Molecules*, 20(5), 8856-8874.
- Hashemi, S. F., Tasharofi, N., & Saber, M. M. (2020). Green synthesis of silver nanoparticles using *Teucrium polium* leaf extract and assessment of their antitumor effects against MNK45 human gastric cancer cell line. *Journal of Molecular structure*, 1208, 127889.
- He, Y., Du, Z., Ma, S., Liu, Y., Li, D., Huang, H., ... & Zheng, X. (2016). Effects of green-synthesized silver nanoparticles on lung cancer cells in vitro and grown as xenograft tumors in vivo. *International journal of nanomedicine*, 11, 1879.
- Iravani, S., Korbekandi, H., Mirmohammadi, S. V., & Zolfaghari, B. (2014). Synthesis of silver nanoparticles: chemical, physical and biological methods. *Research in pharmaceutical sciences*, 9(6), 385.
- Keshari, A. K., Srivastava, R., Singh, P., Yadav, V. B., & Nath, G. (2020). Antioxidant and antibacterial activity of silver nanoparticles synthesized by *Cestrum nocturnum*. *Journal of Ayurveda and integrative medicine*, 11(1), 37-44.
- Khorrami, S., Zarrabi, A., Khaleghi, M., Danaei, M., & Mozafari, M. R. (2018). Selective cytotoxicity of green synthesized silver nanoparticles against the MCF-7 tumor cell line and their enhanced antioxidant

- and antimicrobial properties. *International journal of nanomedicine*, 13, 8013.
- Kiruba Daniel, S. C. G., Mahalakshmi, N., Sandhiya, J., Kasi, N., & Muthusamy, S. (2013). Rapid synthesis of Ag nanoparticles using Henna extract for the fabrication of Photoabsorption Enhanced Dye Sensitized Solar Cell (PE-DSSC). *Advanced Materials Research*, 678, 349-360.
- Lakshmanan, G., Sathiyaseelan, A., Kalaichelvan, P. T., & Murugesan, K. (2018). Plant-mediated synthesis of silver nanoparticles using fruit extract of *Cleome viscosa* L.: assessment of their antibacterial and anticancer activity. *Karbala International Journal of Modern Science*, 4(1), 61-68.
- Le Ouay, B., & Stellacci, F. (2015). Antibacterial activity of silver nanoparticles: A surface science insight. *Nano today*, 10(3), 339-354.
- Logeswari, P., Silambarasan, S., & Abraham, J. (2015). Synthesis of silver nanoparticles using plants extract and analysis of their antimicrobial property. *Journal of Saudi Chemical Society*, 19(3), 311-317.
- Medda, S., Hajra, A., Dey, U., Bose, P., & Mondal, N. K. (2015). Biosynthesis of silver nanoparticles from Aloe vera leaf extract and antifungal activity against *Rhizopus* sp. and *Aspergillus* sp. *Applied Nanoscience*, 5, 875-880.
- Moodley, J. S., Krishna, S. B. N., Pillay, K., & Govender, P. (2018). Green synthesis of silver nanoparticles from *Moringa oleifera* leaf extracts and its antimicrobial potential. *Advances in Natural Sciences: Nanoscience and Nanotechnology*, 9(1), 015011.
- Omar, A. A., Alkelbash, H. M., Alhasomi, Y. F., Al-muntaser, O. M., Elraies, S. S. E., & Khalifa, A. A. (2018). Green synthesis of silver nanoparticles using olive pomace extract. *Journal of science*, 662-9.
- Omar, A. A., Ahmad, N. A., Rajab, M. M., Berrisha, N. E., Alnakkaa, A. A., Alshareef, B. A., & Qadmour, R. R. (2021). Biosynthesis of Silver nanoparticles using Olive Wastewater. *Journal of Materials NanoScience*, 8(1), 11-15.
- Pirtarighat, S., Ghannadnia, M., & Baghshahi, S. (2019). Green synthesis of silver nanoparticles using the plant extract of *Salvia spinosa* grown in vitro and their antibacterial activity assessment. *Journal of Nanostructure in Chemistry*, 9, 1-9.
- Rao, B., & Tang, R. C. (2017). Green synthesis of silver nanoparticles with antibacterial activities using aqueous *Eriobotrya japonica* leaf extract. *Advances in natural sciences: Nanoscience and nanotechnology*, 8(1), 015014.
- Salayová, A., Bedlovičová, Z., Daneu, N., Baláž, M., Lukáčová Bujňáková, Z., Balážová, L., & Tkáčiková, E. (2021). Green synthesis of silver nanoparticles with antibacterial activity using various medicinal plant extracts: Morphology and antibacterial efficacy. *Nanomaterials*, 11(4), 1005.
- Shahmoradi, H., & Naderi, D. (2018). Improving effects of salicylic acid on morphological, physiological and biochemical responses of salt-imposed winter jasmine. *International Journal of Horticultural Science and Technology*, 5(2), 219-230.
- Singh, R., Hano, C., Nath, G., & Sharma, B. (2021). Green biosynthesis of silver nanoparticles using leaf extract of *Carissa carandas* L. and their antioxidant and antimicrobial activity against human pathogenic bacteria. *Biomolecules*, 11(2), 299.
- Tripathy, A., Raichur, A. M., Chandrasekaran, N., Prathna, T. C., & Mukherjee, A. (2010). Process variables in biomimetic synthesis of silver nanoparticles by aqueous extract of *Azadirachta indica* (Neem) leaves. *Journal of Nanoparticle Research*, 12, 237-246.
- Veerasamy, R., Xin, T. Z., Gunasagaran, S., Xiang, T. F. W., Yang, E. F. C., Jeyakumar, N., & Dhanaraj, S. A. (2011). Biosynthesis of silver nanoparticles using mangosteen leaf extract and evaluation of their antimicrobial activities. *Journal of saudi chemical society*, 15(2), 113-120.
- Vivek, R., Thangam, R., Muthuchelian, K., Gunasekaran, P., Kaveri, K., & Kannan, S. (2012). Green biosynthesis of silver nanoparticles from *Annona squamosa* leaf extract and its in vitro cytotoxic effect on MCF-7 cells. *Process Biochemistry*, 47(12), 2405-2410.



Preptin Hormone in Patients with Type 2 Diabetes Induced Post Coronavirus Infection (Covid-19)

Zahraa M. Mahmood and Luay A. Al-Helaly

Chemistry Department, College of Science, Mosul University, Mosul, Iraq.

DOI: <https://doi.org/10.37375/sjfssu.v3i1.46>

A B S T R A C T

ARTICLE INFO:

Received: 02 December 2022

Accepted: 16 January 2023

Published: 17 April 2023

Keywords: Coronavirus, Diabetes, Protein, Fats, Antioxidants, Oxidative Stress.

The research included a study of the levels of the hormone preptin and some biochemical variables in the blood serum of people with type 2 diabetes (T2D) induced post coronavirus infection (Covid-19). Those variables included: glucose, cholesterol, triglycerides, high-density lipoprotein (HDL), low-density lipoprotein (LDL) and measurement of levels of antioxidants (Albumin, uric acid, fucose and glutathione), as well as levels of oxidants compounds: for exaple malondialdehyde and peroxyntirite on (16) a sample for patients and (40) samples for the control group, whose ages ranged between (35-70) years in Mosul city.

The results showed that there was a significant increase in the levels of the preptin hormone, glucose, cholesterol and LDL in addition to the decrease in HDL, among T2D patients induced after corona compared with the control group. No significant difference was observed in the TG, HDL and uric acid between the patients' group and control group.

The results also indicated that there was a state of high oxidative stress reflected in the low levels of antioxidants for glutathione, albumin, and fucose, and a significant increase in the levels of malondialdehyde and peroxyntirite in people with diabetes mellitus developed after corona compared with the control group.

The study concluded that the hormone preptin is a good indicator that reflects the status of T2D patients induced Post coronavirus infection (Covid-19), by comparing them with the levels of antioxidants and oxidants, as well as the levels of fucose and glucose.

1 Introduction

The emerging coronavirus disease in 2019 (Covid-19) led to a serious pandemic in 2020, as classified by the World Health Organization, which led to a great loss in the global economy, loss of lives and lifestyle changes (Goyal *et al.*, 2020). The clinical symptoms of coronavirus differ from one person to another, and it may be asymptomatic or accompanied by serious complications that lead to death (Sheraton *et al.*, 2020). Coronavirus (Covid-19) mainly targets lung systems, but it has unexpected effects on many organs. Previous studies have shown a number of long-term complications of the Corona virus (Nalbandian *et al.*, 2021). Including fibrosis of the lungs, heart attack,

stroke, mood disorder and diabetes developed after infection with the virus (SeyedAlinaghi *et al.*, 2021), which is the most important focus of our research.

As coronavirus can cause the emergence of diabetes in people with it (Chee *et al.*, 2020). As a result of multidirectional changes in glucose metabolism resulting from a defect in the organs and tissues responsible for the main metabolism, including beta cells in the pancreas, fatty tissue, small intestine and kidney (Bornstein *et al.*, 2020). Coronavirus binds to the angiotensin-converting enzyme 2 receptor. It works by inhibiting the angiotensin II-to-angiotensin (7-1) pathway that plays a protective role in diabetes by

improving pancreatic cell survival, stimulating insulin secretion, and reducing insulin resistance (Ni *et al.*, 2020).

Preptin hormone is a peptide hormone with a molecular weight of 3,948 Daltons that was first isolated in 2001 from beta cells of the pancreatic gland of mice (beta-TC6-F7) by Buchanan *et al.* (2001). Preptin hormone consists of 34 amino acids as it is secreted with insulin and amylin from secretory granules of beta cells. Preptin is the newest member of the insulin family discovered. Preptin hormone has many functions in the human body, but the most important function of preptin is energy balance and carbohydrate metabolism by stimulating it to secrete insulin from beta cells when the blood glucose level is high, where it participates along with insulin, amylin and pancreaticin in glucose metabolism. It is a physiological enhancer of insulin secretion caused by high glucose concentration (Wang *et al.*, 2020).

Oxidative stress is a factor that causes metabolic and physiological changes and various diseases of the organism, as it is associated with some chronic diseases such as diabetes, heart diseases and cancer, and is also associated with some types of viral infections that are carried out through RNA, such as coronavirus (Baqi *et al.*, 2020). A study has proven the association of oxidative stress with complications that affect corona patients, such as severe inflammation, blood clotting and cellular oxygen deficiency (Sudre *et al.*, 2021). It has been observed that coronavirus can generate oxidative stress due to the excessive levels of reactive oxygen and nitrogen species in Corona patients, which are randomly generated by immune cells to infected cells and surrounding tissues as a result of acute inflammation. As a result of the oxidative stress caused by infection with coronavirus (Mohiuddin and Kasahara, 2021). Peroxynitrite is the largest of the potent oxidants produced by immune cells and the main mediator associated with inflammation (Ahmed *et al.*, 2020).

The study aims to know the role of the preptin hormone and its relationship with some other measurements in patients with type 2 diabetes developed after infection with coronavirus (Covid-19), and to know the state of oxidative stress.

2. Materials and Methods

This study included (18) patients diagnosed with diabetes developed after infection with coronavirus (Covid-19), where the clinical diagnosis of each case was made by a specialized doctor, and samples were collected during the time period from the beginning of September 2021 to the end of November 2021 from

patients treated at the Al-Wafa Specialized Center for Diabetes and Endocrinology in Mosul city, their ages range from (35-70) years.

The control group consists of 40 normal healthy individuals who have no history of disease and who match the age and body mass index with the patients. Data were collected for patients and the control group, including age, sex, height, weight, body mass index, family medical history, and smoking.

Ten milliliters of venous blood were taken from the patients and control groups and left for 15 minutes at room temperature for coagulation. Then the serum was separated by centrifugation at (3000 x g) for 15 minutes and divided into two parts and kept frozen at (-20°C) until it worked the analysis.

2.1: Methods used in measuring preptin hormone and the variables specified in the research:

The serum preptin was estimated based on linked enzyme immunosorbent assay (ELISA) technique using ready-made assay kits from BT LAB Company /China, which is an immunological method for quantification based on the sandwich principle.

The levels of glucose, total cholesterol, triglycerides and high-density lipoprotein cholesterol (HDL-C) were estimated using ready-made assay (kits) from the company (BIOLABO) and using enzymatic methods (Ambade *et al.*, 1998; Fossati and Prencipe, 1982; Lopez-Virella *et al.*, 1977; Allain *et al.*, 1974), the concentration of low-density lipoprotein cholesterol (LDL-C) in serum was calculated using the following Friedewald equation (Farukhi and Mora, 2018):

$$\text{LDL-C (mmol/L)} = \text{Total cholesterol} - \text{HDL-C} - (\text{TG}/2.2)$$

The albumin concentration was estimated using the Bromocresol green method, in which a ready-made (Kits) from the French company (BIOLABO) was used, which depends on the amount of albumin bound with the reagent (3,3',5,5'-Tetrabromocresol green, BCG) to form the albumin-BCG complex, and the absorbance intensity is measured at the wavelength 630 nm (Dumas *et al.*, 1971). Also, uric acid was estimated using Kits, which depends on the enzyme uricase in the oxidation of uric acid to allantoin and hydrogen peroxide (Walker *et al.*, 1990).

The measurement of fucose was based on the principle of direct interaction between sulfuric acid with components of the blood serum, as the thiol group (-SH) of sulfuric acid interacts with carbohydrates in the serum, and these reactants bind with the amino acid cysteine and form a colored product, which is measured by the intensity of absorption at wavelengths 396 and 430nm (Dische *et al.*, 1948).

The concentration of GSH in serum was determined using the modified method used by researchers (Sedlak and Lindsay, 1968), The method is based on the use of Ellman's reagent, which is [5-5 dithio bis (2-nitrobenzoic acid)], DTNB, which reacts quickly with GSH and reduces it by means of the thiol group (SH group) of GSH forming a colored product, the absorbance is read for it at 412 nm.

MDA was measured in the serum using the method of researchers (Guidet and Shah, 1989) and the method depends on the reaction of MDA with thiobarbituric acid (TBA) and this reaction takes place in an acidic medium and it produces a colored product whose absorbance intensity is measured at the wavelength 532 nm. Peroxynitrite (ONOO-) levels were measured using the method of researcher Vanuffelen *et al.*, 1998), which depends on ONOO- in the nitration of phenol to nitrophenol, which reflects the concentration of ONOO- and its absorbance intensity can be read at 412 nm.

2.2: Statistical analysis

The statistical program SPSS-17 was used to determine the mean (\bar{X}) and standard error (SE) and the

t-test was chosen to compare two variables and find the difference between the values that appeared through the P-value that occurs at ($P \leq 0.05$) significant difference, and at ($P \geq 0.05$) non-significant difference (Hinton, 2004).

3. Results and Discussion

3.1: Comparison of levels of preptin hormone, glucose and lipids in diabetic patients after infection with Covid-19 compared to the control group.

3.1.1: Preptin hormone

The results shown in Table (1) that there is a significant increase in the level of preptin hormone in the serum of people with induced diabetes after infection with coronavirus, compared with the healthy group at ($P=0.036$). The reason for the rise of the preptin hormone is due to the rise in blood glucose in the serum of patients with diabetes, and that the function of the preptin hormone is to stimulate the secretion of insulin in the event of high blood glucose, the higher the level of blood glucose, increased the concentration of preptin hormone (Alubaidi *et al.*, 2018).

Table 1: Comparison of levels of preptin hormone, glucose and lipids in diabetic patients after infection with COVID-19 compared to the control group.

Biochemical variables	Control		Patients		p-value
	\bar{X}	SE	\bar{X}	SE	
age (year)	48.5 a	1.90	48.14 a	4.64	0.574
BMI (body mass index, kg/m ²)	30.3 a	1.22	31.08 b	2.02	0.066
Proptin (ng/mL)	1231.9 a	50.61	1407.65 b	194.4	0.036*
Glucose (mg/100mL)	93.9 a	3.03	134.42 b	5.98	0.017*
Cholesterol (mg/100mL)	162.77 a	8.79	174.71 b	9.04	0.045*
Triglyceride (mg/100mL)	121.19 a	15.06	142.57b	16.38	0.036*
(HDL) (mg/100mL)	46.02 b	2.10	35.24 a	5.69	0.042*
(LDL) (mg/100mL)	93.6 a	7.36	144.52 b	6.34	0.010*

*The difference in the letters (a, b) horizontally indicates that there is a significant difference at a probability level of less than or equal to 0.05 between the studied groups.

3.1.2: Glucose:

The results shown in Table (1) indicated that there is a significant increase at the probability level of 0.017 in the concentration of glucose for patients with diabetes developed after infection with coronavirus compared to healthy group, and these results are consistent with the results of previous studies that showed that there is an increase in blood glucose in some Coronavirus patients (Ren *et al.*, 2020).

The cause of high blood glucose after infection with coronavirus may be the result of the entry of virus through the receptor of the angiotensin-converting enzyme 2 (ACE2) into sites and organs in the body that express these receptors, such as the cells of the pancreas gland, and their infection with infections, which leads to infection of beta cells and a decrease in insulin secretion (Lutz *et al.*, 2020; Murray *et al.*, 2020), or as a result of a defect in ACE2 itself that prevents the conversion of angiotensin II to angiotensin (1-7) and leads to hyperactivity of angiotensin II, which is a critical inducer of insulin resistance (Ren *et al.*, 2020) as well as disrupts the activities of insulin-stimulating pathways, impairing the transmission of Glut-4 (Glucose receptor) is attached to the membrane of insulin-sensitive tissues such as muscle, liver, and adipose tissue (Khunti *et al.*, 2021). In addition, Ang11 also contributes to inflammation by both immune cells and cells in tissues, which leads to an increase in proinflammatory cytokines that block insulin receptors in beta cells leading to a state of insulin resistance similar to that seen in type 2 diabetics (Mahmudpour *et al.*, 2022).

3.1.3: Lipid levels:

The results in Table (1) indicated that there was a significant increase in cholesterol at a probability level of 0.045. These results are consistent with previous studies that showed that cholesterol in the lipids of the cell membrane is a key element in the entry of the virus and the promotion of viral infection, as it plays an important role in the interaction and linkage between the S protein in coronavirus and the angiotensin-converting enzyme receptor 2 and facilitating the process of viral phagocytosis (Meher *et al.*, 2020). Studies have found that using effective lipid-lowering and cholesterol-lowering treatment significantly suppresses coronavirus infection (Katsiki *et al.*, 2020).

The results also indicated a significant increase in triglycerides (TG) and LDL-C in patients compared with healthy people at a probability level of 0.036 and 0.01, respectively, and that there was a significant decrease at a probability level of 0.042 in HDL-C in the group of patients compared to the healthy group, and

these results are consistent with a previous study that showed that inflammation and the increase of cytokines for immune cells as a result of infection change the shape and metabolism of lipids in corona patients and work on an increase in TGs and a decrease in HDL-C (Sorokin *et al.*, 2020).

3.2. Comparison of antioxidants and oxidants levels in patients with diabetes developed after infection with coronavirus with the healthy group.

3.2.1: Antioxidants Levels:

The results in Table (2) indicate that there is a significant decrease in the levels of antioxidants, including fucose and glutathione, in patients with diabetes developed after infection with coronavirus, at a probability level of 0.042 and 0.038, respectively, and these results are consistent with the results of a previous study that indicated a decrease in antioxidant levels in corona patients (Polonikov, 2020).

The reason for the low levels of antioxidants, especially glutathione, in corona patients is due to its depletion in balancing the effect of free radicals, whose level is high due to the increase in oxidative stress in corona patients (Mohiuddin and Kasahara, 2021). As it plays a vital role as an antioxidant, in addition to its other vital properties, has the ability to act as an anti-inflammatory, anti-tumor, and immune-boosting agent. It is used in anti-aging cosmetics, nutritional supplements, or as a treatment for some diseases (Iqbal *et al.*, 2021; Hameed and Al-Helaly, 2021), so we note low levels in patients. In addition, glutathione is one of the most important antioxidants and the main detoxifier of metallic or otherwise, as it works to remove many toxic compounds xenobiotics and remove reactive oxygen species (ROS). It is important in the functioning of the immune system and it is one of the main antioxidants produced by cells (Million *et al.*, 2020; Hameed and Al-Helaly, 2020).

The results also indicate a significant decrease in patients' albumin levels at a probability level of 0.028, and these results are consistent with a previous study (Chen *et al.*, 2020). The reason for the low albumin levels is due to a defect in liver function as a result of infection with coronavirus, as it is an important biomarker for assessing liver function (Clark *et al.*, 2021). The reason for this decrease may also be due to the inflammation caused by the infection of coronavirus, which increases the permeability of the capillaries, which leads to the escape of albumin outside the blood vessels and a decrease in its concentration in the blood (Spada *et al.*, 2021; Qin *et al.*, 2020). The results also indicate an insignificant decrease in uric acid, one of the antioxidants, in patients with diabetes developed after

infection with coronavirus, compared to healthy patients.

3.2.2: Oxidants Levels:

On the other hand, the results in Table (2) showed that there was a significant increase in the level of MDA in diabetic patients induced after infection with t

coronavirus compared to the healthy group at a probability level of 0.015. This is due to the increase in the production of free radicals in corona patients, which in turn works; it destroys lipid membranes and occur lipid peroxidation, and elevated levels of MDA as by-products of the oxidation process (Aninagyei *et al.*, 2019).

Table (2): Comparison of oxidation levels of antioxidants in diabetic patients after infection with corona compared to the control group.

Biochemical variables	Control		Patients		p-value
	\bar{X}	SE	\bar{X}	SE	
Albumin (g/100mL)	4.79 b	0.14	2.27 a	0.11	0.029*
Uric acid (mg/100mL)	5.89 a	0.35	6.21 a	0.36	0.748
Fucose (mg/100mL)	12.44 b	1.18	8.14 a	1.88	0.042*
Glutathione ($\mu\text{mol/L}$)	7.83 b	0.55	4.25 a	1.46	0.038*
Malondialdehyde ($\mu\text{mol/L}$)	5.46 a	0.43	11.45 b	1.87	0.015*
Peroxyntirite ($\mu\text{mol/L}$)	54.39 a	2.95	73.42 b	2.26	0.035*

*The difference in the letters (a, b) horizontally indicates that there is a significant difference at a probability level of less than or equal to 0.05 between the studied groups.

The results also indicated that there was a significant increase in the levels of ONOO- in diabetic patients who developed after infection with the coronavirus compared to the healthy group at the probability level of $P < 0.05$. These results are consistent with previous results that indicated high levels of oxidative compounds, including ONOO-, in corona patients (Ntyonga-Pono, 2020; Derouiche, 2020).

The reason for the high level of ONOO- in corona patients is the inflammation resulting as the body's immune response to protect against different types of infections, and during infections, excessive production of nitric oxide and superoxide anion radical occurs, which results in the formation of ONOO- in the infected body and the resulting oxidation problems different and increase the complications of the disease (Ahmed *et al.*, 2020).

4. Conclusions

The study concluded that the preptin hormone is a good indicator that reflects the status of patients with type 2 diabetes that developed after infection with corona, by comparing it with the levels of antioxidants and oxidants, as well as levels of fucose and glucose, and patients should increase the intake of antioxidants of various kinds to reduce their state of oxidative stress.

Acknowledgements

The author would like to acknowledge those who always encourage and give their guidance, mom and dad.

Conflict of Interest: The authors declare that there are no conflicts of interest.

References

- Ahmed, N. Chakrabarty, A. and Peter F. (2020). Protective Role of Glutathione against Peroxynitrite-Mediated DNA Damage during Acute Inflammation. *Chemical Research in Toxicology* 2020 33 (10), 2668-2674
- Allain, C.C., Poon, L.S., Chan, C.S., Richmond, W. and Fu, P.C. (1974). Determination of serum total cholesterol by enzymatic colorimetric method. *Clini. Chem.* 20(4): 470- 475.
- Alubaidi, A. and Tamara, Mohammd, U. (2018). Estimation of preptin in serum of thyroid dysfunction patients and its relationship with other parameters. *Oriental Journal of Chemistry*, 34(4), 2114–2124.
- Ambade, V. N., Sharma, Y. V., and Somani, B. L. (1998). Methods for estimation of blood glucose: a comparative evaluation. *Medical Journal Armed Forces India*, 54(2), 131-133.
- Aninagyei, E., Tetteh E.T. and Banini, J. (2019) Evaluation of haemato-biochemical parameters and serum levels of 8-iso-prostaglandin F2 α oxidative stress biomarker in sickle cell-malaria comorbidity. *J Appl Microb Res*, 2(1): 32–40
- Baqi, H., M. Farag, H. and El Bilbeisi, A.H. (2020). Oxidative Stress and Its Association with COVID-19: A Narrative Review. *Kurdistan Journal of Applied Research*. 5, 97-105.
- Bornstein, S.R., Dalan, R. and Hopkins, D. (2020). Endocrine and metabolic link to coronavirus infection. *Nat Rev Endocrinol* 16, 297–298.
- Buchanan, C.M., Phillips, A.R. and Cooper, G.J. (2001). Preptin derived from proinsulin-like growth factor II

- (proIGF-II) is secreted from pancreatic islet beta-cells and enhances insulin secretion. *Biochem. J.* 360:431–9
- Chee, Y.J., Ng, S.J.H. and Yeoh, E. (2020) Diabetic ketoacidosis precipitated by Covid-19 in a patient with newly diagnosed diabetes mellitus. *Diabetes Res Clin Pract.* 164:108166.
- Chen, N., Zhou, M. and Dong, X. (2020). Epidemiological and clinical characteristics of 99 cases of 2019 novel coronavirus pneumonia in Wuhan, China: a descriptive study *Lancet*, 395 (10223), pp. 507-513
- Clark, R. Waters, B. and Stanfill, A.G. (2021) Elevated liver function tests in COVID-19: causes, clinical evidence, and potential treatments *Nurse Pract.* 46 (1) pp. 21-26
- Derouiche S. (2020). Oxidative stress associated with SARS-Cov-2 (COVID-19) increases the severity of the lung disease—a systematic review. *J Infect Dis Epidemiol*, 6(3): 1–6.
- Dische, Z. and Shettles, L. B. (1948). A specific color reaction of methylpentoses and a spectrophotometric micromethod for their determination. *Journal of Biological Chemistry*, 175(2), 595-603.
- Doumas, B.T., Watson, W.A. and Biggs, H.G. (1971). Albumen standards and the measurement of serum albumin with bromocresol green. *Clin. Chem. Acta.* 31:87-96.
- Farukhi, Z., and Mora, S. (2018). The future of low-density lipoprotein cholesterol in an era of nonfasting lipid testing and potent low-density lipoprotein lowering. *Circulation*, 137(1): 20–23.
- Fossati, P. and Prencipe, L. (1982). Serum triglycerides determined colorimetrically with an enzyme that produces hydrogen peroxide. *Clin. Chem.* 28 (10): 2077-2080.
- Goyal, P., Choi, J., Pinheiro, L., Schenck, E., Chen, R. and Jabri, A. (2020). Clinical Characteristics of Covid-19 in New York City. *N Engl J Med.*
- Guidet, B. and Shah, S.V. (1989). Enhanced in vivo H₂O₂ generation by rat kidney in glycerol-induced renal failure. *Am J Physiol.* 257(3 Pt 2), F440-F445.
- Hameed, O. M. and Al-Helaly, L. A. (2020). Levels for Some Toxic and Essential Metals in Patients with Neurological Diseases. *Raf. Jour. Sci.* 29(3):27-37.
- Hameed, O. M. and Al-Helaly, L. A. (2021). Evaluation the level of Total Fucose and Some Enzymes in the Blood of Patients with Neurological Diseases. *Egypt. J. Chem.* Vol. 64, No. 10, pp. 5613 – 5618.
- Hinton, P.P. (2004). *Statistics Explained*. 2d Edition by Routledge printed in the USA and Canada pp.85-125.
- Iqbal, M. W., Riaz, T., Mahmood, S., Ali, K., Khan, I. M., Rehman, A., Zhang, W. and Mu, W. (2021). A review on selective l-fucose/d-arabinose isomerases for biocatalytic production of l-fucose/d-ribulose. *International Journal of Biological Macromolecules*, 168(), 558–571.
- Katsiki, N., Banach, M. and Mikhailidis, D. (2020). Lipid-lowering therapy and renin-angiotensin-aldosterone system inhibitors in the era of the COVID-19 pandemic. *Arch. Med. Sci.*, 16, 485–489.
- Khunti K, Del Prato, S. and Mathieu C. (2021) COVID-19, hyperglycemia, and new-onset diabetes. *Diabetes Care* 44:2645
- Lopez-Virella, M. F., Stone, P., Ellis, S., and Gllwell, J. A. (1977). Cholesterol determination in high density lipoprotein separated by three different methods. *Clin. Chem.* 23: 882-884.
- Lutz, C., Maher, L. and Lee, C. (2020). COVID-19 preclinical models: human angiotensin-converting enzyme 2 transgenic mice. *Hum Genomics* 14, 20
- Mahmudpour, M., Vahdat, K. and Keshavarz, M. (2022). The COVID-19-diabetes mellitus molecular tetrahedron. *Mol Biol Rep* 49, 4013–4024.
- Meher, G., Bhattacharjya, S. and Chakraborty, H. (2020). Membrane cholesterol modulates oligomeric status and peptide-membrane interaction of severe acute respiratory syndrome coronavirus fusion peptide. *J. Phys. Chem. B*, 123, 10654–10662.
- Million, M., Armstrong, N. and Khelaifia, S. (2020). The Antioxidants Glutathione, Ascorbic Acid and Uric Acid Maintain Butyrate Production by Human Gut Clostridia in The Presence of Oxygen In Vitro. *Sci Rep* 10, 7705.
- Mohiuddin, M. and Kasahara K. (2021). The emerging role of oxidative stress in complications of COVID-19 and potential therapeutic approach to diminish oxidative stress. *Respir Med.* 187:106605.
- Murray, E., Tomaszewski, M. and Guzik, T. (2020). Binding of SARS-CoV-2 and angiotensin-converting enzyme 2: clinical implications, *Cardiovascular Research*, Volume 116, Issue 7, Pages e87–e89,
- Nalbandian, A., Sehgal, K. and Gupta, A. (2021). Post-acute COVID-19 syndrome. *Nat Med* 27, 601–615
- Ni, W., Yang, X. and Yang, D. (2020). Role of angiotensin-converting enzyme 2 (ACE2) in COVID-19. *Crit Care* 24, 422
- Ntyonga-Pono MP. (2020). COVID-19 infection and oxidative stress: an under-explored approach for prevention and treatment? *Pan African Med* 35(Suppl. 2): 12
- Polonikov, A. (2020) Endogenous deficiency of glutathione as the most likely cause of serious manifestations and death in COVID-19 patients, *ACS Infect Dis* 6 1558–1562.
- Qin, C., Zhou, L. and Hu, Z. (2020) Dysregulation of immune response in patients with coronavirus 2019 (COVID-19) in Wuhan, China. *Clin Infect Dis.*, 71(15): 762- 768.
- Ren, H., Yang, Y. and Wang, F. (2020). Association of the insulin resistance marker TyG index with the severity and mortality of COVID-19. *Cardiovasc Diabetol*, 19:58.
- Sedlak, J. and Lindsay, R. H. (1968). Estimation of total, protein bound and non protein sulfhydryl groups in tissue with Ellman's reagent. *Anal. Biochem.* 25, 192-205.
- SeyedAlinaghi, S., Afsahi A.M. and MohsseniPour M. (2021). Late Complications of COVID-19; a Systematic Review of Current Evidence. *Arch Acad Emerg Med.* 9(1):e14. doi: 10.22037/aaem.v9i1.1058. PMID: 33681819; PMCID: PMC7927752.

- Sheraton M, Deo N, Kashyap R. and Surani S.(2020). A Review of Neurological Complications of COVID-19. *Cureus*. 12(5):e8192.
- Sorokin, A.V., Karathanasis, S.K., Yang, Z-H, Freeman, L, Kotani, K. and Remaley, AT. (2020). COVID-19—Associated dyslipidemia: Implications for mechanism of impaired resolution and novel therapeutic approaches. *The FASEB Journal*.34: 98439853. <https://doi.org/10.1096/fj.202001451>.
- Spada, A. Emami, J. and Tuszynski, J. A. (2021), The uniqueness of albumin as a carrier in nanodrug delivery *Mol. Pharm.*, 18 (5), pp. 1862-1894
- Sudre, C.H.,Murray, B. and Varsavsky, T. (2021). Attributes and predictors of long COVID. *Nat Med* 27: 626–631.
- Vanuffelen, B. E., Van Derzecz, J. and Dekoster, B. M. (1998). Intracellular but not extracellular conversion of nitroxyl anion into nitric oxide leads to stimulation of human neutrophil migration. *Biochem. J.* 330,719-722.
- Walker, H. K., Hall, W. D., and Hurst, J. W. (1990). *Clinical Methods: The History, Physical, and Laboratory Examinations*, 3, 60.
- Wang, H., Wang, Z. and Dong, Y. (2020).Phase-adjusted estimation of the number of Coronavirus Disease 2019 cases in Wuhan, China. *Cell Discov* 6, 10.



A study on Using Plant Extracts as Indicators for the Endpoint in the Acid-Base Titrations

Aisha AL-Abbasi*, Dania Abu Alassad, Ihssin Abdalsamed and Khadija Ahmida

Chemistry Department, Science Faculty, Sebha University, Libya.

DOI: <https://doi.org/10.37375/sjfsu.v3i1.149>

A B S T R A C T

ARTICLE INFO:

Received: 01 December 2022

Accepted: 16 January 2023

Published: 17 April 2023

Keywords:

Acid-Base Titrations, Green Chemistry, Natural Indicators, Methyl Orange; Phenolphthalein.

Acid-base titrations are the key part of volumetric analysis in the first year undergraduate chemistry practical program in Libya. Students are typically taught the procedures and skills necessary for acid-base titrations utilizing chemically synthesized indicators. Frequently utilized Synthetic indicators are sometimes difficult to obtain and highly hazardous to both people and aquatic life. Thus, the best option is to use natural dyes because it has been illustrated that some plant extracts exhibit the characteristics of synthetic dyes, making them usable for their use. Since this research emphasizes a return to green chemistry, it was necessary to search for alternative environmentally friendly indicators that are readily available, simple to prepare, and can be used to detect the endpoint of the reaction. The purpose of this article is to explore nine different types of aqueous extracts from various plants that can be used as indicators in acid-base titrations. The results have show that, similar to phenolphthalein, all of the investigated plant extracts are appropriate for strong-acid and strong-base titration. Moreover, hibiscus flower and cabbage leaf extracts are superior indicators for a strong-acid and strong-base titration to the synthesizers indicators. It is recommended that the use of these plant extracts as acid-base indicators should be combined in the teaching of acid-base titration. The amount of sodium hydroxide consumed at the endpoint were between 9.5 - 10 mL, while the pH of the solutions were between 6 - 9.7.

1 Introduction

Classical analysis methods are still sufficient and have many advantages, although the availability of instrumentational analytical techniques is offered for chemical analyses of various compound. (W. A. Izonfuo, Fekarurhobo, Obomanu, & Daworiye, 2006; Petrucci, 1972) Titration is among the standard analytical methods which are still used currently (Petrucci, 1972). The equivalence point in titration is often achieved by the endpoint titration which is characterized by indicators (W. A. Izonfuo et al., 2006; Mendham, 2004; Petrucci, 1972). The indicator is a chemical compound that is added during titration in a very small amount that causes a noticeable change in one of the physical or chemical properties of the solution and contributes to determining the endpoint of the titration. There are numerous types of indicators available for acid-base titration types

(W. A. Izonfuo et al., 2006; Mendham, 2004; Petrucci, 1972). Commonly used acid-base indicators are synthetic organic dyes such as phenolphthalein, methyl red and methyl orange, phenol red, methyl yellow, bromophenol blue, thymol blue, and others. these indicators are usually expensive and have toxic effects on humans such as diarrhea, pulmonary edema, hypoglycemia, and pancreatitis, and can lead to abdominal cramps, rashes, eruptions, redness, and necrosis of the skin and cause environmental pollution (Kasture, 2005; Okoduwa, Mboru, Adu, & Adeyi, 2015). Thus, researchers have sought ways to measure the pH of solutions other than using synthetic pH indicators (Bhagat, 2008; W. A. Izonfuo et al., 2006). In much of the published research, many flowers, fruits, and vegetables have been used effectively as natural pH indicators (Abugri, 2012;

Alejandre; Bhagat, 2008; Bhise, 204; W. F. Izonfuo, G. Obomanu, F., and Daworiye,L., 2006; Nuryanti, 2013; Okoduwa et al., 2015; Ologundudu, 2009; Pimpodkar, 2014; Vaibhav, 2014). Green indicators are pigments or dyes isolated from a variety of natural sources, including plants, fungi, insects, and algae. They were likely to be cheaper, environmentally friendly and non-toxic, readily available, easy to extract, less toxic to users, and environmentally friendly (Housecroft C. and A. G. Sharpe & 2008; Okoduwa et al., 2015; Pradeep, 2013). Almost any flower that is red, blue, or purple contains a class of organic pigments that change colour with pH [2, 4]. Natural dyes as acid-base indicators were first used in 1664 by Robert Boyle, nowadays, several studies conducted by different scientists have exploring the effectiveness of natural indicators in acid-base titration (Housecroft C. and A. G. Sharpe & 2008; Kadam, 2013; Okoduwa et al., 2015). Others are plants and leaves such as red cabbage extract, raspberry juice, black tea, beet juice, and tomato leaf. (Housecroft C. and A. G. Sharpe & 2008; W. F. Izonfuo, G. Obomanu, F., and Daworiye,L., 2006; Kadam, 2013; Okoduwa et al., 2015). From here, the natural indicator can be defined as a natural substance of plant origin that can be used to determine the pH of another substance (Kadam, 2013; Vaibhav, 2014). Plant pigments that provide natural food colours can be grouped into four primary classes based on their chemical structure, viz., chlorophyll, carotenoids, flavonoids, and betalain. Hence, this research aims to evaluate the properties of some colours natural plants to test the extent of their analytical capabilities as guides for acid and base titrations, tested plants are given in Table 1.

2. Materials and Methods

Materials and Instrumentation

2.1 Chemicals and Instrumentations










The chemicals used are all of a high degree of purity and are produced by well-known companies: Sodium hydroxide (98%), hydrochloric acid (37%), and sodium carbonate (99.8%). a pH device (Thermo).

2.2 Preparation of Standard Solutions

100 mL of a standard 0.1 M (mol/L) sodium carbonate solution was prepared by the direct method, weighing 1.06 g in a 100 mL volumetric flask, the volume was completed with deionized distilled water up to the standard mark. Hydrochloric acid in a concentration (0.1 M) was prepared by taking 8.36 mL) from a bottle of concentrated acid (37%-1.81g/cm³-36.5 g/mol) in a standard volumetric flask (1000 mL) the volume was supplemented with deionized distilled water. It was confirmed that the acid concentration was adjusted by titrating it with an exact titration of sodium carbonate

and a phenolphthalein index. Sodium hydroxide (0.1 M) was prepared by taking 4 g in a standard volumetric flask (1000 mL) the volume was supplemented with deionized distilled water. The control of sodium hydroxide was confirmed by titrating it with titrated hydrochloric acid and phenolphthalein index.

Table 1: Utilized plants to produce an aqueous extract for acid-base titrations

Plant	Discription
	Hibiscus rosa-Sinensis are used for foods and beverages and as a food coloring agent, as they have been known to contain anthocyanins [18-16].
	Red cabbage has an anthocyanin pigment primarily used as a food color and can be used as a pH indicator in pharmaceutical formulations.
	Eggplant has a dark purple or black colour. it ranks among the top 10 fruits and vegetables for its high phenol content and antioxidant properties. The peel of purple eggplant is rich in anthocyanins.
	Beetroot red beets contain a high percentage of betalain. Betalain is a coloured substance that gives some vegetables, fruits, and flowers their colour.
	Capsicum fruit colors vary between green, yellow, red, orange, and yellow. Capsicum extract contains β -carotene, capsanthin, cryptoxanthin, lutein, zeaxanthin, and capsanthin. Capsanthin is a major carotenoid in red pepper.
	Tomatoes ranked as the main source of lycopene, followed by β -carotene and vitamins C. Lycopene and β -carotene is a major contributors to tomato fruit coloration [19].
	Lemon, the outer peel is a light green to yellow and consists of flavonoids, which contain carotenoid pigments, vitamins, and essential oils [20].
	The poinciana tree (Red Acacia) has red flowers that have bioactive substances and antioxidants that are ideal for new natural anti-aging, hydrating, and hair treatments.
	<i>Pistacia Atlantica</i> fruit is orange coloured a small fruit numerous research has proven that it is beneficial for anaemia and increases iron levels (Mahjoub F, 2018).

2.3 Preparation of the Plant Extract

All solutions of the different plant extracts were prepared by dissolving 3.4 gram of each plant (date, flower, or root) in 40 mL of deionized distilled water and shaken for 3 hours. It is used on the same day, and then the filter. From these extracts, drops are added before starting the titration. The color change was tested with titration.

2.4 Acid-Base Titrations for Strong Acid and Strong Base

The hydrochloric acid was first titrated with sodium hydroxide to determine the volume of base needed to reach the equivalence point, using both phenolphthalein and methyl orange indicators. The previous experiment is repeated, but this time by adding drops of different plant extracts, and the calibration is recorded in color before, at, and after reaching the equivalence point. The pH values are also recorded at the endpoint point.

2.5 Measurement of pH and (Uv-Vis) Spectra of Aqueous Extracts.

Stepwise additions of 2 ml of hydrochloric acid (0.5 M) to 5 mL of the aqueous extract were made. Until a pH reached 1, the pH and UV-VIS spectrum were measured with each addition. Similarly, 2 mL of sodium hydroxide solution (0.5 M) is added progressively to 5 mL of the aqueous extract, with the pH and UV-VIS spectrum being recorded after each addition, until pH = 13.69. to calculate pH of 0.5 M NaOH. So, $pOH = -\log$

$$[OH^-] = -\log(0.5) = 0.3010 \text{ Hence, } pH = 14 - pOH = 13.69 .$$

3. Results and Discussion

The flower extract underwent testing to determine its suitability for use as an acid-base indicator in strong acid-strong base titrations. The screening results were comparable to those of conventional indicators methyl orange and phenolphthalein as collected in Table 2.

The endpoint of the aqueous extracts of the different plant extracts mentioned in Table 2 was also determined and it was compared with each of the indicators of methyl orange and phenolphthalein, and the results were included in Table (2) and Figure (1). It is assumed that the consumed volume will be 10 mL as expected by theoretical calculations of (10 mL), however, it is slightly different, these differences in 0.1 ml are due to the precision of the method. In addition, Table (2) includes a description of the colour of the endpoint.

The extracts of both hibiscus flowers and cabbage leaves were selected to study the change in acidity function when sodium hydroxide was added, due to the obvious change in colour at the neutralization point of these two extracts from pink to light green. 0.5 mL of NaOH was added each time and the corresponding value was recorded. As for the rest of the aqueous extracts, values were measured when the break-even point was reached, and the results were included in Table (2) and Figure (1).

Table 2: Screening results of acid-base titrations

	Indicator	Color change at the End point	Burette reading (mL)	pH at the end point
Standard indicator	Methyl Orange	Red to yellow	9.9	8.6
	Phenolphthalein	Colorless to red	9.9	7.5
Plant extract	Cabbage Leaves	Pink to light green	9.7	8.3
	Acacia Flowers	Pink to light green	9.8	6.3
	Eggplant Peels	colorless to light brown	9.6	9.7
	Lemon Peels	colorless to light green	9.5	6
	Beetroots	light orange to light green	10	9
	Hibiscus Flower	pink red to light brown	10	8.4
	Red Pepper	colorless to light green	9.6	7.3
	<i>Pistacia Atlantica</i> Fruit	light brown to light yellow	9.7	6.7
	Tomato Fruit	light green to dark brown	10	9.5

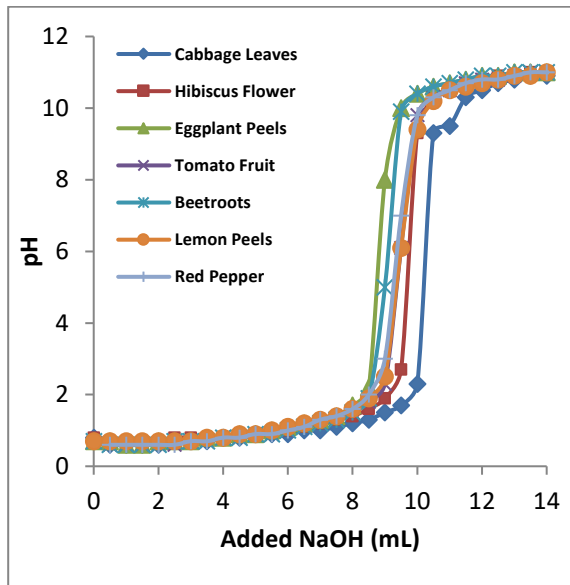


Figure 1: The change of the pH with the addition of NaOH

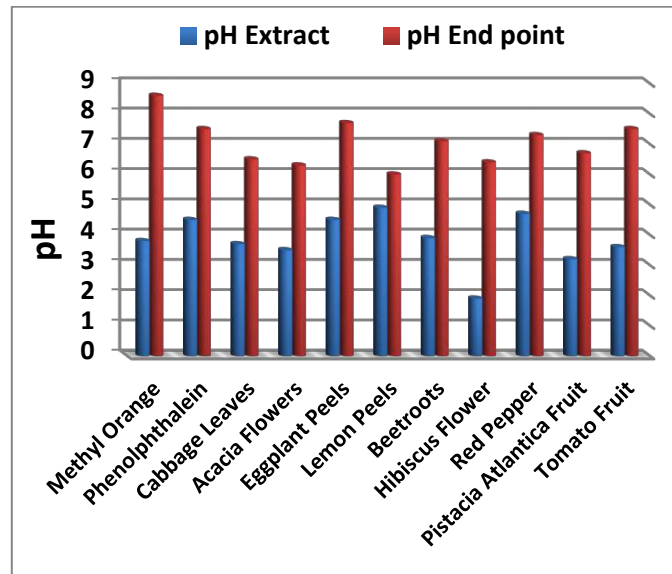


Figure 2: The change of the pH of extracts at the endpoint

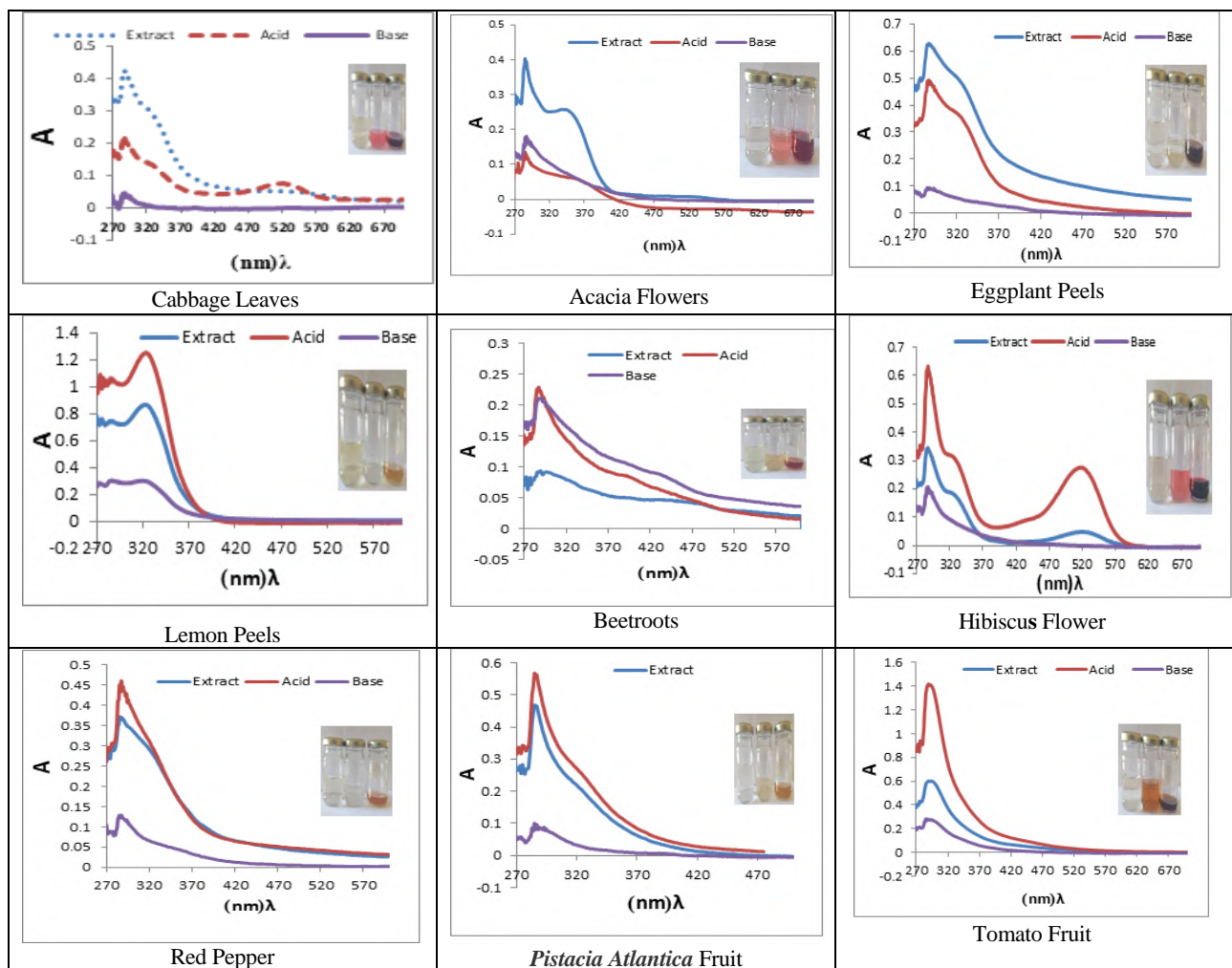


Figure 3: UV-vis spectra of plant extracts in acidic, neutral and basic media

An electronic spectrophotometer (Uv-Vis) was used to determine the absorbance of the extract in the visible region (ie. 200-900 nm) and the wavelength of maximum absorption (λ_{\max}) extrapolated for each extract. The absorption was plotted against the wavelength. It was included in Table (2) and Figure 3, with an explanation of the colour of these extracts in each medium and its comparison with the absorption spectra of the pure extracts.

UV-Vis spectrophotometer analysis of cabbage leaf extract showed that the maximum wavelength at (λ_{\max}) 519 nm is due to anthocyanins, which have an absorption in the region between 465-560 nm, which belongs the anthocyanin pigment that give red colour for its extract. The hibiscus extract has λ_{\max} at 520 nm, as they have been known to contain anthocyanins [18-16]. As for the eggplant peel extract, it was absorbed in 285 nm wavelength and with an overlapping absorption at 320 nm, respectively, this absorption disappear in base medium as the colour is vanish after equivalent point.

Moreover, Figure 3 showed that the extract of Red Acacia flowers absorbs at a λ_{\max} of 285 nm and at 330 nm, respectively. This absorption disappeared in the basal medium as the colour vanish.

The results also showed that lemon peel extract absorbs at a wavelength of 320 nm and this absorption was due to pigments strong. Tomato date extract absorbs only at a wavelength of 285 nm, and pepper extract absorbs at a wavelength of 285 nm which is similar to the spectrum of tomato, which attributed to the extract contains β -carotene.

However, beetroot extract absorbs at a wavelength of 285 nm and with an overlapping absorption in the range of 400-480 nm, respectively, this absorption belongs to a high content of betalain Betalain pigment. *Pistacia Atlantica* fruit seed extract absorbs at a wavelength of 285 nm and with an overlapping absorption at 320 nm, respectively.

4. Conclusion

In this research, dyes were successfully extracted from coloured plants, which could be used as chemical indices and as a guide for acid-base titrations. The behaviour of the coloured aqueous extracts was compared with standard indicator of phenolphthaline and methyl orange. The pH function of the pure aqueous extracts was measured and it was also measured at the equivalence point. The pH values of all aqueous extracts ranged between 1 - 4.5 before titration started, and their values after titration and at the equivalence point ranged between 6-7.7. UV-VIS spectra of pure aqueous extracts were recorded and their maximum wavelength was

determined. The spectra were also recorded in both acid and base medium. The electronic spectra, which were slight differ from the electronic spectra of the pure extracts, indicated the extent of the consistency of these extracts, and their chemical composition change with the change in the acidity function. The obtained results confirmed the possibility of using natural endpoint indicator in chemical titration experiments to identify the break-even point, and thus it is considered safer than using synthetic chemical endpoint indicator.

5. Recommendations

It is advised to investigate the viability of applying these coloured plant extracts to various additional titrations, such as complex formation titrations, precipitation titrations, or other titrations.

Acknowledgements

We would like to thank the Chemistry Department of Sebha University for supporting this work and the Libyan Petroleum Institute in Tripoli for their efforts in providing some of the chemical analysis techniques.

Declaration of Competing Interests

The authors declare that they have no known competing financial interests or personal relationships that could have appeared to influence the work reported in this paper.

References

- Abugri, D., Apea, O. and Pritchett, G. (2012). Investigation of a simple and cheap source of a natural indicator for acid-base titration: effects of system conditions on natural indicators. *Green and Sustainable Chemistry*, 02, 117-122.
- Alejandre, S. A., Ripalda, A. O. *The solvent extraction of rosa rosa (red rose) flower petals and its application as ph indicator*. (BSChE). Eastern Visayas State University, Tacloban City/Republic of the Philippines.
- Bhagat, V., Patil, R., Channekar, P., Shetty, S. and Akarte, A. (2008). Herbal indicators as a substituent to synthetic indicators,. *International Journal of Green Pharmacy*, 2, 162-163.
- Bhise, S., Shinde, N., Surve, B., Pimpodkar, V., and Shikalgar, S. (2004). Acalypha wilkesiana as natural pH indicator. *International Journal of Natural Products Research*, 4, 33-35.
- Housecroft C. and A. G. Sharpe, & , 3rd edition, . (2008). *Inorganic Chemistry* (3 ed.). England, UK: Educational ltd Prentice Hall.
- Izonfuo, W. A., Fekarurhobo, G., Obomanu, F., & Daworiye, L. T. (2006). Acid-base indicator properties of dyes from local plants I: dyes from Basella alba (Indian spinach) and Hibiscus sabdariffa (Zobo). *Journal of Applied Sciences and Environmental Management*, 10. doi:10.4314/jasem.v10i1.17295

- Izonfuo, W. F., G. Obomanu, F., and Daworiye, L. (2006). Acid-base indicator properties of dyes from local plants I: dyes from *Basella alba* (Indian spinach) and *Hibiscus sabdariffa* (Zobo). *Journal of Applied Sciences and Environmental Management* 10(5-8).
- Kadam, S., Yadav, A., Raje, V., and Waghmare K.,. (2013). Comparative study of natural and synthetic indicators. *Der Pharma Chemic*, 5, 296-299.
- Kasture, A., Mahadik, R., Wadodkar, and More, H., . (2005). Textbook of Pharmaceutical Analysis. In (11th edition ed., Vol. 1). Maharashtra, India: Nirali Prakashan.
- Mahjoub F, A. R. K., Yousefi M, Mohebbi M, Salari R. , . (2018). *Pistacia atlantica* Desf. A review of its traditional uses. *phytochemicals and pharmacology. J Med Life*, 3, 80-186.
- Mendham, J., Denney, R., and Barnes, J., Freeman, W. (2004). *Quantitative Chemical Analysis* (Vol. 6th edition). New Delhi, India.
- Nuryanti, S., Matsjeh, S., Anwar, C.,Raharjo, T., Hamzah, B. . (2013). Corolla of Roselle (*Hibiscus sabdariffa* L.) as acid-base indicator. *Eur. J. Chem.*, 4, 20-24.
- Okoduwa, S. I. R., Mbora, L. O., Adu, M. E., & Adeyi, A. A. (2015). Comparative Analysis of the Properties of Acid-Base Indicator of Rose (*Rosa setigera*), Allamanda (*Allamanda cathartica*), and Hibiscus (*Hibiscus rosasinensis*) Flowers. *Biochemistry Research International*, 2015, 381721. doi:10.1155/2015/381721
- Ologundudu, A., Ologundudu, A., Ololade, I., Obi, F. . (2009). Effect of *Hibiscus sabdariffa* anthocyanins on 2, 4- dinitrophenylhydrazine-induced hematotoxicity in rabbits. *J. Biochem. Res.*, 3, 140-144. .
- Petrucci, R. H. (1972). *General Chemistry; Principles and Modern Applications*: Macmillan.
- Pimpodkar, N. S., S., Shinde, N., Bhise, and Surve, B. (2014). *Rhoeo sythacea* and *Allamanda cathartica* extract as a natural indicator in acidity-alkalimetry. *Asian Journal of Pharmaceutical Analysis*, 4, 82–84.
- Pradeep, J. a. D., K. . (2013). A novel, inexpensive and less hazardous acid-base indicator. *Journal of Laboratory Chemical Education*, 1, 34-38.
- Vaibhav, G. V., B., Prashant, D., Ganpatrao, N., Suresh, T., and Ashish, S. (2014). Study of *Nerium odoratum* as natural, economical and effective alternative to synthetic indicator and litmus paper. *International Journal of Pharmaceutical Chemical Science*, 3, 440.



Assessment of the Antimicrobial Activity of Three *Silene* Species (Caryophyllaceae) Against Some Microorganisms

Miloud M. Miloud¹ and Najma A. Senussi²

¹Botany Department, Science Faculty, Benghazi University, Al-abyar branch, Libya.

²Botany Department, Science Faculty, Ajdabiya University, Libya.

DOI: <https://doi.org/10.37375/sjfsu.v3i1.1089>

A B S T R A C T

ARTICLE INFO:

Received: 26 February 2023

Accepted: 5 April 2023

Published: 17 April 2023

Keywords:

Silene species, Antimicrobial activity, well diffusion assay, MIC, MBC/MFC.

Three *Silene* species (*Silene gallical* L., *Silene succulent* Forsk., and *Silene apetala* Willd) were tested for potential anti-microbial activity against some microorganisms (*Staphylococcus aureus*, *Serratia marcescens*, *Acinetobacter boumannii*, *Klebsella* sp., *Aspergillus flavus*, *Aspergillus niger*, *Cladosporium cladosporioides*, and *Alternaria alternata* using the well diffusion assay. Solvents used in the extraction process are ethanol, methanol and acetone. The obtained results from all plant extracts showed clear antimicrobial activity against all tested microbial species, except *S. succulent* extracts, which had no inhibitory activity against *Klebsiella* sp., *A. niger* and *A. flavus*. Moreover, the acetone extract of *S. gallical* and *S. apetala* was the most effective plant extract and showed bacteriostatic, bactericidal, fungistatic and fungicidal activities against the highly susceptible species of microbes (*S. aureus*, *S. marcescens*, *C. cladosporioides*, and *A. alternata*) with MIC ranged from 3.12 to 6.25 mg/ml, MBC and MFC of 6.25 and 12.5 mg/ml. The experiments confirmed the efficacy of selected plant extracts as natural antimicrobials and suggested that they could be used in drugs to treat infectious diseases caused by the tested microbes.

1 Introduction

Despite the progress that has been made in medical science, infectious pathogens remain an important cause of morbidity and mortality (Moellering et al., 2007). Those circumstances have propelled scientists to explore new antimicrobial effective substances from different sources such as medicinal plants (Cordell, 2000). Medicinal plants are a source of efficient substances that act as antibacterial and antifungal agents (Chandra, 2013). Medicinal plant extracts are used for the treatment or prevention of diseases and promotion of good health (El Astal et al., 2005). In this study, we targeted three plants growing southeast of Benghazi, Libya. The selected plants are *Silene gallical* L., *Silene succulent*

Forsk. and *Silene apetala* Willd. (The used part is the leaves), but known for their uses in traditional medicine for various diseases. Many species belongs to *Silene* have been used to treat inflammations, bronchitis, colds, and infections (Ali et al., 1999; Hirst, 2005). The *Silene* belongs to Caryophyllaceae family which comprises annuals, biennials and perennials (Greuter 1995). Most of its species are hermaphrodites and very few numbers of its species are dioecious or gynodioecious (Greuter, 1995). Some *Silene* species contain effective chemical compounds such as ecdysteroids, Phyto-ecdysteroids, flavonoids, saponins and triterpenes (Mamadalieva, 2012). The main objective of current study is to evaluate the antimicrobial activity of leaf extracts of *Silene*

gallica, *Silene succulent* and *Silene apetala* against some microorganisms.

2 Materials and Methods

2.1 Plants extraction preparation

Fresh samples were collected from the leaves of the selected plants in the middle of the spring month of 2022 from the southeast of Benghazi, Libya. The collected plants were watery washed and dried in the shade for 2 weeks. The dried plant leaves of each plant species were crushed into a fine powder using an electric blender. According to the method of Mohammadi *et al.*, (2015), with minor modifications, 50 g of the powder of *Silene gallica*, *Silene succulent*, and *Silene apetala* were filled in the thimble and extracted successively with 200 ml each of ethanol, methanol, and acetone using a Soxhlet apparatus for 24 hours. All the extracts were evaporated using a rotary evaporator. All the crude extracts were dissolved in the same used solvents. One concentration of extracts was prepared, which is 50 mg/ml, and stored at 4 °C in airtight bottles until further use.

2.2 Collection of microorganisms

Bacterial species were collected from the microbiology laboratory of Benghazi Medical Centre (BMC). Fungal species were collected from the Botany Department, Ajdabiya University. In total, eight microorganisms, four bacterial species (*S. aureus*, *S. marcescens*, *A. boumannii*, *Klebsiella sp.*) and four fungal species (*A. niger*, *A. flavus*, *C. cladosporioides*, and *A. alternata*). The bacterial species were maintained on nutrient agar slants and the fungal species were maintained on potato dextrose agar slants at 4 °C.

2.3 Inoculums preparation

Bacteria stock cultures were sub-cultured onto Nutrient Agar (NA) plates and incubated overnight at 37°C (bacterial cultures are 24 hours old). Three to four bacterial colonies were inoculated into 10 ml of Mueller Hinton broth (MHB) and incubated at 37 °C. The overnight bacterial suspensions were adjusted to 0.5 McFarland Standard with sterile MHB broth, approximately 1.5×10^6 cell/ml. To aid comparison, the adjustment of bacterial suspensions to the density of the 0.5 McFarland Standard was done against a white background with contrasting black lines (Teh *et al.*, 2017). The fungal inoculum (spores) was prepared according to the method of Surapuram *et al.*, (2014) with minor modification, by suspending five representative colonies, obtained from fresh, mature (3 to 7 days-old)

cultures grown at 27°C on PDA medium, in potato dextrose broth (PDB). Then the inoculum was adjusted to 0.5 McFarland standard, approximately $1-5 \times 10^6$ spores/ml, by measuring the absorbance in a spectrophotometer at a wavelength of 625 nm.

2.4 Antimicrobial activity of plant extracts

The obtained crude extracts were tested against four bacterial species and four fungal species by MHA medium and PDA medium. A well diffusion assay was used for evaluating the antimicrobial activity (Pawaskar and Kale, 2006; Athanassiadis *et al.*, 2009). Some antibiotics were used as the standard antimicrobial agents. The media was poured into the sterile Petri plates and allowed to solidify to make a base layer. The microbial inoculum was evenly spread over the media. A sterile cork borer was used to punch wells (five wells) in the media. Subsequently, wells were filled with 100 µl of each extract at a concentration of 50 mg/ml and allowed to diffuse at room temperature for 1 hour, then the plates were placed in an incubator at 37 °C for 24 hours in the case of bacteria and at 27 °C for 72 hours in the case of fungi. The resulting diameters of inhibition zones were measured using a ruler in millimeters. The experiments were conducted three times, and the mean zone of inhibition was calculated for each crude extract and standard antibiotic.

2.5 Determination of Minimal Inhibitory

Concentration (MIC) and Minimum

Bactericidal/Fungicidal Concentration

(MBC/MFC) of the effective plant extracts

The MIC test was prepared according to the method of Mostafa *et al.*, (2018), with minor modifications. MIC is defined as the lowest concentration of an antimicrobial that will inhibit the visible growth of microbes after overnight incubation. The crude plant extracts which exhibited strong antimicrobial activity at 50 mg/ml were tested to determine their MIC using a well diffusion assay and to evaluate their efficiency in controlling microbial species causing diseases. different concentrations of the tested plant extracts (1.56, 3.12, 6.25, 12.5, 25, and 50 mg/ml). Mueller-Hinton agar and Potato dextrose agar were poured into sterile Petri dishes and seeded with microbial suspensions of the tested microbes. Wells were filled with 100µl of various plant extracts concentrations and allowed to diffuse at room temperature for 1 hour before being incubated in the incubator at 37 °C for 24 hours (for bacteria) and at 27 °C for 48-72 hours (for fungi). The zones of inhibition were measured by a ruler in millimeters. While, the MBC and MFC are the

concentrations that cause growth inhibition by % 99.9, and this was confirmed by taking a swab from the zones of inhibition and cultivating it on MHA medium and PDA medium again to make sure the bacteria and fungi are killed. The concentration of the plant extract that did not show any microbial growth on the freshly inoculated used media was determined as the MBC and MFC.

3 Results

The results from the experiments were recorded in Table 1 and in Figures 1-3. *S. gallical*, *S. succulent* and *S. apetala* were investigated to evaluate their antimicrobial activity against eight microorganisms, including *S. aureus*, *S. marcescens*, *A. boumannii*, *Klebsiella sp.*, *A. niger*, *A. flavus*, *C. cladosporioides* and *A. alternata*, using a well diffusion assay with a concentration of 50 mg/ml. Ciprofloxacin, Imipenem, Colistin, and Fluconazole were used as a positive controls for the antibacterial and antifungal assays, respectively. The ethanol, methanol, and acetone solvents were used as a negative controls. The obtained results from all plant extracts showed clear antimicrobial activity against all tested microbial species, except *S. succulent* extracts, had no inhibitory

activity against *Klebsiella sp.*, *A. niger* and *A. flavus*. Moreover, the acetone extract of *S. gallical* and *S. apetala* was the most effective plant extract against four microbial species (*S. aureus*, *S. marcescens*, *C. cladosporioides*, and *A. alternata*) compared to the other extracts (ethanolic and methanolic extracts). In the present study, the acetone extract of *S. gallical* and *S. apetala* was the most efficient plant extract in inhibiting microbial species *S. aureus*, *S. marcescens*, *C. cladosporioides*, and *A. alternata*, so the MIC, MBC and MFC values of this extract were tested. The MIC results were recorded in Table 2 and illustrated in Figures 4 and 5. The inhibitory effect of *S. gallical* acetone extract started at 3.12 mg/ml with inhibition zones of 9,8,9 and 8 mm against *S. aureus*, *S. marcescens*, *C. cladosporioides*, and *A. alternata*, while acetone extract of *S. apetala* suppressed microbial growth of these species at a concentration of 6.25 mg/ml with inhibition zones of 9,8,9 and 9 mm respectively. *S. gallical* acetone extract showed potentially bactericidal and fungicidal activities against four microbial species (*S. aureus*, *S. marcescens*, *C. cladosporioides*, and *A. alternata*) with MBC and MFC of 6.25 mg/ml, while the MBC and MFC of *S. apetala* acetone extract reached 12.5 mg/ml against these species.

Table (1). Average zones of inhibition of *Silene* leaf extracts against tested microbial species.

No.	Plant species	The zone of inhibition is measured in millimeter													
		Concentration 50 mg/ml													
		<i>S. gallical</i>			<i>S. succulent</i>			<i>S. apetala</i>			Antibiotics				Controls
Microbial species	A	B	C	A	B	C	A	B	C	Ci	Im	Co	Fl	ABC	
1	<i>S. aureus</i>	13	12	16	12	13	13	11	11	16	23	R	R	R	R
2	<i>S. marcescens</i>	11	10	16	11	10	12	10	12	15	R	21	R	R	R
3	<i>A. boumannii</i>	13	13	13	10	9	11	10	10	12	R	R	13	R	R
4	<i>Klebsiella sp.</i>	11	10	13	R	R	R	12	11	12	18	R	R	R	R
5	<i>A. niger</i>	12	10	12	R	R	R	9	9	10	R	R	R	13	R
6	<i>A. flavus</i>	11	11	12	R	R	R	9	9	10	R	R	R	13	R
7	<i>C. cladosporioides</i>	10	11	17	10	10	13	11	13	15	R	R	R	19	R
8	<i>A. alternata</i>	11	13	16	11	11	12	13	13	16	R	R	R	16	R

A:Ethanol B:Methanol C:Acetone R:Resistant / Ci:Ciprofloxacin, Im:Imipenem, Co:Colistin, Fl:Fluconazole

Table (2). MIC values of acetone extract of *S. gallical* and *S. apetala* against four microbial species.

No.	Plant extract	The zone of inhibition is measured in millimeter				
		Microbial species				
		Concentrations in mg/ml	<i>S. aureus</i>	<i>S. marcescens</i>	<i>C. cladosporioides</i>	<i>A. alternata</i>
1	<i>S. gallical</i>	1.56	R	R	R	R
		3.12	9	8	9	8
		6.25	9	8	9	10
		12.5	12	10	13	11
		25	14	13	15	14
		50	16	16	17	16
2	<i>S. apetala</i>	1.56	R	R	R	R
		3.12	R	R	R	R
		6.25	9	8	9	9
		12.5	12	11	10	10
		25	13	14	12	13
		50	16	15	15	16

R:Resistant

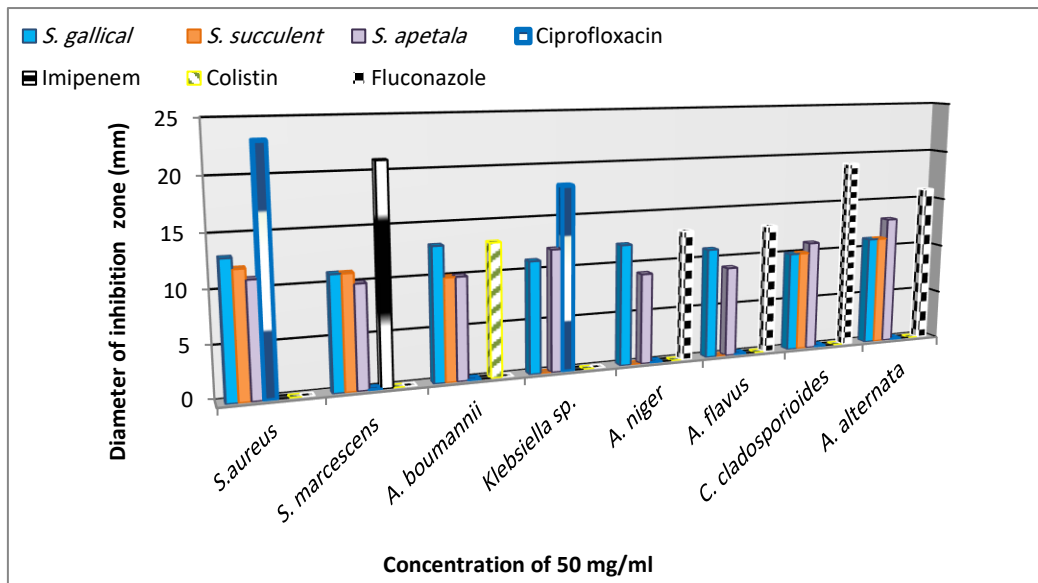


Figure (1): Effect of ethanol extract of *Silene* species against tested microbial species

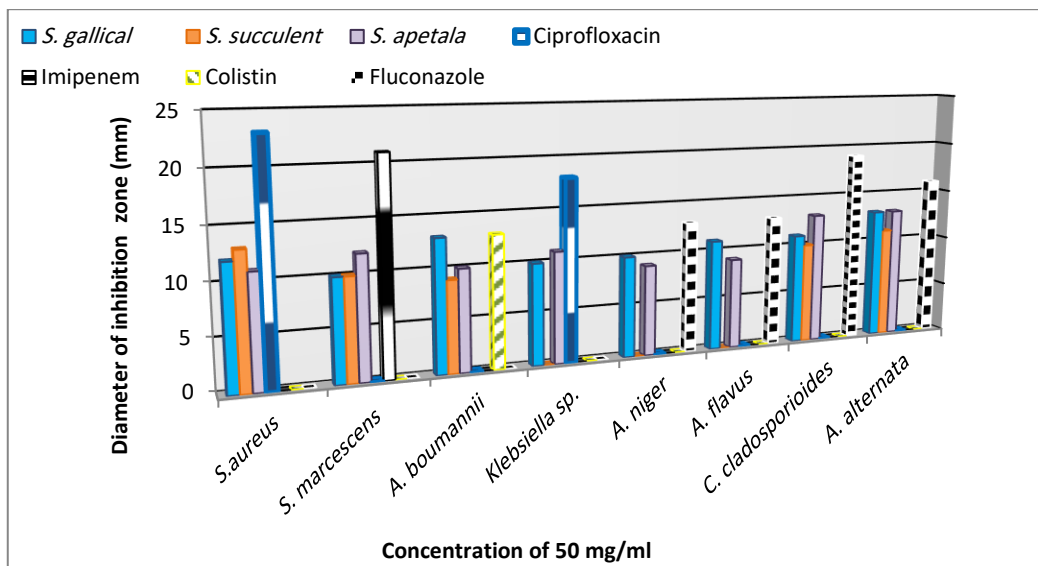


Figure (2): Effect of methanol extract of *Silene* species against tested microbial species

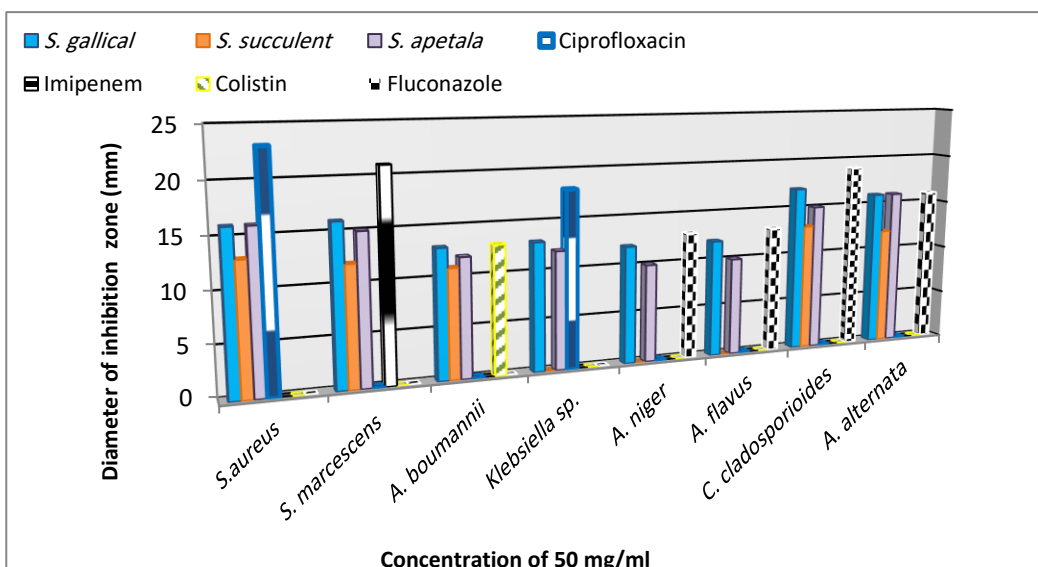


Figure (3). Effect of acetone extract of *Silene* species against tested microbial species.

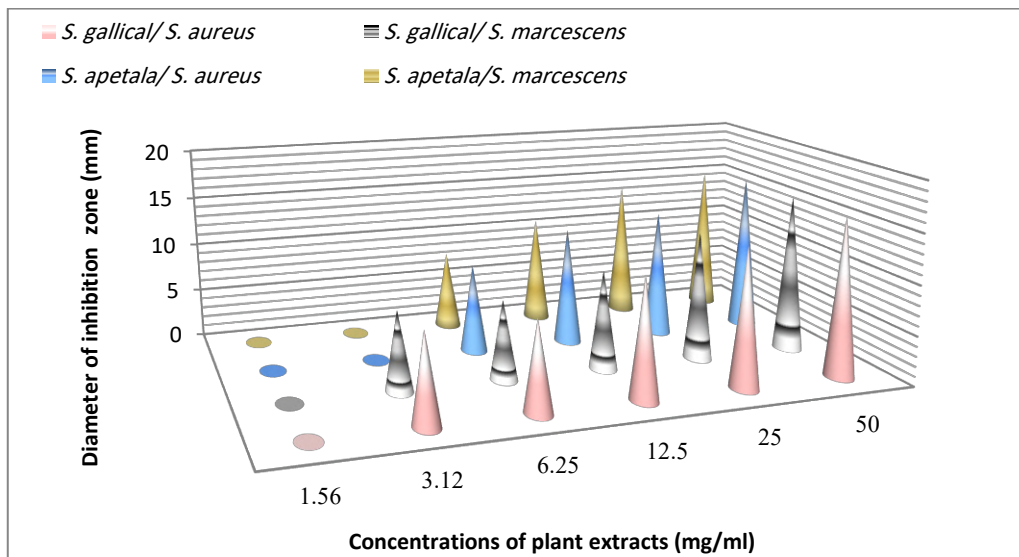


Figure (4). MIC of acetone extract against *S. aureus* and *S. marcescens*

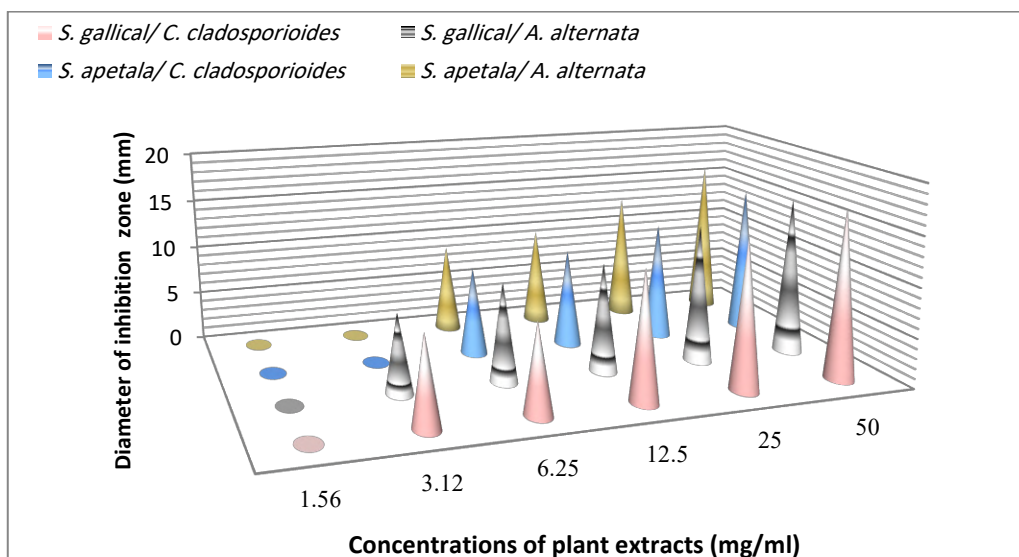


Figure (5). MIC of acetone extract against *C. cladosporioides*, and *A. alternata*

4 Discussion

The agar well diffusion method has been used in this research because it is more sensitive than the agar disc diffusion method (Valgas et al., 2007). Many studies have shown that obtained crude extracts from the *Silene* species inhibit the growth of different microorganisms at various concentrations (Miloud and Senussi, 2021; Keskin et al., 2016; Toroglu et al., 2013; Ertürk et al., 2006). Several studies were conducted to determine the efficacy of plant extracts and their active compounds as antimicrobial agents for microbial growth control. High phenolic compounds, flavonoids, aldehydes, ketones, saponins, and alcohols cause antimicrobial activity (Akgul, 1989; Sindhu and Manorama, 2012). These compounds are known to be abundant in the Caryophyllaceae family. The flavonoids from plant extracts have been found to possess antimicrobial and antioxidant properties in various studies (Amarlal et al., 2009; Lin et al., 2008). Gram positive bacteria were to be more susceptible than Gram negative bacteria. This could be due to the fact that the cell wall of Gram positive bacteria is less complex and lack the natural sieve effect against large molecules due to the small pores in their cell envelope (Hawkey, 1998). Some researchers have suggested that antimicrobial components of plant extracts (terpenoid, alkaloid, and phenolic compounds) interact with enzymes and proteins of the microbial cell membrane, causing its disruption to disperse a flux of protons towards the cell exterior, which induces cell death or may inhibit enzymes necessary for amino acid biosynthesis (Burt, 2004; Gill and Holley, 2006).

5 Conclusions

In conclusion, the used crude extracts of *Silene* species exhibited a good antibacterial and antifungal activities against all tested microbial species, except *S. succulent* extracts had no activity against (*Klebsiella sp.*, *A. niger* and *A. flavus*). The acetone extract of *S. gallica* and *S. apetala* was highly significant against the highly susceptible species of microbes (*S. aureus*, *S. marcescens*, *C. cladosporioides*, and *A. alternate*). Finally, the results of this study clearly elucidate the antimicrobial activity of these plants and provide an evidence to support their use in folk medicine.

Acknowledgements

We would like to thank the Department of Botany, Faculty of Science, Ajdabiya University for providing all the facilities to conduct this study.

Conflict of Interest: The authors declare that there are no conflicts of interest.

References

- Akgul, A. (1989). Antimicrobial activity of black cumin (*Nigella sativa* L.) essential oil. *Gazi Universitesi Eczacilik Fakultesi Dergisi*, 6(1), 63-68.
- Ali, Z., Ahmad, V. U., Ali, M. S., Iqbal, F., Zahid, M., & Alam, N. (1999). Two new C-glycosylflavones from *Silene conoidea*. *Natural Product Letters*, 13(2), 121-129. <https://doi.org/10.1080/10575639908048832>
- Amaral, S., Mira, L., Nogueira, J. M. F., da Silva, A. P., & Florêncio, M. H. (2009). Plant extracts with anti-inflammatory properties—A new approach for characterization of their bioactive compounds and establishment of structure–antioxidant activity relationships. *Bioorganic & medicinal chemistry*, 17(5), 1876-1883. <https://doi.org/10.1016/j.bmc.2009.01.045>
- Athanassiadis, B., Abbott, P. V., George, N., & Walsh, L. J. (2009). An *in vitro* study of the antimicrobial activity of some endodontic medicaments and their bases using an agar well diffusion assay. *Australian Dental Journal*, 54(2), 141-146. <https://doi.org/10.1111/j.1834-7819.2009.01107.x>
- Burt, S. (2004). Essential oils: their antibacterial properties and potential application in foods: A review. *International Journal of Food Microbiology*, 94(3), 223–253. <https://doi.org/10.1016/j.ijfoodmicro.2004.03.022>
- Chandra, M. (2013). Antimicrobial activity of medicinal plants against human pathogenic bacteria. *International journal of biotechnology and bioengineering research*, 4(7), 653-658. <http://www.ripublication.com/ijbbr.htm>
- Cordell, G. A. (2000). Biodiversity and drug discovery—a symbiotic relationship. *Phytochemistry*, 55(6), 463-480. [https://doi.org/10.1016/S0031-9422\(00\)00230-2](https://doi.org/10.1016/S0031-9422(00)00230-2)
- El Astal, Z. Y., Ashour, A. E. R. A., & Kerrit, A. A. M. (2005). Antimicrobial activity of some medicinal plant extracts in Palestine. *Pakistan Journal of Medical Sciences*, 21(2), 187-193.
- Ertürk, Ö., Kati, H., Yayli, N., & Demirbağ, Z. (2006). Antimicrobial properties of *Silene multifida* (Adams) Rohrb. plant extracts. *Turkish Journal of Biology*, 30(1), 17-21. <https://journals.tubitak.gov.tr/biology>
- Gill, A. O., & Holley, R. A. (2006). Disruption of *Escherichia coli*, *Listeria monocytogenes* and *Lactobacillus sakei* cellular membranes by plant oil aromatics. *International Journal of Food Microbiology*, 108, 1–9. <https://doi.org/10.1016/j.ijfoodmicro.2005.10.009>
- Greuter, W. (1995). *Silene* (Caryophyllaceae) in Greece: a subgeneric and sectional classification. *Taxon*, 44(4), 543-581. <https://doi.org/10.2307/1223499>

- Greuter, W. (1995). Studies in Greek Caryophylloideae: *Agrostemma*, *Silene*, and *Vaccaria*. *Willdenowia*, 105-142. <https://www.jstor.org/stable/3996977>
- Gould D, Booker C. Applied microbiology for nurses. Aardvark Editorial, Mcndham, Suffolk; 2000:75-94
- Hawkey, P. M. (1998). The origins and molecular basis of antibiotic resistance. *British Medical Journal*, 317(7159), 657-660. <https://doi.org/10.1136/bmj.317.7159.657>
- Hirst, M. (2005). Dreams and medicines: The perspective of Xhosa diviners and novices in the Eastern Cape, South Africa. *Indo-Pacific Journal of Phenomenology*, 5(2), 1-22. <https://hdl.handle.net/10520/EJC46926>
- Keskin, D., Guvensen, N. C., & Yildiz, K. (2016). Antimicrobial activity of *Silene cariensis* subsp *cariensis* and *Silene pungens* from Turkey. *Advances in Environmental Biology*, 10(7), 167-173. <http://www.aensi.org/aeb.html>
- Lin, S. Y., Wang, C. C., Lu, Y. L., Wu, W. C., & Hou, W. C. (2008). Antioxidant, anti-semicarbazide-sensitive amine oxidase, and anti-hypertensive activities of geraniin isolated from *Phyllanthus urinaria*. *Food and Chemical Toxicology*, 46(7), 2485-2492. <https://doi.org/10.1016/j.fct.2008.04.007>
- Mamadalieva, N. Z. (2012). Phytoecdysteroids from *Silene* plants: distribution, diversity and biological (antitumour, antibacterial and antioxidant) activities. *Boletín Latinoamericano y del Caribe de Plantas Medicinales y Aromáticas*, 11(6), 474-497. <https://www.redalyc.org/articulo.oa?id=85624607001>
- Miloud, M.M., & Senussi, N.A. (2021). Antibacterial activity of leaf extracts of *Silene succulent* Forsk. (Caryophyllaceae) against clinically important bacteria. *Academia Journal of Microbiology Research*, 9(1): 013-020. <http://www.academiapublishing.org/ajmr>
- Moellering Jr, R. C., Graybill, J. R., McGowan Jr, J. E., & Corey, L. (2007). Antimicrobial resistance prevention initiative—an update: proceedings of an expert panel on resistance. *American journal of infection control*, 35(9), S1-S23. <https://doi.org/10.1016/j.ajic.2007.08.001>
- Mohammadi, S., Asgary, V., Shandiz, S. A. S., Heidari, E., Jozaghkar, H., Cohan, R. A., & Mirzaie, A. (2015). Antimicrobial activity of methanolic root extracts of *Euphorbia condylocarpa* against pathogenic bacteria. *Advanced Studies in Biology*, 7(2), 55-64. <https://doi.org/10.12988/asb.2015.41049>
- Mostafa, A. A., Al-Askar, A. A., Almaary, K. S., Dawoud, T. M., Sholkamy, E. N., & Bakri, M. M. (2018). Antimicrobial activity of some plant extracts against bacterial strains causing food poisoning diseases. *Saudi Journal of Biological Sciences*, 25(2), 361–366. <https://doi.org/10.1016/j.sjbs.2017.02.004>
- Pawaskar, S. M., & Kale, K. U. (2006). Antibacterial activity of successive extracts of *Mimosa pudica*. *INDIAN DRUGS-BOMBAY-*, 43(6), 476.
- Sindhu, S., & Manorama, S. (2012). Screening of *Polycarpha corymbosa* lam.(Caryophyllaceae) for its in vitro antioxidant activity. *Asian Journal of Pharmaceutical and Clinical Research*, 5(4), 175-8.
- Surapuram, V., Setzer, W. N., McFeeters, R. L., & McFeeters, H. (2014). Antifungal activity of plant extracts against *Aspergillus niger* and *Rhizopus stolonifer*. *Natural Product Communications*, 9(11), 1603 – 1605. <https://doi.org/10.1177/1934578X1400901118>
- Teh, C. H., Nazni, W. A., Nurulhusna, A. B., Norazah, A., & Lee, H. L. (2017). Determination of antibacterial activity and minimum inhibitory concentration of larval extract of flyvia resazurin-based turbidometric assay. *BMC Microbiology*, 17(36), 1-8. <https://doi.org/10.1186/s12866-017-0936-3>
- Toroglu, S., Keskin, D., Dadandi, M. Y., & Yildiz, K. (2013). Comparison of antimicrobial activity of *Silene laxa* Boiss. & Kotschy and *Silene caramanica* Boiss. & Heldr different extracts from Turkey. *JOURNAL OF PURE AND APPLIED MICROBIOLOGY*, 7, 1763-1768.



Mobile Phones as a Source of Bacterial Infection

Najla A. Najam¹ and Fauzia Garabulli²

¹Microbiology Department, Assistant Lecturer at the Higher Institute of Science and Technology-Suluq, Benghazi, Libya.

²Botany Department, Benghazi University, Benghazi, Libya.

DOI: <https://doi.org/10.37375/sjfssu.v3i1.155>

ABSTRACT

ARTICLE INFO:

Received: 01 December 2022

Accepted: 10 April 2023

Published: 17 April 2023

Keywords:

Benghazi, mobile phone, pathogens, nosocomial, reservoir, antibiotics.

Background: The wide spread of mobile phones in recent years inevitably raises the question of whether they are an exogenous source of infections.

Design: A cross-sectional study was carried out among some teachers, educational staff, doctors, and nurses selected using the multi-stage stratified random sampling technique. 100 samples were collected from some teachers, educational staff, doctors, and nurses in some hospitals in Benghazi.

Results: The organisms sequentially isolated in this study, based on colonial, morphological, and biochemical characteristics, were coagulase-negative Staphylococci (58%), *Staphylococcus aureus* (12%), *Corynebacterium urealyticum* (6%), *Bacillus cereus* (5%), *Tatumella ptyseos* (3%), *Leuconostoc lactis*, *Pseudomonas aeruginosa*, All isolates were resistant to more than one antibiotic. This revealed that mobile phones may have a notable role in the transmission of multidrug-resistant nosocomial pathogens.

Conclusions: This study showed microbial contamination on personal mobile phones and hands. Some of the contaminated mobile phone microorganisms (such as *Staphylococcus aureus*) were epidemiologically important nosocomial drug-resistant pathogens. These isolates of bacteria were resistant to commonly used antimicrobials such as amoxicillin, gentamicin, and ciprofloxacin. These results showed that mobile phones and personal's hands were contaminated with various types of bacteria, which suggested that mobile phones (used by people in daily practice) may be a source of nosocomial infections.

1. Introduction

Mobile phones have become an integral part of modern social life and are in the hands of billions of users worldwide every day. Between 2011- 2018 the adoption rate of mobile phones within the community skyrocketed from 10 to 60 percent while the upward trend reaches 79% by 2025 (Tiron *et al.*, 2020). The real problem is that the number of bacterial strains that develop resistance to disinfectants and especially antibiotics is increasing very quickly. Some of these resistant microorganisms (bacteria) are difficult to destroy and can survive for a longer time on the floor and other surfaces. Resistant bacterial strains are now

spreading to our houses and other places where people live or work (Eltablawy and Elhifnawi, 2009).

National Center for Radiation Research and Technology (NCRRT) (Eltablawy and Elhifnawi, 2009) reported that there are no safe objects. Tables, utensils, computers, doorknobs, gym equipment, and other objects were shown to be contaminated with potentially dangerous pathogens. Bacterial contamination has been discovered on cell phones as well as the mouse and keyboard of personal computers. All these items and surfaces can be potential sources for cross-infections and transmitting microorganisms.

In fact, microorganisms are found almost everywhere in air, water, soil, food, plants and animals, including humans and may be transmitted, either directly, through hand-to-hand contact, or indirectly via food or other inanimate objects such as cell phones, money and coins (Angelakis *et al.*, 2014) without enough washing performed and using personal cell phone in the course of a working day give the potential act of cell phones as a source of microbial transmission is considerable (Schultz *et al.*, 2003, and Rafferty & Pancoast, 1984).

Additionally, infectious individuals who use their hands when covering a cough divert infective pathogens from the droplet route to the hand-fomite route, which has the potential to increase fomite transmission from highly touched devices (Zhao *et al.*, 2012). Recently, the COVID-19 virus is rapidly transmitted from person to person via respiratory droplets that come out of the infected person when they cough, sneeze, breathe or talk.

Mobile phones are widely used by most adults and many children in many countries, including Libya. Therefore, cell phones have become one of the indispensable accessories of professional and social life, which makes them a good pathogenic carrier or reservoir. The reservoir of any organism, which may be animate or inanimate objects, in the epidemiology of any bacterial disease is very important (Haydon *et al.* 2002). The pathogens live and/or multiply in the reservoir on which their survival depends, such as flies. Many epidemiological studies have confirmed that contaminated surfaces play a major role in the spread of infectious diseases (Hendley, Wenzel, and Gwaltney, 1973).

These pathogens pass from the contaminated hand and skin of the user to another user, through which there is exchange of flora between the users (Famurewa and David, 2009). The adult human is covered with approximately 2m² of skin, with a surface area supporting about 10¹² bacteria (Mackowiak, 1982). The normal microbes of the skin include other; coagulase negative staphylococci, Diphtheroids, staphylococcus aureus, streptococci (various species), Bacillus spp (Joanne and Christopher, 2008).

The increased use of mobile phones is seen against a background of rising nosocomial infection rates reported by ecological findings (Brady *et al.*, 2006). Mobile phones can harbor various potential pathogens

and become an exogenous source of nosocomial infections among hospitalized patients and also a potential health hazard for themselves and family members (Gurang *et al.*, 2008).

In view of the above, knowing the types of bacteria spread among the health and education sectors in Benghazi is important. This will provide programs that encourage Keep the mobile phone away from our children and pay attention to personal hygiene.

2. Materials and Methods

2.1 Collection of samples:

Random samples were collected from cell phones and the hands of the user using sterile cotton swabs. For each person, a sterile swab was rotated over the surface of both sides of his or her cell phone. A second swab was rubbed over the entire ventral surface of the hands, including the ventral surface of the thumb and the fingers. Both swabs were immediately sent to the laboratory at the Benghazi Center for Infectious Diseases and Immunology, the Al-Jalaa Hospital for Surgery and Accidents, and the Central Reference Laboratory.

Sub-culture: Samples were inoculated into Brain Heart Infusion (BHI) broth as a transport medium and incubated at 37°C for 24 hours aerobically. This was to ensure that any microbes present in the cotton swab diffused into the broth. Brain Heart Infusion is a general-purpose liquid medium used in the cultivation of fastidious and non-fastidious microorganisms, including aerobic and anaerobic bacteria, from a variety of clinical and nonclinical materials. It is used for the cultivation of microorganisms, including bacteria, yeasts, and molds.

For isolation and purification, organisms were sub-cultured on blood agar, MacConkey agar, and nutrient agar plates. Petri plates were incubated at 37°C for 24–48 hours aerobically. Plates were observed for growth and colonial morphology of the isolates and used for identification tests for more accurate biochemical tests.

2.2 Identification of bacteria:

Bacteria were identified in culture by conventional methods such as microscopic examination and morphological analysis, with the help of the Phoenix fully automated identification system, the analytical profile index (API) system, and biochemical methods to confirm the identification.

2.3 Gram Technique:

This is the most important staining method in bacteriology and the first step in the identification procedure. In this study, it was employed for the diagnostic identification of various organisms as Gram-positive or Gram-negative due to differences in their cell wall structure.

2.4 Biochemical methods:

Different biochemical tests were carried out for bacterial identification using the medical laboratory manual (Mukhtar and Tukur, 2019).

2.5 Antibiotic sensitivity tests:

Bacterial species vary in their sensitivity to different chemotherapeutic and antibiotic agents. These variations and the continuously increasing number of antimicrobial agents necessitate the selection of the proper agent for each organism to be used for therapeutic purposes. The antibiotic sensitivity pattern of the selected isolate was studied by the disc diffusion method (Bauer, 1966). All isolated strains were streaked on Mueller-Hinton agar plates. The tested antibiotics on Gram negative and Gram positive bacteria were amoxicillin-clavulanic acid, amoxicillin, ampicillin, penicillin, ceftriaxone, ciprofloxacin, chloramphenicol, erythromycin, gentamicin, imipenem, levofloxacin, sulfamethoxazole /trimethoprim, Kanamycin and tetracycline. After 24 hours of incubation at 37°C, the zones of inhibition were measured and compared to the manufacturer's instructions and the criteria of the National Committee for Clinical Laboratory Standards (Wikler, 2006).

2.6. Analysis of results:

The data was analyzed using SPSS 8.0. Tests of significance were done using the Chi square test.

3. Results

3.1. Bacterial Identification:

A total of 100 hands and mobile phones screened in this study showed bacterial growth. These bacteria were identified using Bergey's Manual of Determinative Bacteriology (Holt *et al.*, 1994). The organisms recovered are from sixteen different genera, including Coagulase-negative Staphylococci (CNS), *Staphylococcus aureus*, *Corynebacterium urealyticum*, *Bacillus cereus*, *Tatumella ptyseos*, *Leuconostoc lactis*,

Pseudomonas aeruginosa, *Citrobacter youngae*, *Gaffkya tetragena*, *Kocuria kristinae*, *Aeromonas hydrophila*, *Chryseobacterium meningosepticum*, *Enterobacter cloacae*, *Aerococcus viridans*, *Gardnerella vaginalis*, and *Leclercia adecarboxylata*. The recovery rate ranges between 1% and 58% (Table 1). The organisms were consistently isolated from the mobile phone and human hands.

Table 1: Bacterial agents isolated from mobile phones and hands.

Bacterial types	Number of isolation	Percent
coagulase-negative staphylococci	58	58%
<i>Staphylococcus aureus</i>	12	12%
<i>Corynebacterium urealyticum</i>	06	6%
<i>Bacillus cereus</i>	05	5%
<i>Tatumella ptyseos</i>	03	3%
<i>Leuconostoc lactis</i>	02	2%
<i>pseudomonas aeruginosa</i>	02	2%
<i>Citrobacter youngae</i>	02	2%
<i>Gaffkya tetragena</i>	02	2%
<i>Kocuria kristinae</i>	02	2%
<i>Aeromonas hydrophila</i>	01	1%
<i>Chryseobacterium meningosepticum</i>	01	1%
<i>Enterobacter cloacae</i>	01	1%
<i>Aerococcus viridans</i>	01	1%
<i>Gardnerella vaginalis</i>	01	1%
<i>Leclercia adecarboxylata</i>	01	1%
Total	100	100

3.2 Level of Contamination:

The results showed that isolated organisms from individuals' hands and mobile phones, which included coagulase-negative staphylococcus (CNS), were the most common, followed by *S. aureus*, *C. urealyticum*, *B. cereus*, and *T. ptyseos*. While *G. vaginalis*, *A. viridans*, *E. cloacae*, *L. adecarboxylata*, *C. meningosepticum*, and *A. hydrophila* were the less commonly isolated from individuals' hands and mobile phones. In this study, the contamination rate of mobile phones and hands was 100% (table 2). The percentage of gram-positive bacteria in mobile phones was higher (90%) than in hands (88%), while the percentage of gram-negative bacteria in mobile phones was lower (10%) than that in hands (12%).

Table 2: Distribution of gram-positive and gram-negative bacteria isolated from people's phones and hands.

Bacteria: Gram positive (GP)	Phones N=50%	Hands N=50%
<i>Staphylococcus epidermidis</i>	10 (20%)	10 (20%)
<i>Staphylococcus haemolyticus</i>	3 (6%)	3 (6%)
<i>Staphylococcus warneri</i>	1 (2%)	4 (8%)
<i>Staphylococcus sciuri</i>	3 (6%)	1 (2%)
<i>Staphylococcus pasteurii</i>	1 (2%)	0
<i>Staphylococcus capitis</i>	1(2%)	0
<i>Staphylococcus cohnii</i>	2 (4%)	2 (4%)
<i>Staphylococcus lentus</i>	2 (4%)	2 (4%)
<i>Staphylococcus simulans</i>	1 (2%)	0
<i>Staphylococcus hominis</i>	6 (12%)	6 (12%)
<i>Staphylococcus aureus</i>	5 (10%)	7 (14%)
<i>Gardnerella vaginalis</i>	1 (2%)	0
<i>Bacillus cereus</i>	3 (6%)	2 (4%)
<i>Corynebacterium urealyticum</i>	3 (6%)	3 (6%)
<i>Gaffkya tetragena</i>	1 (2%)	1 (2%)
<i>Kocuria kristinae</i>	1 (2%)	1 (2%)
<i>Aerococcus viridans</i>	0	1 (2%)
<i>Leuconostoc lactis</i>	1 (2%)	1 (2%)
Total	90%	88%
Bacteria: Gram negative (GN)	Phones N=50%	Hands N=50%
<i>Tatumella pytyseos</i>	2 (4%)	1 (2%)
<i>Citrobacter youngae</i>	1 (2%)	1 (2%)
<i>Enterobacter cloacae</i>	1 (2%)	0
<i>Leclercia adecarboxylata</i>	0	1 (2%)
<i>pseudomonas aeruginosa</i>	1 (2%)	1 (2%)
<i>Chryseobacterium meningosepticum</i>	0	1 (2%)
<i>Aeromonas hydrophila</i>	0	1 (2%)
Total	10 %	12 %
Total bacteria GN & GP	100 %	100 %

S. epidermidis was the most commonly isolated microorganism from mobile phones (20%) and hands (20%), followed by *S. hominis*, which had the same incidence (12%) in the mobile phones and hands, the presence of *S. aureus* (14%) in the hands was higher than in the mobile phones (10%). While *C. urealyticum* and *S. haemolyticus* are represented by (6%) in both mobile phones and the hands. Some isolated bacteria were more prevalent in the hands than on mobile phones, such as *B. cereus* (6%) in the mobile phones and (4%) in the hands; *S. warneri* (2%) in the mobile phones and (8%) in the hands; and *S. cohnii* and *S.*

lentus, both represented by 4% in the mobile phones and hands. *S. sciurir* is represented by 6 percent of mobile phones and (2%) of the hand. However, the percentage (2%) of isolated bacteria was equal in both mobile phones and person hands, as in the case of *S. pasteurii*, *S. capitis*, *S. simulans*, *L. lactis* and *G. vaginalis*. *K. kristinae* and *G. tetragena* were both (2%) in mobile phones and hands, and *A. viridans* was (2%) only in hands. In gram- negative bacteria, *T. pytyseos* is represented by (4%) in mobile phones and by (2%) in the hands. *P. aeruginosa*, *C. youngae* were both (2%) in the mobile phones and hands. *A. hydrophila*, *L. adecarboxylata* and *C. meningosepticum* were represented by (2%) only in the hand. *E. cloacae* was (2%) on mobile phones only.

3.3. Antimicrobial susceptibility testing:

For gram-negative bacteria, antibiotics which included 8 antibiotics were used show in (Table 3). Most of the organisms isolated in the study were sensitive to most of the antibiotics that were used. For gram-positive bacteria of 13 antibiotics were used (Table 4).

Table 3: Antimicrobial susceptibility patterns of gram-negative bacterial identified.

Antibiotic ^c	<i>T. pytyseos</i>				<i>C. youngae</i>				<i>P. aeruginosa</i>			
	Phone s n = 2		Hands n = 1		Phone s n = 1		Hands n = 1		Phone s n = 1		Hands n = 1	
	S	R	S	R	S	R	S	R	S	R	S	R
CHL	2	-	1	-	1	-	1	-	-	1	-	1
KAN	2	-	1	-	1	-	1	-	1	-	-	1
IPM	2	-	1	-	1	-	1	-	1	-	1	-
AMP	2	-	1	-	-	1	-	1	1	-	1	-
TET	1	1	1	-	1	-	1	-	-	1	-	1
GEN	2	-	1	-	1	-	1	-	1	-	-	1
CIP	2	-	1	-	1	-	1	-	1	-	1	-
SXT	2	-	1	-	1	-	1	-	-	1	-	1

CHL→ Chloramphenicol. KAN →Kanamycin. IPM → Imipenem. AMP → Ampicillin. TET →Tetracycline. GEN→ Gentamicin. CIP → Ciprofloxacin. SXT→ Sulfamethoxazole /trimethoprim. S; sensitive, R; resistant.

Table 4: Antimicrobial susceptibility patterns of gram-positive bacterial identified.

Antibiotic	<i>S. haemolyticus</i>				<i>S. warneri</i>				<i>S. sciurir</i>				<i>S. cohnii</i>				<i>S. lentus</i>				<i>B. cereus,</i>				<i>C. urealyticum</i>				<i>K. kristinae</i>				<i>G. tetragena</i>				<i>L. lactis</i>			
	Phones n = 3		Hands n = 3		Phone s n = 1	Hand s n = 4	Phone s n = 3	Hands n = 1	Phone s n = 2	Hand s n = 2	Phone s n = 2	Hand s n = 2	Phone s n = 3	Hand s n = 2	Phones n = 3	Hand s n = 3	Phone s n = 1	Hand s n = 1	Phones n = 1	Hands n = 1	Phone s n = 1	Hands n = 1	Phones n = 1	Hands n = 1	Phone s n = 1	Hands n = 1	Phones n = 1	Hands n = 1												
	S	R	S	R	S	R	S	R	S	R	S	R	S	R	S	R	S	R	S	R	S	R	S	R	S	R	S	R	S	R	S	R	S	R						
AMC	-	3	1	2	1	-	4	-	2	1	-	1	2	-	2	-	-	2	2	-	-	3	1	1	-	3	-	3	1	-	1	-	1	-	1	-	1	-		
AMX	2	1	2	1	1	-	3	1	3	-	1	-	1	1	2	-	1	1	2	-	-	3	-	2	-	3	-	3	1	-	1	-	1	-	1	-	1	-		
AMP	-	3	-	3	-	1	-	4	-	3	-	1	-	2	2	-	-	2	-	2	-	3	-	2	3	-	-	3	1	-	1	-	1	-	1	-	1	-		
P	-	3	-	3	-	1	-	4	-	3	-	1	-	2	1	1	-	2	-	2	-	3	-	2	2	1	-	3	1	-	1	-	1	-	1	-	1	-		
CRO	1	2	1	2	1	-	4	-	1	2	-	1	1	1	-	2	1	1	2	-	-	3	-	2	-	3	-	3	-	1	-	1	-	1	-	1	1	-	1	-
CIP	3	-	3	-	1	-	4	-	1	2	1	-	1	1	2	-	2	-	2	-	3	-	2	-	1	2	1	2	1	-	1	-	1	-	1	-	1	-	1	-
CHL	2	1	3	-	1	-	4	-	1	2	1	-	2	-	1	1	2	-	2	-	3	-	2	-	3	-	3	-	1	-	1	-	1	-	1	-	1	-		
ERY	-	3	-	3	1	-	3	1	1	2	1	-	2	-	2	-	-	2	2	-	3	-	2	-	-	3	-	3	-	1	-	1	1	-	1	-	1	-	1	-
GEN	3	-	3	-	1	-	4	-	1	2	1	-	2	-	2	-	2	-	2	-	3	-	2	-	-	3	2	1	1	-	1	-	1	-	1	-	1	-	1	-
SXT	2	1	3	-	1	-	4	-	1	2	1	-	2	-	1	1	1	1	2	-	1	2	-	2	-	3	-	3	1	-	1	-	1	-	1	-	1	-	1	-
LVX	3	-	3	-	1	-	4	-	1	2	1	-	2	-	2	-	2	-	1	1	3	-	2	-	-	3	-	3	1	-	1	-	1	-	1	-	1	-	1	-
TET	2	1	2	1	1	-	4	-	2	1	1	-	2	-	2	-	2	-	2	-	1	2	-	2	2	1	-	3	1	-	1	-	1	-	1	-	1	-	1	-
IPM	3	-	1	2	1	-	4	-	1	2	-	1	2	-	1	1	-	2	2	-	3	-	2	-	-	3	-	3	1	-	1	-	1	-	1	-	1	-	1	-

AMC → Amoxicillin- clavulanic acid. AMX → Amoxicillin. AMP → Ampicillin. P → Penicillin. CRO → Ceftriaxone. CIP → Ciprofloxacin. CHL → Chloramphenicol. ERY → Erythromycin. GEN → Gentamicin. SXT → Sulfamethoxazole /trimethoprim. LVX → Levofloxacin. TET → Tetracycline. IPM → Imipenem.

All *S. aureus* isolates from hands and mobile phones were sensitive to imipenem and sulfamethoxazole/trimethoprim. They are also sensitive to amoxicillin-clavulanic acid, amoxicillin, and gentamicin, except one isolate was resistant in each case. The incidence of resistance strains of *S. aureus* to chloramphenicol and erythromycin was higher in samples of mobile phones and hands. Most isolated *S. aureus* were sensitive to ampicillin, penicillin, ciprofloxacin and levofloxacin except one isolate on a mobile phone and two at the hands and also sensitive to ceftriaxone and tetracycline except two and one isolate respectively on the hands. (Table 5).

Table 5: Antibiotic sensitivity patterns of *S. aureus* isolated from mobile phones and hands.

Antibiotic	Mobile phones (n=5)		Hands (n=7)	
	S	R	S	R
Amoxicillin-clavulanic acid	4	1	6	1
Amoxicillin	4	1	6	1
Ampicillin	4	1	5	2
Penicillin	4	1	5	2
Ceftriaxone	5	-	5	2
Ciprofloxacin	4	1	5	2
Chloramphenicol	1	4	5	2
Erythromycin	1	4	4	3
Gentamicin	4	1	6	1
Sulfamethoxazole /trimethoprim	5	-	7	-
Levofloxacin	4	1	5	2
Tetracycline	5	-	6	1
Imipenem	5	-	7	-

All isolates of *S. epidermidis* from mobile phones and hands were sensitive to ciprofloxacin and levofloxacin. Also, they were sensitive to amoxicillin-clavulanic acid amoxicillin, chloramphenicol, and sulfamethoxazole /trimethoprim except one strain was resistant in each case and two on the last. They were susceptible to erythromycin and imipenem except for two resistant strains on the mobile phones and one on the hands. There were many *S. epidermidis* isolates that resistant to penicillin, ampicillin and ceftriaxone with different incidence. Sensitive to gentamicin and tetracycline but resistant only one in each case for mobile phone only. The highest incidence of resistant strains was ceftriaxone resistant bacteria from personal hands and ampicillin resistant once isolated from a mobile phone. Twenty-five resistance *S. epidermidis* strains were that isolated from the mobile phones and twenty-three that

isolated from the hands most of them were ampicillin, penicillin, and ceftriaxone higher than other antibiotics resistant (Table 6).

Table 6: Antibiotic sensitivity patterns of *S. epidermidis* isolated from mobile phones and hands.

Antibiotic	Mobile phones (n=10)		Hands (n=10)	
	S	R	S	R
Amoxicillin-clavulanic acid	9	1	9	1
Amoxicillin	10	-	9	1
Ampicillin	3	7	5	5
Penicillin	5	5	7	3
Ceftriaxone	4	6	1	9
Ciprofloxacin	10	-	10	-
Chloramphenicol	10	-	9	1
Erythromycin	8	2	9	1
Gentamicin	9	1	10	-
Sulfamethoxazole /trimethoprim	10	-	8	2
Levofloxacin	10	-	10	-
Tetracycline	9	1	10	-
Imipenem	8	2	10	-

The isolates of *S. hominis* from hands and mobile phones were sensitive to ceftriaxone, ciprofloxacin, chloramphenicol, gentamicin and levofloxacin. Where are sensitive to amoxicillin-clavulanic acid and imipenem but was resisted on the hands only. The number of resistant strains of *S. hominis* was higher in samples isolates from mobile phones 17 than in samples isolates from the hands was equal 15. In both samples, data revealed that isolated six samples had resistance activity more than one antibiotic or sensitive to all tested antibiotics (Table 7).

Table 7: Antibiotic sensitivity patterns of *S. hominis* isolated from mobile phones and hands.

Antibiotic	Mobile phones(n=6)		Hands (n=6)	
	S	R	S	R
Amoxicillin-clavulanic acid	6	-	5	1
Amoxicillin	4	2	6	-
Ampicillin	-	6	-	6
Penicillin	-	6	-	6
Ceftriaxone	6	-	6	-
Ciprofloxacin	6	-	6	-
Chloramphenicol	6	-	6	-
Erythromycin	5	1	5	1
Gentamicin	6	-	6	-
Sulfamethoxazole /trimethoprim	5	1	6	-
Levofloxacin	6	-	6	-
Tetracycline	5	1	6	-
Imipenem	6	-	5	1

4. Discussion

In this study, mobile phone use by many people have not only shown a high rate of bacterial contamination, but also, more importantly, contamination by nosocomial pathogens. The results showed that about 100% of individual's hands and 100% of their mobile phones had bacterial contamination, these result are similar with Ilusanya *et al.*, 2012 mention that the rate of bacterial contamination of food vendor's mobile phones was 100% and with Angadi *et al.*, 2014 90% of the mobile phones and hands of all 100% the health care workers were contaminated with organisms known to cause hospital acquired infections.

Coagulate-negative staphylococcus (CNS) most prevalent bacterial agent isolated from 100 (58%) mobiles and hands in this study, may account for high levels of bacterial pathogen contamination observed. This result agree with Karabay *et al.*, 2007 in which CNS was the most frequently encountered bacterial agent isolated from 68.4% of the subjects evaluated. Brady *et al.*, 2006 had shown that the combination of constant handling and heat generated by the phones creates a prime breeding ground for microorganisms that are normally found on our skin. This may be because the increase incidence of bacterial agents isolated from hands and mobile phones was attributed to the poor hygiene and the body temperature that is a suitable environment for these organisms.

This research has shown that CNS (58%) it was the highest percentage among types specifically *S. epidermidis* and *S. hominis*. This result is similar to Banawas *et al.*, 2018 who reported coagulase-negative staphylococci were the most frequently isolate bacteria among healthcare workers (60.5%), particularly *S. epidermidis* and *S. hominis*. It was determined that coagulase-negative staphylococci are responsible for blood infections, of which *S. epidermidis* causes 67% of infections and other coagulase-negative staphylococci cause 33% (Gatermann, Koschinski, and Friedrich, 2007). Also various sub-species of *S. hominis* had been implicated for nosocomial outbreaks causing bloodstream infections in patients with underlying malignancies (Roy *et al.*, 2014).

In the present study, *S. aureus* was isolated from mobile phones 5 (10%) and hands 7 (14%) These results converge to study carried out at King Abdul-Aziz University in Saudi Arabia, out of 105 cell phones screened, 17 (16.2%) mobile phones were found to harbor *S. aureus* (Zakai *et al.*, 2016). *S. aureus* is an opportunistic bacteria, responsible for nosocomial and community infections (Lalaouna *et al.*, 2018). In addition, *S. aureus* can invade tissues and cause infections such as cutaneous abscesses, endocarditis, and septic shock (Lalaouna *et al.*, 2018).

As shown in **Table 4**, our antimicrobial susceptibility results indicate that most of the coagulase-negative staphylococci isolate from mobile phones and hands were resistant to erythromycin, ampicillin and

penicillin was observed in *S. hominis*, *S. haemolyticus*, *S. warneri*, *S. sciurir*, and *S. lentus*. Similarly, Morad *et al.*, 2016 reported that coagulate-negative staphylococci isolates from nosocomial bloodstream infections in Najran -Saudi Arabia- were highly resistant to penicillin and erythromycin. It has been believed that coagulase-negative staphylococci are important reservoirs of antimicrobial resistance genes and resistance-associated mobile genetic elements, which can be transferred between staphylococcal species. *S. hominis*, *S. epidermidis*, and *S. haemolyticus* are reported to be multiple drug resistant coagulase-negative staphylococci (Bouchami *et al.*, 2011, Becker, Heilmann, and Peters, 2014).

In the present study, we showed some of the *S. aureus* strain sensitive to ampicillin this differ with a previous study in Nigeria revealed that 42% of *S. aureus* isolated from mobile phones of non-health care workers was resistant to ampicillin (Nwankwo, Ekwunife, and Mofolorunsho, 2014). The study also showed some strains of *S. aureus* sensitive to penicillin this contradicts with Chambers *et al.*, 2009 reported that penicillin developing resistance to *S. aureus* since the 1960 and some strains resistant to ciprofloxacin this differ with Deyno *et al.*, 2017 who reported the pooled prevalence of *S. aureus* resistance to ciprofloxacin was 19%.

5. Conclusions

This study showed microbial contamination on personal mobile phones and hands. Some of the contaminated mobile phones microorganisms (such as *S. aureus*) were epidemiologically important nosocomial drug resistant pathogens. These isolates of bacteria were resistant to commonly used antimicrobials such as chloramphenicol, erythromycin, and ciprofloxacin. These results showed that mobile phones and personal's hands were contaminated with various types of bacteria, which suggested that mobile phones (used by people in daily practice) may be a source of nosocomial infections. Users of mobile phone are hence advised to use antibacterial wipes to make their mobile phones germ free at all times.

Acknowledgements

Gratitude is expressed for the microbiology laboratory at Al-Jalaa hospital, Benghazi reference laboratory, Infectious and immunity disease center, and Department of plant protection for providing facilities and support to this research work.

Conflict of Interest: The authors declare that there are no conflicts of interest.

References

- Angadi, Kalpana M., et al. "Study of the role of mobile phones in the transmission of Hospital acquired infections." *Medical Journal of Dr. DY Patil University* 7.4 (2014): 435.
- Angelakis, Emmanouil, et al. "Paper money and coins as potential vectors of transmissible disease." *Future microbiology* 9.2 (2014): 249-261.
- Banawas, Saeed, et al. "Multidrug-resistant bacteria associated with cell phones of healthcare professionals in selected hospitals in Saudi Arabia." *Canadian Journal of Infectious Diseases and Medical Microbiology* 2018 (2018).
- Bauer, A. W. M. M., W. M. M. Kirby, and J. C. Turck Sherris. "Turck, Turck M. Antibiotic susceptibility testing by a standardized single disk method." *American journal of clinical pathology* 45.4 (1966): 493.
- Becker, Karsten, Christine Heilmann, and Georg Peters. "Coagulase-negative staphylococci." *Clinical microbiology reviews* 27.4 (2014): 870-926.
- Brady RR, Wasson A, Stirling I, McAllister C, Damani NN. Is your phone bugged? The incidence of bacteria known to cause nosocomial infection on healthcare worker's mobile phones. *J. Hosp. Infect.* , (2006); 62: 123-125.
- Bouchami, O., et al. "Antibiotic resistance and molecular characterization of clinical isolates of methicillin-resistant coagulase-negative staphylococci isolated from bacteremic patients in oncohematology." *Folia microbiologica* 56 (2011): 122-130.
- Chambers, Henry F., and Frank R. DeLeo. "Waves of resistance: *Staphylococcus aureus* in the antibiotic era." *Nature Reviews Microbiology* 7.9 (2009): 629-641.
- Cheesbrough M. *Medical Laboratory Manual for Tropical Countries*, First edition, Vol 2. Thetford press Ltd. (1984), England.
- Deyno, Serawit, Sintayehu Fekadu, and Ayalew Astatkie. "Resistance of *Staphylococcus aureus* to antimicrobial agents in Ethiopia: a meta-analysis." *Antimicrobial Resistance & Infection Control* 6.1 (2017): 1-15.
- Eltablawy, S. Y., and H. N. Elhifnawi. "Microbial contamination of some computer keyboards and mice in National Center for Radiation Research and Technology (NCRRT)." *World Applied Sciences Journal* 6.2 (2009): 162-167.
- Famurwa O, David OM. cell phone: A Medium of transmission of bacterial pathogens. *World Rural Observations*, (2009); 1:69-72.
- Gatermann, S. G., T. Koschinski, and S. Friedrich. "Distribution and expression of macrolide resistance genes in coagulase-negative staphylococci." *Clinical microbiology and infection* 13.8 (2007): 777-781.
- Gurang, B., et al. "Do mobiles carry pathogens." *J Microbiol* 23 (2008): 45-76.
- Haydon, Daniel T., et al. "Identifying reservoirs of infection: a conceptual and practical challenge." *Emerging infectious diseases* 8.12 (2002): 1468-1473.
- Hendley JO, Wenzel RP, Gwaltney JMJ. Transmission of rhinovirus colds by self-inoculation. *New. Eng. J. Med.*, (1997); 288: 1361-1664.
- Holt, John G., et al. "Bergey's Manual of determinate bacteriology." (1994).
- Ilusanya, O. A. F., et al. "Personal hygiene and microbial contamination of mobile phones of food vendors in Ago-Iwoye Town, Ogun State, Nigeria." *Pakistan journal of nutrition* (2012).
- Joanne MW, Linda MS, Christopher JW. Prescott, Harley and Kleins Microbiology, 7th Edition, Mc. Graw-Hill International. (2008) Pp.1-17.
- Karabay, Oguz, Esra Koçoglu, and Mustafa Tahtaci. "The role of mobile phones in the spread of bacteria associated with nosocomial infections." *J Infect Dev Ctries* 1.1 (2007): 72-73.
- Lalaouna, David, et al. "MS2-affinity purification coupled with RNA sequencing approach in the human pathogen *Staphylococcus aureus*." *Methods in enzymology*. Vol. 612. Academic Press, 2018. 393-411.
- Mac kowiak PA. The normal Microbial Flora. *N. Engl. J. Med.*, (1982); 307:83-93.
- Morad Asaad, Ahmed, Mohamed Ansar Qureshi, and Syed Mujeeb Hasan. "Clinical significance of coagulase-negative staphylococci isolates from nosocomial bloodstream infections." *Infectious Diseases* 48.5 (2016): 356-360.
- Nwankwo, E. O., N. Ekwunife, and K. C. Mofolorunsho. "Nosocomial pathogens associated with the mobile phones of healthcare workers in a hospital in Anyigba, Kogi state, Nigeria." *Journal of epidemiology and global health* 4.2 (2014): 135-140.
- Rafferty KM, Pancoast SJ. Brief report: Bacteriological sampling of telephones and other hospital staff hand-contact objects. *Infect. Control*, 1984; 5: 533-535.
- Roy, Priyamvada, et al. "Multidrug-resistant *Staphylococcus hominis* subsp. *novobiosepticus* causing septicemia in patients with malignancy." *Indian Journal of Pathology and Microbiology* 57.2 (2014): 275.
- Schultz M, Gill J, Zubairi S, Huber R, Gordin F. Bacterial contamination of computer keyboards in a teaching hospital. *Infect. Control Hosp. Epidemiol.*, 2003; 24:302-303.
- Tiron, Roxana, et al. "Screening for obstructive sleep apnea with novel hybrid acoustic smartphone app technology." *Journal of Thoracic Disease* 12.8 (2020): 4476.
- Wikler, Matthew A. "Performance standards for antimicrobial disk susceptibility tests: approved standard." (No Title) (2006).
- Zakai, Shadi, et al. "Bacterial contamination of cell phones of medical students at King Abdulaziz University, Jeddah, Saudi Arabia." *Journal of Microscopy and Ultrastructure* 4.3 (2016): 143-146.
- Zhao, Jijun, et al. "Model analysis of fomite mediated influenza transmission." *PloS one* 7.12 (2012): e51984.



Detection of Bacterial Species Causing Urinary Tract Infections in Brega City Region, Isolation, Identification, and Antibiotic Sensitivity Testing

Mifthah S. Najem¹, Suliman F. Alsdig² and Youssef F. Lawgali^{3,4}

¹Dentistry Faculty, Oral Microbiology Department, Benghazi University, Libya.

²Institute of Medical Technolog¹, Ajdabiya, Libya.

³Sciences Faculty, Microbiology Department, Benghazi University, Libya.

⁴The Environmental and Biological Chemical Research Center, Tokara, Libya.

DOI: <https://doi.org/10.37375/sjfsu.v3i1.1140>

A B S T R A C T

ARTICLE INFO:

Received: 07 March 2023

Accepted: 10 April 2023

Published: 17 April 2023

Keywords:

bacterial species, urinary tract infection and antibiotic sensitivity testing, Libya

The purpose of the study is to ascertain the prevalence of Gram-positive and Gram-negative bacteria that cause urinary tract infections in patients in Brega of various Libyan ages. Inpatients and outpatients at Brega Qarawi Hospital (third zone), Family Clinic (first zone), and Industrialized Clinic (first zone) provided 500 mid-stream urine (MSU) specimens. These people ranged in age from 15 to 65 and included 285 men and 215 women.

According to this study, UTI was 45% common in Brega City, with males having a higher frequency than females (46% vs. 44%). Adults (72.4%) were the age group most likely to have UTIs, followed by the elderly (16.4%) and teenagers (11.1%). The majority of those with UTI were outpatients (62.2%) and inpatients (37.7%). With 49.7% of infections caused by it, *Escherichia coli* was the most prevalent uropathogen. *Pseudomonas aerogenosa* and *Klebsiella pneumoniae* were each in charge of 10.2% and 20.8% of the cases, respectively. UTIs were less commonly caused by the gram-positive bacteria *Staphylococcus aureus* (5.3%) and *Staphylococcus saprophyticus* (2.6%). With the highest sensitivity of the antibiotics examined in this study, Imipenem is the one to use.

1. Introduction

The urinary system is made up of many bodily parts that produce, store, and excrete urine. There is always a chance that bacteria, in particular, will invade these organs. Urinary tract infections (UTIs) are a group of clinical conditions characterized by microbial invasion of the tissues lining the urinary system, which extends from the renal cortex of the kidneys to the urethral meatus. The invasive microorganism may affect the whole tract, or it may be limited to the upper area of the kidneys (pyelonephritis), the lower region, where the invaded organs are the bladder (cystitis), prostate (prostatitis), and urethra (urethritis), or it may simply affect the urine (Tenover, 2006).

The study's goal is to Goals in general particular goals discovery and isolation of the bacterial species responsible for urinary tract infections in the Brega region.

figuring out how common the germs that cause urinary tract infections are in Brega city among patients of various ages. the evaluation of isolated bacteria's susceptibility to antibiotics.

Urinary tract infections continue to be among the most prevalent infectious illnesses due to their vast spectrum of clinical symptoms and impacted host groups, but they are also among the most difficult and little understood. The endogenous micro flora, which also includes Gram-

positive bacteria like Enterococci and Gram-negative bacteria like *Escherichia coli*, frequently causes mono infections such urinary tract infections (Heisig., 2010).

Although though fatality rates are normally not high, community-acquired urinary tract infection is one of the most prevalent infectious illnesses and a frequent reason for out-patient treatment presentations. Gram-negative bacteria, mostly *Escherichia coli* and *Klebsiella pneumoniae*, but also *Acinetobacter* and *Enterobacter* spp., are responsible for UTIs (Heisig., 2010; Drekonja and Johanson., 2008).

Bacteriological reports are becoming more crucial for private practice physicians as well since it is only through an understanding of the resistance patterns of the causative organisms that treatment failures and their repercussions may be avoided (Blieblo and Baiu, 1999; Inglis, 1996; Greenwood *et al.*, 1997).

Escherichia coli's Ur pathogenicity cannot be solely attributed to its serotype. A crucial procedure known as Pilus-mediated adherence of *E. coli* to uroepithelial cells contributes to the pathogenicity of urinary tract infection (Kisielius *et al.*, 1989).

Klebsiella pneumoniae is the major pathogen in the genus *Klebsiella*, while *K. oxytoca* can also cause bacteriuria. The frequent isolation of *K. pneumoniae* biotypes 16 and 17 from haemodialysis fluid encouraged researchers to examine strains seen in regular samples from nephrological patients (Kolmos, 1984).

Staphylococcus aureus, a rare urinary isolate, was responsible for about (0.5–6%) of all positive urine cultures. The most important predisposing factors in the urinary system included indwelling catheters (63%) followed by obstruction (56%) and surgery (43%) (Arpi and Rennerberg 1980).

Although (Makii and Tambyah., 2010) discovered that microbes could enter the urinary tract through lymphatic or haematogenous spread, there is a wealth of clinical and experimental data demonstrating that the ascent of microbes from the urethra is the most frequent pathway leading to a UTI, particularly for organisms with enteric origin (i.e., *Escherichia coli* and other *Enterobacteriaceae*).

2. Materials and Methods

specimen collection

In-patients and out-patients at the Brega Qarawi Hospital (the third zone), Family Clinic (the first zone), and Industrialized Clinic (the first zone) in Brega city provided 500 Mid-stream urine (MSU) specimens. Their ages varied from 15 to 65 years old, and there were 285 males and 215 girls. These samples were

gathered between the months of March and June 2013. The questionnaire page for the patient was appropriately labeled with the sterile universal container containing the sample, and the patients were given instructions on how to collect the sample (the folded equipped private collection of urine sample and directions on how to clean the area carefully).

Urine cultivation

Samples were first cultivated on Cysteine lactose electrolyte-deficient (CLED), MacConkey, and blood agar medium (OXOID LTD) after being received at the lab, according to standard laboratory protocols.

The loop in use may move 0.01 milliliters of urine sample. The plates were inoculated and then placed on the bench for the urine to soak into the agar media. The plates were then turned over and incubated aerobically for 24 hours at 37°C. Omnipresent container housing the sample

Identification of bacteria and antimicrobial sensitivity test using BD Phoenix 100 system

Principles of the procedure

Many of the tests used in the phoenix ID panels are modifications of the classical methods. These include tests for fermentation, oxidation, degradation and hydrolysis of various substrates. In addition to these, the Phoenix system utilizes chromogenic and fluorogenic substrates as well as single carbon source substrates in the identification of organisms. A maximum of 100 identification and antimicrobial susceptibility tests can be performed in the Phoenix instrument at a time using Phoenix ID/AST combination panels. A sealed and self-inoculating moulded polystyrene tray with 136 micro-wells containing dried reagents, serves as the Phoenix disposable. (National Committee for Clinical Laboratory Standards, 2003).

The combination panel includes an ID side with dried substrates for bacterial identification, an AST side with varying concentrations of antimicrobial agents and growth and fluorescent controls at appropriate wells locations. The Phoenix system utilizes an optimized colorimetric redox indicator for AST, and a fluorometric indicators for ID. The AST broth is cation-adjusted (e.g., Ca⁺⁺ and Mg⁺⁺) to optimize susceptibility testing performance. The Phoenix panel is comprised of a 51 wells ID side and an 85 wells AST side. The ID side

contains 45 wells with dried biochemical substrates and 2 fluorescent control wells.

The AST side contains 84 wells with dried antimicrobial agents and 1 growth control well panels are available as ID only (Phoenix NID panels, Phoenix PID panels), AST only (Phoenix NMIC panels, Phoenix PMIC panels), or ID/AST combination (Phoenix NMIC/ID panels, phoenix PMIC/ID panels). Unused wells are reserved for future Phoenix panels are inoculated with a standardized inoculum. Organism suspensions must be prepared only with the BBL crystal spec or BD Phoenix nephelometer. Once inoculated, panels are into the instrument and continuously incubated at 35°C. the instrument test panels every 20 minutes, on the hour at 20 minutes past the hour and again at 40 minutes past the hour up to 16 hours if necessary. Phoenix panels are read only by the instrument. Phoenix panels cannot be read manually. (National Committee for Clinical Laboratory Standards., 2003).

Bacterial identification

The ID portion of the Phoenix panel utilizes a series of conventional chromogenic, and fluorogenic biochemical tests to determine the identification of the organism. Both growth based and enzymatic substrates are employed to cover the different types of reactivity in the range of taxa. The tests are based on microbial utilization and degradation of specific substrates detected by various indicator system. Acid production is indicated by a change in the phenol red indicator when an isolate is to utilize a carbohydrate substrate. Chromogenic substrates produce a yellow colour upon enzymatic hydrolysis of either p-nitrophenyl or p-nitroanilide compounds. Enzymatic hydrolysis of fluorogenic substrates results in the release of a fluorescent coumarin derivative. Organisms that utilize a specific carbon source reduce the resazurin based indicator. In addition, there are other tests that detect the ability of an organism to hydrolyse, degrade, reduce or otherwise to utilize a substrate. (Bohdima, K, A and Topoli, A, S. 2010).

Antimicrobial susceptibility testing

The phoenix AST method is a broth based micro dilution test. The phoenix system utilizes a redox indicator for the detection of organism growth in the presence of an antimicrobial agent. Continuous measurements of change to the indicator as well as

bacterial turbidity are used in the determination of bacterial growth. Each AST panel configuration contains several antimicrobial agents with a range of two-fold doubling dilution concentrations. Organism identification is used the interpretation of the MIC values of each antimicrobial agent producing susceptible, intermediate or resistant (S. I. R.) result classifications.



Figure 1. phoenix 100 system

The components required for testing using the phoenix system include, phoenix panels with panel closures, phoenix ID broth, phoenix AST broth, phoenix AST indicator solution, phoenix inoculation station, phoenix transport caddy, BBL crystal spec or BD phoenix spec Nephelometer, 25ul pipettor and sterile tips, and Miscellaneous lab supplies (listed under materials required but provided). Prior to inoculation , the phoenix panel is placed on the inoculation station with the inoculation ports at the top for filling. Separate inoculum is added manually to the ID and AST ports. The inoculum flow down the panel in serpentine fashion, filling the panel wells as the liquid front progresses toward the pad. The pad absorbs excess inoculums. Closures are manually inserted in the fill ports. An air admittance port is located in the divider area of panel lid to ensure adequate oxygen tension in the panel for the duration of the tests. (Stefaniuk, E. et al., 2003).

Phoenix test results

Organism identification will appear on the Phoenix report form with a probability percentage from the Phoenix database based on the substrate reaction profile. Results from each substrate will appear as +, V or X for each reaction. The MIC result and interpretive Categorical results (S. I. R.) will be shown for the appropriate organism antimicrobial agent combinations. However, the aim of the study isolation and identification of bacterial species causing urinary tract infection in the area of Brega city.

Statistical analysis

The data were subjected to chi-square test using the SPSS computerized software version 11(Chicago, USA). Significance was accepted at $P < 0.05$ levels.

3. Results

Five hundred Mid-stream urine samples from 208 men and 292 women were analyzed between March 2013 and June 2013 for this study. Of these instances, 225 (or 45%) were positive.

Prevalence of UTI among both genders

The prevalence of bacterial urinary tract infections among people of different ages was 225 cases (45%). It was more in males than females, 96 (46%) and 129 (44%), respectively (Fig. 2).

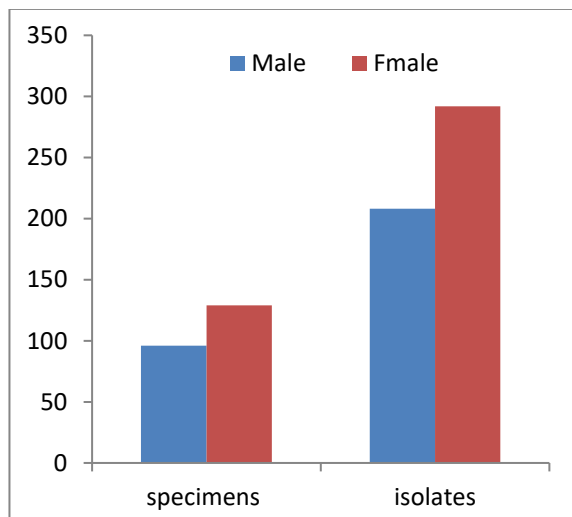


Figure 2. Distribution gender among all collected specimens and isolates.

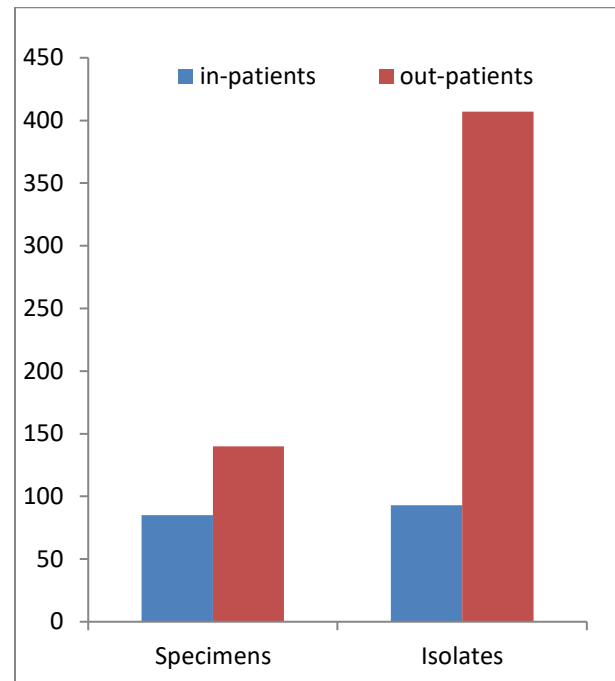


Figure 3. Distribution of the UTI in in-patients and out-patients among all collected specimens and isolates.

UTI among people of different ages

The study showed a distribution of urinary tract infections of patients according to age (Table 1). Positive specimens were different in ages. The results showed that the positive specimens of adolescent (15 years to 21 years) were 25 cases (11.1%), of them 11 males and 14 females, and in adults aged (22 years to 60 years), 163 cases (72.4%), 48 males and 115 females, and in elderly more than (60 years), 37 all affected patients were male (16%), however there were more cases in females than males. (Buzayan, M and Baiu, S., 1998).

Table 1: Bacterial urinary tract infections according to age

Gender	# of pos cases	Adolescents		Adults		Elderly	
		15-21 Year		22-60 Year		Over 60 Year	
		No.	%	No.	%	No.	%
Male	96	11	11	48	50	37	39
Female	129	14	11	115	89	0	0
Total	225	25	11.1	163	72.4	37	16

Table 2: The Frequency of Bactrial Uropatogens

Bacterial Isolates	Frequency	%
<i>Escherichia coli</i>	112	49.7
<i>Klebsiella pneumoniae</i>	47	20.8
<i>Pseudomonas aeruginosa</i>	23	10.2
<i>Proteus mirabilis</i>	16	7.1
<i>Staphylococcus aureus</i>	12	5.3
<i>Staphylococcus saprophyticus</i>	6	2.6
<i>Enterobacter aerogenes</i>	5	2.2
<i>Enterobacter cloacae</i>	4	1.7
	225	100

Distribution of Gram-positive and Gram negative bacteria among Ur pathogens

Gram-negative bacteria were the most common of Ur pathogens responsible for UTI with (92%), in

comparison to (8%) for Gram-positive bacteria as shown in (Table 3) and (Fig.4).

Table 3: Distribution of Gram-positive and Gram-negative bacteria among Ur pathogens

Gram negative bacteria	Total 91.7%	Gram positive bacteria	total % 7.9
<i>Escherichia coli</i>	49.7	<i>Staphylococcus aureus</i>	5.3
<i>Klebsiella pneumoniae</i>	20.8	<i>Staphylococcus saprophyticus</i>	2.6
<i>Pseudomonas aeruginosa</i>	10.2		
<i>Proteus mirabilis</i>	7.1		
<i>Enterobacter cloacae</i>	1.7		
<i>Enterobacter aerogenes</i>	2.2		

Antibacterial Sensitivity Testing *Escherichia coli* isolates from UTI were resistant to Trimethoprim-Sulfamethoxazole, Ampicillin, Augmentin, Ciprofloxacin, Gentamicin, Nitrofurantoin, Ceftazidime and Cefuroxime ; 57%, 55 %, 41 %, 37 %, 34 %, 32 %, 31 % , and 24 % respectively, while it was 80 % sensitive to Imipenem. *Klebsiella pneumoniae* was found to be resistant to Ampicillin, Ceftazidime, Cefuroxime, Trimethoprim-Sulfamethoxazole, Ciprofloxacin, Gentamicin, Augmentin and Nitrofurantoin; 100 % ,51%, 47 %, 43 %, 38 %, 36 %,

30 % and 28.5 respectively. While it was 100% sensitive to Imipenem.

Pseudomonas aeruginosa was found to be resistant to Cefuroxime, Ampicillin, Nitrofurantoin, Trimethoprim-Sulfamethoxazole, Augmentin, Gentamicin, Ciprofloxacin and Ceftazidime; 100 %, 78 %, 65 % , 61 % , 57 % , 26 % , 17 % and 13 % respectively . While it was 100 % sensitive to Imipenem. *Proteus mirabilis* was found to be resistant to Ampicillin, Augmentin, Gentamicin, Nitrofurantoin, Cefuroxime, Trimethoprim.

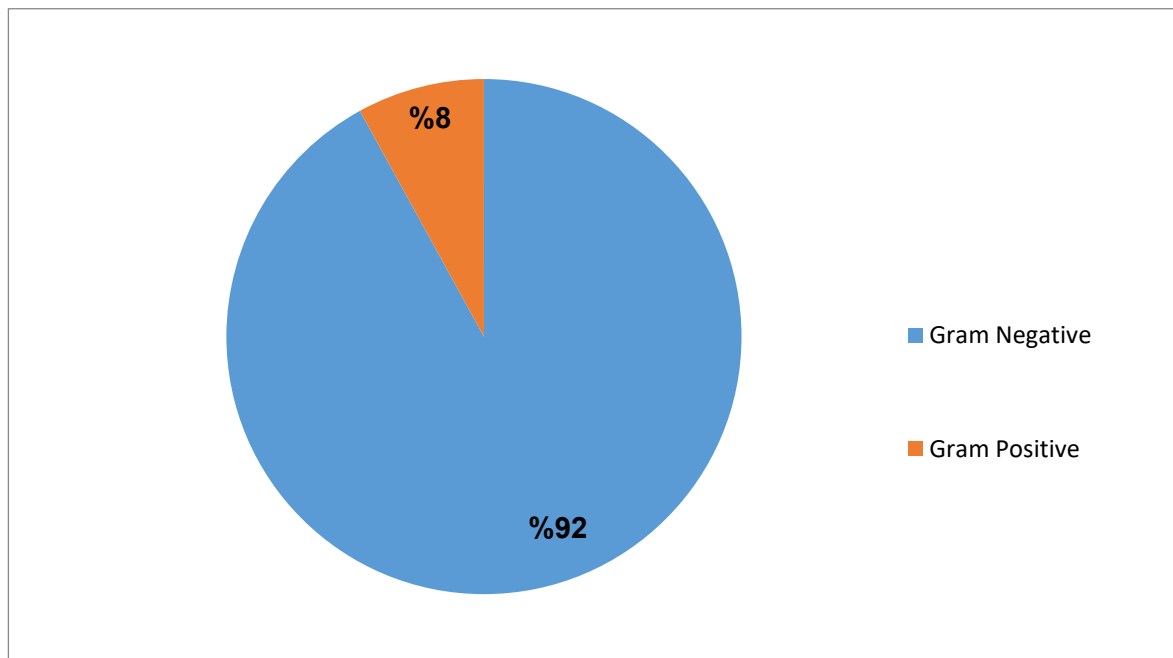


Figure 4. Distribution of Gram-positive and Gram-negative bacteria among Ur pathogens

Table 4: Antibiotic susceptibility patterns of bacterial isolates

Bacterial Isolates									
Antibiotics		<i>Staph.aureus</i> (12 isolates)		<i>Staph. saprophyticus</i> (6 isolates)		<i>Enterobacter aerogenes</i> (5 isolates)		<i>Enterobacter cloacae</i> (4 isolates)	
GN	S	8	67%	5	83%	3	60%	4	100%
	R	4	33%	1	17%	2	30%	0	0%
IMI	S	7	58%	5	83%	5	100%	4	100%
	R	5	42%	1	17%	0	0%	0	0%
XIME	S	5	42%	0	0%	3	60%	4	100%
	R	7	58%	6	100%	2	40%	0	0%
CAZ	S	4	33%	6	100%	5	100%	4	100%
	R	8	67%	0	0%	0	0%	0	0%
AMP	S	3	25%	0	0%	0	0%	0	0%
	R	9	75%	6	100%	5	100%	4	100%
AUG	S	5	42%	6	100%	5	100%	2	50%
	R	7	58%	0	0%	0	0%	2	50%
SXT	S	6	50%	6	100%	4	80%	3	75%
	R	6	50%	0	0%	1	20%	1	25%
CIP	S	10	83%	6	100%	4	80%	3	75%
	R	2	17%	0	0%	1	20%	1	25%
NIT	S	10	83%	6	100%	3	60%	1	25%
	R	2	17%	0	0%	2	40%	3	75%

GN=Gentamicin. IMI=Imipenem. XIME= Cefuroxime. CAZ= Ceftazidime.

AMP= Ampicillin. SXT= Trimethoprim-Sulfamethoxazole.

NIT= Nitrofurantoin. CIP= Ciprofloxacin. S= Sensitive. R = Resistant.

Females had a greater susceptibility to ascending infection, as female's urethra is short and vaginal introitus may become contaminated with fecal organisms. Generally, it is assumed that the short urethra in women accounts for its increased susceptibility to urinary tract infections compared to men. Urinary flow characteristics are important in the initiation of bladder infection (Bohdima, K, and Topoli, A, 2010). Backflow of urine in the females urethra has been observed during micturition. This process will facilitate the spread of colonizing bacteria into the bladder (Noufal and Baiu, 2012).

Females adult groups were the majority of infected cases in this study, they represented (57.3 %) of the total positive cases. This might be interpreted as in this age female genital tract anatomy is different from males and more susceptible to contamination with bacteria from stool (Abu-Daia *et al.*, 2000). In addition to this, prostatic secretions in males can protect bacterial infections (Qunibi.,1982).

In a study on urinary tract infections in sirt area done by Noufal and Baiu in 2003, (19 %) of the patients visiting Ibn-sina Hospital, complaining of urinary tract infections. Females with these infections were more than males , the percentage of occurrence of urinary tract infection in female and male infection, were (4%) and (5%) respectively. In our study urinary tract infections were common in females than males (Bohdima, K, and Tripoli, A, 2010).

4. Discussion

One of the most typical illnesses is a urinary tract infection, particularly in young children. It can lead to consequences including hypertension, renal failure, and permanent kidney damage if it is not treated with the proper antibiotics, and it is still a major health concern

(Steven *et al.*, 2006). In this study, female adult groups made up most of the positive cases (57.3%), making up the bulk of infected patients. This might mean that at this age, female genital tract anatomy differs from male genital system anatomy and is more vulnerable to bacterial contamination from feces (Abu-Daia *et al.*, 2000). Male prostatic secretions can also prevent bacterial infections, according to research (Qunibi.,1982).

According to our research, Gram-negative bacteria account for 48 percent of all UTIs. This was also discovered in a 2007 Saudi research by Wajeha and a 2013 study by Nicolle et al, in which it was shown that

Gram-negative bacteria were to blame for (75.5%), and (88%), respectively, of UTI.

In 2003, Noufal and Baiu, conducted research on urinary tract infections in the Sirt region. Among the patients who visited Ibn-Sina Hospital, 19% reported having an infection. The prevalence of urinary tract infections in males and females was (4%) and (5%), respectively, with females having more of these illnesses than males. In our study, urinary tract infections affected more women than men.

Regarding antibiotic susceptibility of isolated bacteria, the majority of the isolates in our study were extremely susceptible to imipenem, ciprofloxacin, gentamycin, and nitrofurantoin, but resistant to ampicillin. This was supported by the findings of a study carried out at the Mohammad Al-Mgariaf Hospital in the city of Ejdabia by Bohdima and Topoli in 2010, which found that all isolates were ampicillin-resistant and that the most effective antibiotics were imipenem, ceftazidime, nitrofurantoin, and ciprofloxacin. Imipenem, Nitrofurantoin, Gentamicin, and Ciprofloxacin were the most effective antibiotics in El Gotrani and Topoli's, 2011 investigation, which was conducted in the pediatric hospital in Benghazi, although the bacteria were resistant to

Multiple antimicrobial resistance among Gram-negative organisms has been a long-term and well-recognized problem with urinary tract infections. Resistance has been observed in multiple genera, including *Escherichia coli*, *Enterobacter*, *Klebsiella*, *Proteus*, *Serratia*, and *Pseudomonas*. (Noor et al., 2004).

5. Conclusions

1. Our study found that the prevalence of UTI in Brega city was 45% and males were more than affected females 46 %, 44% respectively.

2.The most affected age group with UTI belonged to the adult age group (72.4%), and who were elderly (16.4%), and the adolescents were (11.1%). Most of those suffering from UTI were out-patients (62.2%) and in-patients with (37.7 %).

3.*Escherichia coli* was the most predominant Ur pathogen responsible for (49.7%) of infections. *Klebsiella pneumoniae* and *Pseudomonas aeruginosa* caused (20.8%) and (10.2%) respectively. Also, to less extent the Gram-positive bacteria *Staphylococcus aureus*, *Staphylococcus saprophyticus* that caused UTIs were (5.3%) and (2.6%) respectively.

4.Imipenem is the antibiotic of choice, where it resulted in the highest sensitivity among different antibiotics

used in this study. On the other hand, Ampicillin was resisted by most bacteria.

Conflict of Interest: The authors declare that there are no conflicts of interest.

References

- Abu-Daia, M. ; Al-aaly, A. and De castro, R (2000). Urinary Tract Infection in Childhood Saudi Med.J21(8):711-714.
- Arpi, M. and Rennerberg, J. 1980. The clinical significance of Staphylococcus aureus bacteremia. Jurol. 132:697_700.
- Blieblo, F, A. and Baiu, S, H. (1999). Microbiological findings in Nephrology Center. A Thesis of M.Sc. Department of Botany, Faculty of Science of Garyounis. University Benghazi Libya.
- Bohdima, K, A and Topoli, A, S. (2010). Prevalence of Bacterial Urinary Tract Infection among Patients Ejdabia City. M.Sc. Thesis. Academy of Graduate studies. Ejdabia Branch Libya.
- Buzayan, M,M and Baiu, S, H.(1998). A study of Bacteriuria during pregnancy In Benghazi's Women. A Thesis of M.Sc. Department of Boteny, Faculty of Science Garyounis University. Benghazi Libya.
- Catheter-Associated Urinary Tract Infections. Mayo Clin proc. PMID.74(2):131-6.
- Drekonja, D. and Johason, J. (2008). Urinary Tract Infection. Prim Care.35 (2):345-67.VII.
- El-Gotrani, S and Topoli, A. (2011). Prevalence of Bacterial Urinary Tract Infection among Pediatric Patients at Pediatric Hospital Benghazi. M.Sc. Thesis. Academy of Graduate studies. Benghazi Branch Libya.
- Greenwood, D.; Slack, R. C and Peuthere, J. F. 1997. Medical Microbiology. 15th ed. PP.604_651, Churchill Living stone company Ltd.
- Heisig, P. (2010). Urinary Tract Infections and Antibiotic Resistance. The American Journal of Medicine. A.49(5):612-7.
- Kisielius, P. V.; Schwan, W. R. Amundsen, S. K and Duncan, J. L. 1989. In
- Kolmos, H. J. 1984. Klebsiella pneumonia in a nephrological department J Hos Infect: 5(3):253_259.
- Makii,D and Tampyah, P.(2010). A prospective Study of Pathogenesis of Catheter-Associated Urinary Tract infections. Moy Clin proc. PMID.74(2):131-6.
- National Committee for Clinical Laboratory Standards. 2003. Performance standards for antimicrobial disk susceptibility tests: approved standard, 8th ed. NCCLS document M2-A8. National Committee for Clinical Laboratory Standards, Wayne, Pa.
- Noufal, Y.M.U and Baiu, S.H.(2003). A study on the Urinary Tract Infections (UTI) in Srit Area. A Thesis of M.Sc. Depart of Biology. Faculty of Science. Al-Tahadi University. Sirt Libya.
- Noor,N. ;Ajaz,M. ;Ajaz,S and Pirzada,Z.(2004). Urinary Tract Infections Associated with Multidrug Resistant enteric Bacilli. Characterization and Genitival Studies. Pakistan Jouranl of Pharmaceutical Sciences. Vol 17. No2:115-123.
- Noufal, Y.M.U and Baiu, S.H. (2003). A study on the Urinary Tract Infections. (UTI) in Srit Area. A Thesis of M.Sc. Depart of Biology. Faculty of Science. Al-Tahadi University. Sirt Libya.
- Qunibi,Y.(1982). Urinary Tract Infection. King Faisal Specialist Hospital Journal 2(1): 37-46.
- Steven ; Charg ; Linda and Shortliffe. (2006). Pediatric Urinary Halt Infections. Pediatric Clinic North Amarica. 53:379-400.
- Stefaniuk, E., A. Baraniak, M. Gniadkowski, and W. Hryniewicz. 2003. Evaluation of the BD Phoenix automated identification and susceptibility testing system in clinical microbiology laboratory practice. Eur. J. Clin. Microbiol. Infect. Dis. 22:479-485. [PubMed] [Google Scholar]
- Tenover,F.(2006). Mechanisms of Antimicrobial Resistance in Bacteria. The American Journal of Medicine.119(6):3-10.



The Effects of Indole Butyric Acid and Seaweed (*Posidonia oceanica*) and their Mixture in Improving Photosynthetic Pigments of Salt-Stressed Wheat Cultivar (Marjawi)

Sami M. Salih and Ahmed A. Abdulraziq

Biology Department, Education Faculty, Omar Al-Mukhtar University, Al-Bayda, Libya.

DOI: <https://doi.org/10.37375/sjfssu.v3i1.100>

A B S T R A C T

ARTICLE INFO:

Received: 27 November 2022

Accepted: 21 March 2023

Published: 17 April 2023

Keywords:

Posidonia oceanica, Indole-3-butyric acid, Photosynthetic pigment, Wheat (Marjawi).

Salt stress is one of the most limiting factors in the production of agricultural crops. This study was conducted to test the effect of different salinity levels at concentrations (0.0, 100, 200, and 300 mM) of sodium chloride on the photosynthetic pigments content of *Triticum aestivum* (Marjawi cultivar), and attempting to treat using several transactions of different treatments, include: spraying at 100 mg/L of Indole-3- Butyric Acid (seedlings 2 weeks old), adding crude powder of seaweed *Posidonia oceanica* 25 g/pot (before agriculture), and (mixture) of a crude powder of *P.oceanica* 25 g/pot + spraying IBA, with three replications according to a completely randomized design. The results showed a significant decrease in the content of chlorophyll (a, b), carotenoids, and Total pigments with increasing NaCl concentrations, compared to a control. Moreover, spraying with (IBA) decrease significantly the negative effect of salinity. Also result indicated that adding crude powder of *P.oceanica* was not successful in reducing salt stress, in addition, the result showed that the mixture was superior in recording the best rates in improving the photosynthetic pigments content of wheat salt-stressed, This study concluded that harmful effects of salinity can be mitigated using the mixed treatment.

1 Introduction

Photosynthesis is a sensitive process to various abiotic and biotic stresses in plants, damaged photosynthesis system causes a decrease in the rate of photosynthesis and impairs the productivity of agricultural crops (Sharma *et al.*, 2022). These changes were associated with the production of reactive oxygen species (ROS), resulting from these pressures (Pandey *et al.*, 2022). Salt stress is one of the more abiotic stresses that poses a major threat to the desertification of arable land all across the globe. induces osmotic stress, and ionic stress, both of which impair plant growth and metabolism (Wang *et al.*, 2022; Kapadia *et al.*, 2022). In addition produce oxygen species and reactive nitrogen species (RNS),

which is an imbalance in the homeostasis redox of the cell (Singh *et al.*, 2022). Wheat is considered one of the food crops that are physiologically affected by salt stress, which inhibits the process of nutrient uptake (Ca, Mg, Fe, N, K, P, and Zn), plant water uptake, photosynthesis, protein synthesis, and enzymatic activity, (Kesh *et al.*, 2022; Lata *et al.*, 2022). *Posidonia oceanica* (L.) is classified as an endemic seaweed to libyan coasts (Ezziany *et al.*, 2015), distributed at sea level and reaches a depth of 38 m (Bay,1984). The dead leaves are accumulated on the beaches in huge quantities as waste material, causing great environmental and economical problems (Dural *et al.*, 2011). Seaweed has been reported as a bio-fertilizer in agricultural fields, especially in salt soils, because it contains macro- and micro-nutrients that

stimulate seed germination and improve water and nutrient absorption by rebalancing the ionic and metabolic status (Nabti *et al.*, 2017; Khan *et al.*, 2022). Plant hormones improve tolerance to abiotic stresses by inhibiting the accumulation of reactive (ROS), and stimulating the expression of stress-specific genes (Rachappanavar *et al.*, 2022). For example, chlorophyll (a, b), total chlorophyll, and carotenoids content were enhanced in a wheat plant salt-stressed 150 mM of NaCl, through the application of salicylic acid and gibberellic acid (Iqbal *et al.*, 2022). Also, Abbas *et al.*, (2022) noted an increase in stomatal conductance and chlorophyll (a, b), and total chlorophyll contents, of wheat SARC1 and SARC5 genotypes, using a combined application of potassium and humic acid. Moreover, spraying foliar ascorbin up to 1000 ppm promoted increased chlorophyll, protein, relative water content, and cell membrane stability (Dadrwal *et al.*, 2022).

Therefore, our aims were to:

Evaluation effect of different salinity levels on the content of photosynthetic pigments (chlorophyll a, b and carotenoids) in leaves of wheat.

investigate whether (indole-3-butyric acid or *Posidonia oceanica* or a mixture) applications are more effective in alleviating salinity stress in cultivar wheat Marjawi.

2 Materials and Methods

2.1 Seed Selection:

Seeds of wheat cultivar Marjawi were obtained, From the Department of Crops / faculty of Agriculture / Omar Al-Mukhtar University, were cleaned of impurities, and viability was tested by soaking in distilled water to get rid of empty seeds floating on the surface, were soaked in 1% sodium hypochloride solution for 3 minutes, and washed with distilled water (Dafaallah *et al.*, 2019).

2.2 Collection and Preparation of Seaweed Samples:

Fresh *Posidonia oceanica* (leaves and rhizomes) were collected from the coastline of Al-Hamamah, north of Al-Bayda city / Al-Jabal Al-Akhdar / Libya, and classified in the Department of Biology / Faculty of Education / Omar Al-Mukhtar University, They were washed and rinsed with distilled water in order to eliminate sand and plankton, after that, they were dried at room temperature, ground by an electric grinder and kept until use.

2.3 Preparation of the Used Solutions:

The brine was prepared using sodium chloride salt NaCl (100, 200, and 300), as follows:

$1\text{m Mol} = \text{molecular weight of the solute} / 1000 * \text{concentration}$

$100\text{ m Mol} = 58.5 / 1000 * 100$

$100\text{ m Mol} = 5.85\text{ g/L}$

take weight 5.85g of NaCl salt, then dissolve it in a standard flask of capacity 1000 ml and complete the volume with distilled water to the mark and the same steps for the rest of the concentrations.

Then prepare the concentration of 100 mg / L of indole3-butyric acid (IBA).

2.4 Pot Experiments:

Sterilized seeds germinated in sterile petri dishes containing a damp sterile filter paper, sterile distilled water was added at intervals to keep the paper and germinated seeds wet, dishes were incubated at 30 °C for 2-3 days or until the radicals length were 2-3 cm. Ten germinated seeds were planted into each pot. Five kilograms of dried clay-sandy soil were put into pots. the ratio of 2:1 (weight to weight), ten germinated seeds were planted into each pot. When the growing plants were about 12 cm in length. They were thinned down to five per pot. Pots were divided into four groups, and each of them was irrigated with different concentrations of saline solutions (0.0, 100, 200 and 300 m M NaCl) from the beginning of agriculture to 60 days:

- The first group: was irrigated with the saline solution to reach the salinization level.

- The second group: spraying the seedlings (2 weeks old) three times with 100 mg/L of Indole3- Butyric Acid (IBA) (10 cm³ per pot)+ (saline solution).

- The third group: was treated by adding 25g/pot of *Posidonia oceanica* crude powder + (saline solution).

- The fourth group: a mixture (the crude powder 25g / pot of *Posidonia oceanica* + spraying the seedlings IBA) + (saline solution).

2.5 Photosynthetic Pigment:

The photosynthetic pigments (chlorophyll a, chlorophyll b and carotenoids) were extracted from fresh weight of leaves wheat Marjawi in 85% aqueous acetone to a

certain concentration for spectrophotometric measurements. were determined spectrophotometrically according to (Metzner *et al.*, 1965).The pigments extract was measured against a black of pure 85% aqueous acetone at three wavelengths of 452.5, 644 and 663 nm. After 60 days of sowing. using following equations:

$$\text{Chlorophyll} = 10.3 * 663 - 0.918 * 644 = \text{mg/ml}$$

$$\text{Chlorophyll b} = 19.7 * 644 - 3.87 * 663 = \text{mg/ml}$$

$$\text{Carotenoids} = 4.2 * 452.5 - 0.0264 * \text{chl. a} + 0.4260 * \text{chl. b}$$

Statistical Analysis:

The study experiences were designed according to the complete random design (CRD). Statistical analysis was performed using Minitab 17 program and ANOVA variance analysis tables. The averages were compared using Tukey's test at $P < 0.05$ (Salih and Abdulraziq, 2021).

3 Results and Discussion

3.1 An effect of Salinity Levels on Photosynthetic Pigments of Wheat.

Current work shows in table (1) the effect of salinity levels (0.0, 100, 200, and 300mM) on photosynthetic

pigments of the cultivar wheat (Marjawi). Chlorophyll content (a, b), carotenoids, and total pigments decreased compared to a control, after 60 days of sowing. The concentration of 100 mM caused a decrease of chlorophyll (a, b), carotenoids, and total pigments from (100%) of a control to (79.0%) of chlorophyll (a, b), (74.3%) of carotenoids and total pigments by up to (78.3 %). The rates of decrease of photosynthetic pigments increased with increasing salinity. The concentration of 200 mM recorded a decrease in chlorophyll (a, b), carotenoids, and total pigments with (60.4%, 58.8%, 51.3% and 58.2 %) respectively, while the harmful effect of saline stress was clear at a concentration of 300mM, where recorded the highest inhibition rates of chlorophyll (a, b), carotenoids, and Total pigments with (34.8%, 46.5%, 32.8%, and 37. 5%) respectively. The detrimental effects of salt stress on photosynthetic pigments were reported in studies on wheat (Ahanger *et al.*, 2019; Kesh *et al.*, 2022). This was probably due to an inhibition of ribulose-1,5-bisphosphate enzyme or formation of proteolytic enzymes such as chlorophyllase, Responsible for chlorophyll synthesis (Santos, 2004), thus resulting in a reduction of Calvin cycle enzymes, and inactivation of photosystem II (PSII) reaction centers (Ma *et al.*, 2020).

Table (1): Effect of salinity levels and different treatments on photosynthetic pigments of wheat.

Treatments	NaCl	Chlorophyll a		Chlorophyll b		carotenoids		Total pigments	
		mg/g	%	mg/g	%	mg/g	%	mg/g	%
NaCl	0.0	4.3 ab	100	2.04 cd	100	1.52 b	100	7.86 d	100
	100	3.4 abcde	79.0	1.63 e	79.9	1.13 cd	74.3	6.16 g	78.3
	200	2.6 bcde	60.4	1.20 gh	58.8	0.78 f	51.3	4.58 k	58.2
	300	1.5 e	34.8	0.95 j	46.5	0.50 hi	32.8	2.95 n	37.5
IBA	0.0	4.5 ab	104.6	2.32 b	113.7	1.62 b	106.5	8.44 b	107.3
	100	3.9 abcd	90.6	1.88 d	92.0	1.25 c	82.2	7.03 f	89.4
	200	3.0 bcde	69.7	1.35 fg	66.0	0.96 e	63.1	5.31 i	67.55
	300	2.0 de	46.5	1.00 j	49.0	0.70 fg	46.0	3.7 m	47.0
Crude powder	0.0	4.2 abc	97.6	2.05 c	100.4	1.50 b	98.6	7.75 e	98.6
	100	3.0 bcde	69.7	1.51 ef	74.0	1.17 cd	76.9	5.68 h	72.2
	200	2.2 cde	51.0	1.18 hi	57.8	0.60 gh	39.4	3.98 l	50.6
	300	1.6 e	37.2	1.02 ij	50.0	0.42 i	27.6	3.04 n	38.5
Mixed	0.0	5.2 a	120.9	2.53 a	124.0	1.80 a	118.4	9.53 a	121.2
	100	4.5 ab	104.6	2.00 cd	98.0	1.51 b	99.3	8.01 c	101.9
	200	3.7 abcd	86.0	1.42 f	69.6	1.09 de	71.7	6.21 g	79.0
	300	2.9 bcde	67.4	1.21 gh	59.3	0.81 f	53.2	4.92 j	62.5

3.2 An Effect of Spraying Application of (IBA) on Photosynthetic Pigments of Salt-Stressed of Wheat.

The results also in table (1) showed that spraying of Indole-3- Butyric acid of wheat under salinity levels significantly increased the content of photosynthetic pigments, which increased by (11.6%, 12.1%, 7.9% and 11.1%) of treatment (IBA + 100 mM NaCl), (9.3%, 7.2%, 11.8% and 9.35%) of treatment (IBA + 200 mM NaCl), and (11.7%, 2.5%, 13.2% and 9.5%) treatment (IBA + 300 mM NaCl) of chlorophyll contents (a, b), carotenoids, and total pigments respectively, compared to the untreated plant. Our results are consistent with those (Iqbal *et al.*, 2022; Yilmaz *et al.*, 2022), which found Foliar application of phytohormones of (GA3, and SA) improved the growth traits of salinized wheat. Maybe because they enhance essential inorganic nutrients as well as maintain membrane permeability, balance, and osmotic capacity in plants and Increase activity of antioxidant enzymes that regulate ROS levels (kaya *et al.*, 2010; Piotrowska-Niczyporuk *et al.*, 2018), which Improves efficiency of photosystem II (Aroca *et al.*, 2013).

3.3 An Effect of Adding a Crude Powder of *P. oceanica* on Photosynthetic Pigments of Salt-Stressed of Wheat.

Results showed that adding a crude powder of *P.oceanica* (25 g /pot) had no significant effect compared with different salinity levels, on chlorophyll (a, b), carotenoids, and total pigments, the achieved results were in accordance with (Latique *et al.*, 2013) who found that high concentrations of *Ulva rigida* extract had no effect in enhancing chlorophyll content compared to control, this result differed with a study (Castaldi and Melis, 2002) which confirmed that can be used *P.oceanica* as an agricultural fertilizer because it contains a good proportion of carbon, nitrogen, and phosphorus. The reason for ineffectiveness of *P.oceanica* may be the high levels of growth-promoting substances such as indole-3-acetic acid (IAA), gibberellins A and B, cytokinins (Kalaivanan and Venkatesalu, 2012), or chromosome abnormalities caused by effect of seaweed (Hamouda *et al.*, 2022).

3.4 An Effect of Mixed (crude powder of *P.oceanica* and IBA) Photosynthetic Pigments of Salt-Stressed of Wheat.

The application of mixed(crude powder of *Posidonia oceanica* + IBA) was the most effective treatment, significantly highest increased the content of the

photosynthetic pigments, by (25.6%, 18.1%, 25.0%, and 23.6%)of content chlorophyll (a, b), carotenoids, and total chlorophyll respectively, as compared with 100 mM NaCl, and with an increase in the concentration of NaCl to 200 and 300mM, treatment Mixed recorded an increase by (25.6%, 10.8%, 20.4%, 20.8%) and (32.6%, 12.8%, 20.4%, 25.0%) of content chlorophyll (a, b), carotenoids, and total pigments for two concentrations, respectively.

4 Conclusion

Salt stress leads to disruption of chlorophyll synthesis, This was clear from this study's results on photosynthetic pigments content of wheat under different salinity levels. Treatment of the (mixture) of adding crude powder of *Posidonia oceanica* 25 g/pot, and spraying with 100 mg/L of IBA was the most effective treatment in alleviating, salt stress and increasing improving the photosynthetic pigment content, followed by the spraying of IBA, while the treatment of adding 25g/pot crude powder of *P.oceanica* was not successful in reducing salt stress. So this study recommends a combination of treatments as a way to overcome salinity damage in wheat (Marjawi).

Conflict of Interest: The authors declare that there are no conflicts of interest.

Reference

- Abbas, G., Rehman, S., Siddiqui, M. H., Ali, H. M., Farooq, M. A., & Chen, Y. (2022). Potassium and humic acid synergistically increase salt tolerance and nutrient uptake in contrasting wheat genotypes through ionic homeostasis and activation of antioxidant enzymes. *Plants*, 11(3), 263.
- Ahanger, M. A., Qin, C., Begum, N., Maodong, Q., Dong, X. X., El-Esawi, M., ... & Zhang, L. (2019). Nitrogen availability prevents oxidative effects of salinity on wheat growth and photosynthesis by up-regulating the antioxidants and osmolytes metabolism, and secondary metabolite accumulation. *BMC Plant Biology*, 19(1), 1-12.
- Aroca, R., Ruiz-Lozano, J. M., Zamarre, A. M., Paz, J. A., García-Minak, J. M., Pozo, M. J. and Lopez-Raez, J. A. (2013). Arbuscular mycorrhizal symbiosis influences strigolactone production under salinity and alleviates salt stress in lettuce plants. *J. Plant Physiol.* 170:47- 55.
- Bay, D. (1984). A field study of the growth dynamics and productivity of *Posidonia oceanica* (L.) Delile in Calvi Bay, Corsica. *Aquatic Botany*, 20(1-2), 43-64.
- Castaldi, P., & Melis, P. (2002). Composting of *Posidonia oceanica* and its use in agriculture. In *Microbiology*

- of composting (pp. 425-434). *Springer*, Berlin, Heidelberg.
- Dadrwal, B. K., Bagdi, D. L., Kakralya, B. L., & Sharma, M. K. (2022). Foliar treatment with ascobin reduces the adverse effects of salt stress on physiological and biochemical parameters in wheat. *The Pharma Innovation Journal*, 11(5): 2117-2120.
- Dafaallah, A. B., Mustafa, W. N., and Hussein, Y. H., (2019). Allelopathic Effects of Jimsonweed (*Datura Stramonium L.*) Seed on Seed Germination and Seedling Growth of Some Leguminous Crops. *International Journal of Innovative Approaches in Agricultural Research*, Vol. 3 (2): 321-331.
- Dural, M. U., Cavas, L., Papageorgiou, S. K., & Katsaros, F. K. (2011). Methylene blue adsorption on activated carbon prepared from *Posidonia oceanica* (L.) dead leaves: Kinetics and equilibrium studies. *Chemical Engineering Journal*, 168(1), 77-85.
- Ezziany, I. M. Haddoud, D. and Barah, M. (2015). Estimating Distribution of two Libyan Seagrass Species, *Posidonia oceanica* and *Cymodoceanodosa*, that face a Future Decline in Khoms to Misurata in Libyan Shores. *International Journal of Agriculture and Economic Development*, 3(1), 15.
- Hamouda, M. M., Saad-Allah, K. M., & Gad, D. (2022). Potential of Seaweed Extract on Growth, Physiological, Cytological and Biochemical Parameters of Wheat (*Triticum aestivum* L.) Seedlings. *Journal of Soil Science and Plant Nutrition*, 1-14.
- Humphries, E. (1956). Mineral components and ash analysis. In *Moderne Methoden der Pflanzenanalyse/Modern Methods of Plant Analysis Springer*, (pp. 468-502).
- Iqbal, M. S., Zahoor, M., Akbar, M., Ahmad, K., Hussain, S., Munir, S., ... & Islam, M. (2022). Alleviating the deleterious effects of salt stress on wheat (*Triticum aestivum* L.) by foliar application of gibberellic acid and salicylic acid. *Appl. Ecol. Environ. Res*, 20, 119-134.
- Kalaivanan C, Venkatesalu V.(2012) Utilization of seaweed *Sargassum myriocystum* extracts as a stimulant of seedlings of *Vigna mungo* (L.) Hepper. *Span J Agricul Res*. 10(2):466-70.
- Kapadia, C., Patel, N., Rana, A., Vaidya, H., Alfarraj, S., Ansari, M. J., Gafur, A., Poczai, P., and Sayyed, R. Z. (2022). Evaluation of plant growth-promoting and salinity ameliorating potential of halophilic bacteria isolated from saline soil. *Frontiers in Plant Science*, 13:946217.
- Kayai, C., Tuna, A. L., And Okant, A. M. (2010). Effect of foliar applied kinetin And indole acetic acid on maize ,*Turk J Agric Tubitak*, 529-538.
- Kesh, H., Devi, S., Kumar, N., Kumar, A., Kumar, A., Dhansu, P., Sheoran.,P., and Mann, A. (2022). Insights into physiological, biochemical and molecular responses in wheat under salt stress.
- Khan, Z., Gul, H., Rauf, M., Arif, M., Hamayun, M., Ud-Din, A., Sajid, Z.A., Khilji, S. A., Rehman, A., Tabassum, A., Parveen.Z.,and Lee, I. J. (2022). *Sargassum wightii* aqueous extract improved salt stress tolerance in *Abelmoschus esculentus* by mediating metabolic and ionic rebalance. *Frontiers in Marine Science*, 9,pp1-19.
- Lata, C., Kumar, A., Mann, A., Soni, S., Meena, B., & Rani, S. (2022). Mineral nutrient analysis of three halophytic grasses under sodic and saline stress conditions. *Indian Journal Of Agricultural Sciences*, 92(9), 1051-1055.
- Ma, Y., Dias, M. C., and Helena Freitas, H. (2020). Drought and salinity stress responses and microbe-induced tolerance in plants. *Front. Plant Sci.* 11: 591911.
- Metzner, H., Rau, H., & Senger, H. (1965). Untersuchungen zur synchronisierbarkeit einzelner pigmentmangelmutanten von *Chlorella*. *Planta*, 65(2), 186-194.
- Metzner, H., Rau, H., and Senger, H., (1965). Studies on synchronization of some pigment-deficient *Chlorella* mutants. *Planta*, 65, 186-194.
- Nabti, E., Jha, B., & Hartmann, A. (2017). Impact of seaweeds on agricultural crop production as biofertilizer. *International Journal of Environmental Science and Technology*, 14(5), 1119-1134.
- Pandey, J., Devadasu, E., Saini, D., Dhokne, K., Marriboina, S., Agepati, R. S., & Subramanyam, R. (2022). Reversible changes in structure and function of photosynthetic apparatus of pea (*Pisum sativum*) leaves under drought stress. *The Plant Journal*. 113(1), 60-74.
- Piotrowska-Niczyporuk, A., Bajguz, A., Zambrzycka-Szelewa, E., & Bralska, M. (2018). Exogenously applied auxins and cytokinins ameliorate lead toxicity by inducing antioxidant defence system in green alga *Acutodesmus obliquus*. *Plant Physiology and Biochemistry*, 132, 535-546.
- Rachappanavar, V., Padiyal, A., Sharma, J. K., & Gupta, S. K. (2022). Plant hormone-mediated stress regulation responses in fruit crops-a review. *Scientia Horticulturae*, 304, 111302.
- Salih, S. M., and Abdulrazziq, A. A., (2021). Auto-Resistance to Seeds Germination of Invasive *Acacia saligna* Trees at AlJabal Al-Akhdar region. *Scientific Journal for the Faculty of Science-Sirte University* , Vol 1, Issue (2): 20-24.
- Santos, C. V. (2004). Regulation of chlorophyll biosynthesis and degradation by salt stress in sunflower leaves. *Scientia horticulturae*, 103(1), 93-99.
- Sharma, S., Bhatt, U., Sharma, J., Kalaji, H. M., Mojski, J., & Soni, V. (2022). Ultrastructure, adaptability, and alleviation mechanisms of photosynthetic apparatus

- in plants under waterlogging: A review. *Photosynthetica*, 60(3), 430-444.
- Singh, P., Kumari, A., and Gupta, K. J. (2022). Alternative oxidase plays a role in minimizing ROS and RNS produced under salinity stress in *Arabidopsis thaliana*. *Physiologia Plantarum*, 174(2), e13649.
- Wang, C. F., Han, G. L., Yang, Z. R., Li, Y. X., and Wang, B. S. (2022). Plant salinity sensors: current understanding and future directions. *Frontiers in plant science*, 13: 859224.
- Yilmaz, M., Kizilgeçi, F., Tazebay, N., Ufuk, A. S. A. N., Iqbal, A., & Iqbal, M. A. (2022). Determination of the effect of salicylic acid application on salinity stress at germination stage of bread wheat. *Yuzuncu Yil University Journal Of Agricultural Sciences*, 32(2), 223-236.



Phytoremediation of Crude Oil-Polluted Soil by Maize (*Zea mays*) and Sunflower (*Helianthus Annus*)

Farag Abu Drehiba¹, Abubaker Edkymish², Abdurrazzaq Braydan¹, Otman Ermithi¹, Mohamed Mukhtar¹ and Elmundr Abughnia¹

¹Libyan Biotechnology Research Center Department tissue culture plant.

²Libyan Authority for Scientific Research, Tripoli, Libya.

DOI: <https://doi.org/10.37375/sjfssu.v3i1.940>

A B S T R A C T

ARTICLE INFO:

Received: 9 February 2023

Accepted: 10 April 2023

Published: 17 April 2023

Keywords:

Phytoremediation, hydrocarbon-polluted soil, Maize (*Zea mays*), Sunflower (*Helianthus Annus*).

Recent studies on Phytoremediation of Crude Oil-Polluted Soil gave positive results in both efficiency and cost. The purpose of this study was to evaluate the effectiveness of Maize (*Zea mays*), Sunflower (*Helianthus Annus*) in the biodegradation of total hydrocarbons of soils contaminated with crude oil. The experiment was conducted at the experimental station of The Libyan Center for Biotechnology Research (Tripoli, Libya) to test the ability of the selective plants in stimulating the microbial decomposition of soil pollutants - particularly Crude Oil- decreasing or eliminate these pollutants. The experiment was designed according to Randomized Complete Block Design (RCBD), and the selective plants were (maize and sunflower) planted in pots containing soil treated with different crude oil concentrations (0%, 1.25%, 2.50%, 3.75%, and 5% w/w) for 90 days to test and compare the ability of the studied plants in reducing the pollution in the presence of microbial activity. By the treatment of 3.75% (37,500 ppm) crude oil concentration, the total hydrocarbon concentration decreased to 86.10 ppm by maize and to 77.47 ppm by sunflower, while, by the control of treatment was 188.48 ppm. The total number of the aerobic bacteria at the end of the experiment didn't show significant differences in comparison to zero time except for the 5% pollution treatment by which the total number was 313.23x10⁴ CFU by maize, 164.92x10⁴ CFU by sunflower and 2200.17x10⁴ CFU by the control treatment.

1 Introduction

Today, organic pollutants are generally one of the most important topics in regard to negative effects on environment and human health, especially by crude oil, and organic compounds -such as benzene and polyaromatic hydrocarbons- (Ebadi *et al.*, 2018). Certain hydrocarbons are carcinogenic to people and animals, causing genotoxicity, reproductive toxicity, immunological toxicity, and cancer (Kuppusamy *et al.*

2020). Therefore, removing of hydrocarbons from polluted environments is vital for both ecological stability and human health (Alegbeleye *et al.*, 2017). Worldwide, Libya is one of the most important oil-producing countries, and according to activities related to the extraction, transportation, refining, and storage of oil, a lot of infiltration of harmful compounds infiltrate deep aquifers -water reservoirs- through soil layers. Therefore one liter of petroleum compounds can

contaminate a million liters of groundwater, and thus exposing human beings to dangers by drinking polluted water or absorbing it through the skin when using it for recreational purposes (ATSDR. 1988).

Phytoremediation is one of the most important biological methods used for treatment of oil wastes, by which certain plants are used that have the ability to reduce pollution levels by seizing, removing or decomposition of various pollutants (Singh, 2006). The symbiotic relationship between plant roots and soil microorganisms stimulates decomposition of stable organic pollutants. It remains difficult to increase phytoremediation efficiency. The impact of soil physical and chemical characteristics and microbial activity on the success of phytoremediation of hydrocarbon has been thoroughly established (Ye *et al.*, 2017). According to a preliminary study, phytoremediation may be more effect than using only microorganisms. Also, many studies observed that growing plants in hydrocarbon-contaminated soil increased the decomposition of hydrocarbons compared to uncultivated soils (Siciliano, 1998). To clean up soil pollution, many different methods have been used, including physical, chemical, and biological ones. By using plants and associated soil bacteria, phytoremediation is a low-cost, environmentally friendly process for minimizing the abundance, mobility, or toxicity in soil and water (Arslan *et al.*, 2017).

2 Materials and Methods

This study was conducted by using sandy soil taken from the experimental station of Biotechnology Research Center (BTRC). Used soil were dried, sieved with a 2 mm sieve and then analyzed for determining the physical and chemical properties. The soil was synthetically polluted. Five different crude oil contamination levels (0%, 1.25%, 2.50%, 3.75% and 5%) in 4 replications were used to get 20 experimental plots. Pots were filled with 2 Kg soil and planted with either Maize or sunflower, in addition to control pots without plants, then fertilized with one dose of Ammonium phosphate (120 kg/H). The irrigation was controlled according the field capacity. The total hydrocarbons in the soil and plants, and also the numbers of bacteria in the rhizosphere were estimated at the end of the experiment to assess the ability of the tested plants in treating pollution (Tab. 2). The analysis

of variance ANOVA ($\alpha = 0.05$) and Duncan's multiple range test (Duncan 1958) were performed to evaluate the effect of studied factors.

3 Results and Discussion:

Soil properties and Concentrations of hydrocarbons:

Some parameters of physical and chemical properties of used soil were investigated at BTRC laboratory according (Tab.1).

Table.1: Physical and chemical properties of used soil

pH	EC Mmhos /cm	CaC O3 %	O. M. %	Macro nutrients			Texture %		
				K pp m	P pp m	N %	Cl ay	Si lt	Sa nd
7. 95	2.04	5	0. 33	5. 3	0. 06	0. 46	1. 1	5	93. 9

Concentrations of total hydrocarbons have been determined in the soil, roots, and shoots of both studied plant species. During the experiment sunflower plants did not tolerate the highest pollution treatments, total hydrocarbons up took by sunflower plants in the 1.25% pollution treatment - 420.98 ppm- was about twice as much as by maize. By maize plants, the concentrations ranged between 230 ppm and 245 ppm in the three lowest pollution treatments, while the highest concentration was 749.38 ppm (Fig. 1).

The concentrations of hydrocarbons in planted samples of Maize were lowering than in unplanted - control-samples because of increased microbial activity in the rhizosphere induced by the root system. The concentrations of total hydrocarbons were (28.38, 44.77, 76.52, 86.10, and 78.84 ppm) respectively.

Maize plants were selected due to their global availability, high germination rate, fibrous roots, and versatility (Khan; *et al.*, 2018). In our study hydrocarbon compounds were effectively decreased by maize (fig 2). Similar results were also reported by Zand *et al.*, 2010 at 3.5% pollution level. Murotova, *et al.*, 2003 mentioned that success of phytoremediation of hydrocarbon contaminated soils is related to plant ability in improving microbial activity in the rhizosphere. Microorganisms create a wide range of enzymes to control oxidation reactions that govern the degradation pathways, which cause the mineralization

of hydrocarbons to produce CO₂ and H₂O (Cui, 2020), and (Ali, 2020).

The ability of sunflower plants to endure all levels of pollution for an extended period of time was lacking; for instance, at a 5% pollution level, the plants only perished after two weeks. Even though it had a positive

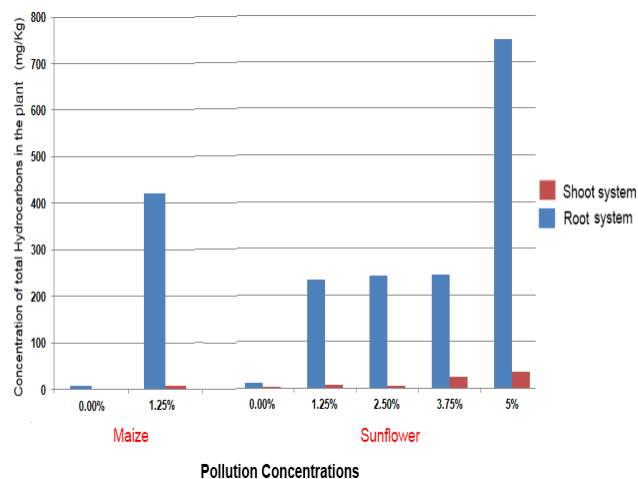


Figure.1: Concentration of total Hydrocarbons in the plant (ppm).

• **Numbers of bacteria in the rhizosphere:**

The injection of crude oil caused the pH of the soil to decrease from 8.00 to 6.50. That was still within the range of growth for bacteria, though. A smaller change in pH values was observed in the soil planted with maize as opposed to the soil planted with sunflowers. According to (Baruah et al. (2013), the pH of soil will decrease as a result of the accumulation of organic acids brought on by the degradation of crude oil.

Relating to the number of bacteria, the results of this study showed a clear increase in the number of bacteria just by the highest pollution level (5%), and this was also found by (Radwan et al., 2005). It also showed that the maize plants had a stimulating effect on the microbial activity in crude oil-contaminated soils, and this was compatible with the study referred to (Norino et al., 2004) that the maize roots had a positive effect on the activity of microorganisms in the contaminated soil compared to the uncontaminated. After while, as demonstrated in (Fig. 3) the unplanted soil having 5% pollution seemed to have the highest level of microorganisms. There were not any significant differences between the contaminated and uncontaminated sunflower plants.

effect on reducing hydrocarbons compared to unplanted soil, for example, 66% of all hydrocarbons were reduced at the 5% pollution level (Fig. 2), this point was confirmed by (Dominguez and Pichtel, 2004), who found that using sunflower plants at a 1.50% pollution treatment reduced the crude oil content by roughly 67%.

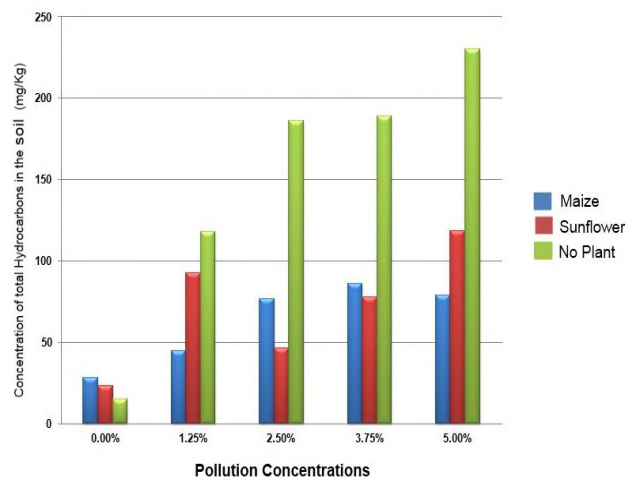


Figure.2: Concentration of total Hydrocarbons in the soil (ppm)

Table.2: Numbers of bacteria in the rhizosphere at zero time and end of experiment

Treatments	Zero Time	End of Experiment		
		Maize	Sunflower	No Plant
%0.00	3.8x10 ⁴ a	2.94x10 ⁴ b	1.73x10 ⁴ a	11.29x10 ⁴ b
%1.25	3.6x10 ⁴ a	4.14 x10 ⁴ b	3.90x10 ⁴ a	8.45x10 ⁴ b
%2.50	4.8x10 ⁴ a	4.45x10 ⁴ b	1.542x10 ⁴ a	10.57x10 ⁴ b
%3.75	2.8x10 ⁴ a	3.71x10 ⁴ b	3.60x10 ⁴ a	12.08x10 ⁴ b
%5	4.1x10 ⁴ a	313.23x10 ⁴ a	164.92x10 ⁴ a	2200.17x10 ⁴ a

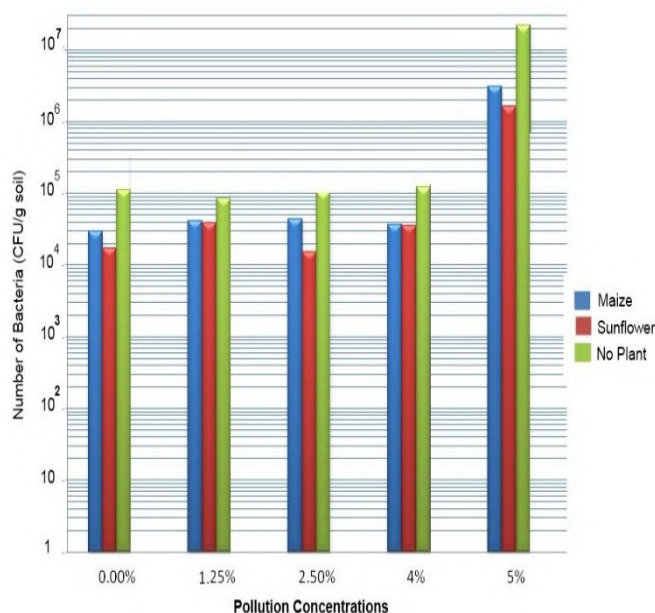


Figure.3: Number of Bacteria (CFU gm/soil) in the soil at the end of experiment.

4 Conclusion

According to the findings, as microorganisms promote plant growth and spread over broad polluted areas, the cooperation between microbes and plants eventually results in the complete removal of pollutants. It is apparent that **Phytoremediation** is a successful method for removing toxins from the soil.

Conflict of Interest: The authors declare that there are no conflicts of interest.

References

- Alegbeleye, O.O.; Opeolu, B.O.; Jackson, V.A. Polycyclic aromatic hydrocarbons: A critical review of environmental occurrence and bioremediation. *Environ. Manag.* 2017, 60, 758–783.
- Ali, M.H.; Sattar, M.T.; Khan, M.I.; Naveed, M.; Rafique, M.; Alamri, S.; Siddiqui, M.H. Enhanced growth of mungbean and remediation of petroleum hydrocarbons by *Enterobacter* sp. MN17 and biochar addition in diesel contaminated soil. *Appl. Sci.* 2020, 10, 8548.

- ATSDR 1988: Health Assessment for York oil company, moira, new York, region 2. *Atlanta, GA: Agency for toxic substances and Disease registry. Report No., PB90-140013: 14.*
- Arslan, M., Imran, A., Khan, Q. M. & Afzal, M. 2017: Plant–bacteria partnerships for the remediation of persistent organic pollutants. *Environmental Science and pollution Research. Res.* 24, 4322–4336.
- Baruah p. p., B. Partha & Deka S. 2013: Removal of hydrocarbon from crude oil contaminated soil by *cyperus brevifolius rottb* 123-130.
- Cui, J.-Q.; He, Q.-S.; Liu, M.-H.; Chen, H.; Sun, M.-B.; Wen, J.-P. Comparative Study on Different Remediation Strategies Applied in Petroleum-Contaminated Soils. *Int. J. Environ. Res. Public Health* 2020, 17, 1606.
- Dominguez-Rosado E., J. Pichtel 2004: Phytoremediation of Soil Contaminated with Used Motor Oil: II Green house Steadies. *Environmental Engineering Science* 21(2): 169-180.
- Ebadi A, Sima N A K, Olamaee M, Hashemi M and Nasrabadi R G 2018 Remediation of saline soils contaminated with crude oil using the halophyte *Salicornia persica* in conjunction with hydrocarbon-degrading bacteria. *J. Environ. Manage.* 219 260-268.
- Khan, M.A.I.; Biswas, B.; Smith, E.; Naidu, R.; Megharaj, M. Toxicity assessment of fresh and weathered petroleum hydrocarbons in contaminated soil-a review. *Chemosphere* 2018, 212, 755–767.
- Kuppusamy, S.; Maddela, N.R.; Megharaj, M.; Venkateswarlu, K. Impact of total petroleum hydrocarbons on human health. In *Total Petroleum Hydrocarbons*; Springer: Cham, Switzerland, 2020; pp. 139–165.]
- Murotova A., T. Hubner, N. Narula, H. Wand, O. Turkovskaya, P. Kusch, R. John & W. Merbach, 2003: Rhizosphere microflora of plants used for the phytoremediation of bitumen-contaminated soil.
- Norino E., O. Norino, S. Zaripore, I. P. Breus 2004: Influence of Cereal Plant on Microorganism of Leached Chernozem Polluted By Hydrocarbons. Orlando, Florida, USA, 2-5, 2003-2004, FO3.
- Radwan S. S., N. Dashti & I. M. El-Nemr, 2005. Enhancing the growth of *Vicia faba* plants by microbial inoculation to improve their phytoremediation potential for oil desert areas. *International, J. Phytoremediation*, (1): 19-32.
- Siciliano S. D. & J. Germida. 1998: Mechanisms of phytoremediation: biochemical and ecological interactions between plants and bacteria. *Environ. Rev.*, 6:65-79.

- Singh H. 2006: Myco-remediation. John Wiley and Sons, Inc. Hoboken, New Jersey. p.592.
- Ye, S.; Zeng, G.; Wu, H.; Zhang, C.; Dai, J.; Liang, J.; Yu, J.; Ren, X.; Yi, H.; Cheng, M. Biological technologies for the remediation of co-contaminated soil. *Crit. Rev. Biotechnol.* 2017, 37, 1062–1076.
- Zand A, D., G. Bidhendi & N. Mehrdadi. 2010: Phytoremediation of total petroleum hydrocarbons (TPHs) using plant species in Iran. *The Turkish Journal of Agriculture and Forestry* 34: 429-438.



Effect of Silver Nitrate (AgNO₃) and Copper Sulphate (CuSO₄) on Callus Formation and Plant Regeneration from Tow Pepper Varieties (Chile Ancho and Misraty) *in Vitro*

Noaman Enfeshi¹, Elshaybani Abdulali¹, Mustafa Salama¹, Zaineb geath¹, Ahmed Shaaban¹, Elmundr Abughnia¹ and Zuhear Ben saad²

¹Libyan Biotechnology Research Center Department Tissue Culture Plant.

²agriculture Factually, Horticulture Department, Tripoli University, Libya.

DOI: <https://doi.org/10.37375/sjfsu.v3i1.943>

A B S T R A C T

ARTICLE INFO:

Received: 09 February 2023

Accepted: 10 April 2023

Published: 17 April 2023

Keywords:

Callus formation, copper sulfate, growth and plant tissue silver nitrate, vegetative.

This study was conducted at the Libyan center for biotechnology research laboratories in order to study the effect of different concentrations of silver nitrate and copper sulfate on the callus formation and plant regeneration of two varieties of pepper plant (Misraty and Chile Ancho). Silver nitrate (AgNO₃) was added at a concentration of 10, 20, 30, 40 and 50 µM/L in the culture media, while copper sulphate (CuSO₄) was added at concentrations of 0.1 (concentration of copper sulfate in MS standard medium), 0.5, 1, 2, 3 and 4 µM/L with presence of 17.8 µM/L of Kin and 1.7 µM/L of NAA. The results indicated that adding silver nitrate to the culture medium did not have a positive effect on the rate of callus formation, while it increased the number of plant growths, especially at a concentration of 30 µM/L. As for copper sulfate, the results showed that, for the plant growth parameter there were no significant differences among the treatments of 2.0, 3.0 and 4.0 µM/L compared to the control treatment in Chile Ancho variety, while the number of seedlings and leaves of the obtained plants improved by increasing the concentration of copper sulfate to record the best average of 4.5 and 7.2, respectively, at a concentration of 3 µM/L. Furthermore for the Misraty variety, the results proved that addition of copper sulfate did not have a positive effect on the rate of callus formation, but it effectively affected the plant growth parameter the percentage of plant growth increased from 15% in the control treatment to 45% in treatment of 3 µM/L. The results showed also that the number of leaves increased by increasing the concentration of copper sulfate by recording average of 7.5 leaves at the treatment of 3 µM/L.

1 Introduction

All peppers belong to the genus *Capsicum* of the Solanaceae family. Chili pepper, chili pepper, and sweet pepper are used interchangeably to describe plants and fruits of the genus *Capsicum* (Dewitt and Bosland, 1993). There are 27 species of pepper, but only five of them are currently domesticated and cultivated. (*C. annum* L. *C. chinense* Jacquin, *C. baccatum* L, *C.*

frutescens L, *C. pubescens*) Barbara Bakersegl has suggested that the first varieties of chilies originated in the distant past of geological times in an area bounded by the mountains of southern Brazil to the east, by Bolivia to the west North-South, Paraguay and Argentina (Dewitt and Bosland, 1993). The pepper genus *Capsicum annum* is the most widely cultivated species in the world. These are the main species grown

in Hungary, Mexico, China, Korea and the East Indies. In Mexico, the term chile (Spanish for chile) refers to all types of hot and sweet peppers, and thus, chili pepper can be used to describe the plants and pods of the capsicum genus Capsicum.

Micropropagation of cells, tissues, and organs is one of the basic applications of biotechnology in many horticultural crops, in addition to its contribution to genetic improvement. The system of reproduction (regeneration) in pepper varieties did not progress as quickly as it occurred in other species of the Solanaceae family, such as potatoes and tobacco, which is considered a model for tissue culture studies, because it has a great ability to reproduce from cells, tissues and organs, while in the case of pepper organs, reproduction was difficult considering that the reproduction of all these plants was obtained from any plant extract or other tissue (Alejo and Malagone 2001). Capsicum explants are very sensitive to ethylene during their in vitro development, a characteristic that has been related to recalcitrance (Gammoudi *et al.*, 2018). In this way, during in vitro culture, pepper explants usually develop chlorosis, abscission of the foliar primordia and loss of vigor (Monteiro *et al.*, 2016). One way to mitigate this effect is using inhibitors of the action of ethylene, which also improve morphogenesis by reducing recalcitrance, achieved by promoting cell elongation and division (Monteiro *et al.*, 2016). Among the ethylene inhibiting substances added to the culture medium, AgNO₃ has been the most used for Capsicum (Gammoudi *et al.*, 2018; Ashwani *et al.*, 2017). To overcome the rosette bud formation (resistance to elongation), silver nitrate (AgNO₃) or phenyl acetic acid (PAA) has been added to the culture media (Gammoudi *et al.*, 2018), although the problem still persists in many materials (Monteiro *et al.*, 2016). Other authors have successfully used copper (Cu) to promote the elongation of shoots (Joshi *et al.*, 2007).

Additionally, differences in the organogenic response have been reported among different Capsicum species and genotypes. In this way, large differences in regeneration have been reported in several Capsicum species, including *C. annuum*, *C. baccatum* and *C. chinense* (Sanatombi and Sharma 2008; Orli and Nowaczyk, 2015; Valadez-Bustos *et al.*, 2009).

The differences found suggest that the variation associated with genotype in Capsicum materials is a limiting factor in the development of widely applicable

regeneration protocols in Capsicum. In fact, individualized protocols are required for different genotypes (Caldas *et al.*, 1990) so, cultivar-specific media formulations have been designed (Dabauza *et al.*, 2001).

This experiment aims to improve the multiplication rates, where the best combination of growth regulators was chosen, which is 17.8 µM/L of Kin with 1.7 µM/L of NAA obtained from previous experiments with the addition of silver nitrate or copper sulfate in several concentrations, as follows:

First: Silver nitrate (AgNO₃) at a concentration of 10, 20, 30, 40 and 50 µM/L.

Second: cupric sulfate (CuSO₄) (MS standard medium concentration, 0.5, 1.0, 2.0, 3.0 and 4.0 µM/L.

2 Materials and Methods

This study was carried out at the Plant Tissue Culture Laboratory which belongs to the Libyan center of biotechnology research, with the aim of improving the vegetative growth rates of two hot pepper varieties (Misraty and the Chilean Ancho). Plant seeds were obtained from the local market for the Misraty variety while, seeds of Chile Ancho variety were obtained from Autonom de Aguascalientes university (Mexico).

The process of preparation and sterilization of the food environment and surface sterilization of seeds and their cultivation in the food environment were summarized. The basic nutrient medium was prepared (Murashige & Skoog MS media) (Murashige and Skoog, 1962). and 45 ml of the nutrient medium was distributed in culture vessels (jars) with a capacity of 330 ml and sterilized in a wet sterilizer (Autoclave) over a temperature of 121°C and an atmospheric pressure of 1.04 kg/cm² for 15 minutes. The prepared media was kept for 3 days before use in the next steps of the study. The experiment was started with preparation of MS which, prepared by addition of 3% sucrose and 0.7% agar at pH of 5.7. The prepared media sterilized in Autoclave for 15 minutes, while about 45 ml of MS media placed in special jars. Prepared media was kept for three days before use.

The seeds were sterilized inside the laminar airflow cabinet using ethanol at concentration of 70% (v/v) for one minute. Then seeds were treated with sodium hypochlorite solution at a concentration of 2.7% (v/v) of commercial Clorox (5.25% Cl₂) for 15 minutes. Finally

seeds were washed by double distilled sterilized water three times for 5 minutes each time. Sterilized seeds were planted on the culture media at a rate of 5 seeds per container, then the cultured plants were incubated in the growth chamber under lighting conditions of 24 $\mu\text{M/L}$ / sec-1 / m-2, a lighting period of 16 hours of light / 8 hours of darkness, and a temperature of $25 \pm 2^\circ \text{C}$. Observation of seed germination was conducted carefully time to time until appropriate size of cultured plants has been obtained. The percentage of germination, contamination, and the beginning of root growth were calculated. Moreover obtained plants were incubated for six weeks before being use in the following studies and analyses.

The cultured media was prepared using MS media supplemented with growth regulators NAA and K with concentration of 1.7 and $17.8\mu\text{M/L}$ respectively whereas, silver nitrate and copper sulfate was added as following First: Silver nitrate (AgNO_3) at a concentration of 10, 20, 30, 40 and $50 \mu\text{M/L}$, Second: cupric sulfate (CuSO_4) (standard MS medium concentration, 0.5, 1.0, 2.0, 3.0 and $4.0 \mu\text{M/L}$). However cultured tissues were directly transferred to the growth chamber whereas, plant tissue samples were incubated under conditions of 16 hours of light and 8 hours of darkness at 25°C to encourage vegetative growth and increase the rate of plant growth for a period

of (90 ± 2) days with application of sub culture twice after 30 and 60 days on the same culture medium. The percentage of callus formation, the percentage of vegetative growth, the average number of shoots and the number of leaves for each vegetative growth were calculated after (90 ± 2) days of culture. However the current experiments were conducted mainly to compare the concentrations of each compound independently.

The complete random system (CRD) was used with 10 replications for data analysis, and when there were significant differences, the averages were isolated using Duncan's multinomial test at the 5% level.

3 Results and discussion

Establishment of free contamination tissue culture considered as one of the most important steps in plant tissue culture technology in order to succeed in the next steps of the study. The result of contamination percentage measurements table (Alejo and malagone, 2001) in this study showed that the contamination rate was low in all the used treatments whereas, in variety of Chile Ancho the contamination rate recorded 8% while, variety of Misraty on contamination was found in all the used treatments.

Table (1): percentage of contamination and seed germination.

Variety	germination (%) after 30 days	Contamination (%)*	No. of days for starting germination**
Misraty	79%	0%	12
Chile Ancho	95%	8%	9

* The percentage of contamination was calculated after 7 days of cultivation.

** The beginning of germination is the exit of the root

percentage of contamination measured after 7days of culture being mentioned before MS media was prepared and supplemented with growth regulators kinetin(K) and Naphthalene acetic acid (NAA) with concentration of 1.7 and $17.8\mu\text{M/L}$ respectively whereas, silver nitrate was added to the same culture media with concentrations of 0.0, 10, 20, 30, 40, $50 \mu\text{M/L}$. The results of this study table (2) showed that

the callus production of Chile Ancho plant samples was significantly higher in treatment of control, 30% 40% silver nitrate compared to other used treatments, whereas control treatment gave a percentage of callus production reached to 80% while treatment of 30% and 40% silver nitrate gave 70% and 65% percentage of callus production respectively. Furthermore the results proved that the other used treatments which are 10, 20,

50 gave lower percentage of callus formation and no significant differences were found among those treatments whereas, those treatments gave a percentage of callus between 40 and 45%. Our obtained results explained that the plant samples of Chile Ancho variety were able to produce callus with large quantities by use of MS culture media supplemented with 30% silver nitrate which mean that addition of silver nitrate with exact concentration has a positive effect on callus formation and induce the plant samples to produce callus. For the vegetative growth parameter the results of this study proved that addition of silver nitrate has a positive effect on plant vegetative growth in general which has been proved in several previous studies whereas, our results proved that addition of 30 and 40 μ M/L silver nitrate gave the best results while those treatments gave vegetative growth with percentage of 43 and 40% respectively followed by control treatment which gave a percentage of 35%. Furthermore the treatments of 30, 40 and control gave a percentage of vegetative growth significantly higher than the other treatments which are 10, 20 and 50 μ M/L. In the same line the treatments of 30 and 40 μ M/L produced the highest number of auxiliary buds those treatments produced 4.7 and 4.9 auxiliary buds for each cultured plant but, there were no significant differences found among the other treatments which are 10, 20 and 50 μ M/L these treatments gave the lowest number of

auxiliary buds and the treatment of 10 μ M/L produced the lowest number of auxiliary buds among all used treatments. However this obtained results proved the positive role of silver nitrate specially when added with concentration of 30 and 40 μ M/L. Our results were in full agreement with (Sharma *et al.*, 2008) the study found that addition of silver nitrate had a positive effect on growth and flowering of pepper plant variety of *C. frutescens*.

Number of leaves parameter. In fact to evaluate the plant growth in this study number of leaf parameter was measured for all plant samples. The results showed that addition of silver nitrate increase the number of leaves in each culture plant while, the treatments of 30 and 40 μ M/L gave the highest number of leaves compared to other treatments whereas, these treatments recorded average of 10.4 and 8.9 leaf for each planted plant respectively. Moreover no significant differences have been found among other used treatments while the treatment of control gave the lowest number of leaves this proved the positive effect of silver nitrate addition on leaf formation for used plant samples. On the same line treatment of control recorded the lowest number of leaf which explain the positive role of silver nitrate by inducing plants to form leaves whereas, control.treatment gave number of leaf of 3.4 leaf in average for each plant sample.

Table (2): Effect of silver nitrate (AgNO₃) on callus formation, vegetative growth, Auxiliary buds and number of leaves after 90 days of growth (variety of Chile Ancho)

Conc.AgNO ₃ μ M/L	Number of leaves	Auxiliary buds (%)	Vegetative (%)	Callus formation (%)
0.0	3.4 ^d	2.6 ^c	80 ^{a*}	35 ^{ab}
10	7.4 ^b	1.6 ^d	45 ^c	11 ^c
20	7.3 ^b	3.2 ^b	40 ^c	28 ^{ab}
30	10.4 ^a	4.7 ^a	70 ^{ab}	43 ^a
40	8.9 ^{ab}	4.9 ^a	65 ^b	40 ^a
50	6.6 ^{bc}	3.2 ^b	40 ^c	20 ^{bc}

* Vertically similar letters, there are no significant differences between them using Duncan's multiple range test at the 5% level.

For Maserati variety results table (Bais *et al.*, 2000) our obtained results showed that for callus formation the results proved that treatments of 30% silver nitrate and control obtained the best results and the highest quantities were obtained by those two treatments, which recorded 90 and 94% respectively. On the other

hand, for vegetative growth the results showed that the treatment of 30% silver nitrate gave the best results followed by 40% and 20% treatment while the results recorded a percentage of 49, 43 and 35% respectively. Furthermore, treatments of control, 10 and 50% gave the lowest levels of vegetative growth and no

significant differences were found among these treatments.

On the other hand, for auxiliary buds formation the results of this study showed that the addition of silver nitrate led to increase the number of auxiliary buds. Moreover the treatment of 30 and 40% gave the best results and they recorded 5.6 and 5.3 buds respectively which prove the positive effect of silver nitrate on plant growth when has been added to nutrition media but, the number of auxiliary buds decreased at concentration of 50% of silver nitrate. which proves that the concentrations 30 and 40% are extremely satiable for pepper vegetative growth in general whereas, the treatment of 50% recorded 3.6 explants. Moreover the lowest recorded results were obtained in treatment of control and 10%. This recorded results were in the same line with (Sharma *et al.*, 2008) who found that the treatment of 30% silver nitrate obtained the best results and addition of silver nitrate has a positive effect on vegetative growth and flowering stage in pepper plant.

For number of leaves parameter the results proved that the addition of silver nitrate led to increase in number of leaves pepper plant variety of Maserati whereas, the treatment of 30% silver nitrate gave the best results and recorded a number of leaves reached to 12.4 leaves which was significantly higher than other used treatments. These obtained results proved the positive effect of silver nitrate on plant growth and explained

the importance role for silver nitrate in pepper plant growth. Nevertheless these results proved also that the high levels of silver nitrate led to negative effect on number of leaves formation and plant growth in general which has been proved in several studies. Our obtained results were in the same line with (Fuentes *et al.*, 2000) (Christopher *et al.*, 1996) who reported that addition of silver nitrate with concentration of 30 to 60 $\mu\text{M/L}$ increased the plant growth of (*Coffeacanephora*) plant whereas, the high levels of silver nitrate led to negative effect on plant growth in general. Furthermore the researcher reported also that high levels act as an ethylene.

blocker and affect the amount of Abscisic acid inside the plant (Kong and Yeung, 1994). However several studies proved that present of ethylene inside the plant cell induces the plant to produce callus and also positively affect the formation of auxiliary buds which may useful in plant tissue culture studies (Giridhar *et al.*, 2004 & Sharma *et al.*, 2008 & Takasaki *et al.*, 2004).

According to our obtained results we found that, the addition of silver nitrate with concentration of 30 and 40 $\mu\text{M/L}$ clearly increase the plant growth in general. Furthermore, the high concentrations of silver nitrate led to negative effect on plant growth whereas, the response to silver nitrate tend to be higher in variety of Maserati than Chile Ancho variety.

Table (3) Effect of silver nitrate (AgNO₃) on callus formation, vegetative growth, Auxiliary buds and number of leaves after 90 days of growth (variety of Maserati)

Conc. AgNO ₃ $\mu\text{M/L}$	Callus formation (%)	Vegetative (%)	Auxiliary buds (%)	Number of leaves
0.0	94 ^a	15 ^c	4.6 ^{bc}	3.2 ^c
10	75 ^c	13 ^d	2.2 ^d	7.6 ^b
20	80 ^b	35 ^{ab}	3.8 ^{bc}	7.8 ^b
30	90 ^a	49 ^a	5.6 ^a	12.4 ^a
40	75 ^c	43 ^a	5.3 ^{ab}	9.5 ^{ab}
50	60 ^d	26 ^{bc}	3.6 ^{cd}	7.3 ^b

* Vertically similar letters, there are no significant differences between them using Duncan's multiple range test at the 5% level.

Effect of copper sulfate on callus induction and plant growth for Chile Ancho and Maserati varieties.

The results of this study (table 5 and 6) showed that the addition of copper sulfate improves the plant growth for both variety. The results proved that for callus

formation parameter it has been found that there was significant differences among the used treatments whereas, the control treatment gave the highest quantity of callus this treatment recorded a percentage of 80 and 94% in Chile Ancho and Maserati variety respectively. However this recorded results explained that there was

no response to callus formation from both varieties. Furthermore for copper sulfate treatments the results showed that the treatments of 3 and 4µM/L copper

sulfate obtained the best results whereas, those treatments recorded 50% of callus formation in Chile Ancho variety and 65% in Maserati variety.

Table (4): effect of (CuSO₄) on callus formation, vegetative growth, Auxiliary buds and number of leaves after 90 days of growth (variety of Chile Ancho).

Conc.CuSO ₄ µM/L	Callus formation (%)	Vegetative (%)	Auxiliary buds (%)	Number of leaves
0.1	80 ^{a*}	35 ^a	2.6 ^b ^c	3.4 ^d
0.5	25 ^c	10 ^c	2.2 ^c	4.8 ^c
1.0	25 ^c	15 ^{bc}	2.4 ^c	4.3 ^c
2.0	45 ^b	25 ^{ab}	3.5 ^{ab}	6.2 ^b
3.0	50 ^b	30 ^a	4.5 ^a	7.2 ^a
4.0	50 ^b	25 ^{ab}	4.6 ^a	6.8 ^{ab}

* Vertically similar letters, there are no significant differences between them using Duncan's multiple range test at the 5% level.

Addition of copper sulfate improves the plant growth in general but the exact concentration of copper sulfate should be studied carefully. Thereby several studies have been applied and studied the effect of copper sulfate on plant growth.

The results of this study showed that the addition of copper sulfate improved that plant growth while, treatment of 3µM/L copper sulfate obtained the best results whereas, recorded a percentage of 30% in Chile Ancho variety and 45% in Maserati variety. Moreover the auxiliary buds formation increased by the addition of copper sulfate whereas, the highest number of auxiliary buds was recorded in treatment of 4µM/L copper sulfate in both varieties whereas, the results recorded an average of 4.6 in Chile Ancho variety and 4.5 in Maserati variety, this obtained results proved the positive effect of copper sulfate on plant growth when added in suitable concentration. On the other hand the

same has been found in number of leaves parameter while the number of leaves increased by the addition of copper sulfate and the treatment of 3µM/L of copper sulfate gave the highest number of leaves followed by the treatment of 4µM/L whereas, those treatments gave an average of number of leaves was significantly higher than the other treatments and those treatments recorded an average of 7.2 and 7.5 for each plant. Our results were in agreement with (Ghaemi *et al.*, 1994) who proved that the addition of copper sulfate improve the plant growth. Furthermore this results were in same line with Kothari and Joshi (Joshi and Kothari, 2007) who found that the addition of copper sulfate increase the plant growth of some pepper variety. In addition our results were in full agree with (Dahleen, 1995) who found that the addition of copper sulfate improve the callus formation of some barely varieties.

Table (5): effect of (CuSO₄) on callus formation, vegetative growth, Auxiliary buds and number of leaves after 90days of growth (variety of Maserati)

Conc.CuSO ₄ µM/L	Callus formation (%)	Vegetative (%)	Auxiliary buds (%)	Number of leaves
0.1	94 ^{a*}	15 ^c	4.6 ^a	3.2 ^d
0.5	30 ^c	15 ^c	2.4 ^b	5.1 ^{bc}
1.0	30 ^c	20 ^b	2.7 ^b	4.4 ^{cd}
2.0	50 ^b	30 ^{ab}	3.2 ^{ab}	6.6 ^b
3.0	65 ^b	45 ^a	3.8 ^a	7.5 ^a
4.0	65 ^b	25 ^b	4.5 ^a	7.2 ^{ab}

* Vertically similar letters, there are no significant differences between them using Duncan's multiple range test at the 5% level.

Conflict of Interest: The authors declare that there are no conflicts of interest.

References

- Alejo, N.O. and R.R.Malagone. 2001. In Vitro chili pepper Biotechnology, In Vitro Cellular and Developmental Biology – Plant. 37:701-729.
- Ashwani, S.; Ravishankar, G.A.; Giridhar, P. 2017. Silver nitrate and 2-(N-morpholine) ethane sulphonic acid in culture medium promotes rapid shoot regeneration from the proximal zone of the leaf of *Capsicum frutescens* Mill. Plant. Cell Tissue Organ. Cult., 129, 175–180.
- Bais, H.P., G. sudha., B. suresh and G. A. ravishankar. 2000. AgNO₃ influences in vitro root formation in *Decalepishamiltonii* Wight, Arn. Current Science, 79: 894-898.
- Beyer, E. M. 1976. A potent inhibitor of ethylene action in plants. Plant Physiology, 58 (3): 268-271.
- Bora, G. H., K. Gogoi and P. J. Handique. 2014. Effect of silver nitrate and gibberellic acid on *in vitro* regeneration, flower induction and fruit development in Naga Chile. Asia-Pacific Journal of Molecular Biology and Biotechnology. 22 (1): 137-144.
- Caldas LS, Haridasan P, Ferreira ME .1990. Meios nutritivos. In: Torres AC, Caldas LS (Eds) Técnicas e Aplicações da Cultura de Tecidos de Plantas (pp 37–70). ABCTP/EMBRAPA-CNPQ, Brasília.
- Ciardi J, Klee H .2001. Regulation of ethylene mediated responses at the level of the receptor. Ann Bot 88(5):813–822. doi:10.1006/anbo.2001.1523
- Chi, G. L. and E. C. Pua. 1989. Ethylene inhibitors enhanced *de novo* shoot regeneration from cotyledons of *Brassica campestris* spp. *in vitro*. Plant Science 64: 243-250.
- Christopher, T. and M. V. Rajam . 1996. Effect of genotype explant and medium on *In vitro* regeneration of red pepper. Plant Cell, Tissue and Organ Culture. 46: 245-250.
- Dabauza, M.; Peña, L. 2001. High efficiency organogenesis in sweet pepper (*Capsicum annuum* L.) Tissues from different seedling explants. Plant. Growth Regul., 33, 221–229.
- Dahleen, L. S. 1995. Improved plant regeneration from barley callus cultures by increased copper levels. Plant Cell, Tissue and Organ Culture. 43: 267-269.
- DeWitt, D.; P.W. Bosland. 1993. The pepper garden. Berkeley, CA: Ten Speed Press; 240 pp.
- Duncan, D. R., M. E. Williams, B. Zehr and J. M. Widholm. 1985. The production of callus capable of plant regeneration from immature embryos of numerous *Zea mays* genotypes. Planta 165 (3): 322-332.
- Fuentes, S. R. L., M. B. P. Calleiros, J. Manetti-Filho and G. E. Vieira. 2000. The effects of silver nitrate and different carbohydrate sources on somatic embryogenesis in *Coffeacaneophora*. Plant Cell, Tissue and Organ Culture, 60: 5-13.
- Gammoudi, N.; Pedro, T.; Ferchichi, A.; Gisbert, C. 2018. Improvement of regeneration in pepper: A recalcitrant species. Plant. Vitro. Cell. Dev. Biol. Plan, 54, 145–153
- Garcia, R. A. and M. A. R. Bahillo. 1990. Tissue and cell culture of pepper (*Capsicum annuum* L. cv. Pico and cv. Piquillo). Acta Horticulturae. 1: 249-254.
- Ghaemi, M., A. Sarrafi and G. Alibert. 1994. The effects of silver nitrate, colchicine, cupric sulfate and genotype on the production of embryoids from anthers of tetraploid wheat (*Triticum turgidum*). Plant Cell, Tissue and Organ Culture, 36: 355-359.
- Giridhar, P., E. P. Indu, K. Vinod, A. Chandrashekar and G. A. Ravishankar. 2004. Direct somatic embryogenesis from *Coffea arabica* L and *Coffeacaneophora* under the influence of ethylene action inhibitor silver nitrate. Acta Physiologia Plantarum 26 (3): 299 -305.
- Joshi, A. S. and L. Kothari. 2007. High copper levels in the medium improves shoot bud differentiation and elongation from the cultured cotyledons of *Capsicum annuum* L. Plant Cell, Tissue and Organ Culture 88:127–133.
- Kim DH, Gopal J, Sivanesan I (2017) Nanomaterials in plant tissue culture: the disclosed and undisclosed. RSC Adv 7:36492–36505.
- Kong, L. and E. C. Yeung. 1994. Effects of ethylene and ethylene inhibitors on white spruce somatic embryo maturation. Plant Science, 104: 71- 80.
- Kothari, S.; Joshi, A.; Kachhwaha, S.; Ochoa-Alejo, N. 2010. Chilli peppers—A review on tissue culture and transgenesis. Biotechnol. Adv., 28, 35–48.
- Kowalska., U., R. Górecki, K. Janas and K. Górecka. 2009. Effect of increased copper concentrations on deformations of the regenerates of carrot obtained from androgenetic embryos. vegetable crops research bulletin, 71: 15 -23.
- Lolkema, P. C. 1985. Copper resistance in higher plants. Doctoral Thesis, Vrije University, Amsterdam.
- Mohiuddin, M., M. Chowdhury, C. A. Zaliha and S. Napis .1997. Influence of silver nitrate (ethylene inhibitor) on cucumber *in vitro* shoot regeneration. Plant Cell, Tissue and Organ Culture, 51: 75-78.
- Malik WA, Mahmood I, Abdul Razzaq, Afzal M, Shah GA, Iqbal A, Zain M, Ditta A, Asad SA, Ahmad I, Mangi N, Ye W. 2021. Exploring potential of copper and silver nano particles to establish efficient callogenesis and regeneration system for wheat (*Triticum aestivum* L.). GM Crops Food 1–22.

- Monteiro do Rêgo, M.; Ramalho do Rêgo, E.; Barroso, P.A.. 2016. Tissue Culture of Capsicum spp. In Production and Breeding of Chilli Peppers (Capsicum spp.); Springer International Publishing: Cham, Switzerland, pp. 97–127..
- Murashige, T and F, Skoog. 1962. A revised medium for rapid growth and bioassays with tobacco tissue cultures. *Physiologia Plantarum*, 15: 473 - 497.
- Podlesna, A. and U. Wojcieszka-Wyskupajtyś. 1996. Collection and use of copper by cereals. *Zesz.Nauk.Komit. Człow. iŚrod.*, 14: 129 -133.
- Purnhauser, L., P. medgysey, M. czako, J. P. dix and L. marton. 1987. Stimulation of shoot regeneration in *Triticumaestivum* and *Nicotianalumbaginifolia* Viv tissue cultures using the ethylene inhibitor silver nitrate, *Plant Cell Reports*, 6 (1): 1- 4.
- Orlińska, M.; Nowaczyk, P.2015. In Vitro plant regeneration of 4 Capsicum spp. Genotypes using different explant types. *Turk. J. Biol.* 39, 60–68.
- Sanatombi, K.; Sharma, G.2008. In Vitro plant regeneration in six cultivars of Capsicum spp. using different explants. *Biol. Plant.*, 52, 141–145.
- Sharma, A., K. Vinod, G. Parvatam and A. R. Gokare. 2008. Induction of *in vitro* flowering in *Capsicum frutescens* under the influence of silver nitrate and cobalt chloride and pollen transformation. *Electronic Journal of Biotechnology*, DOI: 10.2225/vol11-issue2: 1- 8.
- Songstad, D. D., D. R. Duncan and J. M. Widholm. 1988. Effect of 1-aminocycopropane-1-carboxylic acid silver nitrate and norbornadiene on plant regeneration from maize callus cultures. *Plant Cell Reports*, 7(4): 262 -265.
- Steinitz B, Barr N, Tabib Y, Vaknin Y, Bernstein N .2010. Control of in vitro rooting and plant development in *Corymbia maculata* by silver nitrate, silver thiosulfate and thiosulfate ion. *Plant Cell Rep* 29(11):1315–1323.
- Szasz, A., G. Nervo and M. Fasi. 1995. Screening for In vitro shoot forming capacity of seedling explants in bell pepper (*Capsicum annuum* L.) genotypes and efficient plant regeneration using thidiazuron. *Plant Cell Reports*, 14: 666 - 669.
- Takasaki T., Hatakeyama K., Hinata K. 2004. Effect of silver nitrate on shoot regeneration and *Agrobacterium*-mediated transformation of turnip. *Brassica rapa* L. var. *rapifera*. *Plant Biotechnology Journal*, 21: 225 - 228.
- Valadez-Bustos, M.; Aguado-Santacruz, G.; Carrillo-Castañeda, G.; Aguilar-Rincón, V.; Espitia-Rangel, E.; Montes-Hernández, S.; Robledo-Paz, A. 2009. In vitro propagation and agronomic performance of regenerated chili pepper (*Capsicum* spp.) plants from commercially important genotypes. *Vitr. Cell. Dev. Biol. Plant*, 45, 650–658.



Hydrogen Sulphide Strategy in Oil and Gas Field. Review

Ihssin A. Abdalsamed¹, Ibrahim A. Amar¹, Aisha A. Al-abbasi¹, Elfitouri K. Ahmied², Abdusatar A. farouj³, Jamal A. Kawan⁴ and Mohammed A. Awaj⁵

¹Chemistry Department, Sciences Faculty, Sebha University, Sebha, Libya.

²Petroleum Department, Engineering Faculty, Sirte University, Sirte, Libya.

³Corrosion Department, Total Oil Company, Tripoli, Libya.

⁴Production Department, Akakus Oil Company, Tripoli, Libya.

⁵Drilling Department, Zellaf Company for Oil and Gas, Tripoli, Libya.

DOI: <https://doi.org/10.37375/sjfsu.v3i1.74>

A B S T R A C T

ARTICLE INFO:

Received: 26 November 2022

Accepted: 18 March 2023

Published: 17 April 2023

Keywords: H₂S, H₂S Scavenger, Scavenger, Corrosion, mechanisms, Claus process, H₂S safety, Crude oil.

Hydrogen sulphide (H₂S) is one of the most hazardous substances in oil and gas production fields when it comes to the risks posed by its presence. H₂S is a naturally occurring gas found within oil, gas reservoirs, and sewage water. Chemically the gas is extremely toxic, flammable, and corrosive to different materials. H₂S can strongly cause material cracking and environmental pollution and a reduction in oil quality. Thus, prevention measures are very important to produce gas containing even low levels of H₂S. The prevention requires chemical treatment to remove H₂S or convert the gas to an acceptable compound. Therefore, a big challenge was faced to develop a new technological method to manipulate H₂S problems. This review evaluates strategies for crude oil desulfurization by reviewing desulfurization literature. In addition, the effects of hydrogen sulfide on metals and metal protection will be outlined. Finally, some perspectives on the effects of H₂S on personnel health and safety will be discussed.

1. Introduction

Numerous businesses and environmental regulatory authorities have expressed worry about the rising sulfur content of crude oil over time. Hydrogen Sulphide chemically contains one sulfur atom and two hydrogen atoms, the distance between the sulfur atom and hydrogen atom is 133.6 pm, while the angle between hydrogen atoms is 92.1 degrees (Figure 1).^[1] Hydrogen sulphide has many names, such as acidic gas, sour gas, rotten egg gas, stink damp, swamp gas, manure gas, and hydrosulfuric acid.^[2] Recently, reports have found a significant increase in H₂S in the environments.^[3]



Figure (1): The structure of hydrogen sulphide with bond distance and angle

H₂S specification is a colorless, flammable gas with an unpleasant and pungent odor, similar to the smell of rotten eggs. Since H₂S has a density heavier than air, typically usually found in lower places.^[4] Hydrogen sulfide is chemically considered a moderate reducing agent and it plays a significant role in the normal qualitative analysis as it precipitates some metals in the form of sulfides that are insoluble in water in the presence of an acidic medium such as Cu, Hg, Cd, Bi, Sb, Sn and others.^[5] H₂S has many applications used in the manufacture of some medicines and is widely applied in chemical analysis.^[6, 7] H₂S when burn in the air, gives off a faint blue flame. Based on H₂S soluble in water and ethanol (see Table 1).^[6, 8]

Table (1): shows chemical information of H₂S

Formula	H ₂ S
Density	1.36 kg/m ³
Molecular mass	34.0809 g/mol
Boiling point	-60 °C(-76 F; 213 K)
Melting point	-82 °C(-116 F; 191 K)
Solubility	water, ethanol

1.1 H₂S gas sources

Hydrogen sulphide is naturally present in different proportions it is found in high proportions in natural gas and oil and comes out of volcanoes with other gases and in some water wells.^[9] It is produced from the decomposition of biomass due to its fermentation and mildew a product of the processes of decomposition of corpses as well as the decomposition of garbage, as happens with the formation of coal, or the decomposition of tree branches in swamps, or the fermentation of human waste, which leads to the generation of gas.^[10] It is generated because of the interaction of acidic water with components of an underground water tank that contains sulfur compounds, and it is formed when certain types of bacteria that use iron and manganese as part of their food release it, sometimes known as iron bacteria.^[11] Moreover, the gas typically spreads near sewage treatment plants, water pumps, and treatment plants, trucks transporting sewage and chemicals, but it may be emitted from groundwater wells, particularly in areas near oil fields or where wells penetrate limestone layers.^[12] Usually, H₂S gas is extracted from the associated petroleum gas and separated by heat, treated, and condensed to facilitate its transportation as it is exported abroad. The crude is sweet with a sulfur content of 0.5% or less, and it is sour or bitter with a sulfur content greater than that. Nowadays 60% of the oil traded in the world markets is a heavy acid type that contains sulfur.^[13, 14]

1.2 The ways to detect hydrogen H₂S

Due to H₂S being dangerous, it is not permissible to rely on the sense of smell to detect the presence of hydrogen sulphide gas. There are several ways to detect it and its concentration using such as methylene blue liquid and gas chromatography, flame color, digital gas detectors, and adsorption measuring tubes.^[15]

2. Danger levels and precautionary measures

Hydrogen sulphide gas is considered a dangerous gas that affects humans according to its concentration. Hydrogen sulphide is very toxic and its toxicity is higher than that of hydrogen cyanide.^[16] When upon direct exposure to the gas some symptoms occur such as; irritation of the eyes, shortness of breath, disturbances in the nervous system, headache, dizziness, sweating, fatigue, body fatigue, paralysis in the breathing area of the brain, and finally loss of consciousness and sometimes death occur (see Table 2).^[17, 18]

Table (2): shows the safety information of H₂S

Concentration		Effects on humans	The level of risk
mg/m ³	ppm		
1000-2000	1400-2800	Immediate collapse with fatal respiratory paralysis	Fatal
530-1000	530-1000	Central nervous system cell damage, respiratory paralysis leading to death	Very high
320-530	450-750	Acute pulmonary with a high risk of death	High
150-250	210-350	Loss of smell	Moderate
50-100	70-140	Perceived eye damage	Low
10-20	15-30	Eye sensitivity	Normal



Figure (2): Safety sign for H₂S

3. Effect of H₂S gas on equipment in the oil field

Hydrogen sulphide can be dissolved in water and becomes acidic which will be increasing pH, which influences the amount of corrosion damage, resulting in electrochemical corrosion, localized pitting, and pipeline perforation (Figure 3).^[19]



Figure (3): pipeline corroded by H₂S

The hydrogen atoms generated in the corrosion process will be absorbed by the steel and enriched in the metallic defects of the tube, which can lead to the embrittlement of the steel and the initiation of cracks, which leads to cracking (Figure 4).

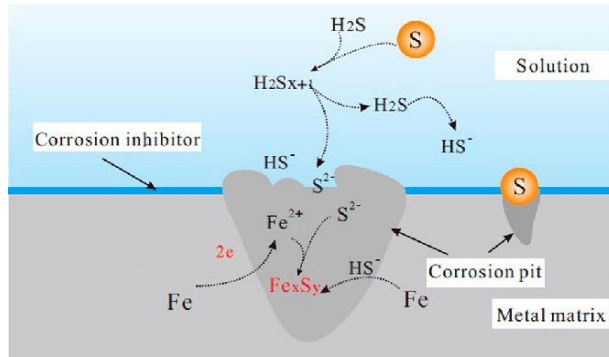


Figure (4) H₂S tendency to attack the metal even corrosion inhibitors are used.

Hydrogen sulphide gas reacts with steel in the presence of water, leading to the formation of iron-sulfur and the release of hydrogen. The iron-sulfur resulting from the reaction will be deposited on the surface of the metal, forming a crust that leads to the formation of a galvanic cell, in which the deposited iron-sulfur plays the role of the cathode (negative), while the steel plays the role of the anode (positive). As a result, several forms of corrosion occur on the metal, the hydrogen atoms released from this reaction penetrate the pores, where these atoms unite with each other to form hydrogen molecules a size larger than the size of the hydrogen atoms (Figure 5). It is necessary to take preventive measures to reduce corrosion as it causes direct and indirect economic losses to oil and gas equipment in the fields.^[20]

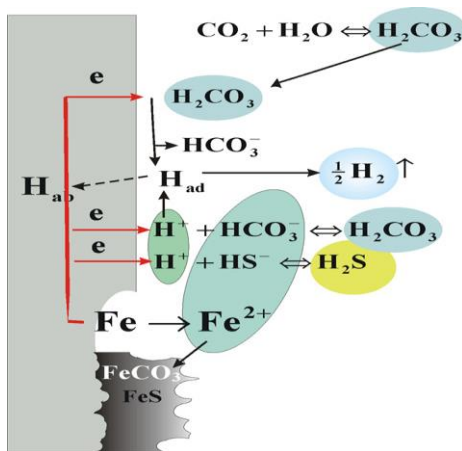


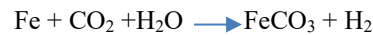
Figure (5): Corrosion mechanism on metal by H₂S enhanced with CO₂.

4. Roles of H₂S gas in corrosion

The majority of pipeline damage is caused by the CO₂ and H₂S-dominated conditions in the oil and gas industry. Since many of the world's oil fields contain H₂S gas, understanding the roles of H₂S gas in corrosion issues is crucial for predicting pipeline corrosion. The impact of H₂S gas in the system has been the subject of much research. It is challenging to estimate H₂S corrosion processes, due to the complicated chemistry and mechanism of the corrosion process. Combinations of responses between the rates of corrosion and film formation may occur during the corrosion process.

4.1 H₂S chemistry in aqueous solution

Corrosion processes can occur under a variety of pipeline environments, and they usually:^[21]



In the pipeline that includes hydrogen sulfide, several chemical processes are taking place, which are mildly acidic when dissolved in water. The chemistry is as follows:^[22, 23]

H₂S dissolution



H₂S dissociation



HS⁻ dissociation



H₂S reduction



FeS formation by precipitation



The pH has an impact on how H₂S reacts in water. The molecular H₂S is the most prevalent form of the sulfide species at low pH (acidic solutions).^[22] This persists until the bisulfide ion is present in large proportions at a pH of around 6. Greater amounts of bisulfide will develop with any pH rise.^[22] The molecular and bisulfide forms are present in equal proportions at a pH of a little around 7. The concentration of the bisulfide ion is around ten folds greater than that of the molecular H₂S at a pH of eight. For pH values higher than 8,^[22, 24, 25] the bisulfide ion is the predominant hydrogen sulfide species iron sulfide can develop in three distinct ways:

I) The dissolution of iron causes a visible black solid film on the surface. The cathodic reaction occurs at the sulfide film/solution interface, and it is constrained by the passage of ferrous ions and electrons through the film.

II) Ferrous ions dissolve in the solution and interact with sulfide ions, preventing the formation of a corrosion product coating on the surface.

III) A mixture of both where ferrous ions react both in solution and on the surface. Iron sulfides form a porous layer as a result.

The cathodic reaction and iron anodic dissolution are made possible by the porous surface.^[22]

5. Factors enhanced the corrosion rate of H₂S

Many factors can enhance hydrogen sulphide tendency to attack the metals such as the following:

I) **Presence of chlorine ions:** Chlorine ions contribute greatly to the continuation of the corrosion process when they are present with hydrogen sulfur and water.

II) **Humidity:** Humidity negatively affects the corrosion of metals with hydrogen sulphide gas, and if moisture is absent, hydrogen sulphide does not affect metals, so drying the gas leads to a significant reduction in the rate of corrosion.

III) **Concentration:** The corrosion rate increases with the increase in H₂S concentration resulting from the increase in the acidity of the medium which the pH increase.^[26]

IV) **Pressure:** The increase in pressure directly affects the rate of corrosion because it increases the concentration of H₂S in one volume, and here severe corrosion is observed even at low pressures. At a partial pressure of 0.05Psia of hydrogen sulphide it causes corrosion to steel alloys.^[27]

V) **Temperatures:** In the gaseous medium, heat affects the rate of corrosion inversely. Corrosion occurs with hydrogen sulphide gas at temperatures of (-6,49) °C.^[28, 29]

VI) **Time:** In the beginning, a layer of iron-sulfur is formed that plays a protective role, and with the passage of time its structure changes, leading to an increase in the rate of corrosion.^[30]

6. Methods of protecting metals from H₂S aggressive

There are many methods to protect the metals used in oil and gas fields from corrosion chemical and non-chemical methods such as a) Good equipment design, b) Treating the surrounding medium, c) Covering, including metallic sheathing (electrochemical nickel-cobalt plating...etc.) or organic coverage (polyethylene - epoxy), d) Injection of corrosion inhibitors, e) Cathodic protection and sacrificial anode. On the other hand, the hydrogen sulphide scavenger is a remarkable method to remove hydrogen sulphide from systems, as well as corrosion allowance, which must be considered by engineering design.^[31, 32]

7. Removal of hydrogen sulfide (H₂S)

Removal of hydrogen sulfide (H₂S) released from various source processes is crucial because this compound can cause corrosion and environmental damage even at low concentration levels.

7.1 H₂S scavenger

H₂S scavengers are widely used in hydrocarbon and chemical processing facilities to remove H₂S with low capital cost.^[33] Triazines and Glyoxal are commonly used as H₂S scavengers in oil and gas production. In offshore plants, triazines are directly injected into the gas streams, while in onshore plants triazines will be injected in contactor towers. Moreover, one mole of triazine can scavenge two moles of hydrogen sulfide.^[34] Glyoxal (C₂H₂O₂) is a hydrogen sulfide scavenger that does not contain nitrogen, which given the glyoxal advantage does not cause corrosion problems in refineries. However, the disadvantage of using glyoxal are; first glyoxal is acidic and it has a low pH that can cause the water phase to have a low pH and result in corrosion at any location, while reaction with H₂S at low temperatures is less efficient, second glyoxal is a slow-acting scavenger and may be corrosive to mild steel.^[35, 36] Moreover, Ethanol amines have been used extensively to remove H₂S from gas streams in sweetening towers while Diglycolamine [2-(2-Aminoethoxy) ethanol] has been used since 1965 for the industrial removal of hydrogen sulphide and /or carbon dioxide from gas streams^[37, 38]. Acrolein (C₃H₄O) has been used as an H₂S scavenger in these instances; Acrolein is an effective scavenger but an extremely toxic substance. On other hand, H₂S reacts with aldehydes across the C=O double bond in a reversible process^[39]. The most common use of formaldehyde. Zinc oxide and zinc carbonate are also used as H₂S scavengers because it has a high to reduce the production of sulphur compounds.^[40] Recently the development and field application of a new Hydrogen Sulfide (H₂S) Scavenger in oilfield mixed production applications is presented.^[41] However, there is disadvantages using H₂S scavenger; the first trail must be done to choose a suitable H₂S scavenger, the second H₂S scavenger maybe reacts with other chemicals such as corrosion inhibitors and demulsifiers.

7.2 Solid bed H₂S scavengers unit

Hydrogen sulfide is mostly removed from associated gas in oil fields using solid bed H₂S scavengers. To protect people and downstream equipment from dangerous and extremely corrosive hydrogen sulfide, the solid-state H₂S removal technology is the best option for gas processors to reduce the quantity of hydrogen sulfide and the outlet pipeline (Figure 6) .^[42, 43]

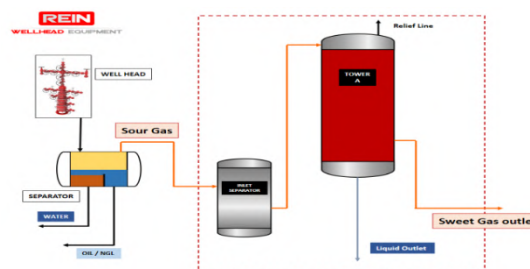
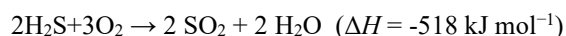


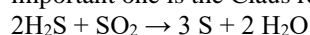
Figure (6): solid bed H₂S scavengers unit.

7.3 Claus process

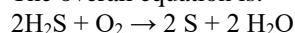
In 1883, the first process to extract and produce sulfur from hydrogen sulphide was invented by the chemist Carl Friedrich Claus. Based on this, the Claus process, which recovers elemental sulfur from gaseous hydrogen sulfide, where the input gas is burnt, is still the most significant gas desulfurizing method. Claus furnaces frequently sustain temperatures beyond 1050°C.^[44] In general, hydrogen sulfide is converted to elemental sulfur in two steps; The first involves the oxidation of a portion of hydrogen sulfide to sulfur dioxide with air oxygen, and then in the second step by conducting a co-proportional reaction between hydrogen sulfide and sulfur dioxide as follows:



The reaction is a strongly exothermic free-flame total oxidation of hydrogen sulfide generating sulfur dioxide that reacts away in subsequent reactions.^[45] The most important one is the Claus reaction is:



The overall equation is:



8. H₂S corrosion monitoring

H₂S Corrosion monitoring has the potential to be a significant asset as part of comprehensive corrosion management since H₂S corrosion affects oil construction.^[46] There are different classical monitoring methods have been various traditional monitoring techniques that employed, including:

8.1 Corrosion coupons

Corrosion coupons can be used in vessels, tanks, and pipes. Corrosion coupons usually can be manufactured in different sizes and shapes. Corrosion coupons are closer resemblance to actual condition, and reliable information for future designs (Figure 7). For measuring the corrosion rate corrosion coupons must be regularly recovered, cleaned, and weight. Determination of the corrosion rate is usually done while the plant is running by using of specialized retrieval equipment. However, because of the risk of H₂S emission, retrieval is usually delayed until shutdown so that the tube part can be isolated, depressurized, cleaned, and aerated. The unit for calculation is MPY which is miles per year. Corrosion rate (CR) can be calculated by the following equation:

$$C.R = 534 \text{ WD/A.T}$$

Where; W is weight loss measured in mg, D is the density of alloy in g/cm³, A is the surface area of the specimen exposed to the solution in cm², and T is the total exposure time in an hour.^[47]

However, if the result is over 1MPY that means a high corrosion rate, as well operation team, have must be done an investigation; of corrosion inhibitors, salinity, H₂Ssolubility, pH, and SRB bacteria count.



Figure (7): corrosion coupon

8.2 Probes detecting corrosion.

There are many probes instruments such as ERP (Electrical Resistance (ER) probe) and Linear Polarisation Resistance (LPR) probes which are instruments mechanism due to electrical conduction (Figure 8), however, it has a disadvantage because the corrosion products, such as iron sulfide deposited on the walls, are electrically conductive and can generate misleading data. These Probes will not measure the corrosion that occurs to such pipe walls; instead, they will merely monitor how corrosive the process fluid is. These devices will break out rapidly as a result of the severe H₂S corrosion as they will be required to be changed and shut down oil constructions.^[46]

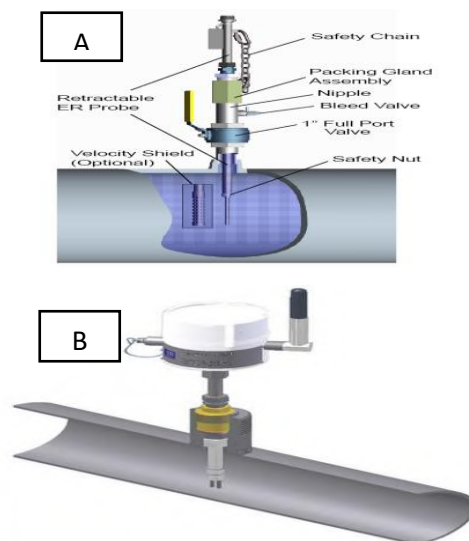


Figure (8): shows A is ERP and B is LPR instrument.

8.3 Wave-guided systems

The method employs acoustic waves that propagate along an elongated structure while guided by its boundaries (Figure 9). Despite in fact that these tools make it possible to verify pipe sections by locating corroded spots. They offer little insight into the possible severity of corrosion damage that can occur, and the data gathered need further manual assessment using conventional methods.^[46, 48]

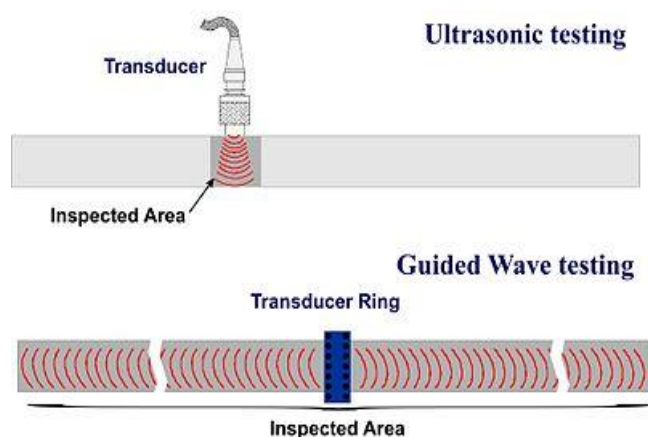


Figure (9): wave guided system.

8.4 Field analysis

Field analysis is usually done for scale corrosion such as CaCO_3 , CaSO_4 , and BaSO_4 , otherwise, field analysis can be done for other types of corrosion to predict whether corrosion is likely or unlikely and if instruments are not available. The type of field analysis that can be done for non-scale corrosion is; water salinity, H_2S solubility, H_2S count, pH, CO_2 solubility, salt in crude oil, and SRB bacteria count. The advantages of field analysis include; simple methods, it can expect corrosion is likely or unlikely as well as some methods do not need instruments for analysis, finally field analysis can expect which type of chemical will be used in the system. However, there are disadvantages likewise first field analysis relies on parameters such as temperature, the second needed skills and experiments of the operator as well as field analysis is a high risk to the safety person and field analysis must be done frequently.

9. Future work

The consequences of H_2S corrosion are contamination, loss of product, and shutdown which leading loss of millions of dollars per year as well as encouraging many scientists related to corrosion science using nanotechnology to try manufacturing plants alloys more resistant than carbon steel and stainless steel such as using three different layers made from three types of metals. Based on this, they are working hard to fabricate transparent plants that could be more non-corrosive and likewise easy to monitor.

10. Summary

Hydrogen sulfide (H_2S) is often present in oil and gas production fluids. Even with low concentration, the gas is poisonous, corrosive to mild steel, and induces localized sulfide corrosion cracking (SCC) in materials with susceptible metallurgical properties. The density of

H_2S is heavier than air and other gases, which is make H_2S found in low places, however for safety person, must stay in high places. The pH will increase with the presence of hydrogen sulphide as hydrogen sulphide can be dissolved in water and becomes acidic. The Chlorine, humidity, temperature, pressure, and time can enhance H_2S to attack the metals. The highly corrosive acid sulfuric acid (H_2SO_4) is chemically created when H_2S reacts with water. Sour corrosion is the name given to corrosion caused by H_2SO_4 . Stock tanks that are submerged in water may sustain severe damage because hydrogen sulfide and water combine rapidly. Moreover, when hydrogen sulfide dissolves in water, it produces a weak acid. As a result, it is a source of hydrogen ions. It has the potential to serve as a catalyst for the adsorption of atomic hydrogen in steel, promoting sulfide stress cracking (SSC) in high-strength steel. Production of liquids and gases containing H_2S can cause severe corrosion because of H_2S stress cracking, especially on equipment that has not been fabricated and designed to deal with sour conditions. In addition, when hydrogen sulfide interacts with elemental sulfur, polysulfides may result. Treatment with H_2S scavengers can enable the use of less-expensive low-alloy carbon steel materials. The H_2S scavenger type must be non-nitrogen-containing, as H_2S scavengers containing nitrogen can make corrosion problems because the amines will react with sulphides/ H_2S to form acid/ base salts in a fully reversible reaction. The oil and gas sector typically uses triazine, the most popular H_2S scavenger, to remove hazardous and corrosive hydrogen sulfide from natural gas, refinery streams, and olefins cracker products. Based on the Claus process, this system is outstanding at converting H_2S to sulfur and has numerous industrial applications. Moreover, Claus's method is exceptional for lowering sulfur compound emissions into the atmosphere. The drawbacks of H_2S scavenger use, however, are low efficiency, corrosively, scalability, and emulsification. Corrosion coupons are remarkable tools for monitoring corrosion rates. They can give accurate corrosion rates in vessels, tanks, and pipes, but they needed the skills of the operator. Moreover, to minimize corrosion rate engineering must be considering as following; the type of metals used to fabricate the plant, chose the suitable area for constructing the plant, the corrosion allowance, and the processing system.

Acknowledgment

The authors like to thank the entire staff at the Al-Shrara field Repsol Oil Company.

Conflict of Interest: The authors declare that there are no conflicts of interest.

References

- Allen, F.H., et al., *Tables of bond lengths determined by X-ray and neutron diffraction. Part 1. Bond lengths in organic compounds*. Journal of the Chemical Society, Perkin Transactions 2, 1987(12): p. S1-S19.
- Pandey, S.K., K.-H. Kim, and K.-T. Tang, *A review of sensor-based methods for monitoring hydrogen sulfide*. TrAC Trends in Analytical Chemistry, 2012. **32**: p. 87-99.
- Toohey, J.I., *The conversion of H₂S to sulfane sulfur*. Nature Reviews Molecular Cell Biology, 2012. **13**(12): p. 803-803.
- Wang, H., D. Fang, and K.T. Chuang, *A sulfur removal and disposal process through H₂S adsorption and regeneration: Ammonia leaching regeneration*. Process Safety and Environmental Protection, 2008. **86**(4): p. 296-302.
- Pudi, A., et al., *Hydrogen sulfide capture and removal technologies: A comprehensive review of recent developments and emerging trends*. Separation and Purification Technology, 2022. **298**: p. 121448.
- Dan, M., et al., *Hydrogen sulfide conversion: How to capture hydrogen and sulfur by photocatalysis*. Journal of Photochemistry and Photobiology C: Photochemistry Reviews, 2020. **42**: p. 100339.
- Powell, C.R., K.M. Dillon, and J.B. Matson, *A review of hydrogen sulfide (H₂S) donors: Chemistry and potential therapeutic applications*. Biochemical Pharmacology, 2018. **149**: p. 110-123.
- Wang, R., *Physiological Implications of Hydrogen Sulfide: A Whiff Exploration That Blossomed*. Physiological Reviews, 2012. **92**(2): p. 791-896.
- Hernández, P.A., et al., *Contribution of CO₂ and H₂S emitted to the atmosphere by plume and diffuse degassing from volcanoes: the Etna volcano case study*. Surveys in Geophysics, 2015. **36**(3): p. 327-349.
- Laprune, D., et al., *Effects of H₂S and phenanthrene on the activity of Ni and Rh-based catalysts for the reforming of a simulated biomass-derived producer gas*. Applied Catalysis B: Environmental, 2018. **221**: p. 206-214.
- Shatalin, K., et al., *H₂S: a universal defense against antibiotics in bacteria*. Science, 2011. **334**(6058): p. 986-990.
- Baawain, M., et al., *Measurement, control, and modeling of H₂S emissions from a sewage treatment plant*. International Journal of Environmental Science and Technology, 2019. **16**(6): p. 2721-2732.
- Demirbas, A., H. Alidrisi, and M. Balubaid, *API gravity, sulfur content, and desulfurization of crude oil*. Petroleum Science and Technology, 2015. **33**(1): p. 93-101.
- Vetere, A., D. Pröfrock, and W. Schrader, *Quantitative and qualitative analysis of three classes of sulfur compounds in crude oil*. Angewandte Chemie International Edition, 2017. **56**(36): p. 10933-10937.
- Shen, X., et al., *Measurement of plasma hydrogen sulfide in vivo and in vitro*. Free Radical Biology and Medicine, 2011. **50**(9): p. 1021-1031.
- Ng, P.C., et al., *Hydrogen sulfide toxicity: mechanism of action, clinical presentation, and countermeasure development*. Journal of Medical Toxicology, 2019. **15**(4): p. 287-294.
- Gao, B., X. Han, and H. Zhang, *Study on H₂S monitoring technique for high risk wellsite*. Procedia Engineering, 2012. **45**: p. 898-903.
- Dagtas, B., O.F. Garnier, and G. Noble. *Management of H₂S risk in total ABK*. in *SPE International Health, Safety & Environment Conference*. 2006. OnePetro.
- Adebayo, A., *Corrosion of steels in water and hydrogen sulphide*. Review of Industrial Engineering Letters, 2014. **1**(2): p. 80-88.
- Salas, B.V., et al., *H₂S pollution and its effect on corrosion of electronic components*. Air Quality—New Perspective, IntechOpen, London, 2012: p. 263-285.
- Fink, J., *Chapter 5 - Corrosion in Pipelines*, in *Guide to the Practical Use of Chemicals in Refineries and Pipelines*, J. Fink, Editor. 2016, Gulf Professional Publishing: Boston. p. 57-82.
- Asmara, Y., *The Roles of H₂S Gas in Behavior of Carbon Steel Corrosion in Oil and Gas Environment: A Review*. Jurnal Teknik Mesin, 2018. **7**: p. 37.
- Nafday, O., *Film Formation and CO₂ Corrosion in the Presence of Acetic Acid*, in *Russ College of Engineering and Technology*. 2004, Ohio University.
- van Hunnik, E.W.J., Pots, B.F.M., Hendriksen, E.L.J.A., *The Formation of Protective FeCO₃ Corrosion Product Layers in CO₂ Corrosion*, in *Corrosion: NACE International*. 1996: Houston.
- Wei Sun, S.N., *Kinetics of Iron Sulfide and Mixed Iron Sulfide/Carbonate Scale Precipitation in CO₂/H₂S*. 2006, Corrosion: NACE International: Houston.
- Romanova, A., M. Mahmoodian, and A. Alani, *Influence and interaction of temperature, H₂S and pH on concrete sewer pipe corrosion*. International Journal of Civil, Environmental, Structural, Construction and Architectural Engineering, 2014. **8**(6): p. 621-624.
- Zhou, C., et al., *The effect of the partial pressure of H₂S on the permeation of hydrogen in low carbon pipeline steel*. Corrosion Science, 2013. **67**: p. 184-192.
- Yongsiri, C., J. Vollertsen, and T. Hvited-Jacobsen, *Effect of temperature on air-water transfer of hydrogen sulfide*. Journal of Environmental Engineering, 2004. **130**(1): p. 104-109.
- Zhang, L., et al. *Effects of temperature and partial pressure on H₂S/CO₂ corrosion of pipeline steel in sour conditions*. in *CORROSION 2011*. 2011. OnePetro.
- Smith, S.N., B. Brown, and W. Sun. *Corrosion at higher H₂S concentrations and moderate temperatures*. in *CORROSION 2011*. 2011. OnePetro.
- Arora, A. and S.K. Pandey. *Review on materials for corrosion prevention in oil industry*. in *SPE International Conference & Workshop on Oilfield Corrosion*. 2012. OnePetro.
- Axmadjonovich, M.A., *Methods of Protecting Pipes from Corrosion*. EUROPEAN JOURNAL OF INNOVATION IN NONFORMAL EDUCATION, 2022. **2**(7): p. 85-88.
- Amosa, M., I. Mohammed, and S. Yaro, *Sulphide scavengers in oil and gas industry—a review*. Nafta, 2010. **61**(2): p. 85-92.
- Taylor, G., et al. *H₂S Scavenger Development During the Oil and Gas Industry Search for an MEA Triazine Replacement in Hydrogen Sulfide Mitigation and*

- Enhanced Monitoring Techniques Employed During Their Evaluation.* in *SPE International Conference on Oilfield Chemistry*. 2019. OnePetro.
- Elkatatny, S., et al. *New Hydrogen Sulfide Scavenger for Drilling Sour Horizontal and Multilateral Reservoirs.* in *SPE Kingdom of Saudi Arabia Annual Technical Symposium and Exhibition*. 2018. OnePetro.
- Patel, N., et al. *Novel Techniques for the Evaluation of Hydrogen Sulfide Scavenger Performance and By-Product Stability.* in *SPE Oil and Gas India Conference and Exhibition*. 2019. OnePetro.
- Spatolisano, E., A.R. de Angelis, and L.A. Pellegrini, *Middle Scale Hydrogen Sulphide Conversion and Valorisation Technologies: A Review.* ChemBioEng Reviews, 2022.
- Shoukat, U., D.D. Pinto, and H.K. Knuutila, *Study of various aqueous and non-aqueous amine blends for hydrogen sulfide removal from natural gas.* Processes, 2019. **7**(3): p. 160.
- Mao, Z., et al., *Hydrogen sulfide as a potent scavenger of toxicant acrolein.* Ecotoxicology and Environmental Safety, 2022. **229**: p. 113111.
- Agbroko, O.W., K. Piler, and T.J. Benson, *A comprehensive review of H₂S scavenger technologies from oil and gas streams.* ChemBioEng Reviews, 2017. **4**(6): p. 339-359.
- Lehrer, S., et al. *Development and Application of a Novel Hydrogen Sulfide Scavenger for Oilfield Applications.* in *SPE International Conference on Oilfield Chemistry*. 2021. OnePetro.
- Ardianto, M.N. and S. Heru Wijaya Pamungkas, *Performance Evaluation of H₂S Adsorbent in Singa Field: Case Study of Adsorbent Pimit-B1.* 2016.
- Jones, R., K. McIntush, and C. Wallace, *Oxygen removal in natural gas systems.* Gas Processors Association Research Report RR-201, GPA Research, 2010(073).
- Eow, J.S., *Recovery of sulfur from sour acid gas: A review of the technology.* Environmental progress, 2002. **21**(3): p. 143-162.
- Chardonneau, M., et al., *Role of toluene and carbon dioxide on sulfur recovery efficiency in a Claus process.* Energy Procedia, 2015. **75**: p. 3071-3075.
- Zhou, H., *Monitoring Hydrogen Sulphide (H₂S) Corrosion in Oil & Gas Upstream Industry.* Aug 5, 2020 | Analytical, Oil & Gas.
- Abdalsamed, I.A., et al., *Corrosion Strategy in Oil Field System.* Journal of Chemical Reviews, 2020. **2**(1): p. 28-39.
- Lowe, M.J., P. Cawley, and A. Galvagni, *Monitoring of corrosion in pipelines using guided waves and permanently installed transducers.* The Journal of the Acoustical Society of America, 2012. **132**(3): p. 1932-1932.

Scientific Journal For the Faculty of Science - Sirte University



Sjsfsu@su.edu.ly



journal.su.edu.ly/index.php/JSFSU



TOGETHER WE REACH THE GOAL



husam